LABORATOIRE DE PHYSIQUE THÉORIQUE ET HAUTES ÉNERGIES

**THÈSE DE DOCTORAT DE**
**L'UNIVERSITÉ PIERRE ET MARIE CURIE**

Spécialité : **Physique**

Présentée par

**Thomas VANEL**

Pour l'obtention du grade de
**DOCTEUR de L'UNIVERSITÉ PIERRE ET MARIE CURIE**

Sujet de la thèse :

# Strongly-coupled systems in gauge/gravity duality

# Systèmes fortement couplés en dualité jauge/gravité

Soutenue le 30 septembre 2014

devant le jury composé de :

| | |
|---|---|
| M. Benoit Douçot | Invité |
| Mme. Johanna Erdmenger | Rapporteuse |
| Mme. Michela Petrini | Directrice de thèse |
| M. Marios Petropoulos | Président du jury |
| M. Giuseppe Policastro | Invité et co-directeur de thèse |
| M. Koenraad Schalm | Rapporteur |
| M. Matthieu Tissier | Examinateur |

# Remerciements

Je tiens tout d'abord à remercier les directeurs successifs du LPTHE, Olivier Babelon et Benoit Douçot, pour m'avoir accueilli au sein du LPTHE, laboratoire qui offre un cadre de travail adéquat et agréable.

Mes remerciements vont à mes directeurs de thèse, Michela Petrini et Giuseppe Policastro, et indissociablement Francesco Nitti, qui m'ont guidé pendant ces trois années. Merci pour votre soutien et vos conseils avisés. J'ai pris beaucoup de plaisir à travailler avec vous, malheureusement je ne suis toujours pas bilingue italien !

Je tiens aussi à remercier Nick Halmagyi et Harold Erbin pour nos collaborations. La supergravité est un domaine fascinant, merci pour ce bout de chemin fait ensemble.

Je remercie Johanna Erdmenger et Koenraad Schalm pour avoir accepté d'être rapporteurs pour cette thèse. Je remercie également Benoit Douçot, Marios Petropoulos et Matthieu Tissier pour avoir bien voulu faire partie de mon jury de thèse.

Merci à mes collègues doctorants, du LPTHE et autres, Demian, Emanuele, Gautier, Harold, Jérémy, Julius, Luc, Konstantina, Pierre, Piotr, Sasha, Stefano, Thibault, Tianhan, Tresa. Je remercie tout particulièrement Emanuele pour avoir parfaitement répondu à mes nombreuses questions sur Mathematica ainsi que Piotr pour sa relecture du manuscrit. Je remercie également Bruno pour sa gentillesse et les nombreux repas que nous avons partagés. Merci aussi à mes amis magistériens, en particulier Binôôôme, Nicolas et l'insaisissable Ruidy.

Merci à mes parents et ma sœur pour leur soutien. Si j'en suis là c'est grandement grâce à vous. J'aimerais aussi remercier mes grands-mères pour leur présence à ma soutenance de thèse. Cela me fait chaud au cœur, j'en suis très heureux.

Cette thèse n'aurait jamais vu le jour sans la présence à mes côtés de ma compagne Margaux. Merci pour ta bonne humeur et tous ces merveilleux moments que nous avons partagés et continuerons à partager. Tu sais combien je tiens à toi.

# Abstract

As an introduction, we present the original formulation of the AdS/CFT correspondence, between $\mathcal{N} = 4$ Super Yang-Mills theory with gauge group $SU(N)$ and type IIB string theory on $AdS_5 \times S^5$. In a first part, we show how the ingredients of the AdS/CFT correspondence can be applied in a phenomenological way to study strongly correlated systems of fermions and present two fundamental models, the electron star and the holographic superconductor. We construct a holographic model for the study of Bose-Fermi systems at finite density and show that the simultaneous presence of bosonic and fermionic degrees of freedom is favoured at zero temperature. By solving the field equation of a probe spinor field in these solutions, we show that the system admits a large number of electron-like and/or hole-like Fermi surfaces and a charged scalar condensate. In a second part, we study asymptotically-$AdS_4$ BPS black hole solutions in the $\mathcal{N} = 2$ gauged supergravity theory. Using the duality transformations in a simple STU model, we find new static and rotating BPS black hole solutions.

# Résumé court

Comme introduction, nous présentons la formulation originale de la correspondance AdS/CFT, entre la théorie de Yang-Mills supersymétrique $\mathcal{N} = 4$ avec groupe de jauge $SU(N)$ et la théorie des supercordes de type IIB sur l'espace $AdS_5 \times S^5$. Dans une première partie, nous montrons comment les ingrédients de la correspondance AdS/CFT peuvent être appliqués de manière phénoménologique à l'étude des systèmes de fermions fortement corrélés et présentons deux modèles fondamentaux, l'étoile à électrons et le supraconducteur holographique. Nous construisons un modèle holographique pour l'étude des systèmes de Bose-Fermi à densité finie et montrons que la présence simultanée de degrés de liberté bosoniques et fermioniques est favorisée à température nulle. En résolvant l'équation du mouvement d'un spineur test sur ces solutions, nous montrons que le système admet un grand nombre de surfaces de Fermi de type électron et/ou trou et un condensat scalaire chargé. Dans une seconde partie, nous nous intéressons à l'étude des solutions de trous noirs BPS asymptotiquement $AdS_4$ dans la théorie de supergravité jaugée $\mathcal{N} = 2$ en 4 dimensions. En utilisant les transformations de dualité dans un modèle STU simple, nous trouvons de nouvelles solutions de trous noirs BPS statiques et en rotation.

# Contents

**Introduction** **1**

**1 The AdS/CFT correspondence** **3**
1.1 Large $N$ limit of gauge theories . . . 3
1.2 The two pictures of $p$-branes . . . 4
1.2.1 $p$-branes in supergravity . . . 4
1.2.2 D$p$-branes in string theory . . . 5
1.3 Decoupling limit . . . 6
1.3.1 Decoupling of the brane/bulk system . . . 6
1.3.2 Near-brane geometry of 3-branes . . . 6
1.4 Tests and properties of the correspondence . . . 7
1.4.1 Strong/weak duality . . . 8
1.4.2 Matching symmetries . . . 8
1.4.3 Matching the spectrum . . . 9
1.5 Partition function and correlation functions . . . 10
1.5.1 Free scalar field in AdS . . . 14
1.6 Generalizations . . . 16

**2 Holography for condensed matter physics** **19**
2.1 Systems of fermions at finite density . . . 19
2.2 Bottom/up approach to the AdS/CFT correspondence . . . 23
2.3 The AdS-Reissner-Nordström black hole . . . 26
2.4 The electron star model . . . 30
2.4.1 Action and field equations . . . 30
2.4.2 Lifshitz symmetry and perturbations towards the boundary region . 33
2.4.3 Solution-generating symmetries and physical parameters . . . 36
2.4.4 Thermodynamics . . . 36
2.4.5 Discussion and extensions . . . 37
2.5 Holographic superconductors . . . 38
2.5.1 Instability of the extremal AdS-Reissner-Nordström black hole . . . 39
2.5.2 Holographic superconductor at zero temperature . . . 40
2.5.3 Other holographic models for superconductivity . . . 44

**3 Holographic Bose-Fermi systems** **47**
3.1 Motivations . . . 47
3.2 Beyond the electron star and the holographic superconductor . . . 48
3.2.1 Scalar instability of the electron star . . . 48
3.2.2 An analysis from the holographic superconductor . . . 49

3.3 A holographic Bose-Fermi model . . . 51
3.3.1 An action for the fluid . . . 51
3.3.2 Field equations . . . 53
3.3.3 UV asymptotics . . . 55
3.3.4 Solutions at finite density . . . 55
3.4 Phase diagrams of charged solutions . . . 59
3.4.1 Free energy and phase diagrams for $\hat{\eta} = 0$ . . . 60
3.4.2 Free energy and phase diagrams for $\hat{\eta} \neq 0$ . . . 61
3.4.3 Charge distribution and screening . . . 62
3.4.4 Comments on the CS/ES and HSC/ERN phase transitions . . . 67
3.5 Low energy fermionic spectrum of holographic Bose-Fermi systems . . . 68
3.5.1 Probe fermion and the Dirac equation . . . 69
3.5.2 The WKB analysis for $|\hat{\omega}| \ll \hat{k} < \hat{k}_F^\star$ . . . 75
3.5.3 The Green's function for eCS and pCS solutions . . . 77
3.5.4 The Green's function for peCS solutions . . . 77
3.5.5 The Luttinger count . . . 80
3.5.6 Fermi surfaces and phase transitions . . . 82
3.6 Discussion . . . 84

**4 AdS black holes from duality in gauged supergravity 87**
4.1 Introduction . . . 87
4.2 $\mathcal{N} = 2$ gauged supergravity . . . 88
4.3 STU-model . . . 90
4.3.1 The basics of $SL(2,\mathbb{R})/U(1)$ . . . 91
4.3.2 Embedding $SO(2)^3$ into $Sp(2n_V + 2, \mathbb{R})$ . . . 93
4.3.3 Two simple generators . . . 93
4.3.4 The third generator . . . 94
4.4 BPS static black holes . . . 94
4.4.1 The supersymmetric static black holes . . . 95
4.4.2 Duality transformations on the CK black holes . . . 97
4.5 Rotating black holes . . . 98
4.6 Conclusions . . . 100

**Conclusion 103**

**A Correlation functions in Lorentzian signature 105**

**B Irrelevant operators and IR Lifshitz solutions 109**

**C The Dirac equation 113**

**D Solving the Schrödinger-like equation 115**
D.1 The WKB solution for one $V < 0$ region . . . 115
D.2 The WKB solution for two $V < 0$ regions . . . 116

**E Duality symmetries and Very Special Kähler Geometry 117**

**F Résumé long en français** **119**
F.1 La correspondance AdS/CFT . . . 119
F.1.1 Supergravité et $p$-branes . . . 119
F.1.2 Théorie des cordes et D$p$-branes . . . 119
F.1.3 Limite de découplage . . . 120
F.1.4 Tests et propriétés de la correspondance . . . 120
F.1.5 Thermodynamique et fonctions de corrélation . . . 121
F.1.6 Généralisations . . . 122
F.2 AdS/CFT pour la matière condensée . . . 122
F.2.1 Systèmes de fermions à densité finie . . . 123
F.2.2 La théorie d'Einstein-Maxwell . . . 124
F.2.3 Le modèle de l'étoile à électrons . . . 124
F.2.4 Le supraconducteur holographique . . . 125
F.3 Systèmes de Bose-Fermi holographiques . . . 126
F.3.1 Modèle . . . 126
F.3.2 Solutions d'étoiles compactes . . . 127
F.3.3 Energie libre . . . 128
F.3.4 Excitations fermioniques de basse énergie . . . 128
F.4 Trous noirs asymptotiquement AdS en supergravité jaugée . . . 129

**Bibliography** **131**

# List of Figures


2.1 Phase diagram of a cuprate material . . . . . 22
2.2 Geometrization of the RG flow . . . . . 25
2.3 Reissner-Nordström black hole . . . . . 29
2.4 Local chemical potential and charge density in the electron star . . . . . 35
2.5 Electron star . . . . . 35
2.6 Free energy of the electron star . . . . . 38
2.7 Holographic superconductor . . . . . 43
2.8 Free energy of the holographic superconductor . . . . . 45

3.1 Scalar hair instability of the electron star . . . . . 50
3.2 Maximum value of the local chemical potential in the holographic superconductor . . . . . 50
3.3 Local chemical potential and charge density in eCS solutions . . . . . 57
3.4 Local chemical potential and charge density in pCS solutions . . . . . 57
3.5 Local chemical potential and charge densities in peCS solutions . . . . . 58
3.6 Free energy of the competing solutions of the Bose-Fermi system (1) . . . . 60
3.7 Free energy of the competing solutions of the Bose-Fermi system (2) . . . . 61
3.8 Phase diagram of the Bose-Fermi system (1) . . . . . 62
3.9 Free energy of the competing solutions of the Bose-Fermi system (3) . . . . 63
3.10 Phase diagram of the Bose-Fermi system (2) . . . . . 64
3.11 Distribution of the electric charge and value of the condensate (1) . . . . . 66
3.12 Distribution of the electric charge and value of the condensate (2) . . . . . 66
3.13 Distribution of the electric charge and value of the condensate (3) . . . . . 67
3.14 Local Fermi momentum in CS solutions . . . . . 70
3.15 Schrödinger potential for eCS and pCS solutions . . . . . 71
3.16 Schrödinger potential for the electron star . . . . . 73
3.17 WKB potential for eCS and peCS solutions . . . . . 76
3.18 Poles of $\mathcal{G}$ for peCS solutions . . . . . 79
3.19 Boundary Fermi momenta for a peCS solution . . . . . 80
3.20 Schematic band structure of (dual of) the compact polarized stars solutions. 86

B.1 Scalar field in the Lifshitz-like hairy electron star . . . . . 110

# Introduction

Originally proposed to explain the arrangement of mesons in Regge trajectories in the late 1960s, string theory became a candidate to the unification of fundamental forces of nature in the early 1980s when it was shown that it was a consistent theory of gravity. In string theory, physics is encoded in a single one-dimensional object, the string, whose vibrations generate all kinds of matter particles and mediating bosons needed for the description of fundamental interactions such as abelian and non-abelian gauge theories, and gravity.

String theory determines uniquely the dimension of spacetime, which turns out to be ten. To recover our four-dimensional spacetime, it is thus necessary to consider string theory on a six-dimensional compact manifold. There is however an infinite number of ways to compactify the theory, and recovering for example the Standard Model of particle physics in the low energy regime is a hard task.

Based on the discovery in 1995 that string theory admits extended objects known as D-branes, a new era has been born in 1997 when Juan Maldacena conjectured that a certain formulation of string theory had an *equivalent* description in terms of an *a priori* unrelated four-dimensional conformal field theory. This conjecture has been quickly generalized to other configurations of string theory and is known as the AdS/CFT correspondence. It relates specific supersymmetric conformal field theories to string theory on a higher-dimensional AdS spacetime.

Beyond the beautiful mathematical structure of the correspondence, the AdS/CFT has proven to be useful for the study of strongly-coupled gauge theories because it provides a dual description in terms of weakly-coupled string theory, i.e. supergravity.

In the AdS/CFT correspondence, supersymmetry and conformality of the field theory can be broken by adding relevant perturbations to the string theory setup, however these models give only qualitative features of realistic field theories such as QCD and quantitative comparison with experiment is difficult. There are however reasons to believe that the AdS/CFT correspondence can be applied to a larger range of theories in a more phenomenological way. This approach is known as the gauge/gravity duality and has been first applied to the study of QCD.

More unexpected, the gauge/gravity duality turns out to be useful to the description of strongly-coupled systems of fermions. Due to strong coupling, these systems do not have a classical limit, but the gauge/gravity duality may provide a dual gravitational description where perturbation theory applies.

In this thesis, we present the applications of the gauge/gravity correspondence both from a string theory approach and a more phenomenological one. In Chapter 1, we review Maldacena's formulation of the AdS/CFT correspondence and discuss its possible generalizations. In Chapter 2, we argue that the ingredients of the AdS/CFT correspondence can be used to study strongly-correlated systems of fermions and we present two fundamental models, the electron star model and the holographic superconductor. In

Chapter 3, we present how these two phenomenological models can be combined to the study of mixture of bosonic and fermionic degrees of freedom in systems at finite density. In Chapter 4, we take a more stringy approach of the correspondence and study black hole solutions in a four-dimensional gauged supergravity theory that can be embedded in M-theory.

Chapters 3 and 4 present the results obtained by the author and collaborators in [1, 2, 3].

# Chapter 1

# The AdS/CFT correspondence

In this chapter we give a brief description of the AdS/CFT correspondence. In its original formulation by Maldacena [4], this is a duality between $\mathcal{N} = 4$ Super Yang-Mills theory in 4 dimensions and type IIB string theory on $AdS_5 \times S^5$.

## 1.1 Large $N$ limit of gauge theories

Yang-Mills theories in four dimensions with gauge group $U(N)$ do not have a dimensionless parameter because the Yang-Mills coupling $g_{YM}$ depends on the Yang-Mills scale $\Lambda_{YM}$ by dimensional transmutation. It results that no clear perturbative expansion can be performed. However, one can consider the rank of the gauge group $N$ as a dimensionless parameter. In the 't Hooft limit [5]

$$N \to \infty\,, \qquad g_{YM} \to 0\,, \qquad \lambda \equiv g_{YM}^2 N \quad \text{fixed}\,, \tag{1.1}$$

where $\lambda$ is the 't Hooft coupling, correlation functions are given by an expansion in $1/N$. For example, the gluon free energy can be written as

$$F = \sum_g N^{2-2g} f_g(\lambda) \tag{1.2}$$

where $g \in \mathbb{N}$ and $f_g$ are functions of the 't Hooft coupling. The expansion (1.2) has in fact a simple geometric interpretation. Each term in the expansion corresponds to the Feynman diagrams which can be drawn on a genus-$g$ Riemann surface. The contribution $f_0$ corresponds to planar diagrams, that can be drawn on the sphere which has genus 0, $f_1$ to the diagrams that can be drawn on the torus, etc. In the large $N$ limit, only planar diagrams survive.

The expansion (1.2) is very similar to the world-sheet expansion of a string. The dominant contribution of the loop expansion of a closed string corresponds to the diagrams having the topology of the sphere and come with a factor $g_s^{-2}$, where $g_s$ is the string coupling constant. More generally, diagrams of genus $g$ contribute to the sting expansion with a factor $g_s^{-2+2g}$. This suggests that the string coupling constant could be identified with the rank of the gauge group,

$$g_s \propto \frac{1}{N}\,. \tag{1.3}$$

The fields in the adjoint representation of the gauge group contribute to the 't Hooft expansion (1.2) with even powers of $1/N$. One can introduce fields in the fundamental

representation of the gauge group. They contribute with odd powers of $1/N$ to the expansion and are suppressed in the large $N$ limit. The expansion is in this case similar to the diagrams of an open string which contribute to the world-sheet expansion with odd powers of $g_s$.

## 1.2 The two pictures of $p$-branes

The similitude between the 't Hooft expansion in Yang-Mills theories and the world-sheet expansion of a string suggests that these two expansions are related. String theory and the AdS/CFT correspondence makes this relation explicit in the case of certain non-abelian conformal field theories and string theory on Anti-de Sitter spacetime. We present here a particular example, the original Maldacena's conjecture [4] that states the equivalence between the $\mathcal{N} = 4$ supersymmetric Yang-Mills theory in 4 dimensions and type IIB string theory on $AdS_5 \times S^5$. The main ingredient of the duality comes from the physics of D$p$-branes, which have two complementary descriptions, in supergravity and string theory.

### 1.2.1 $p$-branes in supergravity

Supergravity theories contain gauge fields of higher rank which generalize the usual potentials of electromagnetism and Yang-Mills theories. These are $p$-forms $C_p$, invariant under generalized gauge transformations. As a particle can be charged under a gauge potential $C_1$ (which is a one-form), supergravity theories admit massive solitonic extended objects which are charged under the potentials $C_{p+1}$. These solutions are called $p$-branes and extend in $p$ space directions plus the time. $p$-branes interact with the gravitational field and the potential $C_{p+1}$ through

$$S_{\text{p-brane}} = \tau \int \mathrm{d}^{p+1}x \, \sqrt{-g} + q \int \mathrm{d}^{p+1}x \, C_{p+1} \,, \tag{1.4}$$

where $\tau$ is the tension of the brane, defined as its energy density in spacetime. The second term generalizes to higher dimensional objets the coupling of a particle to the potential $C_1$. The charge $q$ of the $p$-brane is given by

$$q \propto \int_{S^{8-p}} \star F_{p+2} = N \tag{1.5}$$

where $F_{p+2} = \mathrm{d}C_{p+1}$. Due to the Dirac quantization condition, $N$ is an integer.

Let us focus on the example of type IIB supergravity, which corresponds to the effective description of the massless sector of type IIB string theory. Its bosonic field content is the metric, an antisymmetric tensor $B_{\mu\nu}$, the dilaton $\phi$ and the Ramond-Ramond fields $C_0$, $C_2$ and $C_4$. It admits in particular 3-brane solutions which are charged under the potential $C_4$. When the tension of the brane equals its charge, the 3-brane preserves half of the supersymmetry of the theory. It is thus a BPS object and called an extremal 3-brane. In this case, the 3-brane solution of IIB supergravity is completely determined by an harmonic function $H(u)$ which depends on the radial coordinate $u$ of the directions transverse to the brane. Thanks to supersymmetry, one can also consider a stack of $N$ coinciding 3-branes which will be again specified by an harmonic function. The charge of

each 3-brane under the potential $C_4$ can be taken to be equal to one and the system thus carries a total charge $N$. The solution in this case reads

$$\begin{aligned} \mathrm{d}s^2 &= H^{-1/2}\mathrm{d}x_\mu \mathrm{d}x^\mu + H^{1/2}\mathrm{d}y^2\,, \\ (C_4)_{0123} &= H^{-1}\,, \\ e^\phi &= g_s\,, \\ H(u) &= 1 + \frac{4\pi g_s N \alpha'^2}{u^4}\,, \end{aligned} \tag{1.6}$$

where $g_s$ is the string coupling and $(2\pi\alpha')^{-1}$ the string tension. The directions $y_i$ ($i = 4, \ldots, 9$), with $\mathrm{d}y^2 = (\mathrm{d}u^2 + u^2\Omega_5)$ and $u^2 = \sum_i y_i^2$, are the directions transverse to the branes and $x^\mu$ ($\mu = 0, \ldots, 3$) are the directions of the brane world-volume. The Killing vector $\partial_t$ generating time translations has zero norm at $u = 0$, which is then a Poincaré horizon. This solution has a $SO(1,3) \times SO(6)$ isometry. The tension $\tau$ of the brane is related to its charge, the string coupling and the string tension by

$$\tau = \frac{N}{(2\pi)^3 g_s \alpha'^2}\,, \tag{1.7}$$

which shows the non-perturbative nature of $p$-branes.

### 1.2.2 D$p$-branes in string theory

A great progress has been made by Polchinski who showed that in string theory, $p$-branes have a perturbative description in terms of open and closed strings [6]. D$p$-branes are defined as objects on which open strings can end. They arise when one imposes mixed Dirichlet-Neumann conditions on the open strings: their end-points are restricted to move in a $(p+1)$-dimensional hypersurface of the 10-dimensional spacetime [7]. In the case of a D3-brane, the quantization of the open string leads to a massless spectrum corresponding to a vector multiplet with 16 supercharges. These fields interact with the bulk fields arising from the quantization of the closed string. The effective action of the massless modes of the brane/bulk system is

$$S_{\text{bulk/brane}} = S_{\text{brane}} + S_{\text{int}} + S_{\text{bulk}}\,. \tag{1.8}$$

The brane action $S_{\text{brane}}$, which is defined on the (3+1)-dimensional world-volume, is the action of an abelian gauge theory describing the vector multiplet arising from the quantization of the open string. $S_{\text{bulk}}$ is the effective action of 10-dimensional supergravity with higher order derivative corrections. It can be written as

$$S_{\text{bulk}} \sim \frac{1}{\alpha'^4}\int \mathrm{d}^{10}x\,\sqrt{-g}\,\left[e^{-2\phi}\left(R + 4(\nabla\phi)^2\right) + \cdots + \text{h.d.c.}\right] \tag{1.9}$$

where $R$ is the Ricci scalar, $\phi$ the dilaton, the dots correspond to the action for the other supergravity fields and the 'h.d.c.' contain the higher derivative corrections. $S_{\text{int}}$ is the action describing the interactions between the fields living on the D3-brane and the bulk fields. $S_{\text{int}}$ and the higher derivative corrections appearing in (1.9) come with positive powers of $\alpha'$.

If one stacks $N$ extremal D3-branes together, they do not interact since they are BPS objects. There are in this case $N^2$ kinds of open strings, leading to $N^2$ vector fields and a non-abelian gauge theory on the D3-branes world-volume. The world-volume action is

$$S_{\text{brane}} = \frac{1}{g_s} \int \mathrm{d}^4 x \left( \frac{g_{YM}^2}{4\pi} \mathcal{L}_{YM} + \text{h.d.c.} \right) \tag{1.10}$$

where $\mathcal{L}_{YM}$ is the Lagrangian of $\mathcal{N} = 4$ super Yang-Mills (SYM) theory with gauge group $U(N)$ in 4 dimensions which has 16 real supercharges. The term 'h.d.c.' corresponds to the higher derivative corrections which contribute with positive powers of $\alpha'$. The field content of $\mathcal{N} = 4$ SYM theory is a $U(N)$ gauge field, 6 scalar fields and 4 Weyl fermions. In particular, the 6 scalar fields $\phi^i$ parametrize the position of the D3-branes in the transverse directions, $\phi^i = y^i/\alpha'$.

## 1.3 Decoupling limit

We have presented in the previous sections the two interpretations of D3-branes, as solutions of type IIB supergravity and hypersurfaces on which open string can end. We will see here how the original AdS/CFT correspondence [4] arises when the same decoupling limit is taken on the world-volume of the D3-branes and the backreacted solution.

### 1.3.1 Decoupling of the brane/bulk system

In the limit $\alpha' \to 0$, the action $S_{\text{int}}$ vanishes, the bulk theory becomes free and the world-volume fields decouple from the bulk fields. To preserve all the dynamics of the gauge theory living on the world-volume of the branes, it is necessary to keep the ratio $y^i/\alpha'$ finite. The precise limit to take is

$$\begin{aligned} &\alpha' \to 0\,, \\ &g_s \quad \text{fixed}\,, \\ &N \quad \text{fixed}\,, \\ &\phi^i = \frac{y^i}{\alpha'} \quad \text{fixed}\,. \end{aligned} \tag{1.11}$$

In this limit, the brane action thus reduces to the action of $\mathcal{N} = 4$ $U(N)$ SYM theory since all higher order derivatives are suppressed. The comparison of the Lagrangian of $\mathcal{N} = 4$ $U(N)$ SYM theory with the brane action leads to the identification of the string coupling with the Yang-Mills gauge coupling through

$$g_{YM}^2 = 4\pi g_s\,. \tag{1.12}$$

The limit (1.11) means in particular that we are zooming on the near-brane region.

### 1.3.2 Near-brane geometry of 3-branes

D3-branes are also solutions of type IIB supergravity, where the metric, the potential $C_4$ and the dilaton are given by (1.6). In the limit $\alpha' \to 0$ together with the requirement

that the energy measured by an asymptotic observer is finite, i.e. $u/\alpha'$ is kept fixed, the metric becomes

$$\mathrm{d}s^2 = \left(\frac{L^2}{u^2}\mathrm{d}u^2 + \frac{u^2}{L^2}\mathrm{d}x_\mu \mathrm{d}x^\mu\right) + L^2\Omega_5\,, \tag{1.13}$$

which is the metric of $AdS_5 \times S^5$ which both have radius $L$ with

$$L^4 = 4\pi g_s N \alpha'^2\,. \tag{1.14}$$

The potential $C_4$ is

$$(C_4)_{0123} = \frac{u^4}{L^4} \tag{1.15}$$

and we have

$$\int_{S^5} F_5 = N\,. \tag{1.16}$$

On this side, the limit $\alpha' \to 0$ and $u/\alpha'$ fixed is again a decoupling limit, because it decouples the near-brane geometry from the asymptotically flat spacetime at infinity.

The space $AdS_5$ is the maximally symmetric solution of Einstein equations in 5 dimensions with a negative cosmological constant. In Euclidean signature, it corresponds to a 5-dimensional hyperboloid with isometry $SO(1,5)$. The $AdS_5$ space can be defined as an immersed hypersurface in $\mathbb{R}^{2,4}$ with equation

$$X_0^2 + X_5^2 - X_1^2 - X_2^2 - X_3^2 - X_4^2 = L^2\,, \tag{1.17}$$

from which it is evident that the isometry group of $AdS_5$ is $O(2,4)$. $AdS_5$ spacetime has a conformal boundary with topology $S^1 \times \mathbb{R}^3$.

It is useful to consider the universal cover of $AdS_5$ to have not-closed timelike curves. The term in parentheses in (1.13) corresponds to the metric of $AdS_5$ on the Poincaré patch (see e.g. [8]). In Poincaré coordinates, for each value of the radius $u$ the spacetime is isomorphic to 4-dimensional Minkowski space. Moreover, the conformal boundary, situated at $u = \infty$, is $\mathbb{R}^{1,3}$. The subgroup $SO(1,3) \times SO(1,1)$ of the isometry group $O(2,4)$ of $AdS_5$ is manifest in Poincaré coordinates, as can be seen from (1.13).

While the decoupling limit on the side of the brane/bulk system decouples completely the stringy excitations from the world-volume theory, on the bulk side the gravitational theory admits higher-derivative terms in the action and stringy corrections, which means that the correspondence is between $\mathcal{N} = 4$ SYM theory and the full type IIB string theory on $AdS_5 \times S^5$.

## 1.4 Tests and properties of the correspondence

We have obtained two descriptions of the near-brane region. One is $\mathcal{N} = 4$ SYM theory and the other is type IIB string theory on $AdS_5 \times S^5$. Maldacena conjectured that these two theories were equivalent in the sense that they are different descriptions of the same physics. Even if the correspondence is only a conjecture, there are reasons to believe that it holds.

### 1.4.1 Strong/weak duality

The parameters on the two sides match naturally. $\mathcal{N} = 4$ SYM has two dimensionless parameters, the rank of the gauge group $N$ and the 't Hooft coupling $\lambda$, which match to the parameters of the string theory, the string coupling $g_s$ and the inverse string tension $\alpha'$, through

$$\begin{aligned} 4\pi g_s &= \frac{\lambda}{N}\,, \\ \frac{L^2}{\alpha'} &= \sqrt{\lambda}\,. \end{aligned} \tag{1.18}$$

We see that taking the limit $g_s \to 0$ where the strings are non-interacting on the string theory side corresponds to taking $N \to \infty$ while keeping $\lambda$ fixed on the field theory. So indeed, the 't Hooft limit (1.1) corresponds to the planar limit of string theory. If in addition the massive string modes are suppressed, i.e.

$$g_s \to 0\,, \qquad \frac{\alpha'}{L^2} \to 0\,, \tag{1.19}$$

type IIB string theory reduces to type IIB supergravity, which corresponds to taking

$$N \to \infty\,, \qquad \lambda \to \infty\,, \tag{1.20}$$

in the field theory. We conclude that the AdS/CFT correspondence is a strong-weak duality.

The $1/N$ corrections map to $g_s$ corrections in the string theory, i.e. considering string amplitudes beyond the planar limit. On the other hand, the $1/\lambda$ corrections in the field theory correspond to considering $\alpha'$ corrections on the gravity side, i.e. taking into account higher derivative corrections in the supergravity action.

The regime $\lambda \to 0$ and fixed $N$ can be interpreted as a definition for quantum gravity: in this case the field theory is manageable using perturbative methods.

### 1.4.2 Matching symmetries

A first hint that we have an equivalence between these two theories is the matching of symmetries, the symmetry $PSU(2,2|4)$ is realized on the sides. This pattern will be very general, global symmetries in the gauge theory map to isometries of the string theory.

It is believed that $\mathcal{N} = 4$ $SU(N)$ SYM theory is conformal to all orders, meaning that it is a conformal field theory (CFT). The conformal group in 4 dimensions is $SO(4,2)$ and contains the Poincaré symmetries together with the dilatations and the special conformal transformations. By adding the discrete symmetry $x^a \to x^a/x^2$, $\mathrm{d}x^2 \to x^2\mathrm{d}x^2$, it forms the group $O(4,2)$. $\mathcal{N} = 4$ $SU(N)$ SYM theory is supersymmetric, thus the conformal group in 4 dimensions $O(4,2)$ is enhanced by adding the generators of the R-symmetry group $SU(4)_R$ and the conformal supercharges, which are required to close the algebra. The resulting superconformal group is $PSU(2,2|4)$.

The conformal group $O(4,2)$ of $\mathcal{N} = 4$ SYM maps to the isometry group of $AdS_5$. Also, the R-symmetry group $SU(4)_R$ is isomorphic to the isometry group $SO(6)$ of the $S^5$. The field theory contains 16 supercharges plus the 16 conformal supercharges. On the gravity side, type IIB string theory has 16 supersymmetries, but supersymmetry is enhanced on the maximal supersymmetric background $AdS_5 \times S^5$ leading to 32 supersymmetries.

For example, the subgroup $SO(1,3)$ of the isometry group $O(4,2)$ of $AdS_5$ corresponds to the Lorentz group of the field theory. Also, the subgroup $SO(1,1)$ maps to the dilatation transformations in the field theory. They are realized in the bulk by

$$u \to \lambda u\,, \qquad x^\mu \to \frac{x^\mu}{\lambda}\,. \tag{1.21}$$

We can thus roughly identify the radial coordinate $u$ with the energy scale $E$ of the dual field theory,

$$u \sim E\,. \tag{1.22}$$

The near-boundary bulk region $u \to \infty$ will then be identified with the UV regime of the field theory while the near-horizon region $u \to 0$ represents the IR regime.

### 1.4.3 Matching the spectrum

Contrary to usual relativistic theories where particles are identified by their mass and their Lorentz quantum numbers, as for example their spin, a representation of the (super) conformal group contains states with arbitrary energy, because the mass is not a Casimir of the (super) conformal algebra. The observables are the chiral and non-chiral primary operators, which are specified by their conformal dimension $\Delta$, their Lorentz quantum numbers and their R-symmetry quantum numbers when supersymmetry is present. The chiral primary operators are not renormalized because they are protected by the superconformal algebra, and their conformal dimension is given by their canonical dimension.

In the case of $\mathcal{N}=4$ $SU(N)$ SYM theory, the chiral primaries are composite operators of the elementary fields of the vector multiplet. These protected operators form chiral multiplets, also called short multiplets, which are annihilated by half of the supercharges. A chiral multiplet admits operators with spin up to two, and the lowest state is a scalar transforming in the symmetric traceless representation of rank $k$ of the R-symmetry group $SU(4)_R$. It can be shown that the only single-trace chiral multiplets of $\mathcal{N}=4$ $SU(N)$ SYM theory are generated by the operator

$$\mathrm{Tr}\,\phi_{i_1}\dots\phi_{i_k}\,. \tag{1.23}$$

These chiral multiplets are indexed by the integer $k$ and noted $A_k$. The other operators belonging to $A_k$ are obtained by applying supersymmetric transformations on the scalar operator (1.23), which has conformal dimension given by $\Delta = k$. An important short multiplet is $A_2$, the supermultiplet of conserved currents which are the stress-energy tensor, the supercharges and the $SU(4)_R$ R-current. They are obtained by applying supersymmetry transformations on the operator $\mathrm{Tr}\,\phi_1\phi_2$.

On the other hand, the non-chiral primaries get renormalized and have an anomalous dimension, the conformal dimension is not protected by supersymmetry. They correspond to multi-trace operators and form non-chiral multiplets, also called large multiplets. The lowest state is a multi-trace scalar operator.

Thus, the single-trace operators of $\mathcal{N}=4$ SYM theory form chiral multiplets $A_k$, whose lowest states are scalar with conformal dimension $\Delta = k \in \mathbb{N}$. In fact, the chiral multiplets map on the gravity side to the Kaluza-Klein (KK) modes arising from the dimensional reduction of the 10d string massless modes on the 5-sphere.

The 10d massless bulk fields can be decomposed on the spherical harmonics of $S^5$. The resulting 5d fields form short multiplets $A'_k$ of the superconformal algebra, labelled

by an integer $k \geq 2$. The lowest state of each short multiplet $A'_k$ is a scalar with mass $m^2 = k(k-4)/L^2$.

Thus, there exists a short multiplet of the superconformal group both in the field theory ($A_k$) and the gravitational theory ($A'_k$) for all $k \geq 2$. For a given $k$, the two short multiplets contain fields with the same Casimirs, which are the quantum numbers and the conformal dimension $\Delta$. On the string theory side, the Casimir $C_2 = \Delta$ is related to the mass of the KK mode. The relation $\Delta(m)$ is for a single-trace scalar operator

$$L^2 m^2 = \Delta(\Delta - 4) \quad \Longleftrightarrow \quad \Delta = 2 \pm \sqrt{4 + L^2 m^2}\,. \tag{1.24}$$

For a field with different Lorentz representation than a scalar, the mass-dimension relation changes, it is given for fields up to spin two in [8].

For example, $A'_2$ is the graviton multiplet, which contains in particular an $SO(6)$ gauge field and the 5-dimensional metric. These map respectively to the $SU(4)_R \simeq SO(6)$ R-current and the stress-energy tensor of the short multiplet $A_2$ in the field theory. This is coherent with the matching of the isometry of $AdS_5$ and the conformal group $O(4,2)$.

This mapping also applies to the 5d fields resulting from the dimensional reduction of the string massive modes on the 5-sphere, which organize in non-chiral multiplets of the superconformal group. These 5d fields have a mass $m^2 \sim 1/\alpha'$. Again, there is a one-to-one correspondence between a 5d field and a CFT non-chiral primary which have the same Casimirs. For a scalar, the mass-dimension relation is given by (1.24).

In the supergravity limit (1.19), the stringy modes are not protected because $\Delta \sim \lambda^{1/4}$ and they decouple from the KK modes. This maps in the field theory to the decoupling of the non-chiral primaries from the chiral primaries in the limit (1.20).

We should precise that the correspondence is between $\mathcal{N} = 4$ SYM theory with gauge group $SU(N)$ and type IIB string theory on $AdS_5 \times S^5$. Indeed, the gauge group $U(N)$ is isomorphic to $U(1) \times SU(N)$. The factor $U(1)$ corresponds to the center of mass of the $N$ D3-branes and is irrelevant on the gravity side. The duality thus applies for the field theory gauge group $SU(N)$ corresponding to the dynamics of the D3-branes.

Due to the non-zero curvature of $AdS_5$, there is no scale separation between the KK modes with $k = 2$ and $k > 2$. However, it is possible to write an action for the graviton multiplet $A'_2$, which is the $\mathcal{N} = 8$ gauged supergravity in five dimensions. This theory is believed to be a consistent truncation of type IIB string theory on $AdS_5 \times S^5$ in the sense that every classical solution of the 5d theory can be uplifted to a solution in the 10d theory.

## 1.5 Partition function and correlation functions

The AdS/CFT correspondence states the equality of the partition functions of the two theories. Even if it is believed that this equality holds for the whole string theory, it becomes manageable in the supergravity limit (1.19), where the partition function of string theory is given in the saddle point approximation by the on-shell supergravity action. As we shall see, in this limit it is possible to compute correlation functions of the strongly-coupled boundary field theory by studying physics in the bulk. The equality of the generating functions was originally stated in Euclidean signature [9] and we shall present it now[1].

[1]The AdS/CFT correspondence states more generally the equivalence between specific CFTs in $d$ dimensions and string theory on $AdS_{d+1}$. For this reason, we will keep the dimension of the CFT arbitrary.

We make the change of variable $u = L^2/r$ such that the metric of $AdS_{d+1}$ on the Poincaré patch is now given by

$$\mathrm{d}s^2 = \frac{L^2}{r^2}\left(\mathrm{d}r^2 + \mathrm{d}t^2 + \mathrm{d}\vec{x}^2\right) \tag{1.25}$$

in Euclidean signature. The conformal boundary of $AdS_{d+1}$ is now situated at $r = 0$.

Let us consider a single-trace operator $\mathcal{O}$ of the $\mathrm{CFT}_d$. One can introduce a source $\mathcal{S}$ for the operator $\mathcal{O}$. The Euclidean action of the field theory becomes

$$S_{\mathrm{CFT}} \longrightarrow S_{\mathrm{CFT}} + \int \mathrm{d}^d x\, \mathcal{S}(x)\mathcal{O}(x)\,. \tag{1.26}$$

For example, the source of the stress-energy tensor of the CFT is the metric deformation. It is introduced by adding the term

$$\int \mathrm{d}^d x\, g^{\mathrm{CFT}}_{\mu\nu} T^{\mu\nu} \tag{1.27}$$

to the CFT action. Since the CFT stress-energy tensor and the bulk metric have the same quantum numbers, it is natural to consider the source $g^{\mathrm{CFT}}_{\mu\nu}$ as the value of the bulk metric on the conformal boundary of $AdS_{d+1}$. In fact, this applies to all the single-trace operators as we shall see now.

In the regime (1.20) where the CFT is strongly-coupled, the gravitational theory is type IIB supergravity on $AdS_5 \times S^5$. In this regime, a bulk field $\Psi$ is given by its classical solution $\Psi_{\mathrm{cl}}$ which satisfies in general a second-order differential equation. By imposing regularity at infinity, close to the UV boundary the bulk field $\Psi$ behaves on the background $AdS_{d+1}$ geometry as

$$\Psi_{\mathrm{cl}}(x, r) \sim \Psi_-(x)\, r^{\Delta_-} + \Psi_+(x)\, r^{\Delta_+}\,, \qquad r \to 0\,. \tag{1.28}$$

The exponents $\Delta_\pm$ verify $\Delta_+ > \Delta_-$ and depend on the mass and the quantum numbers of $\Psi$. The exponent $\Delta_+ \equiv \Delta$ is the conformal dimension of the operator $\mathcal{O}$ in the CFT. The first and second terms in (1.28) correspond to non-normalizable and normalizable modes, respectively, in the sense that the effective action for $\Psi_-\, r^{\Delta_-}$ and $\Psi_+\, r^{\Delta_+}$ is respectively divergent and finite. There are cases where both terms are normalizable but we leave this case for later considerations. The leading term $\Psi_-$ in (1.28) is identified with the source of the dual field operator $\mathcal{O}$ through

$$\mathcal{S}(x) = \lim_{r\to 0} r^{-\Delta_-}\Psi_{\mathrm{cl}}(x, r) = \Psi_-(x)\,. \tag{1.29}$$

The UV boundary condition $\mathcal{S} = \Psi_-$ can be chosen freely, contrary to the regularity condition imposed at infinity.

We have now a correspondence between the single-trace operators of $\mathrm{CFT}_d$ and the fields living on $AdS_{d+1}$. The AdS/CFT correspondence goes beyond. Its fundamental statement is the equality of the partition functions of the two theories which can be written as

$$\left\langle e^{-\int \mathrm{d}^d x\, \mathcal{S}(x)\mathcal{O}(x)} \right\rangle_{\mathrm{CFT}} = Z_{\mathrm{sugra}}\left[ r^{-\Delta_-}\Psi_{\mathrm{cl}}(x, r)\big|_{r\to 0} = \mathcal{S}(x)\right]\,. \tag{1.30}$$

The left-hand side is the partition function $Z_{\rm CFT}$ of the field theory, where the source $\mathcal{S}$ is arbitrary. The right hand side is the partition function of the supergravity theory, given by the saddle-point approximation

$$Z_{\rm sugra}[\Psi] \simeq e^{-S[\Psi_{\rm cl}]}\,, \tag{1.31}$$

where $S[\Psi_{\rm cl}]$ is the supergravity action evaluated on the classical (on-shell) solution $\Psi_{\rm cl}$, which has the asymptotic behaviour (1.28) close to the UV boundary. Because the bulk spacetime has a boundary and the classical solution expansion (1.28) admits a non-normalizable mode, the on-shell action is in general divergent and needs to be regularized and renormalized. All the divergences of the on-shell action can be cancelled by adding covariant local boundary counterterms determined by the near-boundary behaviour of bulk fields. This procedure is called holographic renormalization [10] (see [11] for a review). Thus, one should replace the classical action in (1.31) by the renormalized, on-shell action $S_{\rm ren}[\Psi_{\rm cl}]$. It is related to the generating functional $W_{\rm CFT} = \log Z_{\rm CFT}$ of the connected correlation functions of the field theory by

$$W_{\rm CFT}[\Psi_-] = -S_{\rm ren}[\Psi_-]\,. \tag{1.32}$$

One can therefore compute connected correlation functions of the single-trace operators of the strongly-coupled CFT theory by taking derivatives of the renormalized on-shell action $S_{\rm ren}$ with respect to the source $\Psi_-$.

The Euclidean connected $n$-point function is then given by

$$\langle \mathcal{O}(x_1)\dots\mathcal{O}(x_n)\rangle = -\left.\frac{\delta^n S_{\rm ren}[\Psi_-]}{\delta\Psi_-(x_1)\dots\delta\Psi_-(x_n)}\right|_{\Psi_-=0}\,. \tag{1.33}$$

To obtain the correlation functions (1.33), one has to compute first the classical solution for the field $\Psi$ in the supergravity theory by solving its field equation. This equation is typically a second order differential equation in the radial coordinate $r$, the solution then involves two functions which depend only on the field theory coordinates $x^\mu$ and asymptotes to (1.28) close to the boundary. One has therefore to impose two boundary conditions on $\Psi_{\rm cl}$. The condition to impose in the near-horizon region is regularity. In the UV, the boundary condition consists in choosing the leading term in the asymptotic solution (1.28), which corresponds to fixing the source $\Psi_-$ in the dual field theory. In most cases, one computes the correlation functions at vanishing source, as in (1.33), which corresponds to choosing the UV boundary condition

$$\Psi_{\rm cl}(x,r) \sim \Psi_+(x)\, r^{\Delta_+}\,, \qquad r\to 0\,. \tag{1.34}$$

This gives the spectrum of the field theory. One can also compute the correlation functions in the presence of a source by choosing (freely) the UV boundary condition.

To compute explicitly the one and two-point functions, one can introduce the renormalized canonical momentum conjugate to the classical solution $\Psi_{\rm cl}$,

$$\Pi_{\rm ren} = \frac{\delta S_{\rm ren}[\Psi_{\rm cl}]}{\delta\Psi_{\rm cl}}\,. \tag{1.35}$$

The one-point function for finite source $\Psi_-$ is therefore given by

$$\langle \mathcal{O}(x)\rangle_{\Psi_-} = -\frac{\delta S_{\rm ren}[\Psi_{\rm cl}]}{\delta\Psi_-(x)} = -\lim_{r\to 0} r^{\Delta_-}\Pi_{\rm ren}(x,r)\,. \tag{1.36}$$

Considering correlation functions at finite source for an operator is also useful to probe the features of a system. One can indeed compute the response of the system to the application of an external source. In the linear response theory, the one-point function $\langle\mathcal{O}\rangle_{\Psi_-}$ is proportional in momentum space to the external source $\Psi_-$,

$$\langle\mathcal{O}(\omega_E,\vec{k})\rangle_{\mathcal{S}} = G_E(\omega_E,\vec{k})\,\Psi_-(\omega_E,\vec{k})\,, \tag{1.37}$$

where the constant of proportionality is the two-point function $G_E(\omega_E,\vec{k})$. Here, $\omega_E$ is the Euclidean frequency. Using (1.37), we then obtain from (1.36) the two-point function

$$G_E(\omega_E,\vec{k}) = \frac{\langle\mathcal{O}(\omega_E,\vec{k})\rangle_{\Psi_-}}{\Psi_-(\omega_E,\vec{k})} = -\lim_{r\to 0} r^{2\Delta_-}\,\frac{\Pi_{\rm ren}}{\Psi_{\rm cl}}\,. \tag{1.38}$$

As we will see on the example of a scalar operator later, the one-point function is in general proportional to the normalizable mode in the UV expansion (1.28),

$$\langle\mathcal{O}(x)\rangle_{\Psi_-} \propto \Psi_+(x)\,. \tag{1.39}$$

Consequently, the two-point function is given in momentum space by the ratio between the normalizable and the non-normalizable modes,

$$G_E(\omega_E,\vec{k}) \propto \frac{\Psi_+(\omega_E,\vec{k})}{\Psi_-(\omega_E,\vec{k})}\,. \tag{1.40}$$

The two-point function has a pole precisely where the source $\Psi_-$ vanishes, that is when we impose the normalizability condition to the bulk field $\Psi$. This corresponds to computing the spectrum of the Euclidean gravitational theory, i.e. the normal modes.

Let us now give the example of a bulk gauge field, which maps to a conserved current in the field theory.

### $U(1)$ current

If the $d$-dimensional CFT contains a global $U(1)$ symmetry, it admits a conserved $U(1)$ current $J^\mu$. The dual gravitational theory must then contain a $U(1)$ gauge field $A = A_a \mathrm{d}x^a$ dual to $J^\mu$. To compute correlation functions of $J^\mu$ in the strongly-coupled regime of the CFT, one shall consider fluctuations of the bulk gauge field $A_a$. The radial component of the bulk gauge field $A_r$ can be set to zero by a $U(1)$ gauge transformation. Close to the UV boundary, the on-shell gauge field behaves as

$$A_\mu \sim B_\mu + \langle J_\mu\rangle\, r^{d-2}\,, \qquad r\to 0\,. \tag{1.41}$$

Herein, $\langle J_\mu\rangle$ is the vacuum expectation value of the boundary conserved $U(1)$ current and $B_\mu$ its source. Notice that for $p$-forms, the subleading term does not give directly the conformal dimension of the operator. Indeed, if one considers a bulk scale transformation $x^\mu \to \lambda x^\mu$, $r\to\lambda r$, the transformed gauge field is

$$A_a(x,r) \to \tilde{A}_a(x,r) = \lambda^{-1} A_a(x/\lambda, r/\lambda)\,. \tag{1.42}$$

Using (1.41), it means that the boundary conserved current and its source transform as $\tilde{J}^\mu(x,r) = \lambda^{1-d} J^\mu(x/\lambda, r/\lambda)$ and $\tilde{B}_\mu(x,r) = \lambda^{-1} B_\mu(x/\lambda, r/\lambda)$, so the conserved current has dimension $\Delta = d-1$. The $U(1)$ gauge symmetry which acts as

$$A_a \to A_a + \partial_a \Lambda(x,r) \tag{1.43}$$

in the bulk translates in the boundary CFT to

$$\int \mathrm{d}^d x\, B_\mu J^\mu = \int \mathrm{d}^d x\, [B_\mu + \partial_\mu \Lambda]\, J^\mu \,, \tag{1.44}$$

which means that indeed the boundary $U(1)$ current $J^\mu$ is conserved. This is a very important feature of the AdS/CFT correspondence: global symmetries of the CFT map to gauge symmetries in the bulk. We have already obtained this result for the original AdS/CFT correspondence: for example, the $SO(6)$ gauge symmetry in type IIB supergravity maps to the $SU(4)_R$ R-symmetry group of $\mathcal{N} = 4$ SYM theory.

### 1.5.1 Free scalar field in AdS

We have given in the previous section the general procedure to compute Euclidean correlation functions of single-trace operators in the strongly-coupled regime of $\mathrm{CFT}_d$ which admit a gravitational dual. In this section, we give the explicit example of a single-trace scalar operator, which is dual to a scalar field in the bulk.

The action for a neutral free scalar field $\varphi$ in Euclidean $AdS_{d+1}$ spacetime is

$$S_{\mathrm{gra}} = \frac{L^{1-d}}{2} \int \mathrm{d}^d x\, \mathrm{d}r \sqrt{g} \left( g^{ab} \partial_a \varphi \partial_b \varphi + m^2 \varphi^2 \right) \tag{1.45}$$

where $g_{ab}$ is the metric of Euclidean $AdS_5$ spacetime (1.25) and $m$ is the mass of the scalar field. In momentum space, the equation of motion for $\varphi$ is the Klein-Gordon equation

$$r^{1+d} \partial_r \left[ r^{1-d} \partial_r \varphi(k,r) \right] - \left[ m^2 L^2 + k^2 r^2 \right] \varphi(k,r) = 0 \tag{1.46}$$

where $k^2 \equiv \delta_{\mu\nu} k^\mu k^\nu$. Close to the AdS boundary, it reduces to

$$r^2 \varphi''(k,r) + (1-d)\, r\, \varphi'(k,r) - m^2 L^2 \varphi(k,r) = 0 \tag{1.47}$$

where primes denote derivatives with respect to the radial coordinate $r$. The asymptotic behaviour of $\varphi$ is then

$$\varphi(k,r) \sim \varphi_-(k)\, r^{d-\Delta} + \varphi_+(k)\, r^{\Delta} \,, \qquad r \to 0 \,, \tag{1.48}$$

where

$$\Delta = \frac{d}{2} + \nu \,, \qquad \nu \equiv \sqrt{m^2 L^2 + d^2/4} \,, \tag{1.49}$$

and $\varphi_\pm(k)$ are arbitrary functions of $k$. If $m^2 < -d^2/4L^2$ the Hamiltonian is not bounded below and the system is unstable. In the following we will only consider fields which satisfy the Breitenlohner-Freedman (BF) bound [12, 13]

$$m^2 \geq -\frac{d^2}{4L^2} \,. \tag{1.50}$$

One can check that for

$$m^2 L^2 \geq -\frac{d^2}{4} + 1 \,, \tag{1.51}$$

the modes $\varphi_-(k)\, r^{d-\Delta}$ and $\varphi_+(k)\, r^{\Delta}$ are respectively non-normalizable and normalizable in the sense that the effective action for $\varphi_-(k)\, r^{d-\Delta}$ and $\varphi_+(k)\, r^{\Delta}$ is respectively divergent and finite. Following the above discussion on the field/operator correspondence, we can already identify the non-normalizable mode $\varphi_-$ as the source of a dual scalar operator $\mathcal{O}$. We will show below that $\varphi_+$ is indeed the one-point function – vev – of $\mathcal{O}$.

We will now show that $\Delta$ appearing in the UV expansion (1.48) of the bulk field $\varphi$ is the conformal dimension of the operator $\mathcal{O}$. Under a scale transformation $x^\mu \to \lambda x^\mu$ and $r \to \lambda r$, the transformed field is

$$\tilde{\varphi}(\lambda x, \lambda r) = \varphi(x, r)\,. \tag{1.52}$$

In terms of the normalizable and non-normalizable modes, we thus have

$$\tilde{\varphi}(x, r) = \varphi_-\left(\frac{x}{\lambda}\right) \lambda^{\Delta-d}\, r^{d-\Delta} + \varphi_+\left(\frac{x}{\lambda}\right) \lambda^{-\Delta}\, r^{\Delta} \tag{1.53}$$

$$\equiv \tilde{\varphi}_-(x)\, r^{d-\Delta} + \tilde{\varphi}_+(x)\, r^{\Delta}\,, \tag{1.54}$$

where $\tilde{\varphi}_-(x) = \lambda^{-\Delta_-}\varphi_-\left(\frac{x}{\lambda}\right)$ and $\tilde{\varphi}_+(x) = \lambda^{-\Delta_+}\varphi_+\left(\frac{x}{\lambda}\right)$. Then, the dimensions of the fields $\varphi_-$ and $\varphi_+$ are respectively $d-\Delta$ and $\Delta$ and the conformal dimension of the operator $\mathcal{O}$ is equal to $\Delta$. We recover here the mass-dimension relation (1.24) for a scalar operator. The scalar operator $\mathcal{O}$ is respectively relevant and irrelevant for $d/2+1 \leq \Delta < d$ and $\Delta > d$. These two cases correspond respectively to $-d^2/4+1 \leq L^2m^2 < 0$ and $L^2m^2 > 0$. The marginal operator ($\Delta = d$) is represented by a massless scalar field in the bulk. On the other hand, when the mass satisfies

$$-\frac{d^2}{4} \leq m^2L^2 < -\frac{d^2}{4} + 1\,, \tag{1.55}$$

the two modes are normalizable and one can impose the standard (alternative) boundary condition by choosing the source to be $\varphi_-$ ($\varphi_+$, respectively). They correspond respectively to operators with dimension $d/2 \leq \Delta < d/2+1$ and $d/2-1 < \Delta \leq d/2$ [14].

To compute the one and two-point functions of the operator $\mathcal{O}$, we need to evaluate the bulk action (1.45) on the solution to the field equation (1.46). Performing an integration by parts and using the field equation for $\varphi$, the action (1.45) becomes

$$S_{\rm gra} = \frac{L^{1-d}}{2} \int \frac{\mathrm{d}^d k}{(2\pi)^d}\, \mathrm{d}r\, \partial_r \left[\sqrt{g}\, g^{rr} \varphi(-k, r) \partial_r \varphi(k, r)\right]\,. \tag{1.56}$$

To deal with the UV divergences, we introduce a UV cutoff $\epsilon \ll 1$ and send it to zero at the end of the computation. By imposing regularity at infinity, the action is therefore

$$\begin{aligned} S_{\rm gra} &= -\frac{1}{2} \int_{r=\epsilon} \frac{\mathrm{d}^d k}{(2\pi)^d}\; r^{-d+1} \varphi(-k, r)\, \partial_r\, \varphi(k, r) \\ &= -\frac{1}{2} \int_{r=\epsilon} \frac{\mathrm{d}^d k}{(2\pi)^d}\; \left[(d-\Delta)\, \varphi_-(-k)\varphi_-(k)\, r^{-2\nu} + d\, \varphi_-(-k)\varphi_+(k)\right]\,, \end{aligned} \tag{1.57}$$

evaluated at $r = \epsilon$. The first term in Eq. (1.57) contains divergences. To cancel these divergences, we introduce the counter-term

$$S_{\rm ct} = \frac{1}{2} \int_{r=\epsilon} \frac{\mathrm{d}^d k}{(2\pi)^d}\, (d-\Delta)\, \varphi(-k, r)\varphi(k, r)\, r^{-d} \tag{1.58}$$

and obtain the renormalized action

$$S_{\rm ren} = S_{\rm gra} + S_{\rm ct} = -\frac{1}{2}\int \frac{\mathrm{d}^d k}{(2\pi)^d}\, 2\nu\, \varphi_-(-k)\varphi_+(k)\,. \tag{1.59}$$

The on-shell renormalized action is then a functional of the two functions $\varphi_-$ and $\varphi_+$. In the standard quantization scheme, the former is the source for the operator $\mathcal{O}$ and will be used to obtain correlation functions. On the other hand, one must impose regularity at infinity, in the interior of the bulk spacetime. By solving explicitly the field equation (1.46) for $r \in [0, \infty[$ in Fourier space, the IR boundary condition fixes the ratio $\chi(k) = \varphi_+(k)/\varphi_-(k)$. We finally obtain

$$S^{(E)}_{\rm ren} = -\frac{1}{2}\int \frac{\mathrm{d}^d k}{(2\pi)^d}\, 2\nu\, \chi(k)\, \varphi_-(-k)\varphi_-(k)\,. \tag{1.60}$$

Following the general discussion above, it is now easy to obtain the one-point function

$$\langle \mathcal{O}(k)\rangle_{\varphi_-} = -\frac{\delta S^{\rm ren}_{\rm gra}[\varphi_-]}{\delta\varphi_-(-k)} = 2\nu\, \varphi_+(k)\,, \tag{1.61}$$

and the two-point function

$$G_E(k) = -\frac{\delta^2 S^{\rm ren}_{\rm gra}[\varphi_-]}{\delta\varphi_-(-k)\,\delta\varphi_-(k)} = 2\nu\, \frac{\varphi_+(k)}{\varphi_-(k)}\,, \tag{1.62}$$

which is consistent with Eq. (1.40). In the present case where the spacetime is pure $AdS_{d+1}$, the solution to (1.46) is analytic and given in terms of Bessel functions. One can then obtain explicitly the function $\chi(k)$ (see e.g. [15]),

$$\chi(k) = \frac{\Gamma(-\nu)}{\Gamma(\nu)}\left(\frac{k}{2}\right)^{2\nu}\,. \tag{1.63}$$

In real space, one recovers the two-point function of a CFT scalar operator,

$$\langle \mathcal{O}(x)\mathcal{O}(x')\rangle \propto \frac{1}{(x-x')^{2\Delta}}\,. \tag{1.64}$$

## 1.6 Generalizations

The original AdS/CFT correspondence states the equivalence between a specific 4d CFT and a string theory on $AdS_5$ spacetime. An other well-established correspondence is the ABJM theory [16] which states the equivalence between $\mathcal{N} = 6$ Chern-Simons-matter theories, which are 3d CFTs, and M-theory on $AdS_4$ times a 7-dimensional compact manifold. More generally, the AdS/CFT correspondence relates $d$-dimensional CFTs ($\mathrm{CFT}_d$) to physics in $AdS_{d+1}$ spacetime. The details of each correspondence (spectrum, symmetries, ...) arise from the two interpretations of D-branes and M-branes in string theory and M-theory.

The correspondence we presented relates physics in $AdS_{d+1}$ to $\mathrm{CFT}_d$ at zero temperature. If we take the example of $\mathcal{N} = 4$ SYM, this is because the D3-branes we considered were extremal. Non-extremal D3-branes lead on the gravity side to the presence of a non-extremal black hole. The Euclidean spacetime is regular at the event horizon if the

Euclidean time is periodically identified with a period equals to $1/T$, where $T$ is the Hawking temperature of the black hole. This is similar to the procedure applied to study field theories at finite temperature. The Hawking temperature is thus identified with the temperature of the field theory. In the AdS/CFT correspondence, a non-extremal black hole maps to a finite temperature state of the dual field theory [9, 17]. Also, from the equality of the partition functions of the two dual theories, the equilibrium properties of the field theory states are given by the black hole thermodynamics.

Interesting features of a thermal field theory are the close to equilibrium physics and dissipative dynamics. To study the linear response of a thermal system using the AdS/CFT correspondence, it is necessary to be able to compute the Lorentzian Green's functions to study the response of the thermal system to the application of an external source. A prescription to compute correlation functions in Lorentzian signature is known and shares many features with the one to compute Euclidean correlation functions (see Section 1.5). One has to solve the field equation of the bulk field dual to the operator that we want to compute the correlation functions. As for the Euclidean prescription, the UV boundary condition corresponds to choosing the source of the dual field theory operator. However, the bulk geometry is not regular anymore in the IR because of the presence of a black hole event horizon. Two boundary conditions can be imposed: the 'in-going' and the 'out-coming' wave conditions. They lead respectively to retarded and advanced Green's functions. To study dissipation phenomena, one must impose the in-going wave condition. The procedure to compute Lorentzian correlation functions is presented in Appendix A.

Also, when the CFT contains a global $U(1)$ symmetry, one can turn on a chemical potential $\mu$ for the associated conserved current $J^\mu$. Since the chemical potential can be interpreted as a source for the conserved current, it is natural to consider $\mu$ as the UV asymptotic value of the time component of the $U(1)$ gauge field dual to $J^\mu$. It means that there is a radial electric field in the bulk.

Finite temperature and finite chemical potential are simply implemented in the AdS-Reissner-Nordström black hole that we will present in Chapter 2. It is a solution of type IIB supergravity on $AdS_5 \times S^5$ and will be essential for the considerations of this thesis.

Conformal invariance of $\mathcal{N} = 4$ SYM means on the gravity side that the metric is $AdS_5 \times S^5$. Considering other embeddings than the simple flat D3-brane setup will deform the AdS spacetime. This corresponds to turning on relevant operators in the boundary CFT. Non-extremal D3-brane configurations, which lead to finite temperature in the dual field theory, also break conformal invariance.

$\mathcal{N} = 4$ SYM contains only fields in the adjoint representation of the gauge group $SU(N)$. It is possible to introduce matter fields which belong to the fundamental representation of $SU(N)$ by considering a stack of D7-branes in addition to the D3-branes [18]. The modes of the strings stretched between a D3-brane and a D7-brane are dual to fields in the fundamental representation of the gauge group, the 'quarks', while strings attached to D7-branes represent quark-antiquark operators or 'mesons'.

In the AdS/CFT correspondence, one can see the field theory as living on the (conformal) boundary of the AdS spacetime. In this sense, the AdS/CFT correspondence is a realization of the holographic principle, which states that the entire information of a volume of space is encoded on its boundary [19, 20]. In the following, we shall sometimes use the word 'holography' to refer to the AdS/CFT correspondence and its generalizations.

# Chapter 2

# Holography for condensed matter physics

In this chapter we show how the AdS/CFT correspondence and its ingredients can be used in a more phenomenological approach to study strongly-coupled field theories which are neither supersymmetric nor conformal, with particular emphasis to systems of fermions. We present two fundamental setups, the electron star and the holographic superconductor models which are believed to describe a non-Fermi liquid and a non-BCS superconductor, respectively.

## 2.1 Systems of fermions at finite density

Many materials can be described by the techniques of quantum field theory. For example, metals are gapless systems where, in the thermodynamic limit, there are excited states of arbitrary low energy since an electric current is created by applying an arbitrary small electric field. The low energy spectrum is insensitive to the details of the short distance problem, one can thus integrate out the short distance degrees of freedom – forget about the lattice – and the high energy interactions and obtain by the renormalization group (RG) procedure an effective quantum field theory describing the low energy physics. The elementary electrons receive corrections and the low energy degrees of freedom are 'dressed electrons'. While the elementary electrons are strongly-coupled in general, for a large range of metals, it happens that the dressed electrons are not strongly-correlated but rather behave as almost free particles, due to resummation of the short distance strong interactions.

These metals are well-described by the Landau's Fermi liquid theory. This theory admits that the system of dressed electrons is adiabatically connected to the gas of free electrons. The distribution of electrons is described by Fermi-Dirac statistics, the ground state is given by filling all the low energy single-particle states. The highest energy state filled has momentum $k = k_F$, called the Fermi momentum[1]. The excitations, which occur around $k = k_F$, are gapless since they can have arbitrary low energy $\omega$. The surface $k = k_F$ is called the 'Fermi surface', it is a $(d-1)$-dimensional sphere in momentum space for a $d$-dimensional system. The excitations around the Fermi surface are weakly-coupled and have a long lifetime.

Near the Fermi surface ($k \ll k_F$), the retarded Green's function for the dressed electron

[1] We consider here rotational-invariant systems.

operator is

$$G_R(\omega, k) = \frac{Z}{\omega - \frac{k_F}{m_\star}(k - k_F) - i\Sigma_2} \tag{2.1}$$

where $\Sigma_2$ is the imaginary part of the electron self-energy $\Sigma$, $k_F$ the Fermi momentum, $m_\star$ the renormalized mass of the electrons and $Z \leq 1$ the spectral weight. The renormalized mass $m_\star$ is not equal to the electron mass in general. Particle-like and hole-like excitations correspond respectively to adding and removing an electron to the system. The spectral function $A(\omega, k) = \mathrm{Im}\, G_R(\omega, k)$ is given by

$$A(\omega, k) = Z\, \frac{\Gamma_k}{[\omega - \frac{k_F}{m_\star}(k - k_F)]^2 + \Gamma_k^2} \tag{2.2}$$

where the spectral weight $Z$ and the width $\Gamma_k = -Z\Sigma_2$ characterize the low energy excitations (resonances).

For a Fermi liquid, the width behaves as

$$\Gamma_k \sim \frac{1}{k_F}(k - k_F)^2 \tag{2.3}$$

close to the Fermi surface and the energy of excitation is

$$\epsilon(k) \sim \frac{k_F}{m_\star}(k - k_F)\,. \tag{2.4}$$

So the width $\Gamma_k$ of the quasiparticle tends to zero much faster that the energy of excitation $\epsilon(k)$ when one approaches the Fermi surface, i.e. $\Gamma_k \ll \epsilon(k)$. The excitations have thus a long lifetime $1/\Gamma_k$. The Green's function in real space is

$$G_R(t, k) \sim Z\, e^{-i\epsilon(k)t - \Gamma_k t}\,, \tag{2.5}$$

which indeed corresponds to an excitation weakly damped. The excitations near the Fermi surface are thus weakly-coupled and called 'quasiparticles'. The spectral weight $Z$ can be smaller than one but remains finite. The rest of the spectral weight $1 - Z$ corresponds to high energy incoherent excitations having a short lifetime. Notice that the quasiparticles carry the same charge as the elementary electrons. Landau's Fermi liquid theory and perturbative methods have been successfully applied to describe most metals. An important feature of Fermi liquids is that their resistivity increases quadratically with temperature,

$$\rho \sim T^2\,. \tag{2.6}$$

Fermi liquids are examples of systems at finite density. These systems have a global $U(1)$ symmetry and one can associate a finite chemical potential to it. In the case of a Fermi liquid, the chemical potential $\mu$ is equal to $k_F^2/m_\star$ and fixes the average number of particles in the system through the Luttinger theorem, which relates the particle density to the volume enclosed by the Fermi surface [21, 22]. Since the number of particles in the system is not fixed – the low energy excitations correspond to adding or removing

electrons – we work in the grand canonical ensemble, i.e. at fixed chemical potential and temperature.

The $U(1)$ symmetry can be for instance the electromagnetic gauge symmetry. The dressed electrons are charged under the $U(1)$ electromagnetic gauge field which can be considered as non-dynamical at low energy because the electromagnetic coupling is typically small and the electromagnetic interaction is screened by the charged medium. The only remaining fields are the dressed electrons, there are no photons. The system has thus a global – rather than local – $U(1)$ symmetry.

The same approach in terms of quasiparticles has been used to describe the onset of superconductivity by BCS-type pairing [23, 24]. Close to the Fermi surface, the quasiparticles interact with phonons – the vibrations of the lattice – and an effective attraction between quasiparticles emerges. This attraction allows the formation of pairs of dressed electrons, the Cooper pairs. They have spin zero and carry twice the electric charge of the electrons. The $U(1)$ symmetry is thus spontaneously broken. Even if superconductivity is strictly speaking explained by the spontaneous breaking of a local $U(1)$ symmetry, as we discussed above this invariance reduces to a global $U(1)$ group when the electric field is screened.

Superconductivity can be onset in many materials by modifying their atom structure. In the field theory approach, it means that we are modifying the chemical potential. The interaction of the fermions with the phonons translates into the presence of an effective four-point interaction between the quasiparticles in the action. In the superconducting phase, the low energy excitations are gapped by an energy equals to the binding energy of the Cooper pairs.

The Landau's Fermi liquid theory for the description of metals is based on the existence of weakly-coupled degrees of freedom at low energy. However, when the system is strongly-coupled, it can happen that the width $\Gamma_k$ is not much smaller than the energy of excitation $\epsilon(k)$ and the low energy excitations have a short lifetime. These systems still admit a Fermi surface because the low energy excitations are gapless, but the dressed electrons do not behave as quasiparticles and the Landau's Fermi liquid description breaks down since the system is not adiabatically connected to the free gas.

There are systems of fermions which exhibit a quantum phase transition together with the lack of quasiparticle-like excitations at low energy. A quantum phase transition is a phase transition which is not driven by temperature as in a thermal phase transition but by a parameter, as for example doping. At the quantum critical point, one typically observes that the energy of fluctuations around the ground state vanishes and the coherence length diverges with scaling properties. The system has consequently an emergent scaling symmetry

$$t \to \lambda^z \, t \,, \qquad x \to \lambda \, x \,, \tag{2.7}$$

where time and space can scale differently. The system is also invariant under rotations, and space and time translations. All together, this forms the Lifshitz group. The dynamical critical exponent $z$ can be equal or larger than one. When $z = 1$, the system is also invariant under Lorentz boosts and special conformal transformations and the symmetry group is enhanced to the relativistic conformal group [25]. For $z > 1$, if the system is also invariant under Galilean boosts, the symmetry in enhanced to the Schrödinger

group. In this case, the system is effectively described by a non-relativistic conformal field theory [25].

The quantum critical point, which is at absolute zero temperature, extends to a quantum critical region where quantum fluctuations are negligible compared to thermal fluctuations. In this region, the system is described by a critical field theory at finite temperature.

The boson Hubbard model with filling fraction one is an example of a quantum critical system [26, 25]. The bosonic particles occupy sites of a squared lattice and can jump from one site to the nearby ones. There is also a repulsive interaction between nearest neighbours. By varying the intensity of this interaction, the system exhibits a superfluid-insulator quantum phase transition which is effectively described by the $O(2)$ vector model. In the superfluid phase, the $SO(2)$ symmetry is broken and the order parameter, the bosonic field, acquires a vacuum expectation value, i.e. it condenses.

However, the Landau-Ginzburg-Wilson paradigm does not hold for 'deconfined' quantum critical systems. In this case, different symmetries are broken in each phase and there is no order parameter which gets a vacuum expectation value in only one of the two phases. Close to a deconfined quantum critical point, the low energy degrees of freedom interact with emergent critical bosonic modes which become massless at the quantum critical point. The critical bosonic modes can be for instance spin density waves or emergent gauge fields. For systems of fermions, an emergent $U(1)$ gauge symmetry can arise from fractionalization of the dressed electrons which split into a spin and a charge degrees of freedom [27]. The dressed electrons can thus be seen as bound states invariant under the emergent $U(1)$ gauge symmetry. When fractionalization occurs in a fermionic system, the Luttinger count is violated.

From the experimental point of view, an interesting class of materials are the cuprates, which are based on a two-dimensional lattice of copper anions together with cations. Cuprates have a rich phase diagram, given in Figure 2.1. They develop in particular high-

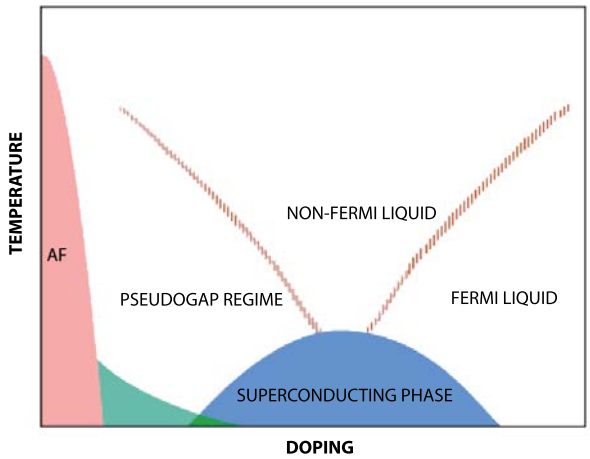


Figure 2.1: Phase diagram of a cuprate material. At small doping, the system is in an antiferromagnetic (AF) phase. In the pseudogap regime, the Fermi surface is gapped only in certain points of momentum space. The non-Fermi liquid phase above the superconducting phase is believed to result from a quantum critical point hidden by the superconducting dome.

Tc superconductivity as has been shown for the first time in 1986 for the oxyde-based

cuprate $La_{2-x}Ba_xCuO_4$ [28]. $x$ represents here hole doping. As can be seen in Figure 2.1, at small doping cuprates are in an anti-ferromagnetic phase. In the pseudogap phase, the Fermi surface is gapped in certain points of momentum space. This is due to the fact that around these points there are very few allowed electronic states. Above the superconducting phase, the system is metallic but is not described by Landau's Fermi liquid theory. It has been found (see e.g. [29] for a review) that in this 'strange metal' phase, the resistivity is linear in the temperature,

$$\rho \sim T\,, \tag{2.8}$$

while it is quadratic for Fermi liquids. This suggests that in addition to the electronic low energy excitations, there are other degrees of freedom which scatter the current-carrying fermions. They must be bosonic because the fermions cannot scatter efficiently close to the Fermi surface [27]. The additional degrees of freedom may come from the fractionalization of the dressed electrons close to a deconfined quantum critical point. This is a reason to believe that under the superconducting dome there is a quantum critical point with a quantum critical region corresponding to the strange metal region.

In cuprates, the onset of superconductivity from the strange metal phase is ill-understood. This is due to the presence of strong interactions at low energy together with a possible fractionalization of the charge carriers. Also, because of strong coupling, the effective action describing the quantum critical system is difficult to find because perturbative methods do not apply. The AdS/CFT correspondence and its extensions offers a new approach to overcome these difficulties. Since many condensed matter systems live effectively in $2+1$ dimensions at low energy as it is the case for cuprates, we will be interested in the study of $(2+1)$-dimensional field theories.

## 2.2 Bottom/up approach to the AdS/CFT correspondence

We have seen in Chapter 1 that the AdS/CFT correspondence was useful to study strongly-coupled conformal field theories with a large number of degrees of freedom, i.e. the rank $N$ of the gauge group is large. The dual string theory reduces in this limit to supergravity. Thus, using the saddle point approximation, one can compute observables in the CFT using the equality of generating functions and the AdS/CFT dictionary between bulk field and CFT single-trace operators.

In the previous section we have seen that there exist systems of fermions at finite density which admit a large number of strongly-coupled degrees of freedom at low energy. They thus share common features with the CFTs accessible from the AdS/CFT correspondence. However supersymmetry is not present in these systems and relativistic conformality may emerge at the critical point (for instance for graphene at vanishing chemical potential, see e.g. [30]) but many quantum critical systems have an emergent scaling symmetry where space and time scale differently, i.e. the dynamical exponent $z$ is different from one (see Eq. (2.7)).

To apply the holographic techniques to the study of strongly-coupled systems of fermions, we will assume that the AdS/CFT correspondence applies not only to top/down models arising from string theory, but also to simple gravitational setups which do not require an UV completion as string theory. Such systems are easier to construct than the top/down models. They do not involve supersymmetry, and the dual field theory is not

a conformal field theory in general. Thus, we assume the correspondence:

| | | |
|---|---|---|
| Large $N$ strongly-coupled field theory in $d$ dimensions | $\Longleftrightarrow$ | Classical gravitational theory on asymptotically-$AdS_{d+1}$ space. |

In the top/down AdS/CFT setups, finite temperature in the CFT arises naturally when one considers non-extremal D-branes. On the gravity side, it means that the spacetime admits an event horizon, i.e. it contains a black hole. Also, because the R-symmetry group contains in general a $U(1)$ subgroup, the CFT can be put at finite density for this $U(1)$ by considering supergravity backgrounds involving a radial electric flux. These two features will be important for the applications of holography to condensed matter. In particular, they will require the presence of a gauge field in the gravitational theory. Thus, we will be more particularly interested in Einstein's gravity coupled to gauge fields and matter fields.

The simplest gravitational setup to consider for the applications of the gauge/gravity duality to condensed matter is 4d Einstein-Maxwell theory with a negative cosmological constant, which has action

$$S = \int \mathrm{d}^4x\sqrt{-g}\left[\frac{1}{2\kappa^2}\left(R + \frac{6}{L^2}\right) - \frac{1}{4e^2}F_{ab}F^{ab}\right] + S_{\mathrm{bdry}} \tag{2.9}$$

where $F = \mathrm{d}A$ is the field strength of the $U(1)$ gauge field $A$, $R$ is the Ricci scalar, $\kappa$ is Newton's constant, $L$ is the asymptotic $AdS_4$ length and $e$ is the $U(1)$ coupling. The cosmological constant is given by $\Lambda = -3/L^2 < 0$. The term $S_{\mathrm{bdry}}$ represents the Gibbons-Hawking term and the counterterms necessary for the holographic renormalization. The Einstein equations resulting from the action (2.9) are

$$R_{ab} - \frac{1}{2}g_{ab}R - \frac{3}{L^2}g_{ab} = \kappa^2\, T^{\mathrm{Mxwl.}}_{ab} \tag{2.10}$$

where the stress-energy tensor of the gauge field is

$$T^{\mathrm{Mxwl.}}_{ab} = \frac{1}{e^2}\left(F_{ac}F_b{}^c - \frac{1}{4}g_{ab}F_{cd}F^{cd}\right) . \tag{2.11}$$

The Maxwell equations are

$$\nabla_a F^{ba} = 0\,. \tag{2.12}$$

We will see in the following that coupling the Einstein-Maxwell theory (2.9) to matter fields leads to interesting holographic models for the study of condensed matter systems such as non-Fermi liquids and superconductors. We will focus on field theories which preserve spacetime rotations and translations, we thus make the homogeneous and isotropic ansatz

$$\mathrm{d}s^2 = L^2\left[-f(r)\mathrm{d}t^2 + g(r)\mathrm{d}r^2 + \frac{1}{r^2}\left(\mathrm{d}x^2 + \mathrm{d}y^2\right)\right] , \qquad A = \frac{eL}{\kappa}h(r)\mathrm{d}t\,, \tag{2.13}$$

for the metric and the gauge field. We have fixed the radial dependence of the metric components $g_{xx}$ and $g_{yy}$ to $L^2/r^2$ by a diffeomorphism transformation and $A_r = 0$ by a gauge transformation.

In Section 1.4.2 we have identified the radial coordinate of $AdS$ spacetime as the energy scale of the dual field theory. We will be here interested in the low energy regime of strongly-coupled systems of fermions. For this reason, we will mainly focus on the interior region of spacetime (IR region) rather than the near-boundary region (UV). However, to apply the ingredients of the AdS/CFT correspondence, we will demand that the spacetime is asymptotically $AdS$ close to the boundary.

Thus, we require that in the UV ($r \to 0$) the metric is that of $AdS_4$,

$$\mathrm{d}s^2 = \frac{L^2}{r^2}\left(-\mathrm{d}t^2 + \mathrm{d}r^2 + \mathrm{d}x^2 + \mathrm{d}y^2\right) , \tag{2.14}$$

i.e. $f(r) \sim g(r) \sim r^{-2}$ for $r \to 0$. However we will allow the field theory to have a non-trivial renormalization group flow, the geometry will be deformed from the UV $AdS_4$ in the interior region of the bulk spacetime. If $g(r) \neq r^{-2}$, the metric (2.13) breaks the bulk scale invariance (1.21) and the field theory is not conformal. In addition, if $f(r) \neq r^{-2}$, the field theory is non-relativistic, i.e. it breaks Lorentz invariance. The bulk 4-dimensional theory can thus be seen as a continuous family of 3d field theories. These theories, each defined at an energy scale, are related by the RG flow, encoded in the metric of the bulk spacetime.

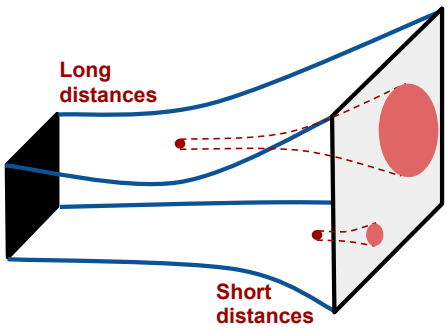


Figure 2.2: Geometrization of the RG flow. UV physics of the field theory is controlled by near-boundary region while IR physics corresponds to the interior region. Figure taken from [27] with consent of the author.

As discussed in Section 1.6, the chemical potential of the boundary field theory is the asymptotic value of the time component of the bulk gauge field close to the boundary. From (1.41) it is also natural to consider the subleading term as related to the conserved $U(1)$ charge of the field theory. Together with the asymptotic $AdS_4$ spacetime condition, we will thus consider solutions of the Einstein-Maxwell theory (2.9) coupled to matter fields which satisfy the UV asymptotics

$$r \to 0 : \qquad f(r) \sim \frac{1}{r^2} , \qquad g(r) \sim \frac{1}{r^2} , \qquad h(r) \sim \hat{\mu} - \hat{Q} r , \tag{2.15}$$

where $\hat{Q}$ is the density of the boundary conserved $U(1)$ charge and $\hat{\mu}$ the associated chemical potential.

Using the ingredients of the AdS/CFT correspondence, we will assume that a gauge-invariant operator of the quantum field theory is dual to a bulk classical field with the same quantum numbers. Again, the conformal dimension of the field theory operator in

the UV CFT maps to the mass of the bulk field. We will thus assume the field/operator correspondence:

| | | |
|---|---|---|
| Field theory gauge-invariant operator $\mathcal{O}$ with spin $s$ and conformal dimension $\Delta$ | $\Longleftrightarrow$ | Gravitational classical field $\Psi$ with spin $s$ and mass $m(\Delta)$. |

For a given gravitational theory, each solution to the bulk field equations will correspond to a state of the dual field theory. When several bulk solutions exist, one must compute the free energy by computing the on-shell action to determine which solution is thermodynamically favoured. We thus have the mapping:

| | | |
|---|---|---|
| State of the field theory | $\Longleftrightarrow$ | Solution to the bulk field equations. |

The observables of the field theory will be obtained by considering the equality of the generating functions of the two dual theories and by applying the prescription to compute correlation functions in Euclidean and Lorentzian signatures (see Section 1.5 and Appendix A).

## 2.3 The AdS-Reissner-Nordström black hole

Einstein-Maxwell theory (2.9) admits an analytic asymptotically $AdS_4$ solution corresponding to a black hole with charge, the AdS-Reissner-Nordström (RN) black hole. The metric is

$$\mathrm{d}s^2 = L^2\left[-f(r)\mathrm{d}t^2 + \frac{1}{r^4 f(r)}\mathrm{d}r^2 + \frac{1}{r^2}\left(\mathrm{d}x^2+\mathrm{d}y^2\right)\right] \tag{2.16}$$

where

$$f(r) = \frac{1}{r^2}\left[1 - \frac{1}{r_+^3}\left(1+\frac{r_+^2\hat{\mu}^2}{2}\right)r^3 + \frac{\hat{\mu}^2}{2r_+^2}r^4\right], \tag{2.17}$$

and the gauge field

$$h(r) = \hat{\mu}\left(1-\frac{r}{r_+}\right). \tag{2.18}$$

At $r = r_+$, the metric component $g_{tt}$ vanishes and the surface $r = r_+$ is infinitely redshifted for an asymptotic observer, which means that the bulk spacetime contains a black hole in the interior with an event horizon with topology $\mathbb{R}^3$ situated at $r = r_+$. To ensure regularity of the gauge field at the event horizon, the constant term in $A_t$ cannot be chosen arbitrarily and is fixed such that $h(r_+) = 0$.

The Hawking temperature [31] of a black hole is obtained by requiring that the Euclidean metric is regular at the horizon. It is the case if one identifies the Euclidean time

$$t_E \sim t_E + 1/T \tag{2.19}$$

where the temperature of the RN black hole is

$$T = \frac{1}{4\pi r_+}\left(3 - \frac{r_+^2\hat{\mu}^2}{2}\right) . \tag{2.20}$$

In Euclidean signature, the holographically dual field theory lives on $\mathbb{R}^4$ where the Euclidean time coordinate $t_E$ is periodically identified by (2.19). It is therefore natural to consider the Hawking temperature of the RN black hole as the temperature of the dual field theory. Also, the parameter $\hat{\mu}$ is identified as the boundary chemical potential from (2.15). The RN black hole is then dual to a field theory state at finite temperature and finite chemical potential.

The introduction of scales, the temperature and the chemical potential, in the boundary CFT breaks the conformal invariance: the gravitational theory is not anymore invariant under the rescaling (1.21) because the bulk spacetime is $AdS_4$ only when one approaches the UV boundary. Indeed, the field theory dual to the RN black hole corresponds to a CFT deformed by two scales, the chemical potential $\hat{\mu}$ and the temperature $T$. By performing the rescalings

$$t \to r_+\, t\,, \qquad r \to r_+\, r\,, \qquad \vec{x} \to r_+\, \vec{x}\,, \qquad \hat{\mu} \to \frac{\hat{\mu}}{r_+}\,, \tag{2.21}$$

$r_+$ can be eliminated from the solution (2.16-2.18). However it remains the free parameter $\hat{\mu}$. This means that a CFT deformed by two scales as a temperature and a chemical potential can only depend on the ratio of them, $T/\hat{\mu}$. The temperature (2.20) vanishes continuously for $r_+ = \sqrt{6}/\hat{\mu}$. This condition corresponds to the extremal limit of the RN black hole.

The bulk gauge field is dual to the conserved $U(1)$ current $J^\mu$ of the field theory. The leading behaviour $\hat{\mu}$ of the time component of the bulk gauge field in the UV is identified with the boundary chemical potential. The subleading term in (2.18) is proportional to the vev of the current operator $J^t$, that is the conserved total charge density of the field theory, which is simply the charge density of the RN black hole,

$$\hat{Q} = \frac{\kappa}{eL}\frac{1}{V_2}\int_{V_2} \star F = \frac{\hat{\mu}}{r_+}\,, \tag{2.22}$$

where $V_2 = \int \mathrm{d}x\, \mathrm{d}y$ is the spatial volume in field theory units.

It is easy to obtain the equilibrium properties – the thermodynamics – of the field theory by computing the Euclidean action

$$S^{(E)} = -\int \mathrm{d}^4x\sqrt{g}\left[\frac{1}{2\kappa^2}\left(R + \frac{6}{L^2}\right) + \frac{1}{4e^2}F_{ab}F^{ab}\right] + \frac{1}{2\kappa^2}\int_{r=0}\mathrm{d}^3x\sqrt{\gamma}\left(-2K + \frac{4}{L}\right) \tag{2.23}$$

on the classical solution. The last term is the sum of the Gibbons-Hawking term, necessary for spacetimes with a boundary to have a well-defined variational problem, and a counterterm for the on-shell action to be finite. Herein, $\gamma_{\mu\nu}$ is the induced metric on the boundary $r = 0$ and $K$ the trace of the extrinsic curvature. In the grand canonical ensemble, the grand potential density $\Omega = -(T/V_2)\log Z^{(E)}_{\mathrm{FT}}$ (which we will call the free energy) is obtained from the Euclidean bulk action evaluated on the solution (2.16)-(2.18). The free energy is then given by

$$\hat{\Omega} = -\frac{1}{2r_+^3}\left(1 + \frac{r_+^2\hat{\mu}^2}{2}\right) \tag{2.24}$$

where we have rescaled the free energy, $\Omega = \frac{L^2}{\kappa^2}\hat{\Omega}$. The thermodynamic quantities are now easily obtained from the free energy (2.24). In particular, the charge density is[2]

$$\hat{Q} = -\frac{\partial\hat{\Omega}}{\partial\hat{\mu}} = \frac{\hat{\mu}}{r_+}\,, \tag{2.25}$$

as anticipated in (2.22). The entropy density is given by

$$\hat{S} = -\frac{\partial\hat{\Omega}}{\partial T} = \frac{2\pi}{r_+^2}\,, \tag{2.26}$$

compatible with the area law since

$$\frac{1}{4G_N}\frac{A_2}{V_2} = \frac{L^2}{\kappa^2}\frac{2\pi}{r_+^2} = S\,, \tag{2.27}$$

where $G_N = \kappa^2/8\pi$ is Newton's constant, $A_2 = L^2V_2/r_+^2$ is the area of the event horizon and $\hat{S} = \frac{\kappa^2}{L^2}S$ the rescaled entropy density. Also, the ADM mass of the black hole is given by

$$\hat{M} = \frac{1}{r_+^3}\left(1 + \frac{r_+^2\hat{\mu}^2}{2}\right) \tag{2.28}$$

and the first law

$$\hat{\Omega} = \hat{M} - T\hat{S} - \hat{\mu}\hat{Q} \tag{2.29}$$

holds.

At zero temperature, the solution reduces to the extremal Reissner-Nordström (ERN) black hole. In this case it is useful to write the function $f$ appearing in (2.16) and the gauge field $h$ as

$$f(r) = \frac{1}{r^2}\left(1 - \hat{M}r^3 + \frac{\hat{Q}^2}{2}r^4\right)\,, \qquad h(r) = \hat{\mu} - \hat{Q}r\,, \tag{2.30}$$

where the mass, the charge and the chemical potential are given in terms of $r_+$ by

$$M = \frac{4}{r_+^3}\,, \qquad \hat{Q} = \frac{\sqrt{6}}{r_+^2}\,, \qquad \hat{\mu} = \frac{\sqrt{6}}{r_+}\,. \tag{2.31}$$

The free energy

$$\hat{\Omega} = \hat{M} - \hat{\mu}\hat{Q} \tag{2.32}$$

of the extremal Reissner-Nordström black hole is simply given by

$$\hat{\Omega} = -\frac{1}{3\sqrt{6}}\hat{\mu}^3\,. \tag{2.33}$$

[2]To compute the thermodynamic quantities, one has to see $r_+$ as a function of the temperature and the chemical potential through (2.20).

It is also interesting to notice that the near horizon geometry ($r \to r_+$) of the ERN black hole is

$$\mathrm{d}s^2 \sim \frac{L^2}{6\rho^2}\left(-\mathrm{d}t^2 + \mathrm{d}\rho^2\right) + \frac{L^2}{r_+^2}\left(\mathrm{d}x^2 + \mathrm{d}y^2\right) , \qquad h(\rho) \sim \frac{1}{\sqrt{6}\,\rho} , \tag{2.34}$$

where we have introduced the new variable

$$\rho \equiv \frac{r_+^2}{6(r_+ - r)} . \tag{2.35}$$

This is the geometry of $AdS_2 \times \mathbb{R}^2$ with $AdS_2$ radius equals to $L/\sqrt{6}$. At finite temperature, it can be shown easily (see e.g. [32]) that in the near-horizon region, the metric becomes a black hole in $AdS_2 \times \mathbb{R}^2$.

The Einstein-Maxwell theory and the RN black hole solution is the simplest holographic setup that one can consider to study field theories at finite charge density. The finite charge density maps to the non-trivial electric flux $F_{rt}$ in the bulk, sourced by the charged black hole, as shown in Figure 2.3.

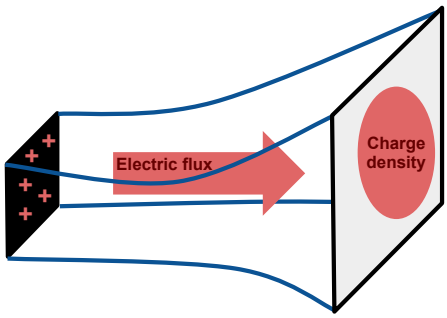


Figure 2.3: The finite charge density of the field theory is represented in the bulk by an electric flux sourced by the charged event horizon of the RN black hole. Figure taken from [27] with consent of the author.

However this model suffers from two main issues. First, at zero temperature, the black hole entropy is non-zero, which suggests that the dual field theory state is degenerate. Second, the finite density is sourced by the charged black hole, there are no matter fields in the bulk. It means that the field theory does not exhibit any gauge-invariant operator and matter is not visible. So where are the low energy fermionic degrees of freedom of the system ? The point is that the fermions are subject to fractionalization, a common process in condensed matter that we discussed in Section 2.1. It was suggested in [33] that the RN black hole could be seen as dual to a totally fractionalized state.

These issues suggest that the RN black hole may be unstable to the formation of matter in the bulk. It has already been shown that low temperature charged AdS black holes are unstable towards many processes, including the formation of a fluid of charged fermions and the condensation of charged scalar fields. This has led to two of the most important holographic models for condensed matter physics that we present and combine in this thesis, the electron star and the holographic superconductor.

We end this section by noticing that the AdS-Schwarzschild black hole obtained from the RN black hole by setting $\hat{\mu} = 0$ is also a solution to the Einstein-Maxwell theory (2.9).

In this case the gauge field is trivial and the black hole is neutral. However, the free energy at fixed temperature of this solution is always larger than that of the RN black hole, so the latter is always thermodynamically favoured. At zero temperature, pure $AdS_4$ (2.14), obtained by setting $\hat{\mu} = 0$ together with the additional condition $r_+ \to \infty$, is also a solution to Einstein-Maxwell theory but it is not favoured because its free energy vanishes. For these reasons, we will not consider these solutions here.

## 2.4 The electron star model

To study non-Fermi liquids with the tools of holography, one needs to introduce fermionic matter in the gravitational theory, which will be dual to the low energy dressed electrons in the quantum critical system. This requires to go beyond the simple Einstein-Maxwell theory, since the RN black hole does not exhibit fermionic degrees of freedom.

The simplest way to introduce fermions in the bulk theory is to consider them as probe fields in the RN black hole (see e.g. [34, 35, 32, 36, 37, 38]). However, to study properties of quantum critical systems, it would be useful to obtain a completely backreacted holographic system with fermionic degrees of freedom. This task is very difficult in principle since fermions cannot be treated classically. However, it is possible to consider the bulk fermions in a 'local Fermi gas approximation' – or Thomas-Fermi approximation – where the set of bulk fermions is treated as an ideal fluid. This was done in a seminal paper by Hartnoll and Tavanfar [39].

### 2.4.1 Action and field equations

Let us consider Einstein-Maxwell theory (2.9) with a negative cosmological constant coupled to a perfect fluid of charged fermions of mass $m_f$ and charge $q_f$ under the gauge group $U(1)$. The fluid contributes to Einstein and Maxwell equations, obtained from the action (2.9), through its stress tensor

$$T^{\text{fluid}}_{ab} = (\rho + p)u_a u_b + p g_{ab} \tag{2.36}$$

and its electromagnetic current

$$J^a_{\text{fluid}} = q_f n u^a \,, \tag{2.37}$$

where $\rho$ is the energy density, $p$ the pressure, $n$ the particle density and $u^a$ the velocity of the fluid normalized so that $u_a u^a = -1$. Einstein equations are

$$R_{ab} - \frac{1}{2} g_{ab} R - \frac{3}{L^2} g_{ab} = \kappa^2 \left( T^{\text{Mxwl.}}_{ab} + T^{\text{fluid}}_{ab} \right) \tag{2.38}$$

where the stress-energy tensor of the gauge field is given by (2.11). Maxwell equations are

$$\nabla_a F^{ba} = e^2 J^a_{\text{fluid}} \,. \tag{2.39}$$

The fluid is a free gas of relativistic fermions at zero temperature in 3+1 dimensions. The local chemical potential $\widetilde{\mu}_l$ for particle number is defined as the tangent frame of the gauge field through the relation

$$\widetilde{\mu}_l = q_f u^a A_a \,, \tag{2.40}$$

it is assumed to be positive for all $q_f$ (positive or negative). This relation is valid only if all the fermionic matter is charged under the $U(1)$ gauge field, which we shall consider later on.

The fluid quantities satisfy the zero-temperature equation of state

$$-p(\widetilde{\mu}_l) = \rho(\widetilde{\mu}_l) - \widetilde{\mu}_l\, n(\widetilde{\mu}_l) \tag{2.41}$$

where the pressure, energy density and charge density are obtained from the local chemical potential $\widetilde{\mu}_l$ by the free gas construction as if the fluid was living in flat space,

$$\rho(\widetilde{\mu}_l) = \int_{m_f}^{\widetilde{\mu}_l} \mathrm{d}\epsilon\, \Theta(\epsilon - m_f)\, \epsilon\, g(\epsilon)\,, \qquad n(\widetilde{\mu}_l) = \int_{m_f}^{\widetilde{\mu}_l} \mathrm{d}\epsilon\, \Theta(\epsilon - m_f)\, g(\epsilon)\,, \tag{2.42}$$

where the density of states at energy $\epsilon$ is

$$g(\epsilon) = \beta\, \epsilon \sqrt{\epsilon^2 - m_f^2} \tag{2.43}$$

and $\Theta$ the Heaviside step function. Notice that $\rho$ and $n$ are positive for $m_f < \widetilde{\mu}_l$ and vanish otherwise. The phenomenological parameter $\beta$ is related to the spin of the constitutive fermions, for spin half fermions $\beta = \pi^{-2}$. All the physics of the fermions is then controlled by the local chemical potential. Instead of working with $n$ and $\widetilde{\mu}_l$, we introduce the charge density

$$\sigma = q_f n \tag{2.44}$$

and the chemical potential for charge density

$$\mu_l = \frac{\widetilde{\mu}_l}{q_f}\,, \tag{2.45}$$

which have the same sign as $q_f$.

As for Einstein-Maxwell theory, we make the homogeneous and isotropic ansatz (2.13). The velocity has then non-zero component $u^t = 1/(L\sqrt{f})$ and the local chemical potential for charge density is a function of the radial coordinate only and given by

$$\mu_l(r) = \frac{e}{\kappa} \frac{h(r)}{\sqrt{f(r)}}\,. \tag{2.46}$$

The classical fluid description, analogous to the Thomas-Fermi approximation, is valid if the local chemical potential $\mu_l$ varies slowly in the radial direction, $\partial_r \mu_l(r) \ll \mu_l(r)^2$, such that the fluid is in local equilibrium at any value of the radial coordinate. This requires the fermions to be at high enough density and their Compton wavelength to be smaller than the characteristic scale of the geometry. The fermion physics it then completely encoded in the metric and the gauge field through the functions $f$ and $h$.

Since we are working in a semi-classical gravity approximation which takes into account the backreaction of the matter fields on the geometry, we must have $\kappa/L \ll 1$ and the left-hand side and the right-hand side of Einstein equations (2.38) must be comparable. It implies that

$$e^2 \sim \frac{\kappa}{L} \ll 1\,. \tag{2.47}$$

One can rescale the fields and parameters to eliminate $e$, $\kappa$ and $L$ from the field equations. We do so by defining hatted quantities through

$$\begin{aligned} \frac{m_f}{|q_f|} &= \frac{e}{\kappa}\hat{m}_f\,, \qquad \beta q_f^4 = \frac{\kappa^2}{e^4L^2}\hat{\beta}\,, \\ \rho = \frac{1}{\kappa^2L^2}\hat{\rho}\,, \qquad p &= \frac{1}{\kappa^2L^2}\hat{p}\,, \qquad \sigma = \frac{1}{e\kappa L^2}\hat{\sigma}\,. \end{aligned} \tag{2.48}$$

In particular, the rescaled local chemical potential is

$$\hat{\mu}_l = h/\sqrt{f}\,. \tag{2.49}$$

We shall now obtain the rescaled fluid quantities $\hat{\rho}$ and $\hat{\sigma}$. From (2.42) and (2.48) we have

$$\begin{aligned} \rho &= \beta \int_{\frac{e}{\kappa}|q_f|\hat{m}_f}^{\frac{e}{\kappa}q_f\hat{\mu}_l} \mathrm{d}\epsilon\; \Theta\left(\epsilon - \frac{e}{\kappa}q_f\hat{m}_f\right)\epsilon^2\sqrt{\epsilon^2 - \frac{e^2}{\kappa^2}q_f^2\hat{m}_f^2}\,, \\ \sigma &= q_f\beta \int_{\frac{e}{\kappa}|q_f|\hat{m}_f}^{\frac{e}{\kappa}q_f\hat{\mu}_l} \mathrm{d}\epsilon\; \Theta\left(\epsilon - \frac{e}{\kappa}q_f\hat{m}_f\right)\epsilon\sqrt{\epsilon^2 - \frac{e^2}{\kappa^2}q_f^2\hat{m}_f^2}\,. \end{aligned} \tag{2.50}$$

Since $q_f\mu_l = \widetilde{\mu}_l > 0$, we can replace in the upper bound of the integrals $q_f\hat{\mu}_l$ by $|q_f||\hat{\mu}_l|$. Replacing $m_f$, $\beta$ and $\mu_l$ by the rescaled quantities (2.48) and performing a simple change of variable, one obtains

$$\begin{aligned} \rho &= \frac{1}{\kappa^2L^2}\hat{\beta}\int_{\hat{m}_f}^{|\hat{\mu}_l|} \mathrm{d}\epsilon\; \Theta\left(\epsilon - \hat{m}_f\right)\epsilon^2\sqrt{\epsilon^2 - \hat{m}_f^2}\,, \\ \sigma &= \frac{1}{e\kappa L^2}\frac{|q_f|}{q_f}\hat{\beta}\int_{\hat{m}_f}^{|\hat{\mu}_l|} \mathrm{d}\epsilon\; \Theta\left(\epsilon - \hat{m}_f\right)\epsilon\sqrt{\epsilon^2 - \hat{m}_f^2}\,, \end{aligned} \tag{2.51}$$

where $|q_f|$ arises from the square root. Since $q_f\hat{\mu}_l > 0$, $|q_f|/q_f = \mathrm{sign}(q_f) = \mathrm{sign}(\hat{\mu}_l)$, using the last line of (2.48) we obtain the final expressions for the rescaled fluid quantities,

$$\begin{aligned} \hat{\rho} &= \hat{\beta}\int_{\hat{m}_f}^{|\hat{\mu}_l|} \mathrm{d}\epsilon\; \Theta\left(\epsilon - \hat{m}_f\right)\epsilon^2\sqrt{\epsilon^2 - \hat{m}_f^2}\,, \\ \hat{\sigma} &= \mathrm{sign}(\hat{\mu}_l)\,\hat{\beta}\int_{\hat{m}_f}^{|\hat{\mu}_l|} \mathrm{d}\epsilon\; \Theta\left(\epsilon - \hat{m}_f\right)\epsilon\sqrt{\epsilon^2 - \hat{m}_f^2}\,, \\ \hat{p} &= -\hat{\rho} + \hat{\mu}_l\hat{\sigma}\,. \end{aligned} \tag{2.52}$$

These expressions are non-zero for $0 < \hat{m}_f < |\hat{\mu}_l|$. The charge density $\hat{\sigma}$ is positive for $0 < \hat{m}_f < \hat{\mu}_l$ and negative for $\hat{\mu}_l < -\hat{m}_f < 0$. The energy density is positive in both cases.

With the ansatz (2.13), the field equations (2.38-2.39) reduce to

$$\frac{1}{r}\left(\frac{f'}{f} + \frac{g'}{g} + \frac{4}{r}\right) + \frac{gh\hat{\sigma}}{\sqrt{f}} = 0\,, \tag{2.53a}$$

$$\frac{f'}{rf} - \frac{h'^2}{2f} + g(3+\hat{p}) - \frac{1}{r^2} = 0\,, \tag{2.53b}$$

$$h'' + \frac{g\hat{\sigma}}{\sqrt{f}}\left(\frac{rhh'}{2} - f\right) = 0\,. \tag{2.53c}$$

### 2.4.2 Lifshitz symmetry and perturbations towards the boundary region

The field equations (2.53) admit the exact solution

$$f = \frac{1}{r^{2z}}\,, \qquad g = \frac{g_\infty}{r^2}\,, \qquad h = \frac{h_\infty}{r^z}\,, \tag{2.54}$$

where the constants $g_\infty$ and $h_\infty$ are given in terms of the (rescaled) mass of the fermions $\hat{m}_f$ and the parameter $\hat{\beta}$ through

$$h_\infty^2 = \frac{z-1}{z}\,, \qquad g_\infty = \frac{6z^2\sqrt{z-1}}{[(1-\hat{m}_f^2)z-1]^{3/2}\hat{\beta}}\,, \tag{2.55}$$

where the parameter $z(\hat{m}_f, \hat{\beta})$ is solution to a complicated equation involving $\hat{m}_f$ and $\hat{\beta}$. The local chemical potential is constant for this solution and given by $\hat{\mu}_l = \pm h_\infty$. For simplicity, we will assume that the fermions are positively charged, i.e. $q_f > 0$. From (2.52), we see that having non-trivial (constant in fact) fluid quantities in the Lifshitz solution requires

$$\hat{\mu}_l = h_\infty = \sqrt{\frac{z-1}{z}}\,. \tag{2.56}$$

The system (2.53) is invariant under charge conjugation which acts on the gauge field as

$$h(r) \to -h(r)\,, \tag{2.57}$$

from which the case $h_\infty < 0$ is easily obtained. It corresponds to a fluid made of negatively charged fermions as can be seen from (2.52) since the local chemical potential becomes negative under (2.57). The geometry (2.54) is a solution to the field equations (2.53) for

$$0 \leq \hat{m}_f < 1\,, \qquad z \geq \frac{1}{1-\hat{m}_f^2} \geq 1\,. \tag{2.58}$$

The solution (2.54) is invariant under the scaling symmetry

$$t \to \lambda^z\, t\,, \qquad x \to \lambda\, x\,, \qquad r \to \lambda\, r\,, \tag{2.59}$$

and is a gravitational realization of the Lifshitz symmetry group [25]. Lifshitz solutions have been studied extensively since the pioneer work [40]. Indeed, we recover here the emergent symmetry of a quantum critical system (see Section 2.1) where $z$ is the dynamical critical exponent, as appearing in the scaling transformation (2.7). Lifshitz symmetry arises typically when massive vector fields become effectively massive [41]. Here, the fermionic charge density screens the electric field which becomes massive and cannot support a near-horizon $AdS_2$ geometry as for the extremal Reissner-Nordström black hole.

We should notice that the Lifshitz spacetime (2.54) is a singular spacetime. Even if the scalar curvature invariants are constant for any $z \geq 1$, Lifshitz spacetime admits a curvature singularity for $r \to \infty$ if $z \neq 1$ which can be seen by computing the tidal forces between infalling observers. It means that Lifshitz spacetime is geodesically incomplete and should be used with caution. The singularity is however expected to be removed

at finite temperature and this spacetime receives strong corrections when embedded in string theory [42].

From the field theory point of view, it is natural to consider the exact Lifshitz solution (2.54) as the holographic low energy description of a quantum critical system of fermions. At low energy, the fermions interact with critical bosonic modes, represented in the gravitational theory by the metric and the gauge field. The scale-invariant low energy theory needs to be connected to the microscopic observables of the system, such as the charge density. This is done in the holographic framework by connecting the Lifshitz-invariant solution (2.54) to a near-boundary $AdS_4$ geometry.

We will then consider the Lifshitz solution as valid in the near-horizon region $r \to \infty$. To connect this asymptotic IR solution to the near-boundary $AdS_4$ geometry, it is necessary to perturb the exact solution (2.54). We write the metric components and the gauge field as

$$f = \frac{1}{r^{2z}} \left(1 + f_1 r^\alpha + \dots\right) , \quad g = \frac{g_\infty}{r^2} \left(1 + g_1 r^\alpha + \dots\right) , \quad h = \frac{h_\infty}{r^z} \left(1 + h_1 r^\alpha + \dots\right) . \tag{2.60}$$

Plugging these perturbations in the field equations (2.53), one obtains the three possible exponents

$$\alpha_0 = 2 + z \,, \qquad \alpha_\pm = \frac{2+z}{2} \pm \frac{\sqrt{9z^3 - 21z^2 + 40z - 28 - \hat{m}_f^2 z (4-3z)^2}}{2\sqrt{(1-\hat{m}_f^2)z - 1}} \,. \tag{2.61}$$

The constants $g_1$ and $h_1$ are solved in terms of $\alpha$ and $f_1$, which remains arbitrary. The exponents $\alpha_0$ and $\alpha_+$ correspond to relevant deformations of the Lifshitz geometry (2.54). Since we want to match this asymptotic IR solution to $AdS_4$, we consider the irrelevant deformation $\alpha_-$. If we want the fluid density not to diverge in the UV region, i.e. if we want the local chemical potential (2.46) to be an increasing function of the radial coordinate $r$, we must have $f_1 < 0$.

By imposing the initial conditions (2.60) on the functions $f$, $g$, $h$ and the derivative $h'$ at a large IR cutoff, it is easy to integrate numerically the field equations (2.53) up to the radius $r = r_s$ where

$$\hat{\mu}_l(r_s) = \hat{m}_f \,. \tag{2.62}$$

The fluid quantities (2.52) vanish at $r = r_s$, which defines the electron 'star' boundary.

For $r < r_s$, the fluid quantities are vanishing and the solution looks like the extremal AdS-Reissner-Nordström, where

$$f = \frac{c^2}{r^2} - \hat{M} r + \frac{\hat{Q}^2}{2} r^2 \,, \qquad g = \frac{c^2}{r^4 f} \,, \qquad h = c \left(\hat{\mu} - \hat{Q} r\right) . \tag{2.63}$$

The constants $c$, $\hat{M}$, $\hat{Q}$ and $\hat{\mu}$ are obtained by matching the exterior solution (2.63) with the numerical solution in the interior region. In general, the constant $c > 0$ is different from one. This is because the constant $f_1$ in (2.60) can be chosen arbitrary. One could choose $f_1$ such that $c = 1$, however it is not necessary, because one can perform a change of time coordinate $t \to \tilde{t} = c\, t$, such that the near-boundary geometry is given by the $AdS_4$ metric (2.14) with $\tilde{t}$ the time coordinate. It means that $\tilde{t}$ is the time coordinate

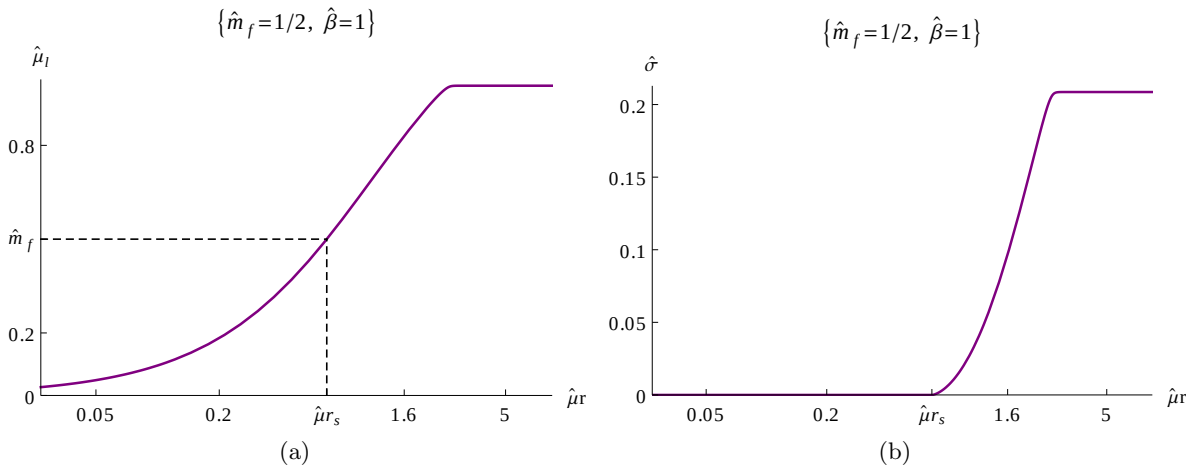


Figure 2.4: Profiles of (a) the local chemical potential and (b) the fluid charge density for an electron star solution.

of the dual field theory. In terms of this variable, the (rescaled) gauge field is given by $\hat{A} = (\hat{\mu} - \hat{Q}r)\mathrm{d}\tilde{t}$. The constant $\hat{\mu}$ is thus identified with the chemical potential of the field theory and $\hat{Q}$ is the total charge of the system. It is easy to verify that the total charge $\hat{Q}$ is given by the integral

$$\hat{Q} = \int_{r_s}^{\infty} \mathrm{d}r \frac{\sqrt{g(r)}}{r^2} \hat{\sigma} \,. \tag{2.64}$$

The electron star solution is displayed in Figure 2.4. In the following, we will refer to the electron star solution at zero temperature by 'ES'.

As for the RN black hole, the electron star model admits a radial electric flux pointing to the UV boundary and responsible for the finite charge density of the boundary field theory. However, in the electron star solution, the electric flux is not sourced by a charged event horizon but by the charged bulk fermions, which occupy the interior region of the bulk spacetime, as shown in Figure 2.5.

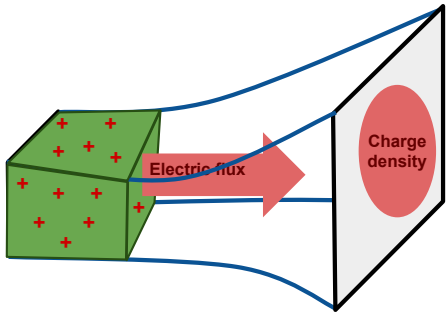


Figure 2.5: In the electron star solution, the boundary charge density is sourced by the charged bulk fermions. Figure taken from [27] with consent of the author.

### 2.4.3 Solution-generating symmetries and physical parameters

The field equations (2.53) are invariant under the two independent symmetries

$$(r, x, y) \to a(r, x, y)\,, \qquad f \to a^{-2} f\,, \qquad g \to a^{-2} g\,, \qquad h \to a^{-1} h\,, \tag{2.65a}$$

$$f \to b^{-2} f\,, \qquad h \to b^{-1} h\,. \tag{2.65b}$$

These symmetries do not leave the ansatz (2.13) invariant. For fixed values of $\hat{m}_f$ and $\hat{\beta}$, the electron star solution is parametrized by the coefficient $f_1$ appearing in (2.60). Changing $f_1$ can be achieved by a symmetry transformation of the kind (2.65a). The constant $c$ can be eliminated from the solution by a transformation of the kind (2.65b). This is equivalent to the rescaling of the time coordinate $t \to c\,t$ as discussed above.

The transformations (2.65a) act on the chemical potential, the charge and the mass of the field theory as

$$(\hat{\mu}, \hat{Q}, \hat{M}) \to (\lambda\hat{\mu}, \lambda^2\hat{Q}, \lambda^3\hat{M})\,. \tag{2.66}$$

Thus, they are solution-generating symmetries, which take one solution of the field equations to a physically different one with different chemical potential, charge and mass.

### 2.4.4 Thermodynamics

Since the solution outside the star is given by the AdS-Reissner-Nordström black hole, the computation of the free energy reduces to the case of Section 2.3. The free energy of the dual field theory state is then given by

$$\hat{\Omega}(\hat{\mu}) = \hat{M}(\hat{\mu}) - \hat{\mu}\hat{Q}(\hat{\mu})\,. \tag{2.67}$$

A solution depends only on one physical parameter. In the grand canonical ensemble, at zero temperature all other physical quantities as the mass or the charge are functions of the chemical potential $\hat{\mu}$. One can check the validity of (2.67) by computing separately the Euclidean on-shell action, the ADM mass and the total charge of the solution. To do so, one needs an action describing the fluid physics. This action and the derivation of the stress-energy tensor (2.36) and the electromagnetic current (2.37) has been given in [39]. We will present an action principle for the fluid in Chapter 3 when we will consider the coupling of the electron star model to a charged scalar field.

Since $\hat{\mu}$ is the only independent variable at zero temperature, the electron star solutions satisfy an equation of state $\hat{Q}(\hat{\mu})$. From the scaling (2.66), we see that the charge must be quadratic in $\hat{\mu}$,

$$\hat{Q}(\hat{\mu}) = c_{\mathrm{ES}}\,\hat{\mu}^2\,, \tag{2.68}$$

where $c_{ES}$ is a constant. By integrating out the thermodynamic relation

$$\hat{Q} = -\frac{\mathrm{d}\hat{\Omega}}{\mathrm{d}\hat{\mu}}\,, \tag{2.69}$$

one obtains the free energy as an explicit function of $\hat{\mu}$,

$$\hat{\Omega} = -\frac{1}{3}\,c_{\mathrm{ES}}\,\hat{\mu}^3\,. \tag{2.70}$$

In this expression, the constant of integration has been eliminated by requiring that the free energy at zero chemical potential vanishes. This case corresponds to the pure $AdS_4$ solution. Inserting (2.70) into the first law (2.67) leads to $\hat{\Omega} = -2\hat{M}$, which is the equation of state of a (2+1)-dimensional conformal field theory. This result is expected since the field theory we are describing is a conformal field theory perturbed by a chemical potential.

For given values of the parameters appearing in the Lagrangian, the constant $c_{\rm ES}$ does not depend on the boundary chemical potential $\hat{\mu}$. In other words, it depends only on the parameters of the theory, which are the fermion mass $\hat{m}_f$ and the phenomenological parameter $\hat{\beta}$. Its knowledge is sufficient to compare the free energy with other solutions. This can be seen from (2.68), which shows that the constant $c_{\rm ES}$ is invariant under the solution-generating transformation (2.66). The constant $c_{\rm ES}$ can be easily obtained from (2.68) using the matching conditions at the star boundary.

In addition to the electron star, the field equations (2.53) also admit the extremal Reissner-Nordström black hole as a solution. Indeed, one recovers the Einstein-Maxwell equations in vacuum for vanishing fluid quantities ($\hat{\sigma} = \hat{\rho} = \hat{p} = 0$). The free energy of this solution is given by (2.33), so the constant $c_{\rm ERN}$, which plays the role of $c_{\rm ES}$ for the extremal charged black hole, is

$$c_{\rm ERN} = \frac{1}{\sqrt{6}}\,. \tag{2.71}$$

For the extremal black hole solution, the parameter which plays the role of $f_1$ is the value of the event horizon $r_+$, which can be changed using the transformations (2.65b). In this case the scaling (2.66) is still valid.

In Figure 2.6, we display the constant $c_i$ ($i = {\rm ERN}, {\rm ES}$) for the extremal black hole and the electron star solutions as a function of the fermion mass $\hat{m}_f$ at fixed $\hat{\beta}$. We see that the electron star solution is always thermodynamically favoured at zero temperature. In the limit where $\hat{m}_f \to 1$, the near-horizon geometry of the electron star solution is $AdS_2 \times \mathbb{R}^2$ and one recovers the ERN black hole solution. Indeed, the free energies of the two solutions match in this limit, as shown in Figure 2.6. The limit $\hat{m}_f \to 1$ means that the dynamical critical exponent $z \to \infty$ which corresponds to the decoupling of the time and space directions of the field theory, as can be seen from (2.59). This is indeed what happens in the extremal black hole, where the near-horizon geometry describes a (0+1)-dimensional CFT.

Since the electron star solution does not admit an event horizon, the entropy is vanishing, which means that the electron star solution is dual to a non-degenerate state of the field theory. This solution being thermodynamically favoured at zero temperature compared to the extremal Reissner-Nordström black hole, we observe a removal of degeneracy by the presence of fermionic degrees of freedom.

### 2.4.5 Discussion and extensions

The electron star model presented above describes a system of strongly-correlated fermions in the vicinity of a quantum critical point at zero temperature. It exhibits an infinite number of closely spaced Fermi surfaces as will be shown in Section 3.5 (see also [43, 44]), each corresponding to the quasiparticle-like excitations of a (fermionic) 'generalized free field' [45]. It is interpreted as the decomposition of the fermionic operator into 'bound states' which behave almost freely, similarly to the hadrons in QCD. Thus one effectively sees a continuum of zero-energy excitations at fixed momentum, instead of a unique

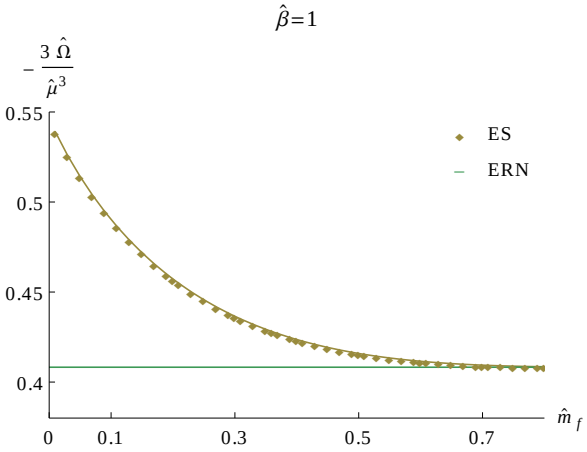


Figure 2.6: Free energy (normalized to the chemical potential) as a function of the fermion mass for the electron star solution and the extremal black hole. The free energy of the ERN in these units is $1/\sqrt{6} \simeq 0.41$.

excitation in the case of a Fermi liquid. It can be shown that the system satisfies the Luttinger theorem [44]. However, the application of an external magnetic field to the system shows that it admits Kosevich-Lifshitz quantum oscillations but only fermions at a given radius contribute to them. It results that the Fermi surface extracted by quantum oscillations does not satisfy the Luttinger theorem [43]. For this reason the electron star solution is dual to a non-Fermi liquid.

The electron star model can be easily generalized to finite temperature [46]. The interior region of the spacetime is occupied by a charged event horizon, responsible for the non-zero temperature of the dual field theory state. The perfect fluid of charged fermions is located in a compact region of spacetime (in the radial direction). In the classical limit, the black hole does not radiate and the zero-temperature construction of the fluid used above applies. The Reissner-Nordström black hole is also a solution to the system, when the fluid quantities vanish identically in the whole spacetime. A continuous phase transition occurs at a critical temperature $T_c$ between the finite-temperature electron star solution and the Reissner-Nordström black hole [46]. This model shows that the Reissner-Nordström black hole is unstable to the formation of fermionic matter at low temperature.

In the electron star model, fermions are treated semi-classically. A procedure to construct backreacted solutions of Einstein-Maxwell theory with fermions treated quantum mechanically has been proposed in [47, 48].

## 2.5 Holographic superconductors

We have seen in Section 2.4 that the Reissner-Nordström black hole is unstable to the formation of fermionic degrees of freedom. It results in the electron star model which describes a non-Fermi liquid. It has also been found that the Reissner-Nordström black hole is unstable to the formation of scalar hair. This has been used to construct gravitational models with non-trivial bosonic degrees of freedom. These models offer a new approach to the study of superconductivity and are called holographic superconductors.

### 2.5.1 Instability of the extremal AdS-Reissner-Nordström black hole

The history of holographic superconductors has started with the discovery by Gubser [49] that charged black holes in AdS have an instability to the formation of charged scalar hair.

Let us consider Einstein-Maxwell theory with a negative cosmological constant coupled to a free scalar field $\psi$ . The action is

$$S = \int \mathrm{d}^4x\sqrt{-g}\left[\frac{1}{2\kappa^2}\left(R+\frac{6}{L^2}\right) - \frac{1}{4e^2}F_{ab}F^{ab} - \frac{1}{2}\left(|\nabla\psi - iqA\psi|^2 + m_s^2|\psi|^2\right)\right] + S_{\mathrm{bdry}} \tag{2.72}$$

where $m_s$ is the mass of the scalar field and $q$ its coupling to the $U(1)$ gauge field. The action $S_{\mathrm{bdry}}$ includes the Gibbons-Hawking term and the counterterms necessary for the holographic renormalization procedure. The Klein-Gordon equation for the scalar field $\psi$ is

$$-\left(\nabla_a - iqA_a\right)\left(\nabla^a - iqA^a\right)\psi + m_s^2\psi = 0\,. \tag{2.73}$$

In an electrically charged black hole background, the charged scalar field acquires an effective mass squared

$$m_{\mathrm{eff}}^2 = m_s^2 + q^2 g^{tt} A_t^2\,, \tag{2.74}$$

where we recall that the inverse metric component $g^{tt}$ is negative. Close to the event horizon, $|g^{tt}|$ is very large, so the effective mass squared $m_{\mathrm{eff}}^2$ may become sufficiently negative to destabilize the scalar field. When the scalar field becomes unstable on the black hole background, it means that one has to take into account the backreaction of the scalar field on the geometry, leading to hairy black hole solutions. This instability is favoured when the black hole is close to extremality. Indeed in this case, in addition to $g_{tt}$, also its first derivative is close to vanish at the event horizon, so $|g^{tt}|$ diverges faster. It means that the formation of haired black holes is favoured at low temperature. There is typically a critical temperature above which the scalar field is not unstable. The fact that the black hole lives in an asymptotically-AdS spacetime is crucial for the formation of hairy black holes. The gravitational potential of AdS prevents the particles created by the Hawking radiation close to the event horizon to escape to infinity. They stay in the near-horizon region and are represented classically by the hair [50].

Let us consider the example of a probe charged scalar field $\psi$ in the extremal Reissner-Nordström black hole. For convenience, we rescale the scalar field, its mass and elementary charge through

$$\psi = \frac{1}{\kappa}\hat{\psi}\,, \qquad m_s = \frac{1}{L}\hat{m}_s\,, \quad q = \frac{\kappa}{eL}\hat{q}\,. \tag{2.75}$$

Imposing the homogeneous and isotropic ansatz (2.13) together with $\hat{\psi} = \hat{\psi}(r)$, the field equation for $\hat{\psi}$ becomes

$$\hat{\psi}'' + \left(\frac{f'}{2f} - \frac{g'}{2g} - \frac{2}{r}\right)\hat{\psi}' + g\left(\frac{\hat{q}^2h^2}{f} - \hat{m}_s^2\right)\hat{\psi} = 0\,. \tag{2.76}$$

In the near-horizon geometry (2.34) of the extremal Reissner-Nordström black hole, the scalar field $\psi$ satisfies the Klein-Gordon equation

$$\rho^2\partial_\rho^2\hat{\psi} - \frac{\hat{m}_s^2 - \hat{q}^2}{6}\hat{\psi} = 0\,. \tag{2.77}$$

Notice that $\rho \to +\infty$ at the horizon. From (1.47), we see that we recover the field equation in $AdS_2$ of a scalar field with effective mass

$$\hat{m}^2_{\text{eff}} = \frac{\hat{m}^2_s - \hat{q}^2}{6} \,. \tag{2.78}$$

If this mass violates the BF bound $\hat{m}^2_{AdS_2} = -1/4$ of $AdS_2$, that is if

$$\frac{\hat{m}_s - \hat{q}^2}{6} < -\frac{1}{4} \,, \tag{2.79}$$

the black hole is unstable or, equivalently, when $\hat{q}^2 > \hat{q}^2_{\text{min}}$ where

$$\hat{q}_{\text{st}} \equiv \sqrt{\frac{3}{2} + \hat{m}^2_s} \,. \tag{2.80}$$

When the scalar field is unstable in the near-horizon region of a black hole solution, its backreaction on the geometry has to be taken into account. It means one has to find a solution to the field equation with a non-trivial profile for the scalar field. This task is not easy in general, however one can first find a near-horizon solution and integrate out numerically the field equations to the UV boundary region, where the charged scalar field behaves as in (1.48). The subleading term in this expansion is generically non-zero, which leads to the concept of holographic superconductors as we shall present below.

### 2.5.2 Holographic superconductor at zero temperature

As we discussed in Section 2.3, the extremal Reissner-Nordström black hole has a finite entropy, essentially because it admits an event horizon with finite area. There should exist other holographic states at finite charge density which have zero entropy at zero temperature. We expect them to be thermodynamically favoured to remove the degeneracy of the extremal Reissner-Nordström black hole. We have already seen that the entropy of the state dual to the electron star solution vanishes. We present here an other solution that exhibits a non-trivial profile for a charged scalar field.

Let us go back to the Einstein-Maxwell-scalar theory (2.72). The metric, the gauge field and the scalar field satisfy the Einstein equations

$$R_{ab} - \frac{1}{2} g_{ab} R - \frac{3}{L^2} g_{ab} = \kappa^2 \left( T^{\text{Mxwl.}}_{ab} + T^{\text{scalar}}_{ab} \right) \,, \tag{2.81}$$

the Maxwell equations

$$\nabla_a F^{ba} = e^2 \left( J^b_{\text{fluid}} + J^b_{\text{scalar}} + J^b_{\text{int}} \right) \tag{2.82}$$

and the Klein-Gordon equation (2.73), where the stress-energy tensor of the scalar field is

$$T^{\text{scalar}}_{ab} = \frac{1}{2} \left( g^c_a g^d_b + g^c_b g^d_a - g_{ab} g^{cd} \right) \left( \nabla_c \psi - i q A_c \psi \right) \left( \nabla_d \psi^* + i q A_d \psi^* \right) - \frac{1}{2} m^2_s g_{ab} \psi \psi^* \tag{2.83}$$

and its electromagnetic current

$$J^a_{\text{scalar}} = -i \frac{q}{2} g^{ab} \left[ \psi^* \left( \nabla_a - i q A_a \right) \psi - \psi \left( \nabla_a + i q A_a \right) \psi^* \right] \,. \tag{2.84}$$

The electromagnetic stress-energy tensor was already defined in (2.11).

By making the isotropic and homogeneous ansatz (2.13) together with $\psi = \psi(r)$, and rescaling quantities as in (2.75), the $r$-component of Maxwell equations is

$$q\left(\hat{\psi}^*\hat{\psi}' - \hat{\psi}\hat{\psi}^{*\prime}\right) = 0\,, \tag{2.85}$$

which implies that when $\hat{\psi}$ is non-trivial, its phase is constant. We fix it to zero in the whole spacetime by a global $U(1)$ transformation. The field $\hat{\psi}$ can now be considered as a real scalar field. The field equations thus reduce to the system

$$\hat{\psi}'' + \left(\frac{f'}{2f} - \frac{g'}{2g} - \frac{2}{r}\right)\hat{\psi}' + g\left(\frac{\hat{q}^2h^2}{f} - \hat{m}_s^2\right)\hat{\psi} = 0\,, \tag{2.86a}$$

$$h'' - \frac{1}{2}\left(\frac{f'}{f} + \frac{g'}{g} + \frac{4}{r}\right)h' - \hat{q}^2gh\hat{\psi}^2 = 0\,, \tag{2.86b}$$

$$g' + \left(\frac{5}{r} + \frac{rh'^2}{2f} + \frac{r}{2}\hat{\psi}'^2\right)g + \left[\frac{r}{2}\left(\frac{\hat{q}^2h^2}{f} + \hat{m}_s^2\right)\hat{\psi}^2 - 3r\right]g^2 = 0\,, \tag{2.86c}$$

$$f' + \left[3rg - \frac{1}{r} + \frac{1}{2}r\hat{\psi}'^2 + \frac{r}{2}g\left(\frac{\hat{q}^2h^2}{f} - \hat{m}_s^2\right)\hat{\psi}^2\right]f - \frac{1}{2}rh'^2 = 0\,. \tag{2.86d}$$

In the near-boundary region ($r \to 0$), in addition to the metric and the gauge field which are given by (2.15), the scalar field behaves as

$$\hat{\psi} \sim \hat{\psi}_- r^{3-\Delta} + \hat{\psi}_+ r^{\Delta}\,, \qquad \Delta = \frac{3}{2} + \frac{3}{2}\sqrt{1 + \frac{4\hat{m}_s^2}{9}}\,. \tag{2.87}$$

While the scalar field can be considered as a probe field in the near-boundary region, if it satisfies the instability condition (2.79) it must modify substantially the interior geometry of the extremal Reissner-Nordström black hole. It means that it is dual to a relevant operator of the field theory. For this reason, we choose the mass squared of the scalar field to be negative, $\hat{m}_s^2 < 0$.

Horowitz and Roberts [51] found an asymptotic solution in the IR ($r \to \infty$) to the field equations (2.86) with a non-trivial scalar. This solution is

$$\begin{aligned} &f(r) \sim \frac{1}{r^2}\,, && g(r) \sim -\frac{3}{2\hat{m}_s^2}\frac{1}{r^2\log r}\,, \\ &h(r) \sim h_0\, r^{\delta}\,(\log r)^{1/2}\,, && \hat{\psi}(r) \sim 2\,(\log r)^{1/2}\,, \end{aligned} \tag{2.88}$$

where

$$\delta = \frac{1}{2} - \frac{1}{2}\left(1 - \frac{24\hat{q}^2}{\hat{m}_s^2}\right)^{1/2} \tag{2.89}$$

must satisfy $\delta < -1$, which means that

$$\hat{q}^2 > -\frac{\hat{m}_s^2}{3}\,. \tag{2.90}$$

At this point the constant $h_0$ appearing in (2.88) is arbitrary. The asymptotic metric in the interior region is then

$$\mathrm{d}s^2 \sim \frac{L^2}{r^2}\left(-\mathrm{d}t^2 + \mathrm{d}\vec{x}^2\right) + \frac{L^2}{2|\hat{m}_s^2|}\frac{\mathrm{d}r^2}{r^2\log r}\,, \qquad r \to \infty\,. \tag{2.91}$$

One can easily see that the temperature and the entropy associated to the horizon $r = \infty$ vanish. However, the curvature invariants diverge logarithmically at $r = \infty$. For example, the Ricci scalar behaves as

$$R \sim \frac{8\hat{m}_s^2}{L^2} \log r \,, \tag{2.92}$$

so the solution (2.88) has a mild singularity at $r = \infty$. However, from a field theory point of view, one can consider to put an IR cutoff and study physics close to the horizon but at finite distance from the singularity. It is also possible that this singularity disappears by turning on a small temperature. We see from (2.91) that Poincaré invariance is restored near the horizon and almost (presence of a logarithmic factor) conformal invariance.

The integration of the field equations (2.86) towards the UV boundary $r = 0$ can be achieved numerically by imposing the initial conditions (2.88) at an IR cutoff $r_{\rm IR} \gg 1$. Close to the UV boundary, the solution is

$$r \to 0 : \qquad \frac{f(r)}{c^2} \sim g(r) \sim \frac{1}{r^2} \,, \qquad h(r) \sim c \left( \hat{\mu} - \hat{Q} r \right) \,, \qquad \hat{\psi}(r) \sim \hat{\psi}_- r^{3-\Delta} + \hat{\psi}_+ r^{\Delta} \,, \tag{2.93}$$

where $\Delta$ is the conformal dimension of the operator dual to $\psi$, defined in (2.87). The constants $\hat{\mu}$ and $\hat{Q}$ are respectively the chemical potential and the total charge of the dual field theory.

The field equations (2.86) are invariant under the transformations (2.65) while the scalar remains invariant. As for the electron star system, the constant $c$ in (2.93) can be eliminated by a transformation of the type (2.65b). The transformations (2.65a) generate new physical solutions, we shall come back to this point later.

The bulk field $\hat{\psi}$ is dual to a charged scalar operator $\mathcal{O}$ in the dual field theory. In the standard quantization scheme, the non-normalizable mode $\hat{\psi}_-$ in the asymptotic UV expansion (2.93) of the scalar field is the source of the boundary operator $\mathcal{O}$ and $\hat{\psi}_+$ its vev. When $\hat{\psi}_+ \propto \langle \mathcal{O} \rangle \neq 0$, the scalar operator $\mathcal{O}$ condenses and the global $U(1)$ symmetry is broken. The field theory state is then interpreted as superfluid. As we have discussed in Section 2.1, in many condensed matter systems the photons are non-dynamical and the local $U(1)$ symmetry reduces to a global $U(1)$ symmetry. We can then interpret the condensation of the scalar operator $\mathcal{O}$ as the sign of the onset of superconductivity. The charged condensate $\langle \mathcal{O} \rangle$ should be thought of as the strong-coupling analogue of a Cooper pair. However it is possible that the condensate is not made of pairs of dressed electrons: the scalar operator $\mathcal{O}$ could be a more complicated operator of the fermionic operator. The $U(1)$ symmetry is spontaneously broken if the scalar operator is not coupled to an external source. Thus we must require that $\hat{\psi}_- = 0$. This can be done by choosing correctly the constant $h_0$ appearing in the IR asymptotic solution (2.88). When this is done, the constant $\psi_+$ is generically non-zero. In the following, we denote this holographic superconductor solution by 'HSC'.

The constant $h_0$, which is now chosen such that $\hat{\psi}_- = 0$ can be positive or negative. The transformation relating these two constants is charge conjugation, which acts on the gauge field and the elementary charge of the scalar field as

$$h(r) \to -h(r) \,, \qquad q \to -q \,. \tag{2.94}$$

Charge conjugation is a symmetry of the field equations (2.86). Each solution is related to a solution with opposite chemical potential and total charge by the charge conjugation transformation (2.94).

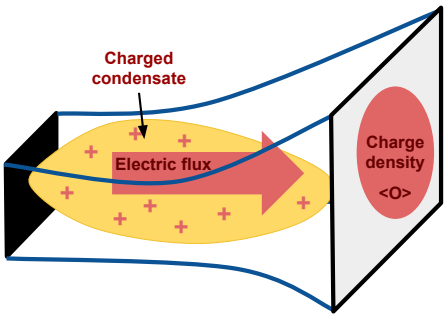


Figure 2.7: In the holographic superconductor models the presence of a charged scalar field is interpreted as the formation of a charged scalar condensate and the breaking of the $U(1)$ symmetry in the field theory. Figure taken from [27] with consent of the author.

As for the electron star solution, the transformations (2.65a) generate solutions with different physical quantities. This can be seen as follows. The free parameter in the IR asymptotic solution (2.88) is not $h_0$ which has to be chosen to ensure the spontaneous breaking of the $U(1)$ symmetry. We can identify a deformation parameter by noticing that if one replaces

$$\log r \to \log r/r_0 \tag{2.95}$$

for an arbitrary $r_0$, (2.88) is still an asymptotic solution to the field equations (2.86). Then, the transformations (2.65a) relate solutions by the same rescaling as for the electron star solution together with the rescaling of the condensate, that is

$$(\hat{\mu}, \hat{Q}, \hat{M}, \hat{\psi}_+) \to (\lambda\hat{\mu}, \lambda^2\hat{Q}, \lambda^3\hat{M}, \lambda^\Delta\hat{\psi}_+)\,. \tag{2.96}$$

It is useful to have a handle of the asymptotics of the metric and the gauge field beyond the leading order (2.93), in particular to understand the corrections due to the condensate. At $\hat{\psi}_+ = 0$ we know the exact solution, i.e. the extremal Reissner-Nordström geometry (2.16-2.18). When the scalar field is non-trivial, it will backreact on the solution, but since we are taking the scalar field to be a purely normalizable mode as $r \to 0$, we can compute the backreaction perturbatively in (2.86). The resulting deformed UV solution with the condensate turned on behaves, as $r \to 0$, as

$$\begin{aligned}
f(r) &= \frac{1}{r^2}\left(1 - \hat{M}r^3 + \frac{\hat{Q}^2}{2}r^4 + \dots\right)\,,\\
g(r) &= \frac{1}{r^4 f(r)}\left(1 - \frac{\Delta}{2}\hat{\psi}_+^2 r^{2\Delta} + \dots\right)\,,\\
h(r) &= \hat{\mu} - \hat{Q}r + \hat{\mu}\frac{\hat{q}^2\hat{\psi}_+^2}{2\Delta(2\Delta-1)}r^{2\Delta} + \dots\,,\\
\hat{\psi}(r) &= \hat{\psi}_+ r^\Delta + \dots\,,
\end{aligned} \tag{2.97}$$

where the dots denote terms which are subleading with respect to those we have included, and whose exact order is unimportant.

Equations (2.97) solve the field equations (2.86) for *arbitrary* values of $\hat{\mu}, \hat{M}, \hat{Q}, \hat{\psi}_+$. This is because the relations (2.31) are imposed at the event horizon where the gauge

field must vanish for regularity and the metric component $g_{tt}$ vanishes. The UV does not know about these relations if it is not connected to a regular IR solution. Remarkably, $f(r)$ receives no corrections to leading order, and $h(r)$ and the relation between $g(r)$ and $f(r)$ are corrected only by terms which are subleading with respect to *all* terms appearing in the exact black hole solution (2.30). This means that the condensate enters into the metric and gauge field at subleading order in $r \to 0$ with respect to the charge and mass parameters of the solution.

To compute the free energy of the holographic superconductor solution, it is possible to apply the same procedure as for the electron star, presented in Section 2.4.4. The reason is that the scalar field deforms the extremal black hole solution in the UV only by terms which are subleading, and do not contribute at all to any of the quantities in (2.32). For the electron star, this was obvious since the solution outside the star coincides with the extremal RN black hole; for the holographic superconductor, this is a consequence of the asymptotic behaviour (2.97) and in particular the fact that $f(r)$ and $h(r)$ are unchanged to the order that gives finite contributions to (2.32). The free energy of the holographic superconductor solution is then simply given by the coefficient $c_{\rm HSC}$ appearing in the expression of the free energy

$$\hat{\Omega} = -\frac{1}{3} c_{\rm HSC}\, \hat{\mu}^3 \,. \tag{2.98}$$

In Fig 2.8, we display the free energy of the ERN and the HSC as a function of the elementary charge $\hat{q}$. The point $\hat{q} = \hat{q}_{\rm min}$, with

$$\hat{q}^2_{\rm min} \equiv -\frac{\hat{m}_s^2}{3} \,, \tag{2.99}$$

is the minimal elementary charge for which the IR geometry in (2.91) is an asymptotic solution to the field equations. Although it is expected, the phase transition between the extremal black hole and the holographic superconductor is not visible in Figure 2.8 because we could not compute the free energy sufficiently close to the possible transition. Another possibility is that another phase emerges between the ERN and the HSC phases.

### 2.5.3 Other holographic models for superconductivity

We have seen that Einstein-Maxwell gravity coupled to a free charged scalar field provides a solution describing a superconducting dual ground state. In this solution, the Poincaré invariance is restored at low energy. It is possible to consider other emergent symmetries. For example, by adding a quartic interaction for the scalar field to the Einstein-Maxwell-scalar action (2.72), the model admits a Lifshitz solution where the metric and the gauge field behave as in (2.54) and the scalar field is constant [52]. Since this solution is a fixed point of the holographic renormalization group (i.e. it is an exact solution of the field equations), one must consider irrelevant perturbations, as in the electron star model, to connect the Lifshitz solution to the near-boundary $AdS_4$ asymptotics. As for the Horowitz-Roberts holographic superconductor, the solution with a non-trivial scalar field is thermodynamically favoured.

Holographic superconductor models were originally discovered at finite temperature by Hartnoll, Herzog and Horowitz in the seminal works [53, 54]. They used the discovery

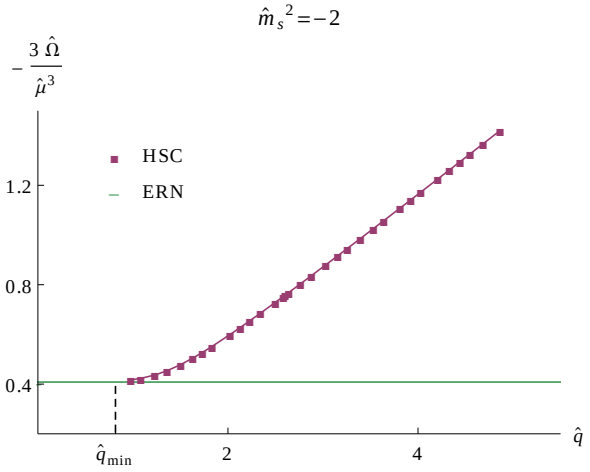


Figure 2.8: Free energy (normalized to the chemical potential) as a function of the elementary charge $\hat{q}$ of the scalar field for the holographic superconductor and the extremal black hole solutions. The free energy of the ERN in these units is $1/\sqrt{6} \simeq 0.41$.

of Gubser that charged black holes are unstable to the creation of charged scalar hair (see Section 2.5.1) to construct the first holographic superconductor. They considered in [53] the Einstein-Maxwell-scalar action (2.72) and treated the gauge field and the scalar field as probe fields on top of the AdS-Schwarzschild black hole. In the second paper [54], they considered the backreaction of these fields on the geometry and found hairy black hole solutions. Both in the probe and the backreacted cases, the scalar field can be non-trivial in the bulk only below a critical temperature $T_c$ and the solution exhibits a non-trivial vev for the dual field theory operator. In this case, the solution is a hairy black hole and it is thermodynamically favoured. The phase transition at the critical temperature $T_c$ between the Reissner-Nordström black hole and the hairy black hole is second order and interpreted as the onset of superconductivity. It is then natural to expect a solution with a non-trivial scalar field to be favoured at zero temperature, which is the case for the models of [52, 51].

The appellation 'holographic superconductor' is not only justified by the condensation of a charged scalar operator, but also by the features of the response of the system to the application of external electric and magnetic fields. The electrical conductivity can be computed by considering the perturbation of the component $A_x$ of the gauge field. It also involves the perturbation of the metric component $g_{tx}$, but it can be eliminated to end up with an ordinary second order equation for the gauge field perturbation $\delta A_x$. Close to the UV boundary $r = 0$, $\delta A_x = \delta A_x^{(0)} + r\,\delta A_x^{(1)} + \ldots$, where $\delta A_x^{(0)}$ is the applied electric field in the field theory and $\delta \hat{A}_x^{(1)}$ the resulting current. From linear response theory, the 'constant' of proportionality between these two quantities is the frequency-dependent conductivity $\sigma(\omega) = -(i/\omega)(\delta A_x^{(1)}/\delta A_x^{(0)})$. In the probe approximation [53], one observes the opening of a gap in energy in the real part of the conductivity for temperatures below the critical temperature. In a metal the conductivity does not admit a gap: for arbitrarily small external electric field, the system is conducting and the induced current is non-zero. The gap observed in the holographic superconductor corresponds to the binding energy of the scalar condensate, which is a composite operator of the fermionic operator. To generate a current in the dual field theory, one must apply a sufficiently large electric field to break the condensate and free the fermionic degrees of freedom. This 'hard gap' is not

present anymore when one considers the backreaction of the gauge field and the scalar field [54]. It is replaced by a 'soft gap': at small frequency, the conductivity becomes very small. The real part of the conductivity also admits a delta function at zero frequency. This is not the infinite DC conductivity observed in superconductivity because it is also present in the normal phase for $T > T_c$. This delta function appears because the system is translationally-invariant: in the presence of an electric field, a finite charge is infinitely accelerated because of the absence of dissipation. However, the coefficient of the delta function grows as the temperature is lowered below $T_c$ [50].

The second interesting characteristic of holographic superconductors is their capacity to expel magnetic fields. In normal superconductors, it is known as the Meissner effect. However, above a critical value the magnetic field can penetrate in the material and it is not superconducting anymore. The phase transition between the superconducting and the normal phases as function of the applied magnetic field can be first order or second order. In holography, the simplest model to consider to study this phase transition is a probe charged scalar field in a black hole with both electric and magnetic charges [55]. It turns out that the phase transition is second order, so the holographic superconductor is type II, as observed in high-Tc superconductors [50].

# Chapter 3

# Holographic Bose-Fermi systems

In this chapter, using holography we study the ground state of a system with interacting bosonic and fermionic degrees of freedom at finite density. The model is based on the combination of the ingredients of the holographic superconductor and the electron star. We show that the system admits solutions which exhibit both fermionic and bosonic degrees of freedom. When they exist, these solutions are thermodynamically favoured. We construct the phase diagrams describing the phase transitions between the different solutions and compute the low energy fermionic excitations of the system.

This chapter presents the results obtained by the author and collaborators in [1, 2].

## 3.1 Motivations

We have seen in Sections 2.4 and 2.5 that a charged black hole in AdS spacetime can suffer from two unrelated instabilities. They allow the creation of bosonic or fermionic matter, whose presence is favoured at low temperature, and lead to pioneering holographic models for the study of non-Fermi liquids and high-Tc superconductors.

It was suggested by Sachdev [33] that the presence of a charged black hole in the bulk could be interpreted as dual to a totally fractionalized state. When the charge is sourced by matter fields in the bulk, it corresponds to matter operators in the boundary field theory. By coupling the electron star model at zero temperature to a neutral scalar field, it was shown in [56] that the presence of the fermionic fluid and/or the extremal charged black hole depends on the UV boundary condition imposed to the scalar field. On the boundary side, this leads to phase transitions between cohesive (presence of the fluid only), partially fractionalized (presence of both the extremal black hole and the fluid) and fully fractionalized (presence of the extremal black hole only) phases as a function of the source for a neutral scalar operator. In the partially fractionalized phase, part of the low energy fermionic degrees of freedom are subject to fractionalization, and the Luttinger theorem is violated: the charge contained in the Fermi surfaces does not account for the total charge of the system. In [57], a similar analysis was done for charged bosonic matter, leading to analogous results (see also [58]). However, the interpretation is different in this case: when the charged scalar field is non-trivial, the $U(1)$ symmetry of the field theory is broken and the system undergoes a phase transition to a superconducting state.

The creation/destruction of Fermi surfaces and the onset of superconductivity have thus been studied independently in holography. In the holographic superconductor models, the boundary bosonic operator that develops a vacuum expectation value is interpreted as a bound state of fermions. However, in these models, there are no fermionic degrees

of freedom, so the competition between those and the condensate is not accessible. The study of such a competition would be interesting for instance to understand the phase diagram of cuprate superconductors, in particular the onset of superconductivity from the strange metal phase (see Figure 2.1).

The competition between fermionic and bosonic degrees of freedom has been first studied in holography in [59]. This was done in the context of a bulk BCS theory in the near-horizon region of the RN black hole. In this approach, the bosonic field, representative of Cooper pairs, interacts with the fermionic field via a Yukawa interaction. However, this approach requires dealing with microscopic fermions and going away from the fluid approximation. In addition, the coupling can only be there in the case where the bosons have twice the charge of the fermions.

An interacting description in the fluid approximation was given in [60], where the scalar is a BCS-like fermion bilinear. The presence of the condensate modifies the equation of state of the fermionic fluid. It was shown that the resulting 'BCS star' solution was favoured at zero temperature and that a pseudo-gap appears in the Fermi spectral function of the boundary theory. However, this model too arises at the microscopic level from a Yukawa interaction when the charge of the scalar is twice that of the fermions.

However, we have seen in Section 2.1 that in the vicinity of a deconfined quantum critical point, the dressed electrons are subject to fractionalization. In strongly-coupled systems of fermions, it is possible that the fermions that condense in the superconducting state are not the elementary fermions but other fermionic excitations which may be fractionalized. For this reason, we would like to keep the ratio of the charges of the bulk bosonic and fermionic degrees of freedom arbitrary.

The bosonic degrees of freedom in the bulk will consist of a charged scalar operator. As for the electron star model (see Section 2.4), we will treat the fermions in the fluid approximation. In the dual field theory, the scalar operator will be interpreted as a bound state of fermions, so bosons and fermions are expected to couple directly. To keep the fluid approximation valid, we will consider in the bulk a simple current-current interaction between the electromagnetic currents of the scalar field and the fermionic fluid. This interaction has the virtue of leaving arbitrary the ratio between the charges.

We will first see in Section 3.2 that there are reasons to believe that bulk solutions exhibiting both bosonic and fermionic degrees of freedom exist. In Section 3.3, we will consider a fully backreacted system, find the homogeneous and isotropic solutions and study the resulting phase diagram. In Section 3.5, we compute the low energy fermionic excitations.

## 3.2 Beyond the electron star and the holographic superconductor

We show in this section why one should expect the combination of the holographic superconductor and the electron star models to lead to bulk solutions with both bosonic and fermionic degrees of freedom.

### 3.2.1 Scalar instability of the electron star

In Section 2.5.1 we discussed the instability of the extremal Reissner-Nordström black hole to the formation of scalar hair. One can wonder if such an instability can also happen

to the electron star. Let us consider a probe charged scalar field $\psi$ with negative mass squared $m_s^2$ satisfying the $AdS_4$ BF bound, with action

$$S = -\frac{1}{2}\int \mathrm{d}^4x\sqrt{-g}\left(|\nabla\psi - iqA\psi|^2 + m_s^2|\psi|^2\right) , \tag{3.1}$$

in the electron star background. In the near-horizon region ($r \to \infty$), where the metric and the gauge field are given by the Lifshitz-like solution (2.54), the scalar field behaves as [1]

$$\psi \sim A_+ r^{(z+2)-\Delta_{\mathrm{IR}}} + A_- r^{\Delta_{\mathrm{IR}}} , \qquad r \to \infty , \tag{3.2}$$

where

$$\Delta_{\mathrm{IR}} = \frac{1}{2}\left[(z+2) - \sqrt{(z+2)^2 - 4g_\infty(h_\infty^2\hat{q}^2 - \hat{m}_s^2)}\right] . \tag{3.3}$$

At infinity, the first term is dominant. We have rescaled the parameters according to (2.48) and (2.75). If the condition

$$\hat{m}_s^2 < \hat{m}_c^2 , \qquad \hat{m}_c^2 \equiv -\frac{(z+2)^2}{4g_\infty} + h_\infty^2\hat{q}^2 , \tag{3.4}$$

is satisfied, the electron star solution becomes unstable to the formation of scalar hair [1]. This is equivalent to the condition $\hat{q}^2 > (\hat{q}^\star_{\mathrm{st}})^2$ where we have defined the stability bound

$$\hat{q}^\star_{\mathrm{st}} = \frac{1}{h_\infty}\sqrt{\hat{m}_s^2 + \frac{(z+2)^2}{4g_\infty}} . \tag{3.5}$$

If the elementary charge $\hat{q}$ of the scalar field vanishes, for $z > 1$ the condition for the instability reduces to

$$-\frac{9}{4} < \hat{m}_s^2 < -\frac{(z+2)^2}{4g_\infty} \tag{3.6}$$

where the first inequality is simply the $AdS_4$ BF bound for a scalar field. This has led to 'hairy electron star' solutions where the neutral scalar field is non-trivial [61]. In this thesis, we focus on the case where $\hat{q}$ is non-zero. In Figure 3.1 is displayed the critical line above which the condition (3.4) is satisfied and the electron star is unstable.

### 3.2.2 An analysis from the holographic superconductor

In the holographic superconductor model of Section 2.5.2, it is possible to define a local chemical potential which controls the formation of the fluid of charged fermions, in the same manner as for the electron star model. This local chemical potential is given by $\hat{\mu}_l = h/\sqrt{f(r)}$ and vanishes both in the UV and in the IR, as can be seen from Eq. (2.88) and (2.93). It also has a maximum, and if this maximum value happens to be larger than the mass of the fermions $\hat{m}_f$, there exist two solutions $r_1$ and $r_2$ to the Eq. (2.62) which define the star edges. Thus, one can start from the IR with the asymptotic solution (2.88) of the holographic superconductor solution. The local chemical potential will increase towards the UV and then at the point $r_2$ we can match the solution with an interior with non-trivial fluid quantities given by (2.52). The density will reach a maximum, then decrease again until it becomes zero at $r_1$. At this point, the solution is matched with a new holographic superconductor solution up to the UV boundary.

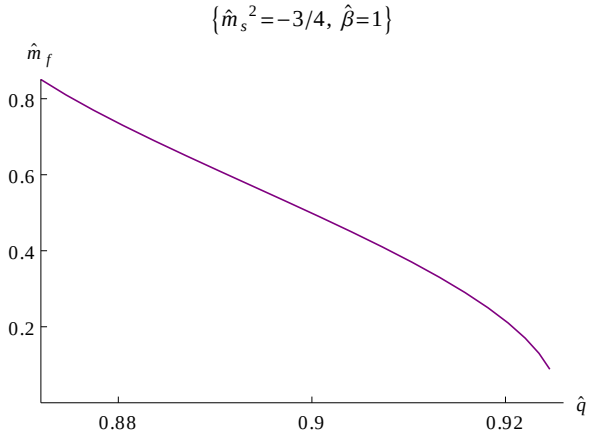


Figure 3.1: The boundary of the stability region for the scalar in the ES background. Above the critical line, the electron star is unstable to the formation of charged scalar hair.

Thus one expects such solution with both non-trivial scalar field and fluid to exist if the condition

$$\hat{m}_f < \hat{\mu}_{\max}(\hat{q}, \hat{m}_s) \tag{3.7}$$

is satisfied, where $\hat{\mu}_{max}(\hat{q}, \hat{m}_s)$ is the maximum value for a HSC solution with parameters $(\hat{q}, \hat{m}_s)$. It is very hard to have an analytic handle of the condition (3.7) as a function of the parameters. One can however compute $\hat{\mu}_{\max}(\hat{q}, \hat{m}_s)$ for a HSC solution numerically [1]. It is displayed in Figure 3.2. The point $\hat{q} = \hat{q}_{\min}$ was defined in (2.99). We also define the

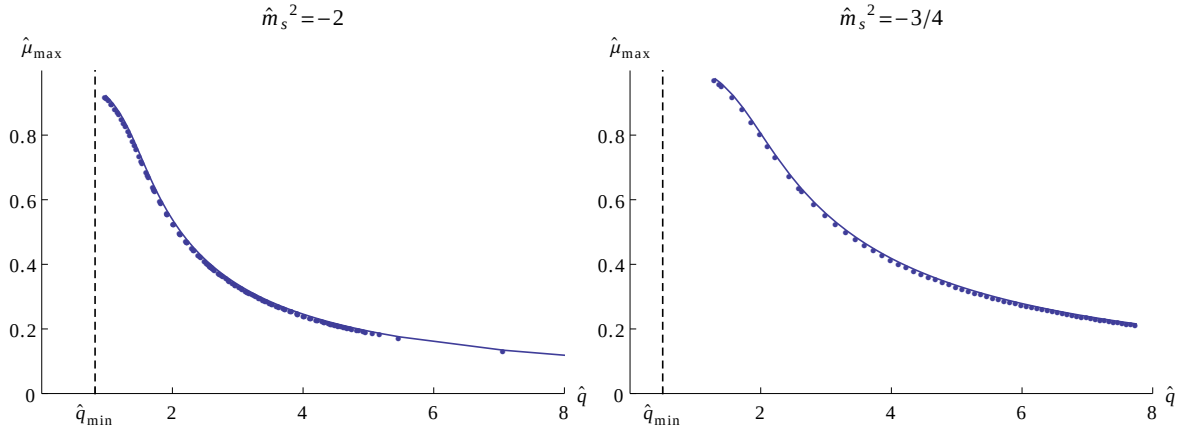


Figure 3.2: Maximum value $\hat{\mu}_{\max}$ of the local chemical potential $\hat{\mu}_l = h/\sqrt{f}$ reached in the HSC solution, as a function of $\hat{q}$, for (a) $\hat{m}_s^2 = -2$ and (b) $\hat{m}_s^2 = -3/4$.

critical elementary charge $\hat{q}_c$ at fixed $\hat{m}_f$ by

$$\hat{\mu}_{\max}(\hat{q}_c, \hat{m}_s) = \hat{m}_f\,. \tag{3.8}$$

When the condition (3.7) is satisfied, in the region of spacetime where the fluid is non-trivial, i.e. for $r_1 < r < r_2$, one has to take into account the contribution of the fluid to Einstein-Maxwell equations to get a totally backreacted solution. The fluid will contribute

and modify the boundary quantities, as the mass, the total charge of the system or the value of the condensate. This has been done first in [1] and [62]. In these models, the action is

$$S = \int \mathrm{d}^4x\sqrt{-g}\left[\frac{1}{2\kappa^2}\left(R + \frac{6}{L^2}\right) - \frac{1}{4e^2}F_{ab}F^{ab}\right] + S_{\text{matter}} + S_{\text{bdry}} \tag{3.9}$$

where

$$S_{\text{matter}} = S_{\text{scalar}} + S_{\text{fluid}} \tag{3.10}$$

is the action for a charged scalar field and a perfect fluid of charged fermions (see Section 2.4). In particular, the action for the scalar field is

$$S_{\text{scalar}} = -\frac{1}{2}\int \mathrm{d}^4x\sqrt{-g}\left[|\partial_a\psi - iqA_a\psi|^2 + m_s^2|\psi|^2 + u|\psi|^4\right] . \tag{3.11}$$

The work of [62] considered the case $u \neq 0$, leading to new Lifshitz solutions involving both non-trivial scalar field and fluid, while the work of [1] focused on the case $u = 0$.

## 3.3 A holographic Bose-Fermi model

In the model (3.9-3.11), the fluid of fermions and the scalar field are not directly coupled and only interact through the exchange of photons. However, as we discussed in Section 3.1, we expect them to interact directly. This will be implemented in the following model.

Let us consider Einstein-Maxwell theory coupled to matter fields consisting of a charged scalar field and a perfect fluid of charged fermions with an action given by (3.9) where the action for the matter fields is

$$S_{\text{matter}} = \int \mathrm{d}^4x\sqrt{-g}\left(\mathcal{L}_{\text{scalar}} + \mathcal{L}_{\text{fluid}} + \mathcal{L}_{\text{int}}\right) . \tag{3.12}$$

The scalar field and the fluid interact through the Lagrangian $\mathcal{L}_{\text{int}}$. We focus the analysis on the case where $u = 0$ in (3.11), so the Lagrangian density of the scalar field $\psi$ is

$$\mathcal{L}_{\text{scalar}} = -\frac{1}{2}\left(|\nabla\psi - iqA\psi|^2 + m_s^2|\psi|^2\right) . \tag{3.13}$$

As before, we will take the scalar field to be dual to a relevant operator such that $-9/4 < \hat{m}_s^2 < 0$. When the Lagrangian of interaction $\mathcal{L}_{\text{int}}$ vanishes, the system reduces to the one studied in [1]. We will come back regularly to the results of this particular case.

### 3.3.1 An action for the fluid

In the electron star model, an action for the fluid was not necessary to compute the solution. The local chemical potential and the fluid quantities were naturally defined in terms of the metric and the gauge field. Here, however, we will need to define an action for the fluid to describe correctly its coupling to the scalar field. Such an action can be defined by introducing Clebsch potentials (see e.g. [39]).

The action for a perfect fluid of particles of elementary charge $q_f$ is

$$\mathcal{L}_{\text{fluid}} = -\rho(n) + nu^a\left(\partial_a\phi + q_fA_a\right) + \lambda(u^au_a + 1) , \tag{3.14}$$

where $\rho$ is the energy density, $n > 0$ the particle number density, $u^a$ the velocity, $\phi$ a Clebsch coefficient, $\lambda$ a Lagrange multiplier and $q_f$ the elementary charge of the fermions. To keep the fluid approximation valid for the fermions, we consider a direct coupling

$$\mathcal{L}_{\text{int}} = \eta J_a^{\text{fluid}} J^a_{\text{scalar}} \tag{3.15}$$

between the scalar field and the fluid through their respective electromagnetic currents, given by (2.37) and (2.84), where $\eta$ parametrizes the intensity of the coupling and can have either sign.

The fluid quantities are encoded in the field equations of $n$, $u^a$, $\phi$ and $\lambda$ resulting from the Lagrangian $\mathcal{L}_{\text{fluid}} + \mathcal{L}_{\text{int}}$. The field equation for $\lambda$ gives the normalizability condition $u^a u_a = -1$ for the fluid velocity. The equation for the particle number density $n$ is

$$\rho'(n) = u^a \left(\partial_a \phi + q_f A_a + \eta q_f J_a^{\text{scalar}}\right) . \tag{3.16}$$

On physical grounds, $\rho'(n)$ is identified with the chemical potential for particle number which is then given by

$$\widetilde{\mu}_l(n) = \rho'(n) = u^a \left(\partial_a \phi + q_f A_a + q_f \eta J_a^{\text{scalar}}\right) . \tag{3.17}$$

We see that when $\eta \neq 0$, the local chemical potential depends explicitly on the scalar field. The field equation of $\phi$ gives the continuity equation

$$\nabla_a J^a_{\text{fluid}} = 0 \tag{3.18}$$

of the fluid current. We define the pressure $p$ through the thermodynamical relation

$$p(n) \equiv -\rho(n) + n\widetilde{\mu}_l(n) . \tag{3.19}$$

Finally, notice that the field equation for the velocity $u^a$,

$$n \left(\partial_a \phi + q_f A_a + \eta q_f J_a^{\text{scalar}}\right) + 2\lambda u_a = 0 , \tag{3.20}$$

allows to determine the Lagrange multiplier as

$$\lambda = \frac{1}{2}\widetilde{\mu}_l n . \tag{3.21}$$

In what follows we set $\partial_a \phi = 0$, so the chemical potential is given by

$$\widetilde{\mu}_l(n) = q_f u^a (A_a + \eta J_a^{\text{scalar}}) . \tag{3.22}$$

This is a choice for the model, since we could in principle allow for a non-zero 'intrinsic' chemical potential for particle number not related to the fermion charge $q_f$. However our choice avoids possible singularities, as discussed in [39].

The fluid is made of non-interacting fermionic particles. Consequently, the energy density $\rho(n)$ is an increasing function of the particle number density $n$ and the chemical potential for particle number $\widetilde{\mu}_l$ is positive for all $q_f$ (positive or negative). As for the electron star model, the particle number density $n$ and the energy density $\rho$ are functions of the local chemical potential (3.22) through the integrals (2.42). We will work instead with the chemical potential for charge density $\mu_l$ defined by (2.45) and the charge density $\sigma$ given by (2.44). Notice in particular that $\mu_l$ has the same sign as $q_f$ since $\widetilde{\mu}_l > 0$.

### 3.3.2 Field equations

We now give the field equations of the system. Einstein equations are

$$R_{ab} - \frac{1}{2}g_{ab}R - \frac{3}{L^2}g_{ab} = \kappa^2\left(T_{ab}^{\text{Mxwl.}} + T_{ab}^{\text{fluid}} + T_{ab}^{\text{scalar}}\right) \tag{3.23}$$

where the stress-energy tensors of the gauge field and the scalar field are given by (2.11) and (2.83), and $T_{ab}^{\text{fluid}}$ is the stress-tensor of the perfect fluid, given by (2.36). The field equation for the scalar field $\psi$ is the Klein-Gordon equation

$$-\left(\nabla_a - iqA_a - 2iq\eta J_a^{\text{fluid}}\right)\left(\nabla^a - iqA^a\right)\psi + m_s^2\psi = 0 \tag{3.24}$$

and Maxwell equations are written as

$$\nabla_a F^{ba} = e^2\left(J^b_{\text{fluid}} + J^b_{\text{scalar}} + J^b_{\text{int}}\right) . \tag{3.25}$$

Herein we have defined

$$J^a_{\text{int}} \equiv \frac{\delta\mathcal{L}_{\text{int}}}{\delta A_a} = -\eta q^2|\psi|^2\sigma u^a . \tag{3.26}$$

Notice that for $\eta = 0$ and $\psi = 0$, the field equations reduce to those of the electron star model, while for vanishing fluid quantities, one recovers the field equations of the holographic superconductor model.

As for the models presented in Chapter 2, we will make the homogeneous and isotropic ansatz

$$\begin{aligned} \mathrm{d}s^2 &= L^2\left[-f(r)\mathrm{d}t^2 + g(r)\mathrm{d}r^2 + \frac{1}{r^2}\left(\mathrm{d}x^2 + \mathrm{d}y^2\right)\right] , \\ A &= \frac{eL}{\kappa}h(r)\mathrm{d}t , \qquad \psi = \psi(r) , \qquad u^a = (u^t(r), 0, 0, 0) . \end{aligned} \tag{3.27}$$

From the normalizability condition $u_a u^a = -1$, the only non-zero component of the fluid velocity is $u^t = 1/(L\sqrt{f})$. Also, in order to simplify the notation and reduce the number of parameters, we perform the following parameter and field redefinitions,

$$\begin{aligned} A_a &= \frac{eL}{\kappa}\hat{A}_a , \qquad \psi = \frac{1}{\kappa}\hat{\psi} , \qquad m_s = \frac{1}{L}\hat{m}_s , \qquad q = \frac{\kappa}{eL}\hat{q} , \\ \eta &= e^2L^2\hat{\eta} , \qquad \mu_l = \frac{e}{\kappa}\hat{\mu}_l , \qquad \frac{m_f}{|q_f|} = \frac{e}{\kappa}\hat{m}_f , \qquad \beta q_f^4 = \frac{\kappa^2}{e^4L^2}\hat{\beta} , \\ \rho &= \frac{1}{\kappa^2L^2}\hat{\rho} , \qquad p = \frac{1}{\kappa^2L^2}\hat{p} , \qquad \sigma = \frac{1}{e\kappa L^2}\hat{\sigma} . \end{aligned} \tag{3.28}$$

These rescalings are similar to these performed for the electron star and the holographic superconductor models with in addition the rescaling of the current-current coupling constant $\eta$. In particular, the rescaled fluid quantities are given by

$$\begin{aligned} \hat{\rho} &= \hat{\beta}\int_{\hat{m}_f}^{|\hat{\mu}_l|}\mathrm{d}\epsilon\ \Theta\left(\epsilon - \hat{m}_f\right)\epsilon^2\sqrt{\epsilon^2 - \hat{m}_f^2} , \\ \hat{\sigma} &= \text{sign}(\hat{\mu}_l)\,\hat{\beta}\int_{\hat{m}_f}^{|\hat{\mu}_l|}\mathrm{d}\epsilon\ \Theta\left(\epsilon - \hat{m}_f\right)\epsilon\sqrt{\epsilon^2 - \hat{m}_f^2} , \\ \hat{p} &= -\hat{\rho} + \hat{\mu}_l\hat{\sigma} . \end{aligned} \tag{3.29}$$

This is because since $\widetilde{\mu}_l > 0$ for all $q_f$, we can still apply the computation of Section 2.4.1 to get the rescaled fluid quantities $\hat{\rho}$ and $\hat{\sigma}$. We allow for both signs of $q_f$, i.e. we allow for the possibility of the fluid to be made up of particles (electrons, $q_f > 0$) and antiparticles (holes, or positrons, $q_f < 0$). For $|\hat{\mu}_l| < m_f$, $\hat{\rho} = \hat{\sigma} = \hat{p} = 0$ due to the Heaviside step functions, and there is no fluid.

With the ansatz (3.27) and the rescalings (3.28), the constants $e$, $L$ and $\kappa$ disappear from the field equations. The $r$-component of Maxwell equations is given by (2.85), so we now consider $\hat{\psi}$ as a real scalar field. The field equations are then [2]

$$\hat{\psi}'' + \left(\frac{f'}{2f} - \frac{g'}{2g} - \frac{2}{r}\right)\hat{\psi}' + g\left(\frac{\hat{q}^2h^2}{f} - \hat{m}_s^2 - 2\hat{q}^2\hat{\eta}\frac{h}{\sqrt{f}}\hat{\sigma}\right)\hat{\psi} = 0\,, \tag{3.30a}$$

$$h'' - \frac{1}{2}\left(\frac{f'}{f} + \frac{g'}{g} + \frac{4}{r}\right)h' - g\left(\sqrt{f}\hat{\sigma} + \hat{q}^2h\hat{\psi}^2 - \hat{q}^2\hat{\eta}\sqrt{f}\hat{\sigma}\hat{\psi}^2\right) = 0\,, \tag{3.30b}$$

$$g' + \left(\frac{5}{r} + \frac{rh'^2}{2f} + \frac{r}{2}\hat{\psi}'^2\right)g + \left[\frac{r}{2}\left(\frac{\hat{q}^2h^2}{f} + \hat{m}_s^2\right)\hat{\psi}^2 + r(\hat{\rho} - 3)\right]g^2 = 0\,, \tag{3.30c}$$

$$f' + \left[rg(\hat{p} + 3) - \frac{1}{r} + \frac{1}{2}r\hat{\psi}'^2 + \frac{r}{2}g\left(\frac{\hat{q}^2h^2}{f} - \hat{m}_s^2\right)\hat{\psi}^2\right]f - \frac{1}{2}rh'^2 = 0\,. \tag{3.30d}$$

They are invariant under the transformations (2.65). Notice that the fluid quantities are functions of the local chemical potential, given by

$$\hat{\mu}_l = \frac{h}{\sqrt{f}}\left(1 - \hat{\eta}\hat{q}^2\hat{\psi}^2\right)\,. \tag{3.31}$$

The fluid parameters $m_f$, $q_f$ and $\beta$ appear in the field equations (3.30) only through the rescaled quantities $\hat{m}_f$ and $\hat{\beta}$. When working with these rescaled quantities, the fermionic charge $q_f$ drops out of the equations, and its sign is encoded in the sign of $\hat{\mu}_l$.

The bulk fluid is made up of 4d Dirac fermions, thus we can have physical states with either sign of the charge. In our conventions, Dirac particles (which we call electrons) have $q_f > 0$, antiparticles (or holes, or positrons) have $q_f < 0$. Thus, a positive chemical potential will fill particle-like states, and a negative one hole-like states.

For the electron star mode (see Section 2.4), the sign of the local chemical potential $\hat{\mu}_l$ is dictated by the sign of the electric potential and it is the same throughout the bulk (for example, it is non-negative if the boundary value of the electric potential is positive). On the other hand, we will see that for the system (3.30), it happens that the sign of the chemical potential is not determined and there can be cases in which $\hat{\mu}_l(r)$ has different signs in different bulk regions.

From Eqs. (3.29), we see that the fluid density is non-zero for $|\hat{\mu}_l| > \hat{m}_f$. The case $\hat{\mu}_l(r) > m_f$ corresponds to a fluid made out of positively charged particles (electrons), whereas a negative $\hat{\mu}_l(r) < -\hat{m}_f$ leads to a fluid of negatively charged particles (positrons). Notice that, in Eqs. (3.29), the energy density $\hat{\rho}(r)$ and the pressure $\hat{p}(r)$ are positive in both cases, whereas the charge density $\hat{\sigma}$ is positive or negative for the electrons and positrons fluids, respectively.

We will see in the next sections that, depending on the parameters, bulk solutions with various arrangements of differently charged fluids are possible (electrons, positrons, or both).

The relevant parameters of the model are thus:

$$\text{scalar: } (\hat{q}, \hat{m}_s)\,, \qquad \text{fluid: } (\hat{m}_f, \hat{\beta})\,, \qquad \text{interaction: } \hat{\eta}\,, \tag{3.32}$$

where the scalar field mass satisfies the $AdS_4$ BF bound $-9/4 < \hat{m}_s^2 < 0$ (i.e. the operator dual to $\psi$ is relevant). We restrict the analysis to the case where the scalar parameters satisfy (2.90) and the fermion mass satisfies $0 < \hat{m}_f < 1$. Then, the holographic superconductor of Section 2.5.2) and the electron star 2.4 are solutions of the system when there is no fluid and the scalar field is trivial, respectively.

### 3.3.3 UV asymptotics

We are looking for solutions dual to field theory states at finite density, so the metric and the gauge field must behave close to $r = 0$ as

$$r \to 0 : \qquad \frac{f(r)}{c^2} \sim g(r) \sim \frac{1}{r^2}\,, \qquad h(r) \sim c\left(\hat{\mu} - \hat{Q} r\right)\,. \tag{3.33}$$

It means in particular that the local chemical potential vanishes close to the UV boundary as

$$\hat{\mu}_l \sim \hat{\mu}\, r, \qquad r \to 0\,, \tag{3.34}$$

so the fluid quantities vanish in the near-boundary region. Thus, if the fluid is present in part of the bulk spacetime, it contributes to the UV asymptotics only through the total charge $\hat{Q}$ (and the chemical potential) appearing in (3.33). As for the holographic superconductor model, we will take the scalar field to be a purely normalizable mode to exhibit a possible spontaneous breaking of the boundary $U(1)$ symmetry. In this case one can compute perturbatively the solution in the UV region and obtains the same asymptotics (2.97) as for the holographic superconductor solution.

### 3.3.4 Solutions at finite density

Given that the UV is fixed to be $AdS_4$ with a non-vanishing electric flux, we already know three solutions to the field equations (3.30) at zero temperature. These are:

- **ERN:** The Extremal Reissner-Nordström black hole (see Section 2.3), which is a solution with trivial scalar field and fluid, $\hat{\psi} = 0$ and $\hat{\sigma} = \hat{\rho} = 0$. The electric charge is all carried by the black hole, corresponding to a completely fractionalized phase, there are no (gauge-invariant) charge carriers in the dual field theory state.

- **ES:** The Electron Star (see Section2.4), where the scalar field is trivial, $\hat{\psi} = 0$. The charge is completely carried by the fluid of electrons. In the dual field theory state, the charge is carried by fermionic degrees of freedom.

- **HSC:** The Holographic Superconductor (see Section2.5.2), where the fluid is trivial, $\hat{\sigma} = \hat{\rho} = 0$. In this case, the charge is carried by the scalar field and has the dual field theory interpretation of a superconducting state.

In addition to these known branches, the discussion of Section 3.2 suggests that there may be other solutions where the charge would be carried both by the scalar field and the fluid of fermions. In particular, as discussed in Section 3.2.2, one can start from the HSC solution in the near-horizon region and take into account the backreaction of the fluid when it can form, that is when the condition (3.7) is satisfied. The analysis of Section 3.2.2 is applicable only when the scalar field and the fluid do not interact directly, that is when

$\hat{\eta} = 0$ in which case the local chemical potential is given by $\hat{\mu}_l = h/\sqrt{f}$. This has been used in [1] to obtain new holographic solutions dual to field theory states exhibiting both a charged scalar condensate and fermionic degrees of freedom. The gravitational solutions consists of a fluid of electrons confined in a shell $r_1 < r < r_2$ together with a non-trivial scalar field everywhere in the bulk spacetime and have been called 'compact stars' [1]. For $r > r_2$, the solution is the same as for the HSC, given by (2.88). The solution for $r < r_1$ is modified compared to the case of the HSC, however the asymptotic solution close to the UV boundary is still given by (2.97) as discussed in Section 3.3.3.

The compact star solutions of [1] have been obtained by considering that the fluid quantities vanish in the near-horizon geometry. One can imagine that there could exist solutions for which the scalar field and the fluid coexist in this region. This would require that the local chemical potential – and consequently the fluid quantities – become constant for $r \to \infty$. Another possibility is that the fluid quantities diverge at infinity, but this is hardly acceptable. The authors of [1] have tried to obtain solutions where the fluid quantities become constant at infinity in the presence of the scalar field, but it appears that such solutions do not seem to exist for $\hat{m}_s^2 < 0$. In fact, for $\hat{m}_s^2 > 0$, the model admits exact Lifshitz-like solutions (given in Appendix B) where the fluid quantities and the scalar field are constant [1]. However these solutions, taken to be the near-horizon solution, are not expected to connect to the UV $AdS_4$ geometry (3.33) because the field theory scalar operator dual to $\hat{\psi}$ is an irrelevant operator which does not permit to 'escape' from the near-boundary geometry.

Lifshitz-like solutions with non-trivial scalar field and fluid can be obtained for $\hat{m}_s^2 < 0$ when the scalar field admits a quartic interaction, i.e. $u \neq 0$ in (3.11). These solutions have been found in [62] and do connect to the near-boundary $AdS_4$ geometry. In this case the fluid quantities vanish at a point of the bulk spacetime which defines the star boundary. Solutions similar to the compact star solutions of [1] have also been found in [62]. In this case the near-horizon geometry is given by the Lifshitz-invariant holographic superconductor solution of [52], and the fluid of electrons is confined in a shell of the bulk spacetime.

Let us now come back to the system (3.30). By using the same arguments that we gave in Section 3.2.2 and [1], one can also construct new solutions in the case where the bulk bosonic and fermionic degrees of freedom interact directly, i.e. for $\hat{\eta} \neq 0$. The first step is to look at the behaviour of the local chemical potential (3.31) in the HSC solution. It vanishes asymptotically both in the UV and in the IR and admits at least one extremum value in the bulk. In the UV, the behaviour of $\hat{\mu}_l$ is given by (3.34). In the IR, it is given by

$$\hat{\mu}_l \sim h_0\, r^{\delta+1}\, (\log r)^{1/2} \left[-4\hat{\eta}\hat{q}^2 \log r + 1\right] + \dots\,, \qquad r \to \infty\,. \tag{3.35}$$

Again, the system is invariant under charge conjugation which acts on the gauge field and the scalar elementary charge by (2.94). We thus choose $h_0$ to be positive, i.e. $h(r) > 0$ in the whole spacetime, such that the boundary chemical potential $\hat{\mu}$ and the total charge $\hat{Q}$ are positive.

For $\hat{\eta} > 0$ the local chemical potential $\hat{\mu}_l$ is negative in the IR, so $\hat{\mu}_l$ has both a negative minimum value and a positive maximum value at finite radii $r_{\min}$ and $r_{\max}$ in the bulk, with $r_{\min} > r_{\max}$. For $\hat{\eta} \leq 0$, the behaviour of $\hat{\mu}_l$ is similar to what happens in the compact star solutions of [1], where it is always positive and admits a maximum. We recall that the IR free parameter $h_0$ is chosen such that the scalar field is a pure normalizable mode in the near-boundary region.

Therefore, in addition to the ERN, ES and HSC, we have found in [2] three kinds of new solutions dual to field theory states at finite density:

- **Compact electron star (eCS)** : a fluid density is confined in a shell whose boundaries $r_1^e$ and $r_2^e$ satisfy $\hat{\mu}_l(r_i^e) = \hat{m}_f$, $i = 1, 2$. The charge density of the fluid is positive, then the fluid is made of electrons. This situation is displayed in Figure 3.3.

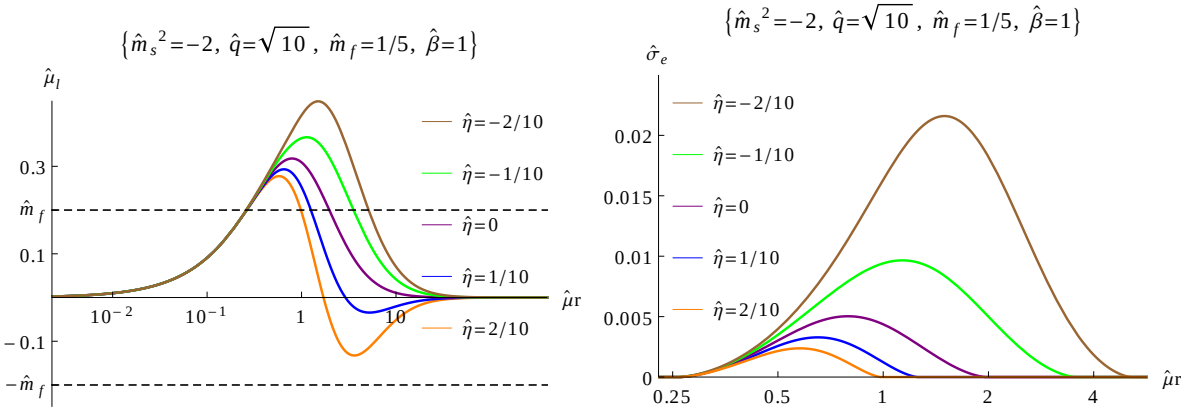


Figure 3.3: Profiles of (a) the local chemical potential and (b) the fluid charge density for eCS solutions.

- **Compact positron star (pCS)** : a fluid density is confined in a shell whose boundaries $r_1^p$ and $r_2^p$ satisfy $\hat{\mu}_l(r_i^p) = -\hat{m}_f$, $i = 1, 2$. The charge density of the fluid is negative, thus the fluid is made of positrons. This situation is displayed in Figure 3.4.

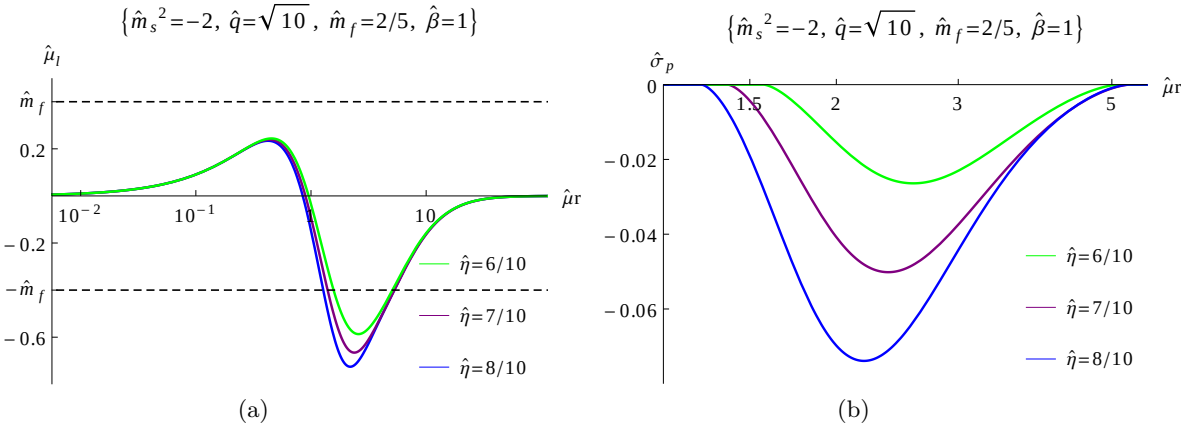


Figure 3.4: Profiles of (a) the local chemical potential and (b) the fluid charge density for pCS solutions.

- **Compact positron/electron stars (peCS)** : In this case, the solution exhibits charge polarization in the bulk: two fluid shells of opposite charges are confined in distinct regions of spacetime, bounded respectively by $(r_1^e, r_2^e)$ and $(r_1^p, r_2^p)$ determined

by the equations

$$\hat{\mu}_l(r_1^e) = \hat{\mu}_l(r_2^e) = \hat{m}_f\,, \qquad \hat{\mu}_l(r_1^p) = \hat{\mu}_l(r_2^p) = -\hat{m}_f. \tag{3.36}$$

The fluid in one region is made of electrons, the one in the other region of positrons. Clearly, for this solutions to exist, the chemical potential must change sign in the bulk. Due to fixed UV asymptotics of the local chemical potential, the fluid of electrons is situated closer to the UV boundary than the fluid of positrons. This situation is displayed in Figure 3.5.

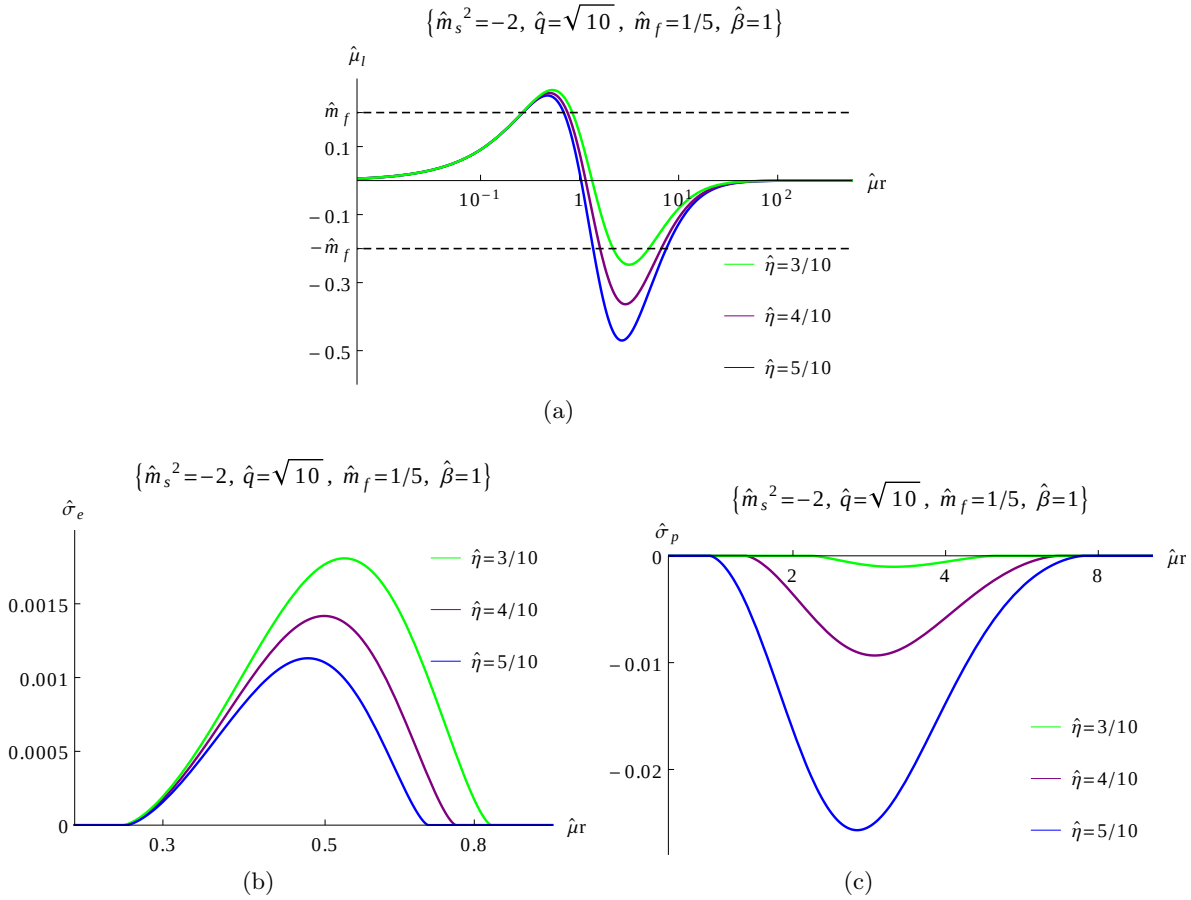


Figure 3.5: Profiles of (a) the local chemical potential, (b), (c) the fluid charge densities for peCS solutions.

The kind of compact star(s) (CS) solutions that may exist depends on the maximum and minimum values of the local chemical potential,

$$\hat{\mu}_{\max}(\hat{m}_s^2, \hat{q}, \hat{m}_f, \hat{\beta}, \hat{\eta}) \equiv \max_{0<r<\infty} \hat{\mu}_l(r)\,, \qquad \hat{\mu}_{\min}(\hat{m}_s^2, \hat{q}, \hat{m}_f, \hat{\beta}, \hat{\eta}) \equiv \min_{0<r<\infty} \hat{\mu}_l(r)\,. \tag{3.37}$$

The possible outcomes are summarized in Table 3.1. We denote the case where no compact star(s) exists by 'noCS'. Notice that $\hat{\mu}_{\max} > 0$ for all $\hat{\eta}$; $\hat{\mu}_{\min}$ is negative when $\hat{\eta} > 0$ and vanishes for $\hat{\eta} \leq 0$. When $\hat{\eta} \leq 0$, the local chemical potential is positive in the whole spacetime and only compact star solutions of the eCS kind can form.

| | $\hat{\mu}_{\min} < -\hat{m}_f$ | $\hat{\mu}_{\min} > -\hat{m}_f$ |
|---|---|---|
| $\hat{\mu}_{\max} > \hat{m}_f$ | peCS, pCS, eCS | eCS |
| $\hat{\mu}_{\max} < \hat{m}_f$ | pCS | noCS |

Table 3.1: Conditions on the minimal and maximal values of the local chemical potential for the existence of the compact star(s) solutions. For given parameters, if the peCS solution exists, the pCS and eCS are also solutions to the system. 'noCS' means that no compact star(s) solution exists, because $|\hat{\mu}_l(r)| < \hat{m}_f$ everywhere in the bulk.

## 3.4 Phase diagrams of charged solutions

In Section 3.3.4 we have seen that different arrangements of fermionic fluids are possible at zero temperature. Depending on the parameter values, we can go from the pure condensate with no fermions (HSC), purely positive or purely negative confined fluid shells (eCS and pCS respectively), and polarized shells of positive/negative charged fluid regions (peCS). In all these configurations, the fermionic charges are surrounded by the scalar condensate, which dominates the UV and IR geometry and confines the fluid in finite regions of the bulk.

Here we determine which is the solution that has the lowest free energy and dominates the grand-canonical ensemble for a given choice of parameter. We work at zero temperature and fixed (boundary) chemical potential $\hat{\mu}$. Thus, different solutions will in general have different charges.

We already know that, when they exist, the ES and the HSC solutions are thermodynamically favoured with respect to ERN black hole (see Figures 2.6 and 2.8). To see whether the CS solutions are favoured or not, we shall compare their free energy, which is obtained by computing the on-shell Euclidean action, with the one of the other solutions. But it turns out that as for the ES and HSC solutions, the free energy for the CS solutions can be put in the form (see Section 2.4.4)

$$\hat{\Omega} = -\frac{1}{3} c_{\rm CS} \hat{\mu}^3 \,. \tag{3.38}$$

The constant $c_{\rm CS}$ and the corresponding constant for the other branches ERN, HSC and ES, are given by

$$c_i = \frac{\hat{Q}_i(\hat{\mu})}{\hat{\mu}^2} \,, \qquad i = \text{peCS}, \text{pCS}, \text{eCS}, \text{HSC}, \text{ES}, \text{ERN}, \tag{3.39}$$

where the charge $\hat{Q}_i$ and the chemical potential $\hat{\mu}$ are read off from the UV asymptotics for each type of solution. Thus, to determine which solution has the smallest free energy, we must compare the values of the constants $c_{\rm ERN}$, $c_{\rm HSC}$, $c_{\rm ES}$ and $c_{\rm CS}$.

We performed this analysis numerically on the solutions described in Section 3.3.4. We checked the relation (3.39) numerically on the various branches, it is obeyed with great accuracy on a large range of values of $\hat{\mu}$ and $\hat{Q}$. This both confirms the validity of (3.39), and constitutes a check of our numerical procedure. The results of the numerical analysis reveal a rich phase diagram, with the interplay of various phase transitions as we shall see now.

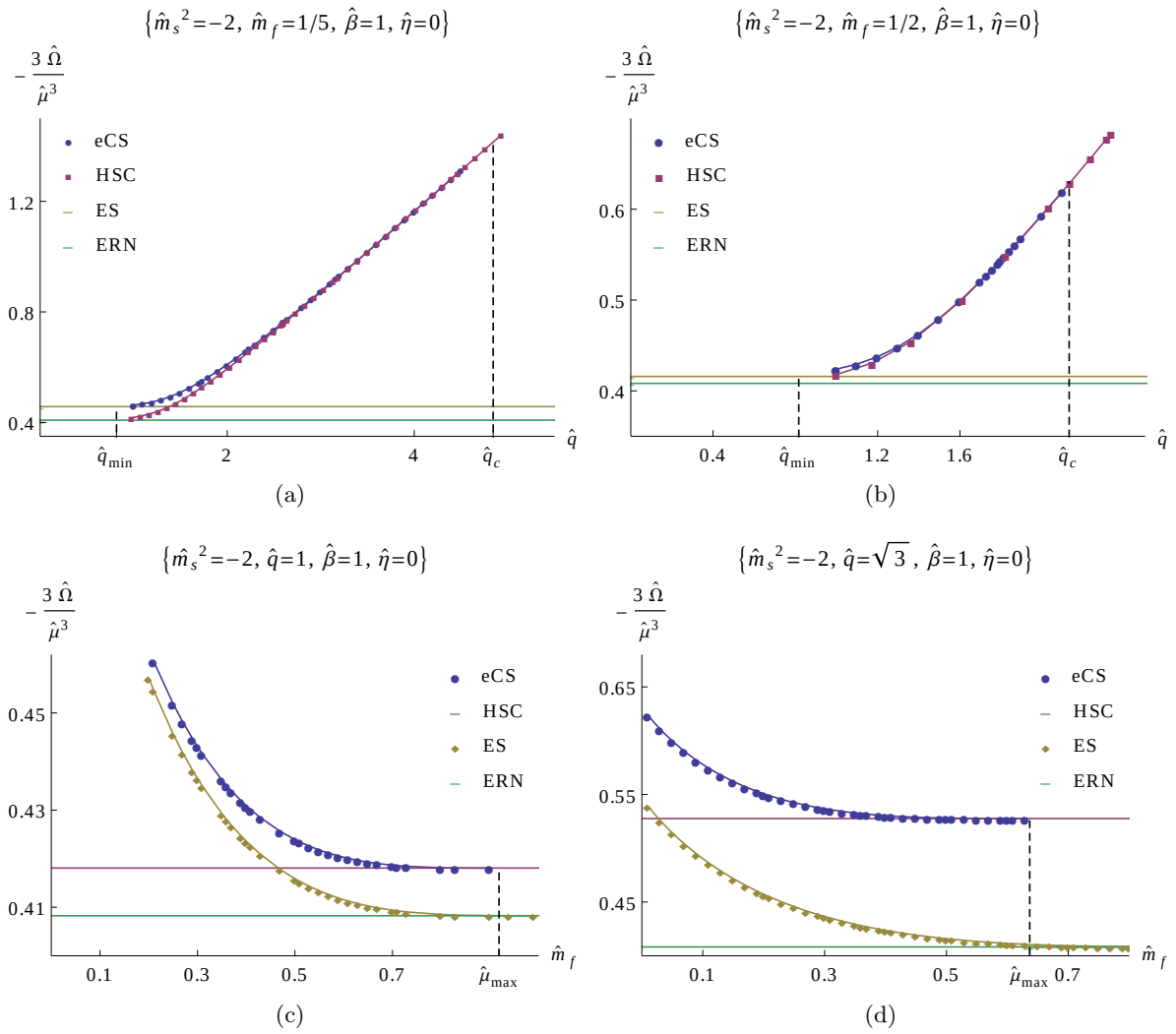


Figure 3.6: Free energy (normalized to the chemical potential) of the four competing solutions, for fixed scalar mass $\hat{m}_s^2 = -2$ and $\hat{\eta} = 0$. In (a) and (b) $\hat{\Omega}$ is plotted as a function of $\hat{q}$ for two fixed values of the fermionic mass $\hat{m}_f$. The HSC and the eCS solution are unknown for $\hat{q} < \hat{q}_{\min}$, whereas the ES and the ERN continue past this point. In (c) and (d) $\hat{\Omega}$ is a function of $\hat{m}_f$ for two fixed values of the scalar field charge . The eCS solution exists only for $\hat{m}_f < \hat{\mu}_{\max}$, where it merges with the HSC. The ES merges with the ERN solution as $\hat{m}_f \to 1$.

### 3.4.1 Free energy and phase diagrams for $\hat{\eta} = 0$

The free energy in the case where the scalar field and the fluid are not coupled directly, i.e. $\hat{\eta} = 0$, has been obtained in [1]. It is displayed in Figures 3.6 and 3.7. In this case the local chemical potential is defined positive and only eCS solutions can form (see Table 3.1). The figures show that the eCS solution is favoured in the region where it exists. There is a crossing of the HSC and ES branches but, as far as we could determine, it is always in the region where the eCS solution is favoured so it does not correspond to a phase transition.

There is instead a phase transition at the point where the eCS branch ceases to exist and it connects to the HSC solution (at $\hat{q} = \hat{q}_c$ for fixed $\hat{m}_f$, where $\hat{q}_c$ is defined by (3.8)).

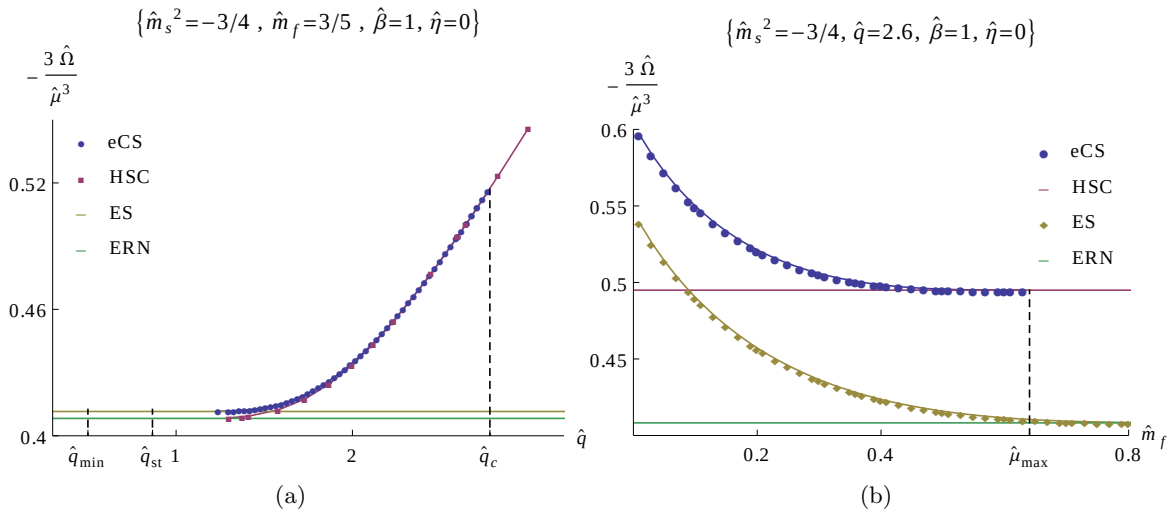


Figure 3.7: Free energy (normalized to the chemical potential) of the four competing solutions, for fixed scalar mass $\hat{m}_s^2 = -3/4$, (a) as a function of $\hat{q}$ for a fixed value of $\hat{m}_f$, (b) as a function of $\hat{m}_f$ for a fixed value of $\hat{q}$. The lines are again merely for visual aid. The point $\hat{q}_{st} = \sqrt{3}/2$ is the stability bound of the ERN defined in (2.80). The stability bound of the ES $\hat{q}^\star_{st}$, defined in (3.5), is not displayed because it is very close to $\hat{q}_{st}$.

The transition appears to be of continuous type as a function of both $\hat{m}_f$ and $\hat{q}$, as can be seen from the figures. This is natural to expect if, as it seems to be the case, the eCS starts dominating at the point where it is allowed as a solution, i.e. on the curve $\hat{\mu}_{\max} = \hat{m}_f$, where it has the same free energy as the HSC solution. As a result we obtain the phase diagram of the system shown in Figure 3.8.

### 3.4.2 Free energy and phase diagrams for $\hat{\eta} \neq 0$

When the scalar field and the fermionic fluid couple directly, new solutions can arise in the system: a star made of negatively charged fermions can form, a positron star. The phase diagram thus becomes richer. We will focus in this section on the CS/HSC transitions obtained in [2]. In Section 3.4.4, we will analyse the transitions CS/ES and HSC/ERN.

We will first analyze what happens if we vary $\hat{\eta}$ keeping other parameters fixed (Figures 3.9a and 3.9b). As we have seen in Section 3.4.1, for $\hat{\eta} = 0$, whenever eCS solutions exist, they dominate the ensemble. Otherwise, the preferred solution is the HSC.

Let us first choose the parameters so that, for $\hat{\eta} = 0$, eCS is the preferred solution (Figure 3.9a): if we dial up a positive interaction term $\hat{\eta}$, eventually the effect of the condensate polarizes the star and, at a critical value $\hat{\eta}_* > 0$, we find a continuous transition to the peCS solution, which now is the one dominating the ensemble. The eCS keeps existing beyond the critical point $\hat{\eta}_*$, where we also see the emergence of a new pCS solution which starts dominating over the HSC solution but not over the peCS solution.

On the other hand, if we start from a point where, for $\hat{\eta} = 0$, there is no eCS solution (Figure 3.9b), we see that dialing up $\hat{\eta}$ either way one gets to a critical point where either a positive or a negative charged star will be formed, and dominate the ensemble henceforth.

For a given (positive) value of $\hat{\eta}$, the type of solution depends on the fermion mass $\hat{m}_f$, as shown in Figure 3.9c. At small mass, the polarized peCS solution dominates over the eCS and pCS solutions. As the mass is increased, one first encounters a continuous

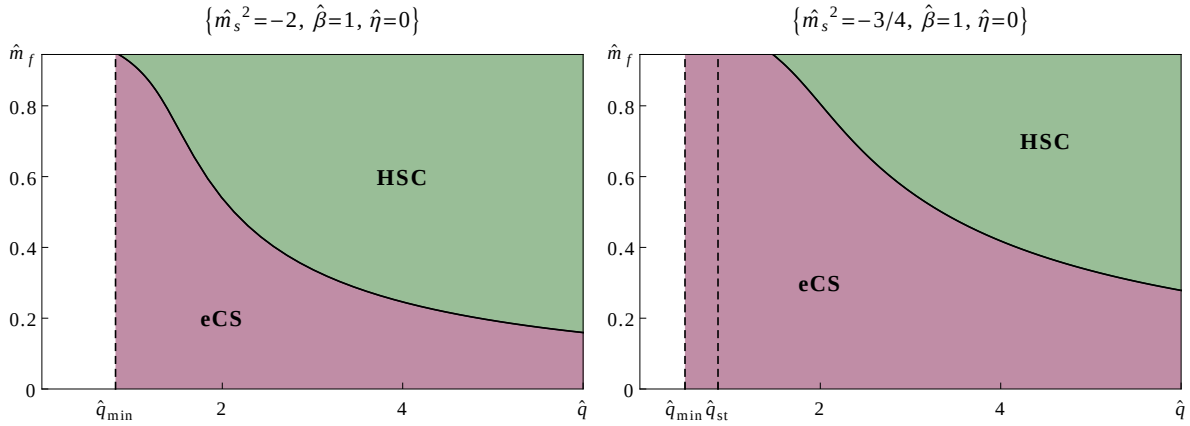


Figure 3.8: Phase diagram showing the transition between the HSC and the eCS solutions at vanishing coupling constant.

transition from the peCS to the pCS solution at the critical value $\hat{m}_{f_*}^{(1)}$. At this point, the (subdominant) eCS solution merges into the (subdominant) HSC solution. Then, at the second critical point $\hat{m}_{f_*}^{(2)}$ the charged fluid disappears and the solution merges into the HCS solution.

We have also analyzed the phase diagram as a function of the scalar charge $\hat{q}$. Phase diagrams of the system are displayed in Figure 3.10, in the plane $(\hat{m}_f, \hat{\eta})$ at fixed scalar charge $\hat{q}$ (Figure 3.10a) and in the plane $(\hat{m}_f, \hat{q})$ at fixed $\hat{\eta}$ (Figures 3.10b-3.10d). The critical lines separating the various phases correspond to the points where the maxima and minima of the local chemical potential are equal in absolute value to $\hat{m}_f$. The different colors correspond to the dominant phase in each region. Thus, all of these transitions are continuous and take place at the points where it is possible to fill the charged fermion states: whenever a fluid solution is possible by the condition $|\hat{\mu}_l| > \hat{m}_f$, that solution will form. Furthermore, solutions in which the charge is distributed between more fluid components are preferred.

### 3.4.3 Charge distribution and screening

In the CS solutions, the electric charge

$$\hat{Q} = \frac{\kappa}{eL}\frac{1}{V_2}\int_{V_2} \star F \tag{3.40}$$

of the system, where $V_2$ is the spatial volume of the field theory, is shared between the scalar field and the fluid(s). With the ansatz (3.27), the electric charge carried by the scalar field in the bulk is

$$\hat{Q}_{\rm scalar} = \int \mathrm{d}r\sqrt{-g}\, J^t_{\rm scalar} = \hat{q}^2 \int_0^\infty \mathrm{d}r \frac{\sqrt{g}}{r^2\sqrt{f}} h\hat{\psi}^2 \tag{3.41}$$

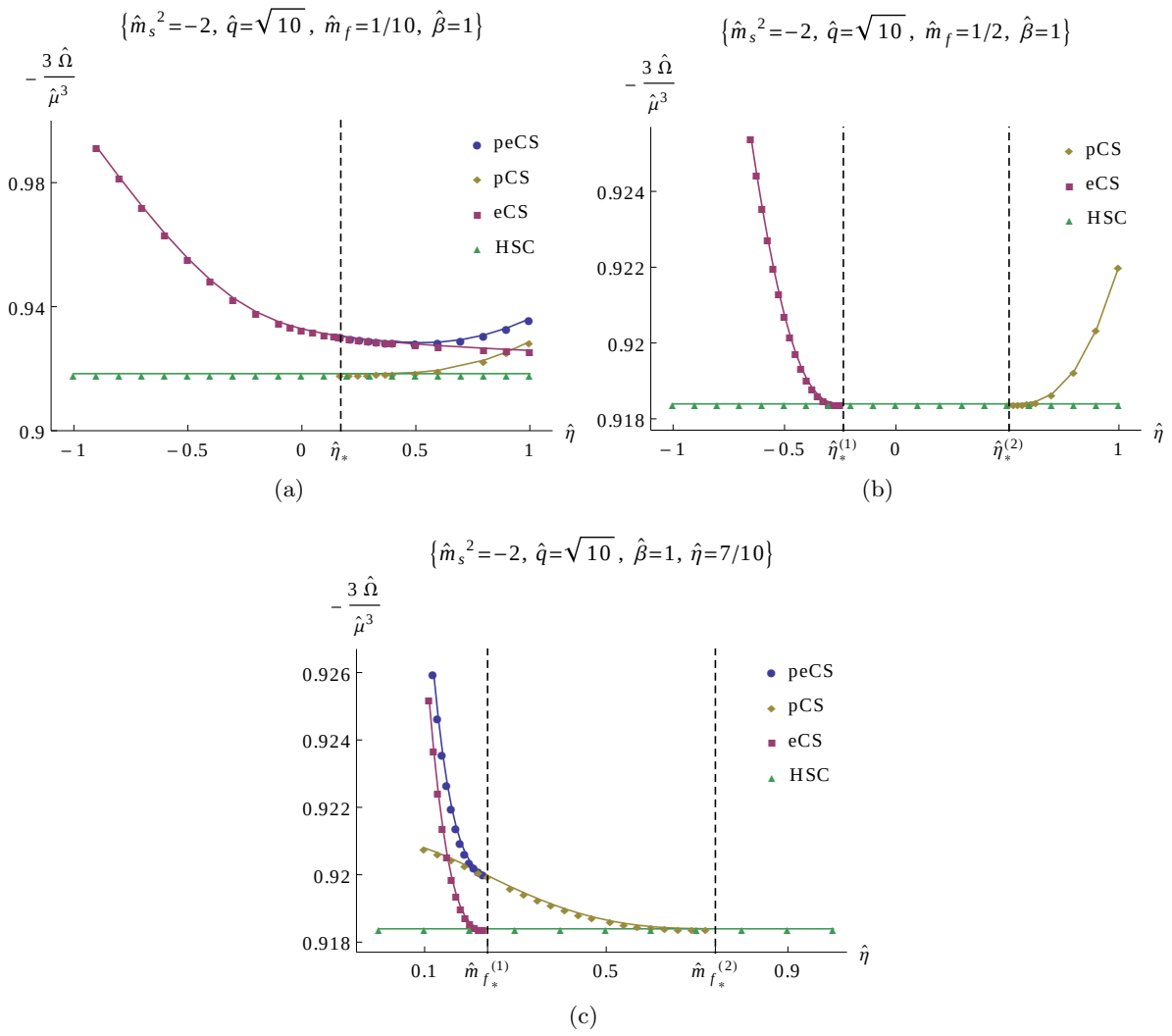


Figure 3.9: Free energy (normalized to the chemical potential). (a) displays the free energy as a function of $\hat{\eta}$ in the transition between eCS and peCS solutions, where $\hat{\eta}_* \simeq 0.17$ is the critical coupling constant. (b) displays the free energy as a function of $\hat{\eta}$ in the transition between eCS, HSC and pCS solutions; $\hat{\eta}_*^{(1)} \simeq -0.24$ and $\hat{\eta}_*^{(2)} \simeq 0.51$ are the critical coupling constants between the eCS and HSC solutions, and the HSC and pCS solutions, respectively. (c) displays the free energy as a function of $\hat{m}_f$ in the transition between peCS, pCS and HSC solutions; $\hat{m}_{f*}^{(1)} \simeq 0.24$ and $\hat{m}_{f*}^{(2)} \simeq 0.74$ are the critical coupling constants between the peCS and pCS solutions, and the pCS and HSC solutions, respectively. To avoid clutter, in (a), (b) and (c) we did not display the (normalized) free energy of the ES and the ERN solutions. They are much smaller than the free energy of the CS and HSC solutions: in (a) and (b), the free energy of the ES solution is equal to 0.49 and 0.42, respectively. In (c), it is between 0.41 and 0.49 depending on $\hat{m}_f$. In all cases, the free energy of the ERN solution is $1/\sqrt{6} \simeq 0.41$.

and the electric charges of the electron and positron fluids are respectively

$$\begin{aligned}\hat{Q}_{\rm e} &= \int {\rm d}r\sqrt{-g}\, J^t_{\rm fluid} = \int_{r_1^e}^{r_2^e} {\rm d}r \frac{\sqrt{g}}{r^2}\hat{\sigma}_{\rm e}\,,\\ \hat{Q}_{\rm p} &= \int {\rm d}r\sqrt{-g}\, J^t_{\rm fluid} = \int_{r_1^p}^{r_2^p} {\rm d}r \frac{\sqrt{g}}{r^2}\hat{\sigma}_{\rm p}\,,\end{aligned} \tag{3.42}$$

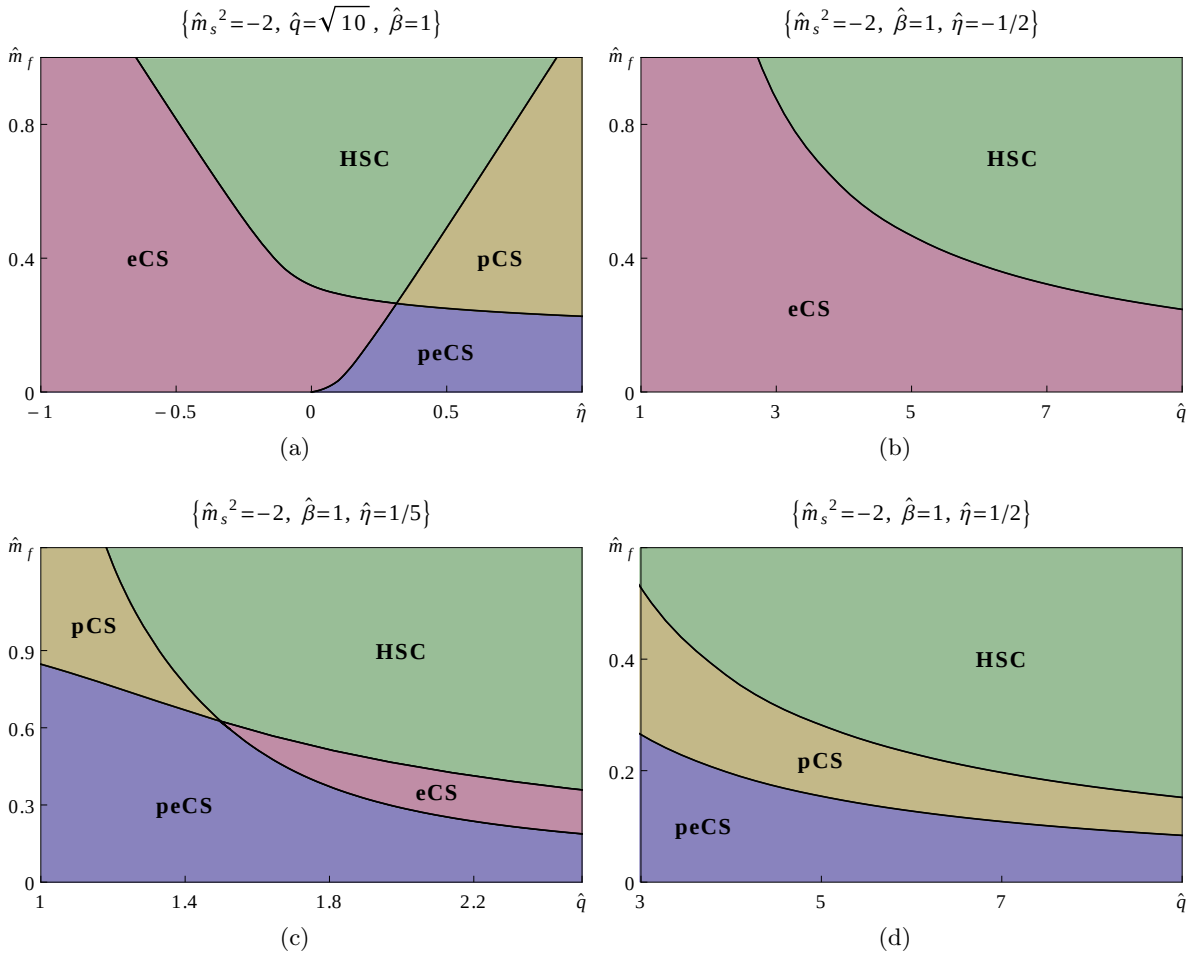


Figure 3.10: Phase diagrams of the CS/HSC transitions. The critical lines (solid black lines) correspond to the minimum and maximum values of the local chemical potential in the HSC solution, which can be seen from the plots the free energy of the different solutions (see Figure 3.9).

where $r_1^e$ and $r_2^e$ are the boundaries of the electron star, and similarly for the positron star. The charge densities of the electron fluid $\hat{\sigma}_{\rm e}$ and the positron fluid $\hat{\sigma}_{\rm p}$ are respectively positive and negative, and given by (3.29) with $\hat{\mu}_l$ respectively positive and negative.

Additionally, due to the current-current interaction term (3.15) and the fact that by Eq. (3.26) the scalar current is linear in the gauge field, there are *screening electric charges*, given by

$$\hat{Q}_{\rm int,e} = -\hat{\eta}\int_{r_1^e}^{r_2^e} {\rm d}r\,\frac{\sqrt{g}}{r^2}\,\hat{q}^2\hat{\psi}^2\,\hat{\sigma}_{\rm e}\,, \qquad \hat{Q}_{\rm int,p} = -\hat{\eta}\int_{r_1^p}^{r_2^p} {\rm d}r\,\frac{\sqrt{g}}{r^2}\,\hat{q}^2\hat{\psi}^2\,\hat{\sigma}_{\rm p}\,, \tag{3.43}$$

which reflect the interaction between the scalar and the fluid made of electrons and positrons, respectively, and it gets contributions from the regions where the fluid density is non-vanishing.

The total electric charge of the system[1]

$$\hat{Q} = \hat{Q}_{\text{scalar}} + \left(\hat{Q}_{\text{e}} + \hat{Q}_{\text{int,e}}\right) + \left(\hat{Q}_{\text{p}} + \hat{Q}_{\text{int,p}}\right) \tag{3.44}$$

matches the UV asymptotic behaviour of the gauge field (3.33),

$$\hat{Q} = -\frac{1}{c}h'(0) \tag{3.45}$$

where $c > 0$ satisfies

$$c^2 = \lim_{r\to 0} r^2 f(r) \tag{3.46}$$

as can be seen from (3.33). This has been verified numerically in all solutions we have constructed.

In Eq. (3.44), the second and third terms represent the total contributions from each charged fluid. Despite the possible presence of local negative charge components, we will show below that all three terms in Eq. (3.44) are positive for all solutions under considerations. This is consistent with our choice $\hat{\mu} > 0$ for the boundary chemical potential in the UV asymptotics (3.33), which implies that the boundary charge $\hat{Q}$ must be positive in all solutions.

To be compared, the physical quantities of different solutions must be given at fixed chemical potential $\hat{\mu}$. The field equations are invariant under (2.65). In particular, the transformations (2.65a) generate physically different solutions through (2.96) and can be used to obtain the different solutions at fixed chemical. Equivalently, one can compare quantities invariant under (2.65a). For the charges, the ratio $\hat{Q}_i/\hat{Q}$ is obviously invariant. For the condensate, the ratio $\langle\mathcal{O}\rangle/\hat{\mu}^{\Delta}$ is invariant.

Let us first consider the scalar field condensate contribution to the total charge. As a consequence of the choice $\hat{\mu} > 0$ in the UV, the electric potential $h(r)$ is positive throughout the bulk[2]. Thus, from Eq. (3.41), one can see that the electric charge of the scalar field $\hat{Q}_{\text{scalar}}$ is positive.

Due to the signs of the local charge densities in (3.42), $\hat{Q}_{\text{e}}$ is positive, and $\hat{Q}_{\text{p}}$ is negative. However, the latter is over-screened by the scalar field through the charge of interaction $\hat{Q}_{\text{int,p}}$, so that $\left(\hat{Q}_{\text{p}} + \hat{Q}_{\text{int,p}}\right) > 0$. This can be seen from Eq. (3.42-3.43) and the fact that, inside the positron fluid, $(1 - \hat{\eta}\hat{q}^2) < 0$, since by Eq. (3.31) this quantity determines the sign of the chemical potential.

By a similar reasoning, $\hat{Q}_{\text{int,e}}$ is positive (negative) for $\hat{\eta} < 0$ ($\hat{\eta} > 0$), but $\left(\hat{Q}_{\text{e}} + \hat{Q}_{\text{int,e}}\right)$ is always positive. Thus, for electrons, there may be charge screening or anti-screening, but never over-screening.

The previous discussion gives a qualitative understanding of why the polarized electron-positron compact stars are stable configurations: although the positron and electron parts of the fluid are made up of positive and negative charge fermionic constituents, respectively, the screening of the negative electric charge by the scalar condensate renders the total charge positive in both fluids. In particular, for peCS solutions, the two charged shells experience electromagnetic repulsion, rather than attraction. Gravitational and electromagnetic forces balance each other, which makes the solution stable.

[1] In all our solutions except the extremal Reissner-Nordström black hole, there is no charged event horizon and the electric charge is shared between the fluid(s) and the scalar field.

[2] There can be, in principle, solutions with HSC IR and UV asymptotics in which $h(r)$ changes sign, but these are expected to have larger free energy [51].

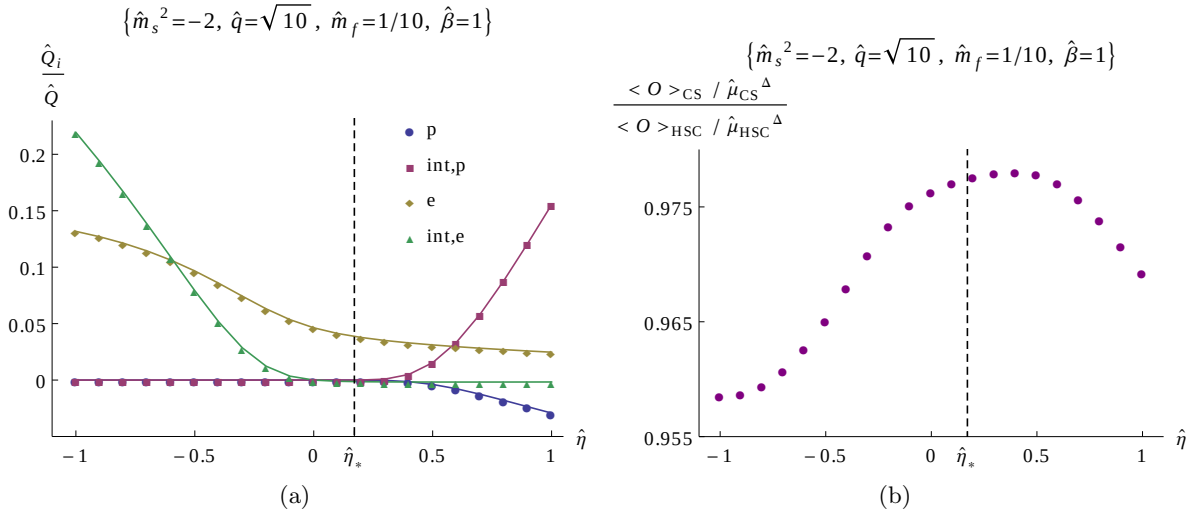


Figure 3.11: (a) Distribution of the electric charge components and (b) value of the condensate in the compact star(s) solutions corresponding to the choice of parameters in Figure 3.9a. To avoid cluttering of the figures, the electric charge of the scalar field $\hat{Q}_{\text{scalar}}$ is not displayed. The dashed line at the critical value $\hat{\eta}_* \simeq 0.17$ marks the transition between the eCS and peCS solutions visible in Figure 3.9a.

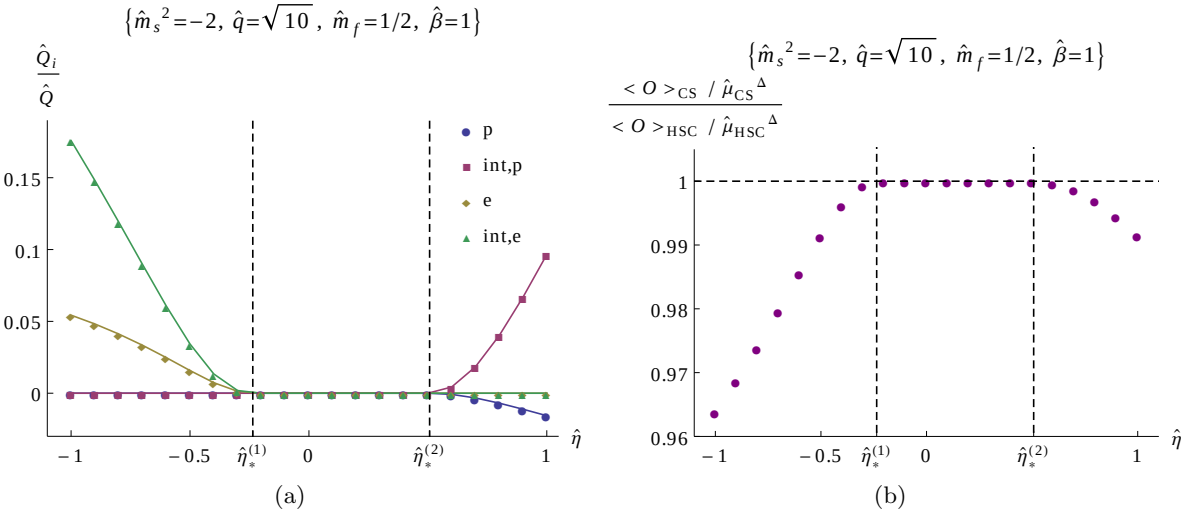


Figure 3.12: (a) Distribution of the electric charge and (b) value of the condensate in the compact star(s) solutions corresponding to Figure 3.9b. The vertical dashed lines indicate the phase transitions visible in Figure 3.9b. The values $\hat{\eta}_*^{(1)} \simeq -0.24$ and $\hat{\eta}_*^{(2)} \simeq 0.51$ are the critical coupling constants marking the transition between the eCS and HSC solutions, and the HSC and pCS solutions, respectively.

In Figures 3.11-3.13 (left) we present the distribution of the total electric charge of the system between the scalar field, the fluids of electrons and positrons and the charges of interaction for different values of the parameters (the same that were used in Figures 3.9). The boundary condensate $\langle \mathcal{O} \rangle$ is also shown in those figures (right). It is interesting to note that it is lower in the CS solutions than in the HSC solution. In Section 3.5 we will show that the presence of fermions in the bulk maps to the formation of Fermi surfaces in the dual field theory. If one interprets the scalar operator $\mathcal{O}$ as being a composite

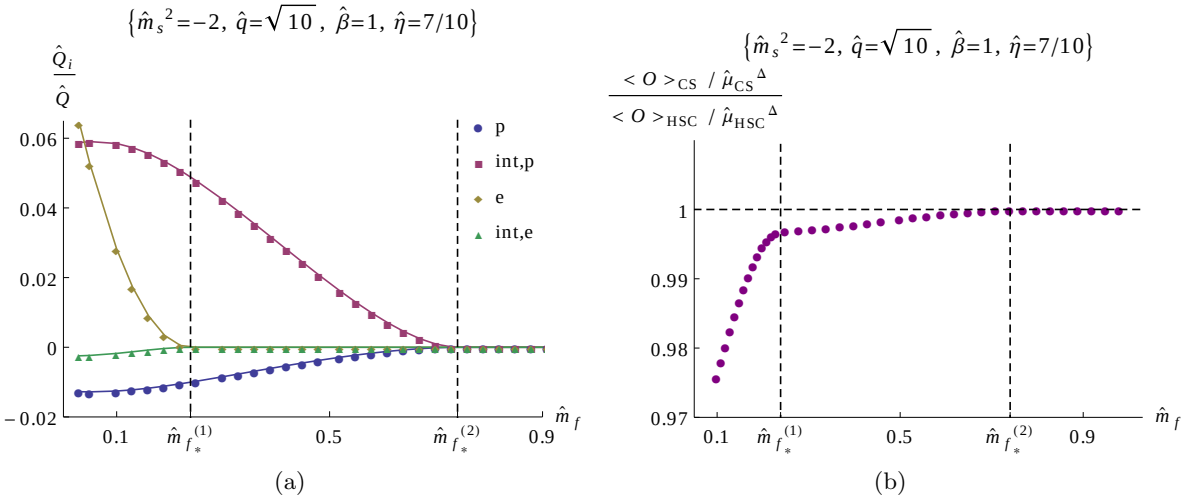


Figure 3.13: (a) Distribution of the electric charge and (b) value of the condensate in the compact star(s) solutions corresponding to Figure 3.9c. The dashed lines at the critical values $\hat{m}_{f*}^{(1)} \simeq 0.24$ and $\hat{m}_{f*}^{(2)} \simeq 0.74$ mark the transitions between the peCS and pCS solutions and the pCS and HSC solutions, respectively. The same value $\hat{m}_{f*}^{(1)}$ corresponds to the (subdominant) transition between the eCS and HSC solutions

operator of the fermionic operator, the suppression of part of the condensate in the CS solutions compared to the HSC solution can be thought of as coming from the breaking of part of the scalar operator excitations.

### 3.4.4 Comments on the CS/ES and HSC/ERN phase transitions

The small $\hat{q}$ region, where the HSC and the eCS approach the ERN and the ES respectively, deserves some further analysis. For simplicity, we will focus on the case $\hat{\eta} = 0$, studied in [1]. As we have mentioned earlier, the branches with non-zero condensate are only known for $\hat{q}^2 > \hat{q}^2_{\rm min}$, where $\hat{q}_{\rm min}$ is defined by (2.99), and this is the range in which our ansatz gives a solution. Additional special values of $\hat{q}$ are given by the stability bounds $\hat{q}_{\rm st}$ and $\hat{q}^\star_{\rm st}$ of the ERN and the ES to the formation of scalar hair, given respectively by (2.80) and (3.5). Thus one can distinguish two cases, depending on whether $\hat{q}_{\rm st}$ and $\hat{q}^\star_{\rm st}$ are larger or smaller than $\hat{q}_{\rm min}$ [1]:

**i** $\hat{q}_{\rm st}\,(\hat{q}^\star_{\rm st}) < \hat{q}_{\rm min}$
For large charge $\hat{q} > \hat{q}_{\rm min}$ the HSC (eCS) dominates over the ERN (ES, respectively). However there is an intermediate region $\hat{q}_{\rm st}\,(\hat{q}^\star_{\rm st}) < \hat{q} < \hat{q}_{\rm min}$ in which a non-trivial solution for the HSC (eCS) should exist but its form is not known. Thus, this region is outside the reach of our investigation, as well as the region of even smaller $\hat{q}$ below the stability bound[3].

**ii** $\hat{q}_{\rm st}\,(\hat{q}^\star_{\rm st}) > \hat{q}_{\rm min}$
In this case, for large $\hat{q}$ again one expects the HSC (eCS) to dominate. For intermediate values of the charge, $\hat{q}_{\rm min} < \hat{q} < \hat{q}_{\rm st}\,(\hat{q}^\star_{\rm st})$, the HSC (eCS) IR geometry is still

[3]In [51] two putative additional branches of solutions with condensate were found in the region $0 < \hat{q}^2 < -2\hat{m}_s^2/5$ but these authors were not able to determine whether such solutions have free tunable parameters to allow them to connect to the UV asymptotics. At any rate one of the two branches seemed to connect smoothly onto the region $\hat{q} > \hat{q}_{\rm min}$.

allowed, but since the IR of the ERN (ES) is stable, the latter should now dominate the ensemble. Either the HSC and the eCS merge smoothly with the ERN and ES, respectively at $\hat{q}_{\rm st}$ at $\hat{q}^{\star}_{\rm st}$, or there is a crossing over (first order phase transition) at a larger critical $\hat{q}$, and then the HSC and eCS disappear into some other subleading solutions at $\hat{q}_{\rm min}$.

The two values of $\hat{m}_s^2$ we considered fall in the two different cases above:

- For $\hat{m}_s^2 = -2$ we have $\hat{q}^2_{\rm min} = 2/3$, and we are always above the stability bound of the ERN since any $\hat{q}^2 > 0$ satisfies (2.79). The same can be said for the ES stability bound for the parameters we have chosen. Thus, we are in case **i**. We see from Figure 3.6 that the eCS and HSC dominate at any $\hat{q}$ above $\hat{q}_{\rm min}$, but unfortunately our level of numerical precision does not allow us to determine whether the HSC (eCS) solution reaches the boundary of this region, or if it stops at some larger $\hat{q}$. In either case, there must be a new solution dominating the ensemble down to $\hat{q}_{\rm st}$ and $\hat{q}^{\star}_{\rm st}$. It would be very interesting to find solutions in the region $\hat{q}^2 < -\hat{m}_s^2/3$.
- For $\hat{m}_s^2 = -3/4$ we have $\hat{q}^2_{\rm min} = 1/4$ and $\hat{q}^2_{\rm st} = 3/4$, thus we are in case **ii**. In Figure 3.7a and 3.8b we have marked the point $\hat{q} = \hat{q}_{\rm st}$ where the scalar mode around the ERN becomes unstable; the point $\hat{q}^{\star}_{st}$ falls very close to $\hat{q}_{\rm st}$ (see Figure 3.1) and it is not displayed. From Figure 3.7a, we cannot determine whether the eCS solution is merging with the ES at $\hat{q}_{\rm st}$ before reaching $\hat{q}_{\rm min}$, or whether the two branches cross. If there is a crossing at some $\hat{q}$ between $\hat{q}_{\rm min}$ and $\hat{q}_{\rm st}$, then there is a phase transition between eCS and ES; if instead the crossing happens for $\hat{q} > \hat{q}_{\rm st}$ then there would be a region where neither the ES nor the eCS is the dominant solution.

## 3.5 Low energy fermionic spectrum of holographic Bose-Fermi systems

In Section 3.3, we have shown that there exist asymptotically $AdS_4$ solutions with both charged fermionic and bosonic matter. By computing the free energy in Section 3.4, we found that the presence of both is favoured. When this happens, the dual field theory state exhibits a non-vanishing vacuum expectation value for a scalar charged operator, interpreted as a sign of the onset of superconductivity. Also, in the electron star model, the presence of a charged fluid of fermions in the bulk has been interpreted as the formation of Fermi surfaces in the dual field theory [43, 44]. Thus, in addition to the scalar condensate, one expects that the Bose-Fermi state allows for gapless low energy fermionic excitations.

The aim of this section is to determine the fermionic spectrum at low energy following the work [44] and to study in more details the transition between the ES and the CS solutions. To do so, we will compute the two-point Green's function – the fermionic propagator – of the Bose-Fermi state of the field theory. This can be done, using the AdS/CFT dictionary, by solving the Dirac equation of a probe spinor field in the background solution [44]. The fluid approximation will allow us to solve this equation in the WKB approximation. The probe spinor field that we will consider is chosen to be the representative field for electrons and will correspond to the electronic excitations of the bulk background. Since the probe field is supposed to be an electron of the electron star, it will carry a positive electromagnetic elementary charge $|q_f|$.

For convenience, we rescale the time coordinate $t \to \tilde{t} = c\,t$ to remove the constant $c$ from the solutions (it appears for example in (3.33)). We recall that this is equivalent to

apply a transformation (2.65b) with $b = c$. In the following, we simply denote the new time coordinate $\tilde{t}$ by $t$.

### 3.5.1 Probe fermion and the Dirac equation

The electromagnetic current of bulk elementary fermions $\chi$ with charge $|q_f|$ is given by

$$J^a_{\rm ferm} = -|q_f|\langle\bar{\chi}\Gamma^a\chi\rangle\,. \tag{3.47}$$

To take into account the current-current interaction between the fermions and the bosons, it is natural to add to the action for free probe fermions $\chi$ the interaction

$$S_{\rm int} = \eta\int d^4x\,\sqrt{-g}J^{\rm ferm}_a J^a_{\rm scal} \tag{3.48}$$

where $J^a_{\rm ferm}$ and $J^a_{\rm scal}$ are given by (C.2).

In Appendix C, we obtain in details the Schrödinger-like equation, but we give here the key steps. By choosing correctly the basis of Gamma matrices, the Dirac equation for a probe spinor field $\chi$ in the background solution can be written as an equation for the two-component spinor $\Phi = r^{-1}f^{-1/4}\chi_1$,

$$\left(\partial_r + \gamma\hat{m}_f g^{1/2}\sigma^3\right)\Phi = g^{1/2}\left\{i\gamma\sigma^2\left[\hat{\omega}f^{-1/2} + \hat{\mu}_l\right] - \gamma\hat{k}r\sigma^1\right\}\Phi \tag{3.49}$$

where we have rescaled the momentum and frequency,

$$\hat{\omega} = \frac{\omega}{\gamma}\,, \qquad \hat{k} = \frac{k}{\gamma} \tag{3.50}$$

by the parameter

$$\gamma \equiv \frac{|q_f|eL}{\kappa} \gg 1 \tag{3.51}$$

which is large in the Thomas-Fermi approximation applied to the bulk fermions. In this limit, the Dirac equation (3.49) is equivalent to the Schrödinger-like equation

$$\Phi_2'' = \gamma^2 V(r)\Phi_2 \tag{3.52}$$

together with the expression

$$\Phi_1 = \frac{1}{\frac{\hat{\omega}}{\sqrt{f}} + \hat{\mu}_l + \hat{k}r}\left(\hat{m}_f\Phi_2 - \frac{1}{\gamma}\frac{1}{\sqrt{g}}\Phi_2'\right) \tag{3.53}$$

for the components $\Phi_1$ and $\Phi_2$ of the spinor

$$\Phi = \begin{pmatrix}\Phi_1\\ \Phi_2\end{pmatrix}\,. \tag{3.54}$$

The potential $V(r)$ can be expressed as

$$V(r) = g(r)\left\{r^2\left[\hat{k}^2 - \hat{k}_F^2(r)\right] - \frac{\hat{\omega}}{f(r)}\left[\hat{\omega} + 2\sqrt{f(r)}\hat{\mu}_l(r)\right]\right\} + \mathcal{O}(\gamma^{-1}) \tag{3.55}$$

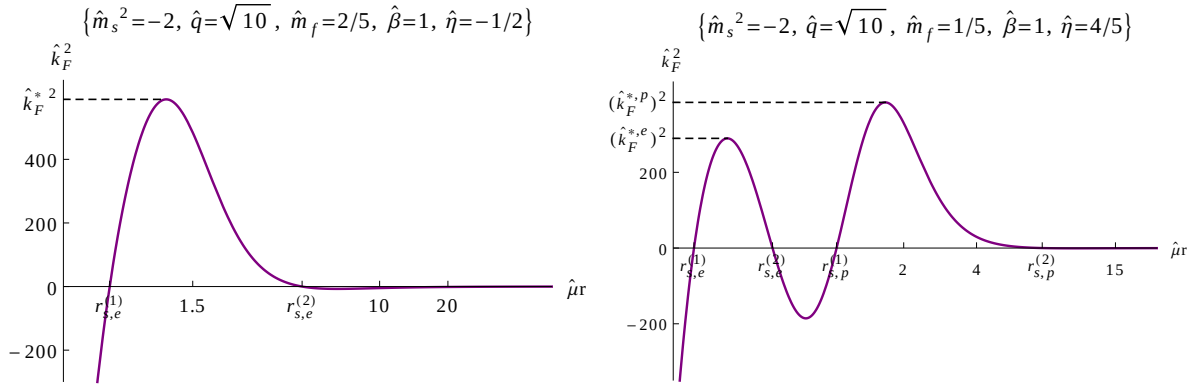


Figure 3.14: Local Fermi momentum squared $\hat{k}_F^2(r)$ for (a) an eCS solution and (b) a peCS solution. It is positive inside the star(s) and negative outside. The points $r_{s,e}^{(1)}$, $r_{s,e}^{(2)}$, $r_{s,p}^{(1)}$ and $r_{s,p}^{(2)}$ are the boundaries of the electron and the positron stars.

where the local Fermi momentum $\hat{k}_F$ is defined as [44]

$$\hat{k}_F^2(r) \equiv \frac{1}{r^2}\left(\hat{\mu}_l^2 - \hat{m}_f^2\right) . \tag{3.56}$$

Notice that $\hat{k}_F^2 > 0$ inside the stars only; these are the regions where $\hat{k}_F$ is relevant for our considerations. The local Fermi momentum is displayed in Figure 3.14 for an eCS solution and a peCS solution. The momentum $\hat{k}$ appears only through $\hat{k}^2$ in the potential (3.55), so we can restrict the analysis to $\hat{k} > 0$ without loss of generality.

**The Schrödinger equation in a standard form**

The potential (3.55) depends on the momentum $\hat{k}$. In order to see the physical interpretation of Eq. (3.52), we put it in a Schrödinger form where $\hat{k}$ plays the role of the energy by introducing the new coordinate $y$, defined by

$$\frac{\mathrm{d}y}{\mathrm{d}r} = r\sqrt{g(r)} . \tag{3.57}$$

We then obtain the equation

$$-\partial_y^2\varphi + \gamma^2\tilde{V}(y)\varphi = -\gamma^2\hat{k}^2\varphi \tag{3.58}$$

for the rescaled field $\varphi \equiv r^{1/2}g^{1/4}\Phi_2$, where

$$\tilde{V}(y) = -\hat{k}_F^2(y) - \frac{\hat{\omega}}{r(y)^2 f(y)}\left(\hat{\omega} + 2\sqrt{f(y)}\hat{\mu}_l(y)\right) + \mathcal{O}\left(\gamma^{-2}\right) \tag{3.59}$$

in the large-$\gamma$ limit. Herein and in the following, $r(y)$ is the inverse map of

$$y(r) = \int^r \mathrm{d}r' r'\sqrt{g(r')} . \tag{3.60}$$

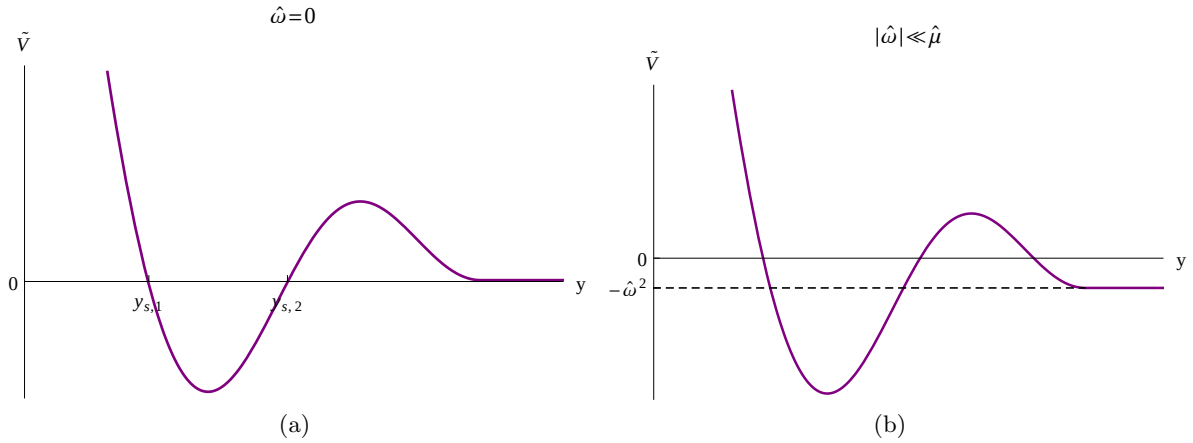


Figure 3.15: Profile of the potential of the Schrödinger equation for an eCS or a pCS solution at (a) zero frequency, (b) small frequency $0 < |\hat{\omega}| \ll \hat{\mu}$. The points $y_{s,1}$ and $y_{s,2}$ are the star boundaries.

Notice that $y \to \infty$ when $r \to \infty$. The equation (3.58) has to be seen as a Schrödinger equation with negative eigenvalue of the energy $E = -\gamma^2\hat{k}^2$. The potential (3.59) is now independent of the momentum $\hat{k}$.

At zero frequency, the potential $\tilde{V}$ is, up to a minus sign, given by the local Fermi momentum squared (3.56). It is negative inside the star and positive outside, and the zero-energy turning points are the star boundaries where $|\hat{\mu}_l(y)| = \hat{m}_f$. Since the local chemical potential $\hat{\mu}_l$ vanishes in the IR as in (3.35), the local Fermi momentum behaves in this region as $\hat{k}_F^2(y) \sim -\hat{m}_f^2/r(y)^2$ where in the IR, the inverse map of $r(y)$ is

$$y(r) \sim \sqrt{\frac{3}{2|\hat{m}_s^2|}}\frac{r}{\sqrt{\log r}}\,, \qquad r \to \infty\,, \tag{3.61}$$

and the potential $\tilde{V}(y) \to 0^+$ at infinity. The potential $\tilde{V}$ for $\hat{\omega} = 0$ is displayed schematically in Figure 3.15a for a compact star solution involving one star (eCS or pCS).

A non-zero frequency $0 < |\hat{\omega}| \ll \hat{\mu}$ affects the behaviour of the potential (3.59) in the near-horizon region. Indeed,

$$\tilde{V}(y) \sim -\hat{\omega}^2 + \frac{\hat{m}_f^2}{r(y)^2}\,, \qquad r \to \infty\,, \tag{3.62}$$

so the zero-frequency limit and the near-horizon limit do not commute. This is also observed in the electron star phase [44] but with a different asymptotic behaviour with respect to the potential (3.59), leading to a different conclusion as we shall see below. Outside the near-horizon region, the effects of small frequency are small and do not affect much the shape of the potential. In particular, the zero-energy turning points of the potential $\tilde{V}$ are close to the star boundaries. In the UV, the potential (3.59) behaves as

$$\tilde{V}(y) \sim \frac{\hat{m}_f^2}{y^2}\,, \qquad y \to 0\,, \tag{3.63}$$

and effects of $\hat{\omega}$ are subleading. The potential for $0 < |\hat{\omega}| \ll \hat{\mu}$ is displayed in Figure 3.15b for a compact star solution involving one star (eCS or pCS).

Our aim is to solve the Schrödinger equation (3.58) for the field $\varphi$ to compute the poles of the retarded two-point Green's function of the gauge-invariant field operator dual to the bulk fermionic particles. To do so, we shall impose the Dirichlet condition on $\varphi$ at the UV boundary and the in-falling condition in the near-horizon region. This second condition can be applied when the solution to Eq. (3.58) is oscillating in the IR, that is when $\tilde{V}(y=\infty) = -\hat{\omega}^2 < -\hat{k}^2$, i.e. for $|\hat{\omega}| > \hat{k}$. The dispersion relation of the Green's function corresponds in this case to quasinormal modes of the wave equation (3.58). For $|\hat{\omega}| < \hat{k}$, the solution is exponential in the near-horizon region and one shall impose the regularity condition, leading to normal modes of the equation (3.58).

The discussion of the previous paragraph allows us to distinguish three different regimes for the spectrum of the Schrödinger equation (3.58). Let us define the extremal local Fermi momentum $\hat{k}_F^\star$ by

$$\hat{k}_F^\star \equiv \max_{y_{s,1}<y<y_{s,2}} \hat{k}_F(y) \tag{3.64}$$

For $\hat{k} > \hat{k}_F^\star$, the 'energy' $-k^2$ lies everywhere below the Schrödinger potential, and there are no eigenstates. In the intermediate region $|\hat{\omega}| < \hat{k} < \hat{k}_F^\star$, we expect to have a discrete spectrum of bound states, which are normal modes of the Schrödinger equation (3.58). Since the region of spacetime where $\tilde{V} < E$ is compact for any frequency, the number of bound states is finite at fixed frequency and is almost independent of the frequency since $\hat{\omega} \ll \hat{\mu}$ only affects the near-horizon region. For $\hat{k} < |\hat{\omega}| \ll \hat{\mu}$, the spectrum of the Schrödinger equation (3.58) is continuous but there is a discrete set of quasinormal modes, which dissipate in the IR region by quantum tunnelling. The number of quasinormal modes is finite at fixed frequency for the same reasons as for the intermediate region. By setting $\hat{\omega} = 0$, one can count the number of Fermi surfaces. From the qualitative behaviour of the Schrödinger potential in Figure 3.15a, the number of boundary Fermi momenta is finite.

In certain parameter regions, although the fluid density is non-zero, there may be no negative energy bound states (thus no Fermi surfaces): this happens for 'small stars', for which the potential $\tilde{V}$ is not deep enough inside the star to allow any bound state.

We then expect to obtain a finite number of boundary Fermi momenta $\hat{k}_n$ ($n = 0, \ldots, N-1$) satisfying $\hat{k}_n < \hat{k}_F^\star$ in the large-$\gamma$ limit. Each boundary Fermi surface admits particle excitations which are stable at low energy $|\hat{\omega}| < \hat{k}$. At larger frequency $|\hat{\omega}| > \hat{k}$ with $|\hat{\omega}| \ll \hat{\mu}$, the excitations are resonances, they can dissipate. This dissipation maps in the bulk to the possible quantum tunnelling of the modes into the near-horizon region. The modes dissipate only at sufficiently large frequency due to the fact that the compact star does not occupy the inner region of the bulk spacetime. From the field theory point of view, the bosonic modes, represented in the bulk by the scalar field, the metric and the gauge field, do not interact with the fermions at sufficiently low energy and the excitations around the $n$-th Fermi surface are stable up to $|\hat{\omega}| \sim \hat{k}_n$.

Let us compare the situation to the electron star phase, studied in detail in [44]. At zero frequency the potential is negative for $y > y_s$, where $y_s$ is the star boundary, and $\tilde{V}(y) \to 0^-$ for $y \to \infty$. For $\hat{\omega} \neq 0$, the potential diverges to $-\infty$ in the IR so dissipation occurs for any non-zero frequency. This is because the fluid does occupy the inner region of spacetime and the boundary fermions interact with the bosonic modes at low energy. For $\hat{\omega} > 0$, the potential admits a local maximum at a point[4] $y_\star \propto \hat{\omega}^{-1/z}$ where

[4]The corresponding point in the original $r$ variable has been computed by Hartnoll et al. in [44].

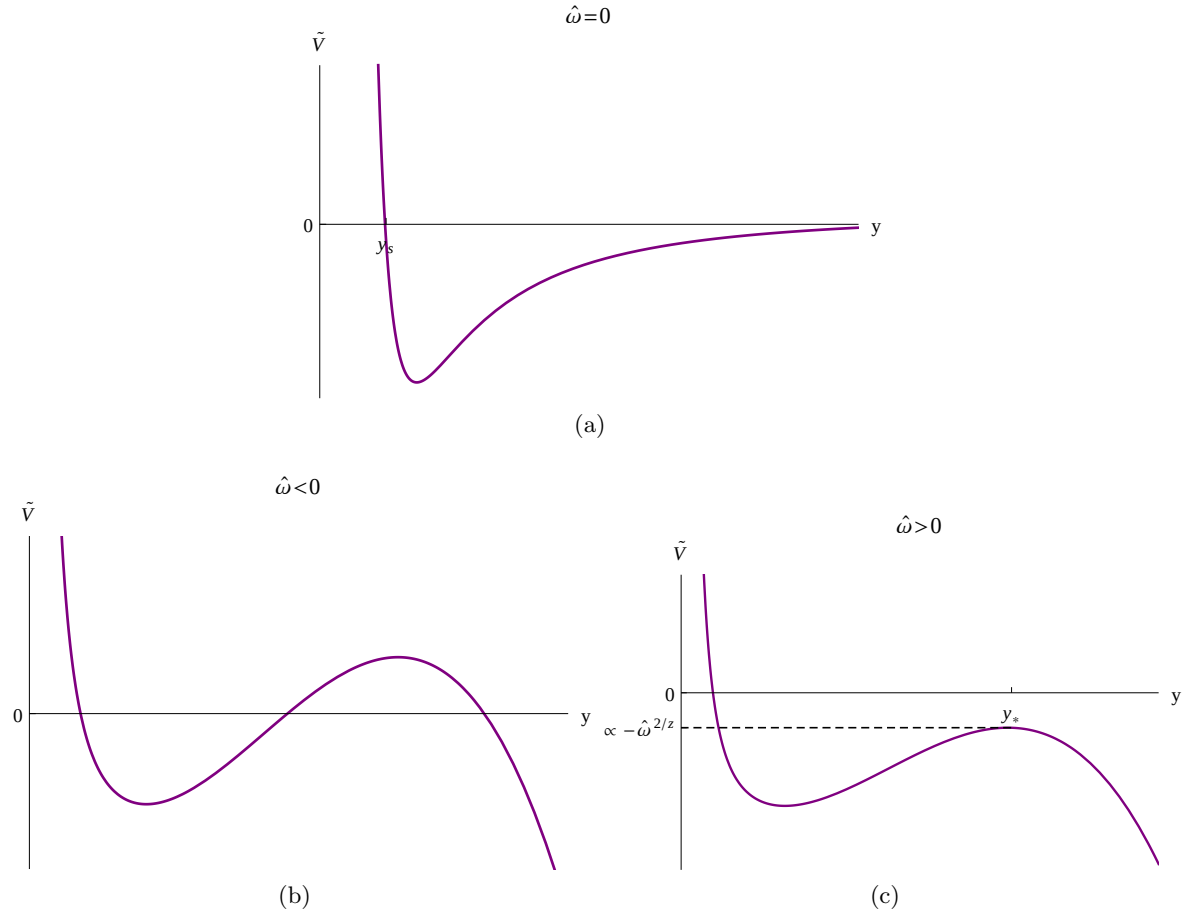


Figure 3.16: Profile of the potential of the Schrödinger equation in the electron star phase at, (a) zero frequency, (b) negative frequency and (c) positive frequency. The point $y_s$ is the star boundary and $y_\star$ is the point where $\tilde{V}$ admits a local maximum in the Lifshitz region for $\hat{\omega} < 0$.

$\tilde{V}(y_\star) \propto -\hat{\omega}^{2/z} < 0$. The constant of proportionality can be easily computed analytically. From the Schrödinger equation (3.58), it means that for positive frequency, the modes are unstable for $\hat{\omega} > \hat{k}^z$ because, as explained in [44], the fermionic excitations strongly interact with the critical modes of the Lifshitz sector. On the other hand, for $\hat{\omega} < 0$, the potential admits two turning points in the Lifshitz region, so there is a region where it is positive. The conclusion is that there is no strong dissipation and one finds a set of quasinormal modes for all $\hat{k} \lesssim \hat{k}_F^\star$ [44]. These situations are displayed in Figure 3.16.

We should notice that for the compact star solutions, $\tilde{V}$ also admits a local maximum, as shown in Figure 3.15. However, this local maximum is positive at zero frequency and not modified at small frequency $|\hat{\omega}| \ll \hat{\mu}$ because it does not belong to the asymptotic IR region. At larger frequencies, the effects of $\hat{\omega}$ are also relevant outside the near-horizon region. It may happen that for sufficiently large frequencies, this local maximum becomes negative. In this case, the potential would be negative for all $y$ larger than the first turning point, leading to unstable states at small momentum.

We have argued above that the number of boundary Fermi momenta dual to the compact star solutions is finite. In the electron star phase on the other hand, at zero

frequency we see from (2.54) that the potential asymptotes to zero in the IR as

$$\tilde{V}(y) \sim -\frac{g_\infty \left(h_\infty^2 - \hat{m}_f^2\right)}{y^2}\,, \qquad y \to \infty\,. \tag{3.65}$$

It means that there is accumulation of levels at small momentum and, as we will explicitly show in Section3.5.6, the number of Fermi surfaces turns out to be infinite [63].

Here, we focus on the regime $|\hat{\omega}| < \hat{k}$ with $|\hat{\omega}| \ll \hat{\mu}$. In this case, all the modes are bound states.

**Bound states for $|\hat{\omega}| \ll \hat{k}$**

In the electron star phase, the dispersion relation of the fermionic excitations around the Fermi surfaces was found to be linear, up to a (imaginary) dissipative term [44]. We will see later that this is also what we obtain for the compact star phases. In the rest of this paper, we will be interested in the behaviour of the particle excitations close to the Fermi surfaces, that is for $|\hat{\omega}| \sim |\hat{k}_n - \hat{k}| \ll \hat{k}_n$. In this case, $|\hat{\omega}| \ll \hat{k}$ and the dependence on $\hat{\omega}$ of the potential (3.59) can be neglected everywhere, in particular in the IR region, and one can consistently set $\hat{\omega} = 0$. The potential is then simply given by

$$\tilde{V}(y) = -\hat{k}_F^2(y)\,. \tag{3.66}$$

It is easy to generalize the above discussion to peCS solutions. In Figure 3.14, we display the local Fermi momentum for an eCS solution and a peCS solution. For convenience, we plot it in the original variable $r$. Doing so does not affect the analysis as it only changes the shape of the local Fermi momentum in the radial direction and does not modify the extremal values of it. It is clear from (3.58) that for $\hat{k} > \hat{k}_F(r)$, the solution is exponential while it is oscillating for $\hat{k} < \hat{k}_F(r)$. There can exist zero, one or two regions where $\hat{k} < \hat{k}_F(r)$ depending on the background solution and the value of $\hat{k}$ compared to the local maxima of $\hat{k}_F$. For eCS and pCS solutions, the extremal local Fermi momentum is

$$\hat{k}_F^\star \equiv \max_{r_s^{(1)} < r < r_s^{(2)}} \hat{k}_F(r) \tag{3.67}$$

and for peCS solutions, there exist two local extrema

$$\hat{k}_F^{\star,p} \equiv \max_{r_{s,p}^{(1)} < r < r_{s,p}^{(2)}} \hat{k}_F(r) \qquad \text{and} \qquad \hat{k}_F^{\star,e} \equiv \max_{r_{s,e}^{(1)} < r < r_{s,e}^{(2)}} \hat{k}_F(r)\,. \tag{3.68}$$

The bounds in the maxima are the star boundaries of the star(s) of the different solutions. The conditions for oscillations are detailed in Table 3.2. When oscillations can occur, as discussed above we expect in the large-$\gamma$ limit that we are considering to obtain a finite number of eigenvalues $k_n$, bounded above by the extremal local Fermi momenta. They correspond to oscillations which are localized in the star for pCS and eCS solutions. For peCS solutions, for $\min(\hat{k}_F^{\star,p}, \hat{k}_F^{\star,e}) < \hat{k} < \max(\hat{k}_F^{\star,p}, \hat{k}_F^{\star,e})$ these oscillations are localized in one of the two stars while for smaller momentum there can be quantum tunnelling between the two stars.

| | eCS/pCS | peCS |
|---|---|---|
| $\hat{k} < \hat{k}_F^\star$ | oscillations | $\times$ |
| $\hat{k}_F^\star < \hat{k}$ | no oscillations | $\times$ |
| $\hat{k} < \hat{k}_F^{\star,e}$ and $\hat{k} < \hat{k}_F^{\star,p}$ | $\times$ | oscillations in electron and positron stars |
| $\hat{k}_F^{\star,e} < \hat{k} < \hat{k}_F^{\star,p}$ | $\times$ | oscillations in positron star |
| $\hat{k}_F^{\star,p} < \hat{k} < \hat{k}_F^{\star,e}$ | $\times$ | oscillations in electron star |
| $\hat{k}_F^{\star,p} < \hat{k}$ and $\hat{k}_F^{\star,e} < \hat{k}$ | $\times$ | no oscillations |

Table 3.2: Conditions on the momentum for oscillations. When possible, oscillations occur in the region(s), located in the star(s), where $\hat{k} < \hat{k}_F(r)$.

### 3.5.2 The WKB analysis for $|\hat{\omega}| \ll \hat{k} < \hat{k}_F^\star$

Even if the Schrödinger problem in the standard form allows to have a clear analysis of the spectrum, we can equivalently obtain the Green's function for[5] $\hat{k} < \hat{k}_F^\star$ from the original Schrödinger-like equation (3.52) with potential (3.55) by looking for zero-energy solutions. As noticed above, the parameter $\gamma$ defined by (3.51) is large,

$$\gamma \gg 1\,. \tag{3.69}$$

This allows us to solve Eq. (3.52) for $\hat{k} < \hat{k}_F^\star$ by applying the WKB approximation if the conditions [44]

$$|V'(r)| \ll \gamma |V(r)|^{3/2} \qquad \text{and} \qquad |V''(r)| \ll \gamma^2 |V(r)|^2 \tag{3.70}$$

are satisfied. This is the case if the momentum $\hat{k}$ is not too close to the local extremal Fermi momenta (3.67) and (3.68). This means in particular that the potential vanishes linearly at the turning points.

The potential (3.55) is positive both in the UV and the IR, where it behaves as

$$V \sim \frac{\hat{m}_f^2}{r^2}\,, \qquad r \sim 0\,, \tag{3.71}$$

and

$$V \sim \frac{3}{2|\hat{m}_s^2|}\frac{\hat{k}^2}{\log r}\,, \qquad r \sim \infty\,, \tag{3.72}$$

where we have used the fact that $|\hat{\omega}| \ll \hat{k}$. As explained in the previous section, for $\hat{k} < \hat{k}_F^\star$ there can be one or two regions where $V < 0$; in these regions, the solution is oscillating and we expect to observe bound states. In Figure 3.17, we display these possible situations by plotting the potential (3.55) for the compact star(s) solutions at zero frequency and several values of the momentum.

To get the Green's function of the gauge-invariant fermionic operators dual to the probe bulk fermion $\chi$, we shall relate the UV asymptotics of $\Phi$ with the normalizable and non-normalizable modes of $\chi$. In the UV ($r \to 0$), the asymptotic solution to the bulk Dirac equation (3.49) is [32]

$$\Phi \simeq A(\hat{k},\hat{\omega})\, r^{-\gamma\hat{m}_f}\left[\begin{pmatrix}1\\0\end{pmatrix} + \dots\right] + B(\hat{k},\hat{\omega})\, r^{\gamma\hat{m}_f}\left[\begin{pmatrix}0\\1\end{pmatrix} + \dots\right] \tag{3.73}$$

[5]From now on, we also denote by $\hat{k}_F^\star$ the maximum of $\hat{k}_F^{\star,e}$ and $\hat{k}_F^{\star,p}$ for peCS solutions.

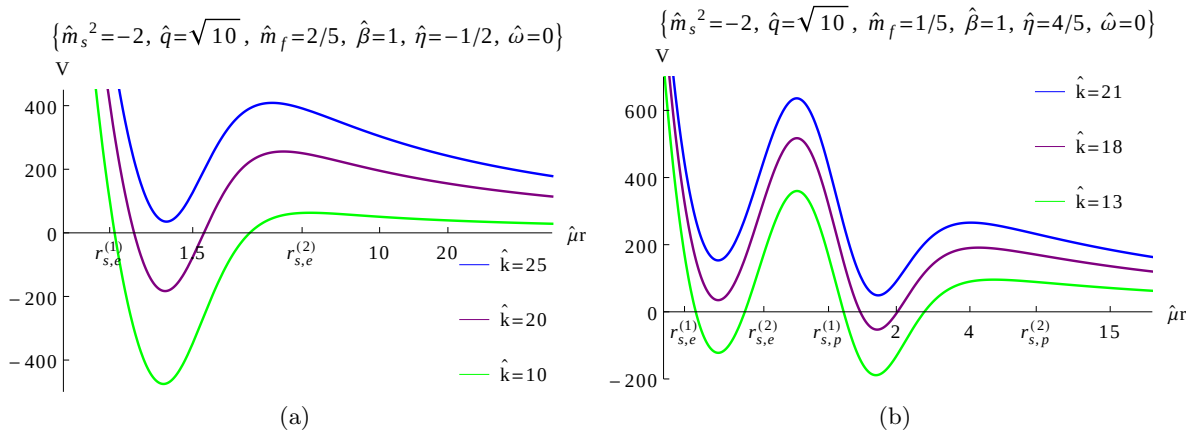


Figure 3.17: Profiles of the potential (3.55) at zero frequency. (a) The potential for an eCS solutions. The extremal Fermi momentum is in this case $\hat{k}_F^\star \simeq 24.3$. (b) The potential for a peCS solution. The extremal Fermi momenta are $\hat{k}_F^{\star,e} \simeq 17.0$ and $\hat{k}_F^{\star,p} \simeq 19.6$. In (a) and (b), the points $r_{s,e}^{(1)}$, $r_{s,e}^{(2)}$, $r_{s,p}^{(1)}$ and $r_{s,p}^{(2)}$ are the boundaries of the electron and the positron stars.

where $A$ and $B$ are independent of the radial coordinate. The Green's function of the fermionic operator dual to the bulk spinor $\Phi$ is then given by

$$G^R(\hat{k},\hat{\omega}) = \frac{B(\hat{k},\hat{\omega})}{A(\hat{k},\hat{\omega})}\,. \tag{3.74}$$

As shown in Appendix D, $\Phi_2$ behaves in the UV as

$$\Phi_2(r) \simeq a_+^\epsilon(\hat{k},\hat{\omega})\left(\frac{r}{\epsilon}\right)^{\gamma\hat{m}_f} + a_-^\epsilon(\hat{k},\hat{\omega})\left(\frac{r}{\epsilon}\right)^{-\gamma\hat{m}_f+1}\,, \tag{3.75}$$

where $\epsilon \ll 1$ is a UV cut-off. Matching this solution with (3.73), the Green's function is fully expressed in terms of the UV asymptotics of the scalar field $\Phi_2$ as

$$G^R(\hat{k},\hat{\omega}) = \frac{\hat{\mu}+\hat{\omega}+\hat{k}}{2\hat{m}_f}\lim_{\epsilon\to 0}\frac{a_+^\epsilon(\hat{k},\hat{\omega})}{a_-^\epsilon(\hat{k},\hat{\omega})}\epsilon^{-2\gamma\hat{m}_f}\,. \tag{3.76}$$

Notice that the functions $a_+^\epsilon(\hat{k},\hat{\omega})$ and $a_-^\epsilon(\hat{k},\hat{\omega})$ depend on the UV cutoff $\epsilon$.

To obtain the ratio $a_+^\epsilon(\hat{k},\hat{\omega})/a_-^\epsilon(\hat{k},\hat{\omega})$ in Eq. (3.76), we must impose normalizability of the wave function in the IR and integrate out Eq. (3.52) from IR to UV. This can be done in the WKB approximation with large parameter $\gamma$. The details of the computation are given in Appendix D. The general form of the Green's function is

$$G_R(\hat{k},\hat{\omega}) = \frac{\hat{\mu}+\hat{\omega}+\hat{k}}{2\hat{m}_f}\,\mathcal{G}(\hat{k},\hat{\omega})\lim_{r\to 0} r^{-2\gamma\hat{m}_f}\exp\left[-2\gamma\int_r^{r_1}\mathrm{d}s\sqrt{V(s)}\right]\,. \tag{3.77}$$

Here, $r_1$ is the turning point of the potential $V$ the closest to the UV boundary. The exponential suppression is due to the fact that the potential is large close to the boundary; the fermion has to tunnel into the spacetime. The function $\mathcal{G}(\hat{k},\hat{\omega})$ depends on the behaviour of the potential $V$ at momentum $\hat{k}$ and frequency $\hat{\omega}$.

### 3.5.3 The Green's function for eCS and pCS solutions

For eCS and pCS solutions, the Green's function has poles when $V < 0$ in one region. In this case, we find in Appendix D that

$$\mathcal{G}(\hat{k}, \hat{\omega}) = \frac{1}{2} \tan W(\hat{k}, \hat{\omega}) \tag{3.78}$$

where

$$W(\hat{k}, \hat{\omega}) = \gamma \int_{r_1}^{r_2} \mathrm{d}r \sqrt{|V(r)|}\,. \tag{3.79}$$

The two points $r_1$ and $r_2$ ($r_1 < r_2$) are the turning points of the potential $V$.

The poles of the Green's function are situated at

$$W(\hat{k}, \hat{\omega}) = \frac{\pi}{2} + n\pi\,, \quad n \in \mathbb{N}\,. \tag{3.80}$$

This equation defines $N$ boundary Fermi momenta $\hat{k} = \hat{k}_n$, where $n = 0, \ldots, N-1$, satisfying

$$0 < \hat{k}_{N-1} < \cdots < \hat{k}_0 < \hat{k}_F^\star\,. \tag{3.81}$$

Since $\gamma \gg 1$, the number $N$ of boundary Fermi momenta is large and the WKB analysis is reliable for large $n$. By computing explicitly the normal modes of the equation (3.52), we have verified that the poles of the Green's function are well-approximated by the WKB analysis. Expanding (3.78) around the poles (3.80), we obtain the Green's function

$$G^R(\hat{k}, \hat{\omega}) = \frac{\hat{\mu} + \hat{\omega} + \hat{k}}{2\hat{m}_f} \sum_{0<\hat{k}_n<\hat{k}_F^\star} \frac{\gamma^{-1} c_n e^{-2\gamma a_n}}{\hat{\omega} - v_n(\hat{k} - \hat{k}_n)} \tag{3.82}$$

where

$$v_n = -\frac{\partial_{\hat{k}} W(\hat{k}_n, 0)}{\partial_{\hat{\omega}} W(\hat{k}_n, 0)}\,, \qquad c_n = -\frac{\gamma}{2}\left[\partial_{\hat{\omega}} W(\hat{k}_n, 0)\right]^{-1}, \tag{3.83}$$

$$a_n = \int_0^{r_1} \mathrm{d}r \sqrt{V(\hat{k}_n, 0)} + \hat{m}_f \log r_1\,. \tag{3.84}$$

Notice that $v_n > 0$ for eCS and $v_n < 0$ for pCS which means that, as expected, the electron star and the positron star form respectively electronic and positronic Fermi surfaces in the dual field theory[6].

### 3.5.4 The Green's function for peCS solutions

For peCS solutions, the Green's function has poles of the same kind as for the eCS and the pCS solutions for intermediate momentum. Indeed, these boundary Fermi momenta $\hat{k}_n$ are bounded as

$$\hat{k}_F^{\star,e} < \hat{k}_{N-1} < \cdots < \hat{k}_0 < \hat{k}_F^{\star,p} \tag{3.85}$$

[6]The electronic excitations have positive energy $\hat{\omega}$. For them to be particle-like excitations ($\hat{k} > \hat{k}_n$), one must have $v_n > 0$. Thus Fermi momenta with $v_n > 0$ ($v_n < 0$) correspond to electron-like (hole-like) Fermi surfaces.

where the oscillations happen in the positron star and vice-versa when they happen in the electron star. Moreover, for small momentum, $V < 0$ in two regions and, as shown in Appendix D, the Green's function reads

$$\mathcal{G}(\hat{k},\hat{\omega}) = \frac{4e^{2X}\sin Y\cos Z + \cos Y\sin Z}{8e^{2X}\cos Y\cos Z - 2\sin Y\sin Z} \tag{3.86}$$

where

$$X(\hat{k},\hat{\omega}) = \gamma\int_{r_2}^{r_3}\mathrm{d}r\sqrt{V(r)}\,, \qquad Y(\hat{k},\hat{\omega}) = \gamma\int_{r_1}^{r_2}\mathrm{d}r\sqrt{|V(r)|}\,, \tag{3.87}$$

$$Z(\hat{k},\hat{\omega}) = \gamma\int_{r_3}^{r_4}\mathrm{d}r\sqrt{|V(r)|}\,. \tag{3.88}$$

The potential $V$ vanishes linearly at the turning points $r_1 < r_2 < r_3 < r_4$. From (3.86) we see that the conditions for $\mathcal{G}$ to have a pole are

$$(Y,Z) = \left(\frac{\pi}{2} + n\pi, m\pi\right) \quad \text{and} \quad (Y,Z) = \left(n\pi, \frac{\pi}{2} + m\pi\right)\,, \quad n,m\in\mathbb{N} \tag{3.89}$$

for all $X$, and

$$e^{2X} = \frac{1}{4}\tan Y\tan Z\,, \qquad \tan Y\tan Z \geq 0\,. \tag{3.90}$$

However the conditions (3.89) are generically not satisfied for any pair $\{\hat{k},\hat{\omega}\}$ and so they do not give rise to poles.

The boundary Fermi momenta $\hat{k}_{\bar{n}}$ are then found by solving (3.90) at zero frequency. Around $\hat{k} = \hat{k}_{\bar{n}}$ and $\hat{\omega} = 0$, (3.86) becomes

$$\mathcal{G}(\hat{k},\hat{\omega}) \simeq \frac{\gamma^{-1}c_{\bar{n}}}{\hat{\omega} - v_{\bar{n}}(\hat{k} - \hat{k}_{\bar{n}})} \tag{3.91}$$

where

$$v_{\bar{n}} = -\frac{8\,e^{2X_{\bar{n}}}\,\partial_{\hat{k}}X_{\bar{n}} - \frac{\tan Z_{\bar{n}}}{\cos^2 Y_{\bar{n}}}\,\partial_{\hat{k}}Y_{\bar{n}} - \frac{\tan Y_{\bar{n}}}{\cos^2 Z_{\bar{n}}}\,\partial_{\hat{k}}Z_{\bar{n}}}{8\,e^{2X_{\bar{n}}}\,\partial_{\hat{\omega}}X_{\bar{n}} - \frac{\tan Z_{\bar{n}}}{\cos^2 Y_{\bar{n}}}\,\partial_{\hat{\omega}}Y_{\bar{n}} - \frac{\tan Y_{\bar{n}}}{\cos^2 Z_{\bar{n}}}\,\partial_{\hat{\omega}}Z_{\bar{n}}} \tag{3.92}$$

and

$$c_{\bar{n}} = \gamma\tan Z_{\bar{n}}\left(1+\tan^2 Y_{\bar{n}}\right)\left[16\,e^{2X_{\bar{n}}}\,\partial_{\hat{\omega}}X_{\bar{n}} - 2\frac{\tan Z_{\bar{n}}}{\cos^2 Y_{\bar{n}}}\,\partial_{\hat{\omega}}Y_{\bar{n}} - 2\frac{\tan Y_{\bar{n}}}{\cos^2 Z_{\bar{n}}}\,\partial_{\hat{\omega}}Z_{\bar{n}}\right]^{-1} \tag{3.93}$$

with

$$X_{\bar{n}} \equiv X(\hat{k}_{\bar{n}}, 0) \tag{3.94}$$

and similarly for $Y$ and $Z$.

The Green's function for peCS solutions with $\hat{k}_F^{\star,e} < \hat{k}_F^{\star,p}$ can therefore be written as

$$G^R(\hat{k},\hat{\omega}) = \frac{\hat{\mu}+\hat{\omega}+\hat{k}}{2\hat{m}_f}\left(\sum_{\hat{k}_F^{\star,e}<\hat{k}_n^Z<\hat{k}_F^{\star,p}}\frac{\gamma^{-1}c_n^Z e^{-2\gamma a_n^Z}}{\hat{\omega} - v_n^Z(\hat{k}-\hat{k}_n^Z)} + \sum_{0<\hat{k}_{\bar{n}}<\hat{k}_F^{\star,e}}\frac{\gamma^{-1}c_{\bar{n}}e^{-2\gamma a_{\bar{n}}}}{\hat{\omega} - v_{\bar{n}}(\hat{k}-\hat{k}_{\bar{n}})}\right) \tag{3.95}$$

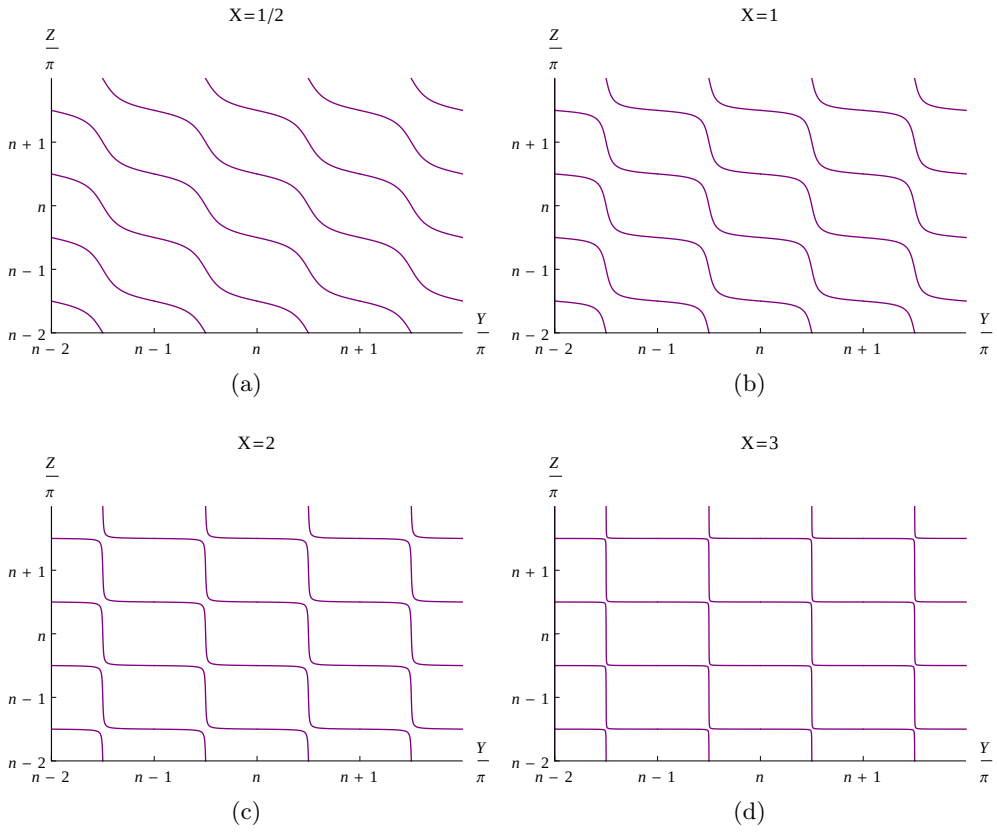


Figure 3.18: Poles of $\mathcal{G}$ for peCS solutions in the (Y-Z)-plan for different values of $X$.

where

$$v_n^Z = -\frac{\partial_{\hat{k}} Z(\hat{k}_n^Z, 0)}{\partial_{\hat{\omega}} Z(\hat{k}_n^Z, 0)}\,, \qquad c_n^Z = -\frac{\gamma}{2}\left[\partial_{\hat{\omega}} Z(\hat{k}_n^Z, 0)\right]^{-1}\,, \tag{3.96a}$$

$$a_n^Z = \int_0^{r_1} \mathrm{d}r \sqrt{V(\hat{k}_n^Z, 0)} + \hat{m}_f \log r_1\,. \tag{3.96b}$$

We have denoted by $\hat{k}_n^Z$ the boundary Fermi momenta obtained when the potential $V$ is negative in one region; in this case we have $Z(\hat{k}_n^Z, 0) = \pi/2 + n\pi$. When $\hat{k}_F^{\star,p} < \hat{k}_F^{\star,e}$, the Green's function for peCS solutions is

$$G^R(\hat{k}, \hat{\omega}) = \frac{\hat{\mu} + \hat{\omega} + \hat{k}}{2\hat{m}_f} \left( \sum_{\hat{k}_F^{\star,p} < \hat{k}_n^Y < \hat{k}_F^{\star,e}} \frac{\gamma^{-1} c_n^Y e^{-2\gamma a_n^Y}}{\hat{\omega} - v_n^Y (\hat{k} - \hat{k}_n^Y)} + \sum_{0 < \hat{k}_{\bar{n}} < \hat{k}_F^{\star,p}} \frac{\gamma^{-1} c_{\bar{n}} e^{-2\gamma a_{\bar{n}}}}{\hat{\omega} - v_{\bar{n}} (\hat{k} - \hat{k}_{\bar{n}})} \right) \tag{3.97}$$

where $v_n^Y$, $c_n^Y$ and $a_n^Y$ are defined by (3.96) where one has to replace $Z$ by $Y$.

In Figure 3.18, we display the poles of (3.86) in the $(Y, Z)$-plan for constant values of $X$. We see that in the large-$\gamma$ limit, the location of the poles of (3.86) are well-approximated by

$$(Y, Z) \simeq \left(\frac{\pi}{2} + n\pi, Z\right) \quad \text{and} \quad (Y, Z) \simeq \left(Y, \frac{\pi}{2} + m\pi\right)\,, \qquad n, m \in \mathbb{N}\,, \tag{3.98}$$

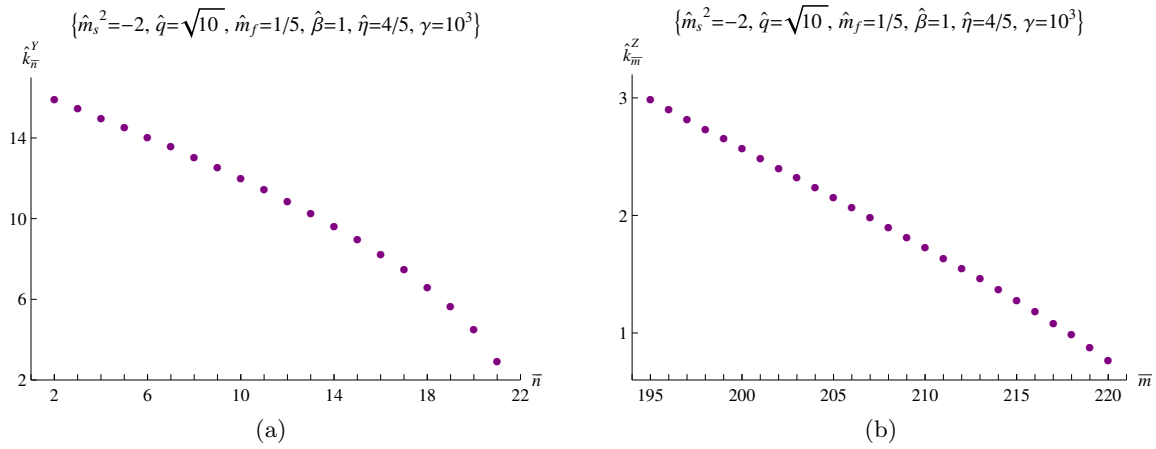


Figure 3.19: Boundary Fermi momenta for a peCS solution. The $\hat{k}^Y_{\bar{n}}$'s and the $\hat{k}^Z_{\bar{m}}$'s are the Fermi momenta of electron-like and hole-like Fermi surfaces in the dual field theory, respectively.

as suggested by Figure 3.18d. We denote by $\hat{k}^Y_{\bar{n}}$ and $\hat{k}^Z_{\bar{m}}$ the boundary Fermi momenta corresponding to the poles (3.98) and computed in the WKB approximation. In Figure 3.19 we give them for a peCS solution. These poles match with a high accuracy to the normal modes of the Schrödinger-like equation (3.52) that we have computed explicitly.

### 3.5.5 The Luttinger count

The Luttinger theorem relates the total charge of a Fermi liquid to the volume enclosed in the Fermi surface. For spin-1/2 particles with charge $|q_f|$ in two spatial dimensions, the Luttinger count is [64]

$$Q_{\rm FS} = |q_f| \sum_i \frac{2}{(2\pi)^2} V_i \,, \tag{3.99}$$

where $V_i$ are the volumes of the Fermi surfaces, given by $V_i = \pi p_i^2$ where $p_i$ is the Fermi momentum of the $i$-th Fermi surface. In the WKB approximation, one can approximate the discrete sum in (3.99) by an integral [44]; for eCS and pCS solutions we have

$$\sum_i \frac{1}{2\pi} p_i^2 = \sum_n \frac{1}{2\pi} k_n^2 = \frac{1}{2\pi} \int_0^{{k_F^\star}^2} {\rm d}E\, E \int_{r_1}^{r_2} {\rm d}r\, r\sqrt{g} \frac{1}{\sqrt{k_F^2 - E}} \tag{3.100}$$

where the Fermi momenta $k_n$ appear (with hats) in the Green's function (3.82). This leads to the relations [44]

$$|q_f| \sum_n \frac{1}{2\pi} k_n^2 = Q_{\rm e} \,, \tag{3.101a}$$

$$-|q_f| \sum_n \frac{1}{2\pi} k_n^2 = Q_{\rm p} \,, \tag{3.101b}$$

for eCS and pCS solutions, respectively, where the charges $Q_e$ and $Q_p$ are defined in Section 3.4.3. It means that as expected, the eCS and pCS solutions admit respectively boundary electronic and positronic Fermi surfaces. This is consistent with the fact that

the particle excitations are electronic in the field theory dual to the eCS solution and positronic in the field theory dual to the pCS solution. The Luttinger relation is

$$|q_f| \sum_i \frac{1}{2\pi} p_i^2 = Q - Q_{\text{scalar}} - Q_{\text{int,e}} \tag{3.102}$$

for eCS solutions and

$$-|q_f| \sum_i \frac{1}{2\pi} p_i^2 = Q - Q_{\text{scalar}} - Q_{\text{int,p}} \tag{3.103}$$

for pCS solutions. These situations are similar to the fractionalized phases of [56]; here the bosonic field takes the role of the charged event horizon, and there is also screening of the fermionic charge by the condensate.

For peCS solutions, the Luttinger count is

$$Q^{\text{e}}_{\text{FS}} = |q_f| \sum_i \frac{1}{2\pi} (p_i^e)^2 + |q_f| \sum_j \frac{1}{2\pi} (q_j^e)^2 \tag{3.104}$$

for electronic Fermi surfaces and

$$Q^{\text{p}}_{\text{FS}} = -|q_f| \sum_i \frac{1}{2\pi} (p_i^p)^2 - |q_f| \sum_j \frac{1}{2\pi} (q_j^p)^2 \tag{3.105}$$

for positronic Fermi surfaces. Here, $p_i^e$ and $q_j^e$ denote the boundary Fermi momenta of electronic Fermi surfaces corresponding to the cases where the potential $V$ is negative in one and two regions respectively in the bulk, and similarly for positrons. For $\hat{k}_F^{\star,e} < \hat{k}_F^{\star,p}$, we have

$$|q_f| \sum_i \frac{1}{2\pi} (p_i^e)^2 = 0\,, \tag{3.106a}$$

$$|q_f| \sum_j \frac{1}{2\pi} (q_j^e)^2 = |q_f| \sum_{\bar{n}} \frac{1}{2\pi} (k_{\bar{n}}^Y)^2 = \frac{|q_f|}{2\pi} \int_0^{(k_F^{\star,e})^2} \mathrm{d}E\, E \int_{r_1}^{r_2} \mathrm{d}r\, r\sqrt{g} \frac{1}{\sqrt{k_F^2 - E}}\,, \tag{3.106b}$$

$$-|q_f| \sum_i \frac{1}{2\pi} (p_i^p)^2 = -|q_f| \sum_n \frac{1}{2\pi} (k_n^Z)^2 = -\frac{|q_f|}{2\pi} \int_{(k_F^{\star,e})^2}^{(k_F^{\star,p})^2} \mathrm{d}E\, E \int_{r_3}^{r_4} \mathrm{d}r\, r\sqrt{g} \frac{1}{\sqrt{k_F^2 - E}}\,, \tag{3.106c}$$

$$-|q_f| \sum_j \frac{1}{2\pi} (q_j^p)^2 = -|q_f| \sum_{\bar{n}} \frac{1}{2\pi} (k_{\bar{n}}^Z)^2 = -\frac{|q_f|}{2\pi} \int_0^{(k_F^{\star,e})^2} \mathrm{d}E\, E \int_{r_3}^{r_4} \mathrm{d}r\, r\sqrt{g} \frac{1}{\sqrt{k_F^2 - E}}\,. \tag{3.106d}$$

We conclude that

$$Q^{\text{e}}_{\text{FS}} = Q_{\text{e}} \qquad \text{and} \qquad Q^{\text{p}}_{\text{FS}} = Q_{\text{p}}\,. \tag{3.107}$$

This result is also valid when $\hat{k}_F^{\star,p} < \hat{k}_F^{\star,e}$. So we have

$$Q^{\text{e}}_{\text{FS}} + Q^{\text{p}}_{\text{FS}} = Q - Q_{\text{scalar}} - Q_{\text{int,e}} - Q_{\text{int,p}}\,. \tag{3.108}$$

Thus, we have shown that the charge that one can assign to fermionic fluid components (which does not include the effect of screening due to the scalar field) is reproduced by the total volume of particle-like and hole-like Fermi surfaces via the Luttinger count.

### 3.5.6 Fermi surfaces and phase transitions

We have shown in the previous sections that the compact star solutions exhibit a large number of boundary Fermi surfaces when the WKB approximation is applicable. Since the field theory is rotationally invariant, they are circular and each of them is specified by a Fermi momentum $\hat{k}_n$, which lie between zero and the maximal value $\hat{k}_F^\star$.

In the WKB approximation, the number of Fermi surfaces with Fermi momentum in the interval $(\hat{k}, \hat{k}_F^\star)$ of a solution with one star – eCS, pCS or ES – is given by the integral [63]:

$$N(\hat{k}, \hat{k}_F^\star) \propto \gamma \int_{y_1}^{y_2} \mathrm{d}y \, \sqrt{\hat{k}_F^2(y) - \hat{k}^2} \tag{3.109}$$

where $y_1$ and $y_2$ are boundaries of the region where $\hat{k}_F^2(y) > \hat{k}^2$. The total number of Fermi surfaces $N$ is then

$$N \propto \gamma \int_{y_{s,1}}^{y_{s,2}} \mathrm{d}y \, \hat{k}_F(y) \tag{3.110}$$

where $y_{s,1}$ and $y_{s,2}$ are the star boundaries. This formula is in fact not exact, because for $\hat{k}$ close to $\hat{k}_F^\star$, the WKB approximation is not valid. However, the contribution of such momenta to the total number of levels is small, and non-vanishing, for eCS, pCS and ES solutions. For the eCS and pCS solutions, the star boundaries $y_{s,1}$ and $y_{s,2}$ are finite, so the total number of Fermi surfaces is finite; this also applies to the peCS solutions. The corresponding Fermi momenta are bounded by zero and the extremal local Fermi momenta.

For the (unbounded) electron star solution, the total number of Fermi surfaces (3.110) can be written as

$$N \propto \gamma \int_{y_s}^{y_0} \mathrm{d}y \, \hat{k}_F(y) + \gamma \int_{y_0}^{\infty} \mathrm{d}y \, \frac{\sqrt{g_\infty(h_\infty^2 - \hat{m}_f^2)}}{y} \tag{3.111}$$

where $y_s$ is the star boundary and $y_0$ is an arbitrary point which belongs to the Lifshitz region. The first term is finite since the boundaries are finite and the integrand is a regular function. However, the second term is logarithmically divergent. Then the electron star solution is dual to a field theory state admitting an infinite number of Fermi surfaces $N = \infty$. Indeed, it can be deduced from (3.109) that the density of levels at small momentum $\hat{k}$ is

$$\rho(\hat{k}) \sim \frac{\gamma}{\hat{k}}\,, \qquad \hat{k} \to 0\,, \tag{3.112}$$

so the number of Fermi surfaces in the interval $(\hat{k}, \hat{k}_0)$ is

$$N(\hat{k}, \hat{k}_0) \sim \gamma \log \frac{\hat{k}_0}{\hat{k}}\,, \qquad \hat{k} \to 0\,, \tag{3.113}$$

where $\hat{k}_0 \ll 1$ is a cutoff such that $\hat{k} < \hat{k}_0$. It means that the Fermi surfaces are accumulating exponentially at small momentum,

$$\hat{k} \sim \hat{k}_0 \, e^{-N(\hat{k}, \hat{k}_0)/\gamma}\,. \tag{3.114}$$

Notice that even if this computation of the total number of Fermi surfaces for the compact star solutions and the electron star applies only in the WKB approximation, the result is also valid when this approximation is not valid, as discussed in Section 3.5.1.

The infiniteness of fermionic modes in the electron star phase is removed at finite frequency. For $\hat{\omega} > 0$, the number of resonances has to be counted between the extremal local Fermi momentum and $\hat{k} \sim \hat{\omega}^{1/z}$. For smaller momentum, the modes are unstable. The total number of resonances is in this case

$$N(\hat{\omega} > 0) \sim \gamma \int_{y_1}^{y_\star} \mathrm{d}y \sqrt{\hat{k}_F^2(y) - \hat{\omega}^{2/z}}\,, \tag{3.115}$$

where $y_1$ is the first turning point of $\tilde{V}$ and $\tilde{V}'(y_\star) = 0$ at $y = y_\star$, which belongs to the Lifshitz region. Since $y_\star \sim \hat{\omega}^{-1/z}$, we conclude that the total number of resonances for small and positive frequency is $N(\hat{\omega} > 0) \sim \gamma \log \hat{\omega}^{-1/z}$. An analogous computation can be done for $\hat{\omega} < 0$ where the integration is taken up to $\hat{k} = 0$. The result is similar and we conclude that at small non-zero frequency, the total number of resonances is

$$N(\hat{\omega} \neq 0) \sim \gamma \log |\hat{\omega}|^{-1/z}\,, \qquad \hat{\omega} \to 0\,. \tag{3.116}$$

This can be seen as the number of Fermi surfaces that admit quasi-particle excitations with frequency up to $\hat{\omega}$. This increases indefinitely as $\hat{\omega}$ is decreased, and as $\hat{\omega} \to 0$, we recover the infinite number of Fermi surfaces of the unbounded Electron star.

On the other hand, for the compact star solutions, the number of resonances does not depend on the frequency because the effects of finite and small $\hat{\omega}$ do not modify the two first turning points of the potential $\tilde{V}$, which are still well approximated by the edges of the star: one finds the same finite number of stable excitations for $\hat{\omega} = 0$ and small $\hat{\omega}$. More precisely, a small frequency $|\hat{\omega}| < \hat{k}_N$ (where $\hat{k}_N$ is the smallest eigenstate of the $\hat{\omega} = 0$ potential) does not change the number of bound states.

A Fermi surface is defined when a system of fermions exhibits gapless low energy excitations around a Fermi momentum $\hat{k}_n$. A Fermi surface is not only defined by the existence of a Fermi momentum but also by a dispersion relation for the low energy excitations around it. For this reason, the result that the number of Fermi surfaces is infinite in the field theory state dual to the electron star needs to be clarified. This result was obtained by setting $\hat{\omega} = 0$. From (3.116), what we should rather say is that in the field theory state dual to the electron star, the number of fermionic excitations at fixed energy and fixed momentum diverges when the energy goes to zero. In other words, at fixed energy the number of fermionic excitations of the system is *arbitrarily large* when the energy tends to zero.

The above discussion suggests that some of the Fermi surfaces disappear between the electron star phase where it is infinite and the compact stars where it is finite. Let us consider the case where the coupling constant $\hat{\eta}$ vanishes, corresponding to the compact star solutions found in [1]. By increasing the elementary charge of the scalar field, one is expected to move from the electron star phase to the compact star phase[7]. Some of the Fermi surfaces are destroyed, they are the Fermi surfaces of the flavours of fermions which become superconducting. These Fermi surfaces have small Fermi momentum, which goes

[7]In fact, although it is expected, a phase transition between the electron star and the compact star was not found explicitly in [1], due to the difficulties in solving the system numerically for parameter values close to the possible transition. Thus, we cannot exclude the possibility of the existence of another phase between the electron star and the compact star phases.

in the opposite direction of what was found in [65] for the Cooper pair creation in the Reissner-Nordström black hole. This suggests that the mechanism leading to superconductivity is here far from being described by the BCS theory and the formation of Cooper pairs. The scalar condensate can rather be though as being a very complicated operator made out of many fermions, which does not have integer charge in elementary fermion charge unit. Indeed, in the bulk we have in general $q \neq 2q_f$.

## 3.6 Discussion

We have considered in this chapter Einstein-Maxwell gravity with a negative cosmological constant coupled to both charged bosonic and fermionic degrees of freedom, represented by a complex scalar field and a perfect fluid of fermionic particles, respectively. They interact directly through a current-current coupling which leaves the fluid approximation for the fermions valid. This system admits already know solutions holographically dual to field theory states at zero temperature and finite density, the extremal charged black hole, the electron star and the holographic superconductor.

In Section 3.2, by studying the field equation of a probe charged scalar field in the near-horizon geometry of the electron star, we have argued that the electron star background is unstable to the formation of scalar hair when the elementary charge of the scalar field is sufficiently large. Also, by studying the shape of the local chemical potential in the holographic superconductor solution, we gave reasons to believe that solutions with both a non-trivial scalar field and a non-zero fluid density could be constructed from the holographic superconductor solution found in [51]: when the maximum value of the local chemical potential exceeds the mass of the fermions, a probe fluid of fermions can exist on the holographic superconductor solution. This approach had already been used in [46] to construct electron star solutions at finite temperature. In this case, the Reissner-Nordström black hole plays the role of the holographic superconductor.

By using the arguments of Section 3.2, we found in Section 3.3 new backreacted solutions to the considered model which exhibit both a scalar field and a fluid density. While the scalar field is non-zero in the whole spacetime, the fluid density is confined in a shell and the charge density of the fluid can be positive or negative, leading to compact electron star solutions and compact positron star solutions, respectively. In our choice where the boundary total charge is positive[8], the formation of a positron star is made possible when the fluid and the scalar field interact directly through the current-current coupling. It exists in this case a charge of interaction between the scalar field and the fluid which is responsible for the screening of the negative charge density of the positron star.

We have also found solutions where a non-trivial scalar field coexists with both an electron star and a positron star, confined in distinct shells of the bulk spacetime. In this case we have a polarized charged system, where the separated shells of positively and negatively charged components of the fluid are immersed in a non-zero scalar field. Due to the screening of the negative electric charge by the scalar field, the two fluid densities are repelled instead of being attracted. The system is kept together by the gravitational attraction, which balances the electromagnetic repulsion. We called these solutions compact electron-positron star solutions.

By computing the free energy of the charged solutions of the system, we have shown in Section 3.4 that when it is possible, the presence in the bulk of both bosonic and

[8]The case where the boundary charge is negative is accessible by charge conjugation.

fermionic degrees of freedom is favoured thermodynamically. In particular, the electron-positron compact star solution is favoured when it exists. These results confirm previous works on the competition of several orders in holography [66, 67, 68, 69, 62, 70, 71, 72, 73].

The interpretation of the bulk charged scalar field in the compact star solutions is clear from the UV asymptotics. The field/operator correspondence presented in Chapter 1 tells us that it represents, in the dual field theory state, a charged scalar condensate which breaks the global $U(1)$ symmetry.

Even if it is natural to believe that the bulk fermionic fluid density is a sign of the presence of fermionic degrees of freedom in the dual field theory state, this is not as simple as for the scalar field. In the fluid approximation, the interpretation of the bulk fermions is not directly obtained from the UV asymptotics as for the scalar field. This is because the boundary fermionic operator is hidden in the fluid approximation of the bulk fermions.

For this reason and to characterize the states dual to the compact star solutions, we computed in Section 3.5 the (quasi-) normal modes of a probe spinor field in these bulk backgrounds. The probe spinor has the dual interpretation of a fluctuation of the fermionic operator of the field theory. The holographic procedure to compute correlation functions can thus be applied and we obtained the propagator, i.e. the retarded two-point Green's function, of the fermionic low energy excitations of the system. It results that the fluid of electrons and the fluid of positrons are dual to electron-like and hole-like Fermi surfaces, respectively. The formation of the Fermi surfaces is controlled by the scalar condensate and the current-current interaction.

As for the electron star, the Luttinger count reproduces the charge carried by the bulk fermions. However it does not correspond to the total charge of the system, which is shared in the boundary field theory by the fermionic and bosonic degrees of freedom; there is also a charge of interaction responsible for the screening of the fermions by the scalar condensate.

On the field theory side, one can interpret the positron-electron compact star solutions in the following way. The field theory state exhibits a scalar condensate and a large number of fermions with different flavours. Each flavour of fermions has a certain band structure but with the zero energy level having an offset that is different for each flavour. It results that a given chemical potential intersects the valence band for some fermions and the conductance band for the others, leading to hole-like and electron-like Fermi surfaces, respectively. A schematic illustration is given in Figure 3.20.

The study of the low energy fermionic spectrum of the mixed Bose-Fermi states has also led to an interesting result. By putting the field equation of the probe spinor in a Schrödinger form, we found that the number of Fermi surfaces in the field theory state dual to the electron star is infinite while it is finite in the compact star solutions. In the ES/CS phase transition between the electron star solution and the compact star solution, part of the boundary Fermi surfaces are gapped and the corresponding fermions condense. The Fermi surfaces which become gapped are the ones with smallest Fermi momenta. As discussed above, this is not expected from the BCS theory point of view where the Fermi surfaces with smallest momenta are the most stable. What happens in our holographic model agrees with the suggestion of [74] that the order the Fermi surfaces are filled in holographic models is characterized by a IR/UV duality: states with lowest Fermi momentum are filled later than the ones with smaller Fermi momentum. They are thus the first to condense at the ES/CS transition.

We also found that for small frequency, the fermionic excitations are stable. Dissipation of excitations around a given Fermi surface occurs only after an energy threshold is

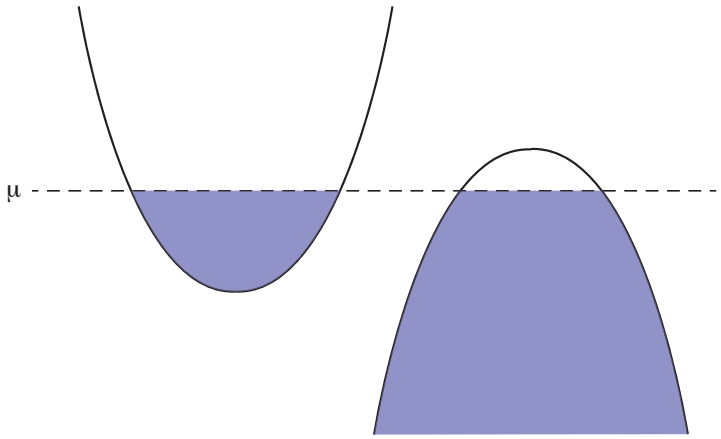


Figure 3.20: Schematic band structure of (dual of) the compact polarized stars solutions.

reached, meaning that the Fermi system does not interact with the bosons at arbitrarily low energy. On the other hand, for the non-compact electron star, the quasi-particle states can decay into the critical bosonic Lifshitz modes in the IR. When the scalar field has a W-shaped potential, hairy electron star solutions with constant fluid quantities in the IR can be constructed [62]. It would be interesting to compute the boundary fermionic Green's function in this case and study the dissipation properties at low energy.

As was shown in [74], the fact that the number of constituent fermions is infinite in the non-compact electron star can be seen as a consequence of working in the regime where the constituent charge $eq_f$ is very small compared to the total charge of the system. As its value is increased, the number of Fermi surfaces decreases until finally one arrives at the Dirac hair solution with only one species of fermions. It would be interesting to study the effect of turning on a scalar condensate in the finite $q_f$ regime, where already for zero condensate there is a finite number of Fermi surfaces.

Notice that the WKB analysis we applied is valid when a large number of hole-like and/or electron-like Fermi surfaces is present and for Fermi momenta not comparable to the extremal local Fermi momentum. Since the WKB approximation is valid for small Fermi momenta and those correspond to the first Fermi surfaces being gapped, one can study the formation and destruction of Fermi surfaces in these regions of the phase diagram which are far from the critical lines. Also, for larger momenta close to the extremal local Fermi momentum, the Schrödinger potential does not vanish linearly at the turning points. Matching at these turning points with Airy functions is not possible anymore. However, following the study done in this situation for the electron star model [44], we also expect Fermi surfaces to form.

It would be interesting to characterize better the properties of the excitations around the Fermi surfaces, determining the Fermi velocity and the residues as done for the electron star in [44]. It would also be interesting to compute the electrical conductivity and especially the Hall conductivity, which would determine the global nature of the fermionic system. One could also study the temperature dependence of the system. Finally, the onset of superconductivity and the ES/CS transition would deserve further analysis. This requires to find a holographic superconductor solution for small elementary charge of the scalar field. One IR asymptotic solution was found in [51], but there is no free parameter that can be fixed such that the source of the dual scalar operator vanishes.

# Chapter 4

# AdS black holes from duality in gauged supergravity

In this chapter, we study a STU model of $\mathcal{N} = 2$ gauged supergravity that is a truncation of the 4d $\mathcal{N} = 8$ gauged supergravity [75] and as such has a lift to eleven-dimensional supergravity on the seven-sphere. By using duality transformations, we obtain new static and rotating BPS black holes.

The new solutions were obtained by the author and a collaborator in [3].

## 4.1 Introduction

Black branes in gauged supergravity are of particular interest due to their ability to possess AdS asymptotics and they have numerous applications to holography. Somewhat recently [76] an exact analytic solution for static quarter-BPS black holes was found as well as an analytic quarter-BPS rotating black hole in [77]. This work was performed in an $\mathcal{N} = 2$ truncation of the four dimensional $\mathcal{N} = 8$ gauged supergravity theory of de Wit-Nicolai [75] and as such these black holes can be lifted to M-theory. Generalizing these solutions to new analytic families of supersymmetric $AdS_4$ black holes is the focus of our current work.

The static black holes of [76] can be understood within the context of the far-reaching work of Maldacena and Nunez [78]; in M-theory they correspond to a stack of M2-branes wrapped on a Riemann surface $\Sigma_g$ of genus $g \geq 0$. The initial work [78] found $AdS_p \times \Sigma_g$ geometries in $(p+2)$-dimensional gauged supergravity only when $g > 1$ and $p = 1, 3$ but the method was clearly universal and there has since been much work establishing the phase space of solutions for arbitrary genus and various $p$[1]. The work of Cacciatori and Klemm (CK) should be singled out for special mention since this is the only example with non-trivial scalar field profiles where the entire black-brane geometry is known analytically[2]. In addition, from a purely general relativistic point of view, four dimensional black holes with spherical horizons are traditionally of substantial interest as compared to black branes in higher dimensions.

In this work we apply a tried and true method of generating solutions in supergravity theories: the awful power of the Geroch group [89]. In Section 4.3 we find by explicit computation that the bosonic sector of our gauged STU model has a $G = U(1)^3$ invariance

[1] See for example [79, 80, 76, 81, 82, 83, 84, 85] and some aspects are nicely reviews in [86].

[2] We should mention the constant scalar black branes which exist for $p = 2, 3$ and $g > 1$ [87, 88].

and one can use this group to act on any solution of the theory. We denote the diagonal $U(1)$ subgroup of $G$ by $U(1)_g$ and find reason to conjecture that $G/U(1)_g$ is in addition a symmetry of the fermionic sector of the theory.

In Section 4.4 we look at the CK solutions. They depend on three charges; there are initially four charges but one BPS condition enforces a Dirac quantization condition and reduces this to a three dimensional parameter space. We act on the CK solutions with the two generators of $G/U(1)_g$ and generate static BPS black holes with two additional charges. In the symplectic frame adapted to the M-theory lift, the CK solution has purely magnetic charges whereas our two additional parameters are electric charges. Another point of comparison is that our new solutions have non-trivial axions whereas in the CK solutions the axions are trivial. Acting on the CK solutions with $U(1)_g \subset G$ breaks the supersymmetry of the solutions and also appears to violate the Dirac quantization condition, as a result we focus on the generators of $G/U(1)_g$. We also act on the CK solutions with equal magnetic charges and generate a new parameter.

In Section 4.5 we perform a similar action of $G/U(1)_g$ on the BPS rotating black holes of [77]. The solutions of [77] have equal magnetic charges which are inversely proportional to the gauge coupling and they depend on two parameters. One parameter corresponds to angular momentum the other represents a deformation of the boundary M2-brane theory. The static limit is a solution from [76] with a single parameter corresponding to a deformation of the boundary M2-brane theory. Another limit sets the deformation parameter to zero and corresponds to the constant scalar black hole with rotation. While this constant scalar black hole is a fixed point of our duality group, from the solutions of [77] we generate one additional parameter. The full solution space of BPS rotating black holes now has three parameters; angular momentum, one deformation parameter and our new parameter.

When lifted to M-theory the charges of the CK solutions correspond to twists of the $S^7$ bundle over $\Sigma_g$ [78]. From another point of view one can view these solutions as the near horizon limit of a stack of M2-branes wrapping a Riemann surface inside a local Calabi-Yau fivefold $X_5$ which is the product of four line bundle over $\Sigma_g$. The magnetic charges of the CK solution are proportional to the Chern numbers of these four line bundles. In this same duality frame, the electric charges we find correspond to the spin of the M2-branes along a pair of circles: $U(1)^2 \subset S^7$.

## 4.2 $\mathcal{N} = 2$ gauged supergravity

Let us consider $\mathcal{N} = 2$ Fayet-Iliopoulos-gauged supergravity coupled to $n_V$ vector multiplets. We use the $\mathcal{N} = 2$ supergravity conventions of [90] except we use the mostly plus signature $(- + ++)$. The theory contains the gravitational multiplet and $n_V$ vector multiplets. The bosonic content is the metric $g_{\mu\nu}$, the graviphoton $A^0$, $n_V$ gauge bosons $A^i$ $(i = 1, \ldots, n_V)$ and $n_V$ complex scalars $z^i$. The scalars parametrize a special Kähler manifold $\mathcal{M}_V$ of complex dimension $n_V$.

The bosonic part of the supergravity action is given by

$$S_{4d} = \int d^4x\sqrt{-g}\left[\frac{1}{2}R - g_{i\bar{\jmath}}\partial_\mu z^i \partial^\mu \bar{z}^{\bar{\jmath}} + \mathcal{I}_{\Lambda\Sigma}F^\Lambda_{\mu\nu}F^{\Sigma\,\mu\nu} + \mathcal{R}_{\Lambda\Sigma}F^\Lambda_{\mu\nu}\left(\frac{1}{2}\epsilon^{\mu\nu\rho\sigma}F^\Sigma_{\rho\sigma}\right) - V_g\right], \quad (4.1)$$

where $\mu, \nu, \rho, \sigma = 0, \ldots, 3$ are spacetime indices, $g_{i\bar{\jmath}}$ is the metric on the scalar manifold $\mathcal{M}_V$, $F^\Lambda_{\mu\nu}$ $(\Lambda = 0, \ldots, n_V)$ are the field strenghts of the graviphoton and the gauge bosons.

The only difference of the gauged supergravity action (4.1) compared to the ungauged case is that the potential for the scalars $V_g$ is non-vanishing.

The scalar manifold $\mathcal{M}_V$ is a special Kähler manifold that describes the self-interactions of the vector multiplets. We will assume that there exists a prepotential that determines in particular the metric on $\mathcal{M}_V$, the scalar potential $V_g$ and the matrices $\mathcal{I}_{\Lambda\Sigma}$, $\mathcal{R}_{\Lambda\Sigma}$ that appear in the action (4.1).

The prepotential $F$ is determined in terms of a symmetric tensor $d_{ijk}$ and given by

$$F \;=\; -d_{ijk}\frac{X^i X^j X^k}{X^0} \tag{4.2}$$

where the special coordinates are given in terms of the complex scalar fields,

$$X^\Lambda \;=\; \begin{pmatrix}1\\ z^i\end{pmatrix}, \qquad z^i = x^i + iy^i\,. \tag{4.3}$$

We define the dual sections $F_\Lambda = \partial_\Lambda F$ by

$$F_\Lambda \;=\; \begin{pmatrix} d_{ijk}z^i z^j z^k \\ -3d_{z,i}\end{pmatrix} \tag{4.4}$$

and the Kähler potential $K$ and metric $g_{i\bar{j}}$ are

$$e^{-K} \;=\; 8d_y\,, \qquad g_{i\bar{j}} = \partial_i\partial_{\bar{j}}K\,. \tag{4.5}$$

The rescaled sections are defined as

$$\mathcal{V} = \begin{pmatrix} L^\Lambda \\ M_\Lambda\end{pmatrix} = e^{K/2}\begin{pmatrix} X^\Lambda \\ F_\Lambda\end{pmatrix}\,. \tag{4.6}$$

The kinetic and topological terms for the vector fields in (4.1) come from the tensor

$$\mathcal{N}_{\Lambda\Sigma} \;=\; \mathcal{R}_{\Lambda\Sigma} + i\,\mathcal{I}_{\Lambda\Sigma} = \overline{F}_{\Lambda\Sigma} + 2i\frac{\mathrm{Im}\,F_{\Lambda\Delta}\mathrm{Im}\,F_{\Sigma\Upsilon}X^\Delta X^\Upsilon}{\mathrm{Im}\,F_{\Delta\Upsilon}X^\Delta X^\Upsilon} \tag{4.7}$$

where $F_{\Lambda\Sigma} = \partial_\Lambda\partial_\Sigma F$. The dual gauge-field strength is

$$G_\Lambda = \mathcal{R}_{\Lambda\Sigma}F^\Sigma - \mathcal{I}_{\Lambda\Sigma} * F^\Sigma\,. \tag{4.8}$$

We define the tensor[3]

$$\widehat{d}^{ijk} = \frac{g^{il}g^{jm}g^{kn}d_{ijk}}{d_y^2} \tag{4.9}$$

which has the crucial property that it is constant whenever $\mathcal{M}_V$ is a homogeneous space. We use the following shorthand for contraction of objects with the symmetric tensors $d_{ijk}$ and $\widehat{d}^{ijk}$:

$$\begin{aligned} &d_g = d_{ijk}g^i g^j g^k\,, \quad d_{g,i} = d_{ijk}g^j g^k\,, \quad d_{g,ij} = d_{ijk}g^k\,,\\ &\widehat{d}_g = \widehat{d}^{ijk}g_i g_j g_k\,, \quad \widehat{d}^i_g = \widehat{d}^{ijk}g_j g_k\,, \quad \widehat{d}^{ij}_g = \widehat{d}^{ijk}g_k\,. \end{aligned} \tag{4.10}$$

[3]The hat index here does not refer to any particular duality frame, hopefully this does not cause confusion on the part of the reader.

The theory is 'covariant' under the symplectic group $Sp(2n_V+2,\mathbb{R})$ which acts on the scalar fields, the gauge fields and the gaugings of the theory. It means that the action (4.1) is not invariant under such a transformation but the field equations are.

The scalar potential $V_g$ is defined in terms of the symplectic invariant quantities

$$\mathcal{L} = \langle \mathcal{G}, \mathcal{V} \rangle \,, \qquad \mathcal{L}_i = \langle \mathcal{G}, D_i \mathcal{V} \rangle \,, \tag{4.11}$$

where $\langle ., . \rangle$ is the symplectic product of two symplectic vectors and

$$\mathcal{G} = \begin{pmatrix} g^\Lambda \\ g_\Lambda \end{pmatrix} \tag{4.12}$$

is the symplectic vector for gaugings. The scalar potential is given in terms of these quantities by

$$V_g \;\; = \;\; g^{i\bar{\jmath}} D_i \mathcal{L} D_{\bar{\jmath}} \overline{\mathcal{L}} - 3|\mathcal{L}|^2 \,. \tag{4.13}$$

We will be interested here in black hole solutions which satisfy the BPS equations. These black holes have electric charges $q_\Lambda$ and magnetic charges $p^\Lambda$ defined by

$$q_\Lambda = \frac{1}{\mathrm{vol}(\Sigma_g)} \int_{\Sigma_g} G_\Lambda \,, \qquad p^\Lambda = \frac{1}{\mathrm{vol}(\Sigma_g)} \int_{\Sigma_g} F^\Lambda \,, \tag{4.14}$$

where $\Sigma_g$ is the event horizon space and $\mathrm{vol}(\Sigma_g)$ its volume. BPS equations depend only on the gauge fields through the symplectic vector

$$\mathcal{Q} = \begin{pmatrix} p^\Lambda \\ q_\Lambda \end{pmatrix} \,, \tag{4.15}$$

on the scalar fields through the sections $\mathcal{V}$ and on the gaugings $\mathcal{G}$. The action of a symplectic transformation on these symplectic vectors leads to a physically equivalent BPS black hole solution but in a different symplectic frame where $\mathcal{V}$, $\mathcal{Q}$ and $\mathcal{G}$ have a different form.

In the following we focus the analysis on a simple STU model of $\mathcal{N}$=2 FI-gauged supergravity which contains three vector multiplets ($n_V = 3$).

## 4.3 STU-model

We start in the symplectic duality frame where the STU-model of four dimensional supergravity has the prepotential

$$F = -\frac{X^1 X^2 X^3}{X^0} \,. \tag{4.16}$$

This implies that $d_{123} = \frac{1}{6}$ and $\widehat{d}^{123} = \frac{32}{3}$. This model has the vector-multiplet scalar manifold

$$\mathcal{M}_V = \Big( \frac{SL(2,\mathbb{R})}{U(1)} \Big)^3 \tag{4.17}$$

and thus the global symmetry $\big[SL(2,\mathbb{R})\big]^3$. We include a very specific dyonic gauging, namely we take

$$\mathcal{G} = \begin{pmatrix} g^\Lambda \\ g_\Lambda \end{pmatrix} \,, \qquad g^\Lambda = \begin{pmatrix} 0 \\ g^1 \\ g^2 \\ g^3 \end{pmatrix} \,, \qquad g_\Lambda = \begin{pmatrix} g_0 \\ 0 \\ 0 \\ 0 \end{pmatrix} \tag{4.18}$$

and using a duality symmetry from Appendix E with

$$\begin{aligned} &\beta = \log\Big[\frac{g_0}{g}\Big]\,, \qquad && B^i{}_i = -\log\Big[-\frac{g^i (g_0)^{1/3}}{g^{4/3}}\Big]\,, \\ &a^i = b_j = 0\,, && B^i{}_j = 0\,, \quad \text{for} \;\; i \neq j \end{aligned} \tag{4.19}$$

we set the magnitudes of the gauge couplings equal

$$g^\Lambda = -\begin{pmatrix} 0 \\ g \\ g \\ g \end{pmatrix}\,, \qquad g_\Lambda = \begin{pmatrix} g \\ 0 \\ 0 \\ 0 \end{pmatrix}\,. \tag{4.20}$$

There is a simple reason for choosing this seemingly obscure gauging: this model is known to be a truncation of $\mathcal{N} = 8$, de Wit-Nicolai theory [91, 92, 93] with $n_V = 3$ and can thus be uplifted to M-theory[4]. The model given by (4.16) and (4.20) is related by a symplectic transformation

$$\mathcal{S} = \begin{pmatrix} A & B \\ C & D \end{pmatrix}\,, \qquad A = D = \mathrm{diag}\{1,0,0,0\}\,, \quad B = -C = \mathrm{diag}\{0,1,1,1\} \tag{4.21}$$

to the perhaps more familiar model with prepotential, gaugings and sections given by

$$\breve{F} \;=\; -2i\sqrt{\breve{X}^0\breve{X}^1\breve{X}^2\breve{X}^3}\,, \quad \breve{g}^\Lambda = 0\,, \qquad \breve{g}_\Lambda = g\,, \tag{4.22}$$

$$\breve{X}^\Lambda \;=\; \begin{pmatrix} 1 \\ -z^2 z^3 \\ -z^3 z^1 \\ -z^1 z^2 \end{pmatrix}\,, \quad \breve{F}_\Lambda = \begin{pmatrix} z^1 z^2 z^3 \\ -z^1 \\ -z^2 \\ -z^3 \end{pmatrix} \tag{4.23}$$

but we are particularly fond of the frame (4.16) because it makes the action of the symplectic group $Sp(2n_V + 2, \mathbb{R})$ manifest and thus is the natural frame to understand the unbroken symmetries. Of course both frames are physically indistinguishable.

With dyonic gaugings such as (4.20) it is convenient to use the formalism of [96] which is a natural symplectic completion of the electrically gauged theory. For the STU model with gaugings given by (4.20), from (4.13) the scalar potential has the following explicit form:

$$V_g = -g^2 \sum_{i=1}^{3} \Big[\frac{1}{y^i} + y^i + \frac{(x^i)^2}{y^i}\Big]\,. \tag{4.24}$$

Our first goal is to analyze the subgroup of $\big[SL(2,\mathbb{R})\big]^3$ which remains unbroken in the bosonic sector of the gauged theory to do so it is sufficient to analyze the invariances of $V_g$.

### 4.3.1 The basics of $SL(2,\mathbb{R})/U(1)$

This section contains some details about the coset $SL(2,\mathbb{R})/U(1)$. We are aware that this material is quite elementary but see no reason not to spell out our steps in modest detail.

[4]There has been recent work [94] refining the explicit uplift [95] of this $\mathcal{N} = 8$ theory to eleven dimensional supergravity and thus proving that it is a consistent truncation.

Indeed, the symmetries of this particularly interesting STU-model of gauged supergravity are remarkably straightforward, nonetheless to the best of our knowledge have never been worked out or utilized.

The coset representative is

$$V = e^{H\frac{\phi}{2}} e^{E\chi} \tag{4.25}$$

where the generators of $\mathfrak{sl}(2,\mathbb{R})$ are

$$H = \begin{pmatrix} 1 & 0 \\ 0 & -1 \end{pmatrix}, \quad E = \begin{pmatrix} 0 & 1 \\ 0 & 0 \end{pmatrix}, \quad F = \begin{pmatrix} 0 & 0 \\ 1 & 0 \end{pmatrix}. \tag{4.26}$$

To construct the metric on the coset, one takes

$$M = V^T V \tag{4.27}$$

and under the right action of $\Lambda \in SL(2,\mathbb{R})$ these transform as

$$V \;\rightarrow\; V\Lambda\,, \qquad M \rightarrow \Lambda^T M \Lambda\,. \tag{4.28}$$

The transformation (4.28) ruins the parametrization (4.25) but one uses a compensating, local, left acting $SO(2)$ transformation to bring $V$ back to the form (4.25). From (4.28) we see that $\mathrm{Tr}M$ is invariant under $\Lambda \in SO(2)$. The kinetic terms for the coset are then given by

$$\mathcal{L}_{kin} = -\frac{1}{4}\mathrm{Tr}(\partial_\mu M \partial^\mu M^{-1}) \tag{4.29}$$

and are invariant under (4.28) for $\Lambda \in SL(2,\mathbb{R})$.

Explicitly, using (4.25) and (4.27) we have

$$M = \begin{pmatrix} e^{\phi} & e^{\phi}\chi \\ e^{\phi}\chi & e^{-\phi} + e^{\phi}\chi^2 \end{pmatrix} \tag{4.30}$$

and using the standard coordinate redefinition

$$z = x + iy = \chi + ie^{-\phi} \tag{4.31}$$

we find that

$$\mathrm{Tr}M = \frac{1}{y} + y + \frac{x^2}{y}\,. \tag{4.32}$$

So we see that the scalar potential of our gauged supergravity theory (4.24) is given by canonical objects from the coset:

$$V_g = -g^2 \sum_{i=1}^{3} \mathrm{Tr}M_i \tag{4.33}$$

where $M_i$ is (4.27) for the $i$-th $SL(2,\mathbb{R})/U(1)$ coset. Thus we have demonstrated that the scalar potential and thus the bosonic sector of the STU model of Section 4.3 is invariant under

$$SO(2)^3 \subset SL(2,\mathbb{R})^3\,. \tag{4.34}$$

### 4.3.2 Embedding $SO(2)^3$ into $Sp(2n_V+2,\mathbb{R})$

We now embed this symmetry group $SO(2)^3$ into $Sp(8,\mathbb{R})$ using the work of [97, 98], key aspects of this work are summarized in Appendix E. The three rotations corresponding to (4.34) are given by the exponentiation of the elements $\underline{\mathcal{S}} \in \mathfrak{sp}(8,\mathbb{R})$ from (E.3) with

$$\beta = B^i{}_j = 0\,, \qquad a^i = -b_i\,. \tag{4.35}$$

We find that these are given by

$$\mathcal{O}_i(\alpha) \;=\; \begin{pmatrix} Q_i(\alpha) & R_i(\alpha) \\ S_i(\alpha) & T_i(\alpha) \end{pmatrix} \tag{4.36}$$

where

$$Q_1(\alpha) = T_1(\alpha) = \begin{pmatrix} c_\alpha & s_\alpha & 0 & 0 \\ -s_\alpha & c_\alpha & 0 & 0 \\ 0 & 0 & c_\alpha & 0 \\ 0 & 0 & 0 & c_\alpha \end{pmatrix}, \quad R_1(\alpha) = -S_1(\alpha) = \begin{pmatrix} 0 & 0 & 0 & 0 \\ 0 & 0 & 0 & 0 \\ 0 & 0 & 0 & -s_\alpha \\ 0 & 0 & -s_\alpha & 0 \end{pmatrix},$$

$$Q_2(\alpha) = T_2(\alpha) = \begin{pmatrix} c_\alpha & 0 & s_\alpha & 0 \\ 0 & c_\alpha & 0 & 0 \\ -s_\alpha & 0 & c_\alpha & 0 \\ 0 & 0 & 0 & c_\alpha \end{pmatrix}, \quad R_2(\alpha) = -S_2(\alpha) = \begin{pmatrix} 0 & 0 & 0 & 0 \\ 0 & 0 & 0 & -s_\alpha \\ 0 & 0 & 0 & 0 \\ 0 & -s_\alpha & 0 & 0 \end{pmatrix},$$

$$Q_3(\alpha) = T_3(\alpha) = \begin{pmatrix} c_\alpha & 0 & 0 & s_\alpha \\ 0 & c_\alpha & 0 & 0 \\ 0 & 0 & c_\alpha & 0 \\ -s_\alpha & 0 & 0 & c_\alpha \end{pmatrix}, \quad R_3(\alpha) = -S_3(\alpha) = \begin{pmatrix} 0 & 0 & 0 & 0 \\ 0 & 0 & -s_\alpha & 0 \\ 0 & -s_\alpha & 0 & 0 \\ 0 & 0 & 0 & 0 \end{pmatrix}$$

and we use the notation $s_\alpha = \sin\alpha$ and $c_\alpha = \cos\alpha$.

We know from Section 4.3.1 that simultaneously acting with $\mathcal{O}_i$ on both the sections $\mathcal{V}$ and the vector fields is a symmetry of the Lagrangian. Now by construction the theory is invariant under the simultaneous action of any symplectic matrix $\mathcal{T}$ on the gaugings $\mathcal{G}$, charges $\mathcal{Q}$ and the sections $\mathcal{V}$:

$$(\mathcal{G},\mathcal{Q},\mathcal{V}) \to (\mathcal{T}\mathcal{G},\mathcal{T}\mathcal{Q},\mathcal{T}\mathcal{V})\,, \qquad \mathcal{T} \in Sp(2n_V+2,\mathbb{R}) \tag{4.37}$$

and so we can surmise that for our particular theory we could equally well just act on the gaugings

$$\mathcal{G} \to \mathcal{O}_i(\alpha)\mathcal{G} \tag{4.38}$$

and this should be a symmetry of the Lagrangian. Indeed explicit calculation shows this to be true.

### 4.3.3 Two simple generators

For two of these transformations we can see this quite explicitly since for the particular gaugings (4.20) something even stronger is true, the gaugings themselves are invariant:

$$\mathcal{O}_{12}(\alpha)\mathcal{G} \;=\; \mathcal{G}\,, \qquad \mathcal{O}_{23}(\alpha)\mathcal{G} = \mathcal{G} \tag{4.39}$$

where

$$\mathcal{O}_{ij}(\alpha) = \mathcal{O}_i(\alpha)\mathcal{O}_j^{-1}(\alpha)\,. \tag{4.40}$$

This leads us to conclude that the generators $\mathcal{O}_{12}(\alpha)$ and $\mathcal{O}_{23}(\alpha)$ commute with the gauge group. In particular this means that solutions generated using $\mathcal{O}_{12}$ and $\mathcal{O}_{23}$ from a supersymmetric seed solution will preserve the same amount of supersymmetry.

### 4.3.4 The third generator

The final generator can be taken to be

$$\mathcal{O}_g(\alpha) = \mathcal{O}_1(\alpha/3)\mathcal{O}_2(\alpha/3)\mathcal{O}_3(\alpha/3) \tag{4.41}$$

and we find that the gaugings are not invariant:

$$g^\Lambda \to -g \begin{pmatrix} s_\alpha \\ c_\alpha \\ c_\alpha \\ c_\alpha \end{pmatrix}, \qquad g_\Lambda \to -g \begin{pmatrix} -c_\alpha \\ s_\alpha \\ s_\alpha \\ s_\alpha \end{pmatrix}. \tag{4.42}$$

Nonetheless the whole bosonic Lagrangian is invariant; the kinetic terms are invariant because this transformation is a duality transformation of the underlying ungauged supergravity theory and we have shown explicitly that the scalar potential is invariant. Note however that the two terms in (4.13) are not separately invariant, only the sum is. As a result we can freely generate solutions to the bosonic equations using $\mathcal{O}_{123}$.

In [96] a comment was made regarding a particular $SO(2) \subset SL(2,\mathbb{R})^3$ which is identified with the gauging of the graviphoton and thus what we referred to in the introduction as $U(1)_g$. We understand this generator to be $\mathcal{O}_g$. In fact we find it difficult to make the Dirac quantization condition (4.44) compatible with this generator, it is the generators $\mathcal{O}_{12}$ and $\mathcal{O}_{23}$ which are particularly useful for our purposes. In a different context [99], it was emphasized to great utility that the duality group of a gauged theory is the commutant of the gauge group inside the duality group of the ungauged theory. In our particular example we understand that the gauge group is identified with the $SO(2)$ generated by[5] $\mathcal{O}_g$ and the commutant of the gauge group to be the $SO(2)^2$ generated by $\mathcal{O}_{12}$ and $\mathcal{O}_{23}$. Solutions generated with $\mathcal{O}_g$ will typically break the supersymmetry of the seed solution and $\mathcal{O}_g$ will not appear in the following sections.

## 4.4 BPS static black holes

We now analyze the action of $\mathcal{O}_i(\alpha)$ on the supersymmetric static black holes of [76], which we will first review. The metric ansatz is

$$ds^2_{BH} = -e^{2U}dt^2 + e^{-2U}dr^2 + e^{2(V-U)}d\Sigma_g^2 \tag{4.43}$$

where $d\Sigma_g^2$ is the constant curvature metric on $(S^2, \mathbb{R}^2, \mathbb{H}^2)$ and the scalar fields depend only on the radial coordinate. The BPS equations can be found in [96] but we will not utilize them here. It is however worth mentioning in general there is a Dirac quantization condition $\langle \mathcal{G}, \mathcal{Q} \rangle \in \mathbb{Z}$ which for supersymmetric solutions is strengthened to

$$\langle \mathcal{G}, \mathcal{Q} \rangle = -\kappa\,, \tag{4.44}$$

where $\kappa = (1, 0, -1)$ for $\Sigma_g = (S^2, \mathbb{R}^2, \mathbb{H}^2)$ respectively.

[5] One should note however that before gauging, the scalar fields are neutral under the global $U(1)$ which is gauged. In the gauged theory the scalars are not minimally coupled to any gauge fields.

### 4.4.1 The supersymmetric static black holes

The black holes of [76] require the charges

$$\mathcal{Q} = \begin{pmatrix} p^\Lambda \\ q_\Lambda \end{pmatrix}, \qquad p^\Lambda = \begin{pmatrix} p^0 \\ 0 \\ 0 \\ 0 \end{pmatrix}, \qquad q_\Lambda = \begin{pmatrix} 0 \\ q_1 \\ q_2 \\ q_3 \end{pmatrix} \tag{4.45}$$

and we define some rescaled sections

$$\widetilde{L}^\Lambda = e^{V-U} L^\Lambda \,, \qquad \widetilde{M}_\Lambda = e^{V-U} M_\Lambda \,. \tag{4.46}$$

In the duality frame given by (4.23) the charges would be purely magnetic:

$$(\breve{p}^\Lambda)^T = (p^0, q_1, q_2, q_3) \,, \qquad \breve{q}_\Lambda = 0 \,. \tag{4.47}$$

The solution is mildly cumbersome but completely explicit, it has recently been extended in [100] to a large class of $\mathcal{N} = 2$ U(1)-gauged supergravity theories and a covariant form of the solution is presented there. It is given by

$$e^V = \frac{r^2}{R} - v_0 \,, \tag{4.48}$$

$$\widetilde{L}^0 = \frac{r}{4gR} + \beta^0 \,, \tag{4.49}$$

$$\widetilde{M}_i = \frac{r}{4gR} + \beta_i \,, \tag{4.50}$$

where $R$ is the $AdS_4$ radius

$$R = \frac{1}{\sqrt{2}\, g} \tag{4.51}$$

and[6]

$$\beta^0 = \frac{\epsilon}{2\sqrt{2}\, g} \sqrt{\frac{v_0}{2R} - g p^0} \,, \tag{4.52}$$

$$\beta_i = -\frac{\epsilon}{2\sqrt{2}\, g} \sqrt{\frac{v_0}{2R} - g q_i} \,, \tag{4.53}$$

$$v_0 = 2R \Big[ g p^0 + \frac{27 (d_{ijk} g^i \Pi^j \Pi^k)^2}{32 d_\Pi} \Big] \,, \tag{4.54}$$

where $\epsilon = \pm 1$ and $\Pi^i$ is a certain function of the charges:

$$\Pi^i = -\frac{4}{3g} (2q_i + p^0 - q_1 - q_2 - q_3) \,. \tag{4.55}$$

From these expressions one obtains the other metric function $e^U$ and the scalars $y^i$ from (4.48)-(4.50) and (4.52)-(4.54):

$$e^{4U} = \frac{1}{64} \frac{e^{4V}}{\widetilde{L}^0 \widetilde{M}_1 \widetilde{M}_2 \widetilde{M}_3} \,, \qquad y^i = \frac{3}{64} \frac{\widehat{d}^{ijk} \widetilde{M}_j \widetilde{M}_k}{\sqrt{\widetilde{L}^0 \widetilde{M}_1 \widetilde{M}_2 \widetilde{M}_3}} \,, \quad i = 1, 2, 3 \,. \tag{4.56}$$

[6] To maintain covariance in the expression for $v_0$ we have left $g^i$ which should be set $g^i = -g$.

This CK solution has vanishing axions and is specified by three independent charges; there are four charges (4.45) with one constraint (4.44). One would typically not refer to the CK solutions as dyonic since in the symplectic frame (4.23) the gaugings are electric and the charges are purely magnetic. There are regular CK black holes for horizons $\Sigma_g$ for all $g \geq 0$ but still regularity places bounds on the values of the magnetic charges.

**Equal charges**

When the charges are all equal then from the above analysis we arrive at the well known flow with constant scalar fields for which $\kappa = -1$ as well as

$$\Pi^i = 0\,, \qquad v_0 = 2Rgp\,, \qquad \beta^0 = \beta_i = 0\,. \tag{4.57}$$

Taking into account the Dirac quantization condition (4.44) the charges are fixed (they do not give an independent parameter)

$$p^0 = q_i = \frac{1}{4g} \tag{4.58}$$

and the horizon is at

$$r = r_h = \frac{R}{\sqrt{2}} \tag{4.59}$$

which is positive and thus the black hole is regular.

There is a whole family of solutions which satisfy (4.58) and are missed by the above analysis because of some degeneracy in the BPS equations, this solution has a free parameter $\beta$ corresponding. The metric and sections have

$$v_0 = \frac{R}{2} + 16Rg^2\beta^2\,, \tag{4.60}$$

$$\beta^0 = \beta_1 = \beta\,, \tag{4.61}$$

$$\beta_2 = \beta_3 = -\beta \tag{4.62}$$

and the resulting scalar fields are purely imaginary (the axions vanish)

$$z^1 = i\,\frac{r+\Delta}{r-\Delta}\,, \qquad z^2 = z^3 = i\,, \tag{4.63}$$

where with a view towards the next section we have defined a new parameter

$$\Delta = 4gR\beta = 2\sqrt{2}\,\beta\,. \tag{4.64}$$

This solution was originally found in [76] from the model with $\widehat{F} = -i\widehat{X}^0\widehat{X}^1$ and we elaborate in the next section on how this is related to the STU model. This gives the metric

$$ds^2_{BH} \;=\; -\frac{\left(r^2 - \frac{R^2}{2} - \Delta^2\right)^2}{R^2(r^2-\Delta^2)}dt^2 + \frac{R^2(r^2-\Delta^2)}{\left(r^2 - \frac{R^2}{2} - \Delta^2\right)^2}dr^2 + \left(r^2-\Delta^2\right)d\Sigma_g^2 \tag{4.65}$$

where the metric on $\Sigma_g = \mathbb{H}^2/\Gamma$ is

$$d\Sigma_g^2 \;=\; d\theta^2 + \sinh^2\theta d\phi^2\,. \tag{4.66}$$

The horizon is at

$$r_h = \sqrt{\frac{R^2}{2} + \Delta^2}\,, \tag{4.67}$$

while the scalar field $z^1$ is singular when

$$r = r_s \equiv \Delta\,. \tag{4.68}$$

but $r_h > r_s$ so the singularity is cloaked by a horizon and the black hole is regular. The conserved charges are independent of $\Delta$ but the metric and scalar field depend nontrivially on $\Delta$. The $\Delta \to 0$ limit gives the constant scalar black hole.

The UV behaviour of the $\Delta$ dependence scales as $\mathcal{O}(\frac{1}{r})$ and in principle there is a choice of quantization schemes [14] which allows us to interpret this as a source *or* a vev in the boundary M2-brane theory. To clarify this it is instructive to study the horizon geometry. We find the radius of the horizon to be independent of $\Delta$

$$R^2_{\Sigma_g} = \frac{R^2}{2} \tag{4.69}$$

which is comforting since the Bekenstein-Hawking entropy should not depend on continuous parameters. However the $AdS_2$ radius does depend on $\Delta$:

$$R^2_{AdS_2} = \frac{R^2}{4\big(1 + \frac{2\Delta^2}{R^2}\big)}\,. \tag{4.70}$$

By general principles of holography the effective $\mathrm{AdS}_2$ radius is a measure of the degrees of freedom in boundary superconformal quantum mechanics. This should not depend on the expectation value of any operator and as such we interpret the $\Delta$ dependence to represent an explicit deformation of the boundary M2-brane theory by a dimension one operator. This is on top of the mass terms induced from the curvature of $\Sigma_g$ when twisting of the world-volume M2-brane theory [78].

### 4.4.2 Duality transformations on the CK black holes

Our new solutions with non-trivial axions and genuinely dyonic charges are given by

$$\begin{aligned} e^V &= e^V|_{CK} \\ e^U &= e^U|_{CK} \\ \mathcal{V}_\alpha &= \mathcal{O}_{12}(\alpha_1)\mathcal{O}_{23}(\alpha_2)\mathcal{V}_{CK} \\ \mathcal{Q}_\alpha &= \mathcal{O}_{12}(\alpha_1)\mathcal{O}_{23}(\alpha_2)\mathcal{Q}_{CK} \\ \mathcal{G}_\alpha &= \mathcal{G}\,, \end{aligned} \tag{4.71}$$

where $\mathcal{Q}_{CK}$ refers to (4.45) and $\mathcal{G}$ refers to (4.20). The scalar fields transform by fractional linear transformations:

$$z^1_\alpha = \frac{c_{\alpha_1} z^1 - s_{\alpha_1}}{s_{\alpha_1} z^1 + c_{\alpha_1}}\,, \tag{4.72}$$

$$z^2_\alpha = \frac{c_{\alpha_{21}} z^2 - s_{\alpha_{21}}}{s_{\alpha_{21}} z^2 + c_{\alpha_{21}}}\,, \tag{4.73}$$

$$z^3_\alpha = \frac{c_{\alpha_2} z^3 + s_{\alpha_2}}{-s_{\alpha_2} z^3 + c_{\alpha_2}}\,, \tag{4.74}$$

where $\alpha_{21} = \alpha_2 - \alpha_1$ and one can observe that non-trivial axions are generated. Importantly, one can check that the Dirac quantization condition is invariant:

$$\langle \mathcal{G}, \mathcal{O}_{12}(\alpha_1)\mathcal{O}_{23}(\alpha_2)\mathcal{Q}_{CK}\rangle = \langle \mathcal{G}, \mathcal{Q}_{CK}\rangle \,. \tag{4.75}$$

This space of supersymmetric static black holes now depends on five charges; three initial charges from the CK solutions and the parameters $(\alpha_1, \alpha_2)$ generate two new charges. As such there is no duality frame where the charges of the entire family are purely magnetic; they are genuinely dyonic black holes. In [101] a complete solution was found for BPS horizon geometries of the form $\mathrm{AdS}_2 \times \Sigma_g$ in FI-gauged supergravity. It was found in [101] that the space of BPS horizon geometries should be $2n_V$-dimensional. The counting works as follows: the gaugings $\mathcal{G}$ define the theory and therefore are fixed. There are $n_V+1$ electric charges and $n_V+1$ magnetic charges. Then there is the Dirac quantization condition (4.44) and in [101] one additional constraint was found leaving $2n_V$ parameters. For the model at hand $n_V = 3$ and this space is six dimensional. Assuming that every BPS solution of the form $\mathrm{AdS}_2 \times \Sigma_g$ can be completed in the UV to a genuine $\mathrm{AdS}_4$ black hole, it would seem there is still one dimension of the black hole solution space missing. We will comment on this further in the conclusions.

For equal charge solutions with (4.58), there is an additional branch of solutions. The charges are invariant under (4.71) but with $\Delta \neq 0$ the scalar fields $(z^2, z^3)$ are invariant while $z^1$ transforms according to (4.72):

$$z^1_\alpha = \frac{2r\Delta s_{2\alpha} + i(r^2 - \Delta^2)}{r^2 + \Delta^2 - 2r\Delta c_{2\alpha}} \,, \tag{4.76}$$

$$z^2_\alpha = z^3_\alpha = i \,. \tag{4.77}$$

The metric is invariant and given by (4.65). When $\Delta = 0$ the whole solution is invariant. The regularity of the black hole can be easily analyzed, when $\alpha = 0$ the scalar $z^1$ diverges at $r = \Delta$ while for $\alpha \neq 0$ the imaginary part $\mathrm{Im}\,(z^1)$ vanishes at $r = \Delta$. Nonetheless this is still shielded by the horizon whose position is independent of $\alpha$. So for the fixed charges (4.58) the full solution space is now a family of solutions with two parameters $(\Delta, \alpha)$. Since the metric does not depend on $\alpha$ the effective $\mathrm{AdS}_2$ radius does not depend on $\alpha$ and we interpret this mode as an expectation value.

## 4.5 Rotating black holes

We now apply our duality transformations to rotating black holes. We focus on the BPS rotating black holes in $\mathrm{AdS}_4$ are those of [77], these solutions were originally found in the gauged supergravity model with prepotential and sections given by[7]

$$\widehat{F} = -i\widehat{X}^0\widehat{X}^1 \,, \qquad \widehat{X}^\Lambda = \begin{pmatrix} 1 \\ \tau \end{pmatrix} \,, \qquad \widehat{F}_\Lambda = \begin{pmatrix} -i\tau \\ -i \end{pmatrix} \,, \qquad \tau = x + iy \,. \tag{4.78}$$

This model does not have a frame where it is given by a cubic prepotential but one can embed it into the STU-model in the frame (4.22) and (4.23). We now describe this

[7]To be clear, the hatted variables refer to the model of (4.78), the variables with a breve "$\breve{}$" refer to the STU-model in the frame given by (4.22) and (4.23) while the un-hatted, un-breved variables refer to STU model obtained from the cubic prepotential (4.16). The duality rotations (4.36) act in the frame of (4.16).

embedding in some detail and then the resulting action of the duality group. To do so we take the scalar fields

$$z^1 = i\tau\,, \tag{4.79}$$
$$z^2 = z^3 = i \tag{4.80}$$

and sections

$$\breve{X}^0 = \breve{X}^1 = \widehat{X}^0\,, \quad \breve{X}^2 = \breve{X}^3 = \widehat{X}^1\,, \quad \breve{F}_0 = \breve{F}_1 = \widehat{F}_0\,, \quad \breve{F}_2 = \breve{F}_3 = \widehat{F}_1\,. \tag{4.81}$$

The scalar potential of this model is

$$\widehat{V}_g = -\frac{\widehat{g}^2}{2}\Big[4 + \frac{1}{x} + x + \frac{y^2}{x}\Big]\,. \tag{4.82}$$

The gauge fields and couplings between the models are related by $\widehat{g}^\Lambda = \breve{g}^\Lambda = 0$ and

$$\frac{1}{\sqrt{2}}\widehat{g}_0 = \breve{g}_0 = \breve{g}_1\,, \quad \frac{1}{\sqrt{2}}\widehat{g}_1 = \breve{g}_2 = \breve{g}_3\,, \qquad \breve{A}^0 = \breve{A}^1 = \frac{1}{\sqrt{2}}\widehat{A}^0\,, \qquad \breve{A}^2 = \breve{A}^3 = \frac{1}{\sqrt{2}}\widehat{A}^1\,.$$

For this embedding the dual sections are $\widehat{M}_0 = -i\widehat{L}^1$ and $\widehat{M}_1 = -i\widehat{L}^0$ so that in total we have the following symplectic vector of sections

$$\breve{\mathcal{V}}^T = \frac{1}{\sqrt{2}}(\widehat{L}^0, \widehat{L}^0, \widehat{L}^1, \widehat{L}^1, -i\widehat{L}^1, -i\widehat{L}^1, -i\widehat{L}^0, -i\widehat{L}^0)\,. \tag{4.83}$$

The duality transformation $\mathcal{O}_{23}(\alpha)$ acts trivially while $\mathcal{O}_{12}(\alpha)$ acts on the sections as follows:

$$\breve{\mathcal{V}}_\alpha \;=\; \mathcal{S}\,\mathcal{O}_{12}(\alpha)\,\mathcal{S}^{-1}\breve{\mathcal{V}} \tag{4.84}$$

where $\mathcal{S}$ is given in (4.21). From (4.84) one can work out that after the transformation we retain the identity $z^2 = z^3 = i$ but this is also clear since they are fixed points of the fractional linear transformations (4.72-4.74). The scalar field $z^1$ transforms by a fractional linear transformation

$$z^1_\alpha \;=\; \frac{c_\alpha z^1 - s_\alpha}{s_\alpha z^1 + c_\alpha}\,. \tag{4.85}$$

The new gauge field strengths are obtained from

$$\begin{pmatrix}\breve{F}^\Lambda \\ \breve{G}_\Lambda\end{pmatrix}_\alpha = \mathcal{S}\,\mathcal{O}_{12}(\alpha)\,\mathcal{S}^{-1}\begin{pmatrix}\breve{F}^\Lambda \\ \breve{G}_\Lambda\end{pmatrix}$$

where we have used the dual field strength defined in (4.8) and one finds that this too is invariant. As a result $\mathcal{O}_{12}$ acts directly on the model of (4.78).

Now we can act on a particular solution such as the black hole of [77] in a straightforward manner. This seed solution can be found explicitly in [77, 102] which we briefly review and add a few comments regarding the parameter space of this solution.

The space-time metric for this rotating solution is given by

$$\begin{aligned} ds^2 \;=\; & \frac{\rho^2 - \Delta^2}{\Delta_r}dr^2 + \frac{\rho^2 - \Delta^2}{\Delta_\theta}d\theta^2 + \frac{\Delta_\theta \sinh^2\theta}{\rho^2 - \Delta^2}\big(jdt - (r^2 + j^2 - \Delta^2)d\phi\big)^2 \\ & - \frac{\Delta_r}{\rho^2 - \Delta^2}\big(dt + j\sinh^2\theta d\phi\big)^2 \end{aligned} \tag{4.86}$$

and the complex scalar fields are

$$z^1 = -\frac{2j\Delta\cosh\theta}{j^2\cosh^2\theta+(r-\Delta)^2} + i\,\frac{j^2\cosh^2\theta+r^2-\Delta^2}{j^2\cosh^2\theta+(r-\Delta)^2}\,, \tag{4.87}$$

$$z^2 = z^3 = i \tag{4.88}$$

where

$$\rho^2 = r^2 + j^2\cosh^2\theta\,, \qquad \Delta_r = \frac{1}{R^2}\Big(r^2+\frac{j^2-R^2}{2}-\Delta^2\Big)^2\,, \qquad \Delta_\theta = 1+\frac{j^2}{R^2}\cosh^2\theta\,.$$

The gauge field is given by

$$\breve{A}^\Lambda \;=\; \frac{1}{8\breve{g}}\frac{\cosh\theta}{(\rho^2-\Delta^2)}\big(jdt-(r^2+j^2-\Delta^2)d\phi\big)\,, \quad \Lambda=0,1,2,3\,. \tag{4.89}$$

This is a rotating generalization of the solution in Section (4.4.1). The parameter $\Xi$ which appears in [77] is unphysical and in our expression has been absorbed by a rescaling of the coordinates which appear there. As with the static solution in Section (4.4.1) all charges are equal as in (4.58). The parameter $j$ is the rotation parameter, $\Delta$ represents a deformation of the boundary theory by a source.

After setting up these pieces, it is completely straightforward to utilize a non-trivial action of $\mathcal{O}_{12}(\alpha)$ on this solution under which the metric, gauge fields and $(z^2, z^3)$ are invariant while $z^1$ transforms exactly as (4.85):

$$z^1 \to \frac{c_\alpha\big[-2j\Delta\cosh\theta+i(j^2\cosh^2\theta+r^2-\Delta^2)\big]-s_\alpha\big[j^2\cosh^2\theta+(r-\Delta)^2\big]}{s_\alpha\big[-2j\Delta\cosh\theta+i(j^2\cosh^2\theta+r^2-\Delta^2)\big]+c_\alpha\big[j^2\cosh^2\theta+(r-\Delta)^2\big]}\,. \tag{4.90}$$

This results in a family of rotating solutions with rotation parameter $j$ and two additional parameters $(\Delta,\alpha)$. The discussion below (4.76) is equally valid for this black hole. When $\Delta=\alpha=0$ we recover the constant scalar rotating solution of [87].

## 4.6 Conclusions

We have demonstrated that a well-known and simple STU-model of four dimensional gauged supergravity has a powerful and previously un-utilized duality group. The duality group is a property of the theory itself and as such can be used to act on any given solution, we have used this group to generate new classes of supersymmetric $AdS_4$ black holes.

When acting on the generic supersymmetric static black holes of [76] we have generated two additional directions in the solution space, both supersymmetric. In the symplectic duality frame in which this directly embeds into the de Wit-Nicolai $\mathcal{N}=8$ theory, these new directions include two additional electric charges and have non-trivial profiles for the axions. One particular representative of our new solutions had been previously constructed numerically in [101]. Using the results of [101] for the static BPS horizon geometries in $\mathcal{N}=2$ $U(1)$-gauged supergravity theories, we have conjectured that with the new results of this paper in hand, the known solution space of supersymmetric static black holes in the STU-model is now co-dimension one within the full space of solutions. The sixth and final dimension of the solution space remains undiscovered and we predict that it should involve a non-trivial profile for the phase of the supersymmetry parameter,

much like the quite complicated supersymmetric static black holes with hypermultiplets found in [103]. We have not presented a strategy by which one could use duality to generate this final branch but one could surely use numerics to confirm its existence.

When acting on the black holes of [76] with equal charges, we have generated a new parameter in the solution space. This black hole now has two free parameters, one is dual to an explicit mass term in the world-volume M2-brane theory, this is in addition to the mass terms induced from twisting of the theory and the curvature couplings [78]. The new parameter we have generated must then correspond to a vev.

We have also used the duality group to generate supersymmetric rotating black holes by using the rotating black hole of Klemm [77] as a seed solution. This family remains within the $\widehat{F} = -i\widehat{X}^0\widehat{X}^1$ model but to generate this family we had to first embed this model into the STU-model. Our new solutions have one additional parameter with respect to the Klemm black hole. In the recent work [104] a new family of rotating $AdS_4$ black holes was found by explicitly solving the second order field equations, generalizing the work of [105, 106]. The Killing spinor conditions were not checked in that work and they do not reference [77] but it would certainly be interesting to establish whether there is overlap between our results in Section 4.5 and the results of [104]. The supersymmetric black hole of [105] and its generalizations have a lower bound on the angular momentum whereas the rotating black holes of Section 4.5 have a regular static limit. There is clearly more work to be done regarding supersymmetric $AdS_4$ black holes even in the STU model; there remains the open problem of constructing a supersymmetric rotating black hole which has a regular CK black hole with $S^2$ horizon as its zero-rotation limit.

There has been much recent work developing non-BPS black holes in gauged supergravity [102, 104, 107, 108, 109, 110, 111, 112] and one can straightforwardly use our duality group on these as well. For non-BPS black holes which are finite temperature generalizations of the CK black holes, one would expect to find qualitatively similar results to ours. The space of static non-BPS solutions discussed in [104] has no overlap with our solution space of supersymmetric black holes in Section 4.4 but it would appear that our duality transformations would not generate new solutions in the class of static black holes found in [104] since in that class all charges are already accounted for. Nonetheless it would be interesting to check this in detail.

Our solution generating technique is reminiscent of the TST duality [113] used in the study of AdS solutions of IIB and eleven-dimensional supergravity. In that work, families of AdS solutions were generated which correspond to the gravity dual of the deformation of the superconformal field theory by exactly marginal operators. This is clearly not directly related to our duality group since the de Wit-Nicolai theory (of which our STU-model is a truncation) contains the $AdS_4$ scalars dual to *relevant* operators, nonetheless we find it an interesting point of comparison. While Lunin-Maldacena focused on BPS solutions, using the techniques of [113] one can find additional non-BPS directions in the solution space [114]. Like the generator $\mathcal{O}_g(\theta)$ in Section 4.3.4, these resulted from dualizing along directions where the bosonic fields are neutral but the Killing spinor is charged. For solutions of IIB supergravity which are topologically of the form $AdS_5 \times S^5$, the solution space is conjectured to admit an additional direction[8] [116] than that found in [113]. This is the dual of the so-called *cubic* deformation of $\mathcal{N} = 4$ SYM and cannot be obtained in any known way through duality. If finding the exact supergravity solution for the final direction of our conjectured solution space of static BPS black holes is a problem

[8]This search for the resulting supergravity solution remains a long-standing open problem, the state of the art in perturbation theory can be found in [115].

of comparable difficulty, one should note that this would be quite a formidable problem.

Duality in gauged supergravity has rarely been employed in the literature. An attempt to use the Geroch group in reductions to three dimensions was carried out in [117] but such a method has not yet proved as useful for generating rotating black holes as it is for ungauged supergravity. It is possible that our results for these $\mathcal{N} = 2$ U(1)-gauged supergravity theories could help in this regard, certainly it should be possibly to understand duality for black holes with hypermultiplets [103]. More generally we hope and expect that the synthesis of our new duality techniques with the numerous recents works on black holes in gauged supergravity will result in much further progress in the study of asymptotically AdS black holes.

# Conclusion

In this thesis, we have seen that the AdS/CFT correspondence and its generalizations provide a new tool to study strongly-coupled field theories. The dual gravitational theory is weakly-coupled and perturbative methods apply. The correspondence is particularly powerful to compute the equilibrium properties and the close to equilibrium correlation functions. Thermodynamic quantities of the field theory are obtained by computing the on-shell gravitational action. The procedure to compute correlation functions is well-defined and consists basically in solving second-order differential equations.

The top/down approach to the AdS/CFT correspondence provides an equivalent description of certain strongly-coupled supersymmetric conformal field theories in terms of supergravity. In this approach, the supergravity theory is the low energy description of string theory or M-theory and the equivalence is believed to hold due to the two descriptions of D-branes and M-branes.

The effective supergravity theory arising from the backreaction of the branes is gauged. It admits a non-vanishing potential for the scalars that behaves as an effective negative cosmological constant in the classical limit. Gauged supergravities thus admit asymptotically AdS solutions. The top/down approach has developed the study of BPS and non-BPS black holes in gauged supergravity. In Chapter 4, we have seen how new BPS black hole solutions could be constructed from duality transformations in 4-dimensional $\mathcal{N} = 2$ gauged supergravity with Fayet-Iliopoulos gaugings.

We have also shown in this thesis how the AdS/CFT correspondence can be used in a more phenomenological way. In this bottom/up approach, minimal gravitational models are constructed to describe strongly-coupled field theories. We have focused the analysis on the study of strongly-correlated fermionic systems at finite density. Surprisingly, simple models such as the electron star model and the holographic superconductor have features related to the physics of non-Fermi liquids and high-Tc cuprate superconductors, as discussed in Chapter 2.

By combining these two models, we have constructed in Chapter 3 new gravitational solutions, dual to field theory states at finite density and zero temperature, which exhibit both bosonic and fermionic degrees of freedom. The study of the low energy fermionic spectrum has led to interesting conclusions about the onset of superconductivity in the model.

The holographic study of systems of fermions is also possible in the D-brane approach to the AdS/CFT correspondence. In particular, the D3-D7' model, obtained by T-dualizing the D4-D8 system, has been used as a model of strongly-interacting fermionic matter in 2+1 dimensions. This model exhibits several familiar phenomena appearing in condensed matter, for example the quantum Hall effect and the zero sound (see e.g. [118]).

The bottom/up holographic models that we presented describe translationally-invariant field theories. One consequence is that the system has an infinite DC conductivity

(the real part of the electrical conductivity admits a delta peak at zero frequency) due to the absence of a lattice. This limitation can be overcome by considering models involving a spatially periodic deformation. The lattice can be for example modulated on the gravity side by a neutral scalar field whose leading behaviour near the boundary is oscillating in the field theory spatial directions [119]. Breaking of the translational invariance can also be realized by considering an oscillating boundary chemical potential [120]. Holographic models with broken translational symmetry have also been considered in the context of massive gravity (see e.g. [121]).

As we have seen on the examples of the electron star and the holographic superconductor models, Lifshitz solutions, which geometrize the Lifshitz invariance of finite density systems at quantum criticality, can be realized as solutions of Einstein-Maxwell gravity coupled to matter fields. However, in the context of the AdS/CFT correspondence, these solutions must connect to an asymptotically AdS solution. Thus, even if one observes an emergent scaling invariance in the near-horizon region, the dual field theory verifies the thermodynamics of a relativistic theory, and the properties of quantum critical points with dynamical critical exponent different from one are not all accessible. Non-relativistic holographic dualities beyond AdS/CFT are thus being constructed.

Gravity duals for systems realizing the Lifshitz symmetry have been proposed in [122] where the relativistic gravitational theory consists in the massive vector model in $d+1$ dimensions where $d$ is the dimension of the field theory (see also [41]). Other models for Lifshitz holography are based on (non-relativistic) Hořava-Lifshitz gravity, proposed in [123, 124] as a renormalizable theory of quantum gravity, which admits Lifshitz spacetime as a vacuum solution [125]. The Schrödinger group can also be realized geometrically, as first proposed almost simultaneously by Son [126] and Balasubramanian and Mc Greevy [127]. The gravitational theory must live in $d+2$ dimensions to realize the full algebra of the Schrödinger group.

Lifshitz and Schrödinger geometries also arise as solutions of string theory. Embedding of the Schrödinger and Lifshitz solutions have first been realized in [128, 129, 130] and [131, 132, 133, 134], respectively. Lifshitz solutions can also be found in the context of four-dimensional $\mathcal{N}=2$ gauge supergravity [135, 136].

The gauge/gravity correspondence has many other applications. The quark-gluon plasma that forms after ion-ion collisions has been studied in the context of the D3/D7 system (see e.g. [137, 138]) and from a bottom/up perspective (see e.g. [139]). Another interesting application is the fluid/gravity correspondence, which maps black hole solutions to fluid dynamics in strongly-coupled field theories. In this context, Navier-Stokes equations are recovered from Einstein equations in suitable near-boundary and near-horizon limits (see e.g. [140, 141, 142]). From the dynamics of the gravitational theory, one can extract the hydrodynamic transport coefficients.

# Appendix A

# Correlation functions in Lorentzian signature

In this appendix, we present the prescription to compute field theory correlation functions in Lorentzian signature.

Since the Euclidean Green's function can be obtained holographically following the prescription of Section 1.5, the retarded Green's function $G_R$ is given by the analytic continuation

$$G_R(\omega, \vec{k}) = G_E(-i(\omega + i\epsilon), \vec{k})\,. \tag{A.1}$$

However in most interesting examples, the Euclidean Green's function is not known exactly and it becomes difficult to perform the analytic continuation to the Lorentz signature. It is then important to be able to compute directly the correlation functions in Lorentzian signature. One could think of applying the procedure developed in Section 1.5 to compute the Lorentzian Green's function. However at finite temperature the Lorentzian bulk spacetime contains a black hole in the interior region so the regularity condition imposed previously is not applicable. A procedure to compute Lorentzian Green's functions has then be proposed in [143] and justified in [144]. We present below the procedure, based on the analytic continuation of the Euclidean asymptotic solution close to the event horizon.

The Euclidean bulk field $\Psi$ satisfies in general a second order differential equation. The asymptotic solution close to the horizon is typically

$$\Psi(t, x, r) \sim A\, e^{\omega_E[t - f(r)]} + B\, e^{\omega_E[t + f(r)]}\,, \qquad r \to r_H\,, \tag{A.2}$$

where $f(r)$ is a positive and increasing function of $r$ which diverges at the event horizon $r = r_H$. The regularity condition is then $B = 0$. The asymptotic solution in Lorentzian signature, obtained by analytic continuation from (A.1) by setting $\omega_E = -i\omega$, is

$$\Psi(t, x, r) \sim A_{\text{in}}\, e^{-i\omega[t - f(r)]} + B_{\text{out}}\, e^{-i\omega[t + f(r)]}\,, \qquad r \to r_H\,, \tag{A.3}$$

i.e. the superposition of two propagating modes: an 'in-going' wave and an 'out-coming' wave. The former propagates from the UV to the IR and the latter in the opposite direction. The regularity condition in Euclidean signature translates into the 'in-falling' boundary condition $B_{\text{out}} = 0$. The in-falling boundary condition turns out to be very natural since classical information can fall into the black hole but cannot come out.

To give an example, let us consider a probe scalar field $\varphi$ in the AdS-Schwarzschild black hole obtained by setting $\hat{\mu} = 0$ in the AdS-Reissner-Nordström black hole presented in Section 2.3. In Lorentzian signature, the bulk action for $\varphi$ is given by

$$S_{\rm gra} = -\frac{L^{1-d}}{2} \int \mathrm{d}^d x \, \mathrm{d}r \, \sqrt{-g} \left( g^{ab} \partial_a \varphi \partial_b \varphi + m^2 \varphi^2 \right) \tag{A.4}$$

where $g_{ab}$ is the metric of the AdS-Schwarzschild black hole. In the near-horizon region, the Klein-Gordon equation for $\varphi$ is simply, in momentum space,

$$\partial_u^2 \varphi + \omega^2 \varphi = 0 \tag{A.5}$$

where $u(r)$ is a new variable defined by

$$u = \int^r \frac{\mathrm{d}r'}{f(r')} \, . \tag{A.6}$$

Since $u(r) \to \infty$ for $r \to r_H$, the regular asymptotic solution in Euclidean signature is $\varphi \sim e^{\omega_E (t-u)}$ which indeed corresponds, by analytic continuation, to the in-falling wave mode

$$\varphi \sim e^{-i\omega(t-u)} \, . \tag{A.7}$$

In the saddle-point approximation, the equivalence of the generating functions of the two theories in Lorentzian signature can then be written as

$$\left\langle e^{i \int \mathrm{d}^d x \, \Psi_-(x) \mathcal{O}(x)} \right\rangle_{\rm FT} \simeq e^{i S_{\rm cl}[\Psi_-]} \, , \tag{A.8}$$

where the bulk field $\Psi$ dual to the operator $\mathcal{O}$ has the classical UV expansion

$$\Psi_{\rm cl}(x, r) \sim \Psi_-(x) \, r^{\Delta_-} + \Psi_+(x) \, r^{\Delta_+} \, , \qquad r \to 0 \, . \tag{A.9}$$

The procedure to compute the one and two-point correlation functions then consists first in finding the action to quadratic order of the bulk field $\Psi$ dual to $\mathcal{O}$ and in finding a solution to the field equation which satisfies both the in-falling condition in the near-horizon region and the UV asymptotics (A.9). As for the Euclidean version of the field/operator correspondence, $\Psi_-$ is the source for the operator $\mathcal{O}$ (in the standard quantization scheme), the renormalized on-shell action $S_{\rm ren}[\Psi_{\rm cl}]$ is related to the generating functional of the connected correlation functions $W_{\rm FT} = -i \log Z_{\rm FT}$ by

$$W_{\rm FT}[\Psi_-] = S_{\rm ren}[\Psi_-] \tag{A.10}$$

and the connected correlation functions are obtained by taking derivatives of the renormalized on-shell action $S_{\rm ren}[\Psi_{\rm cl}]$. One can also introduce the renormalized canonical momentum conjugate to the classical solution $\Psi_{\rm cl}$,

$$\Pi_{\rm ren} = \frac{\delta S_{\rm ren}[\Psi_{\rm cl}]}{\delta \Psi_{\rm cl}} \, , \tag{A.11}$$

in terms of which the one-point function is

$$\langle \mathcal{O}(\omega, \vec{k}) \rangle_{\Psi_-} = \lim_{r \to 0} r^{\Delta_-} \Pi_{\rm ren} \, . \tag{A.12}$$

The in-falling boundary condition is the analogue to the regularity condition imposed in Euclidean signature following the analytic continuation (A.1). It is also possible to consider the analytic continuation $\omega = i\omega_E$ instead of $\omega = -i\omega_E$, which leads to the advanced Green's function. However we focus here on the retarded Green's function as it has an important role in the close to equilibrium physics. In the linear response theory, the response of the system to the application of an external source $\delta\mathcal{S}$ for an operator $\mathcal{O}$ is proportional to the applied source and given by the Kubo formula [145]

$$\delta\langle\mathcal{O}(\omega,\vec{k})\rangle_{\mathcal{S}} = G_R(\omega,\vec{k})\,\delta\mathcal{S}(\omega,\vec{k})\,, \tag{A.13}$$

where the 'constant' of proportionality is the retarded Green's function which characterizes the response of the system. This allows to compute the retarded Green's function in momentum space, from (A.12) we get

$$G_R(\omega,\vec{k}) = \lim_{r\to 0} r^{2\Delta_-}\frac{\Pi_{\text{ren}}}{\Psi_{\text{cl}}}\,. \tag{A.14}$$

# Appendix B

# Irrelevant operators and IR Lifshitz solutions

In this Appendix,we are looking for Lifshitz-like solutions to the field equations (3.30) in the case where $\hat{\eta} = 0$. One can verify that such solutions do not arise if the scalar field mass squared is negative, i.e. the dual boundary operator is a relevant one. However, for $\hat{m}_s^2 > 0$, solutions with Lifshitz symmetry with both non-trivial scalar field and fluid exist.

We assume that the metric, the gauge field and the scalar field are of the form

$$f(r) = \frac{1}{r^{2z}}\,, \qquad g(r) = \frac{g_\infty}{r^2}\,, \qquad h(r) = \frac{h_\infty}{r^z}\,, \qquad \hat{\psi}(r) = \hat{\psi}_\infty\,, \tag{B.1}$$

where $g_\infty$ and $h_\infty$ are positive constants and $z > 1$. In particular, the scalar field is assumed to be constant. On such backgrounds the local chemical potential is constant and equals to $h_\infty$, so the fluid quantities are also constant and we denote the charge density, the energy density and the pressure of the fluid by $\hat{\sigma}_\infty$, $\hat{\rho}_\infty$ and $\hat{p}_\infty$.

These geometries arise both as exact solutions (for $\hat{\eta} = 0$) to the system (3.30) for trivial scalar field and trivial fluid, separately. We present here Lifshitz-like solutions where both the fluid and the scalar field are turned on. It is useful to rescale the scalar field by

$$\hat{\psi} \to \tilde{\psi} = \hat{q}\hat{\psi}\,. \tag{B.2}$$

After this rescaling, (B.1) is a solution of the system if the constants satisfy

$$h_\infty = \sqrt{\frac{z-1}{z}}\,, \tag{B.3a}$$

$$g_\infty = \frac{2z\sqrt{z-1}}{\sqrt{z}\hat{\sigma}_\infty + \sqrt{z-1}\tilde{\psi}_\infty^2}\,, \tag{B.3b}$$

$$\tilde{\psi}_\infty = \left(\frac{z}{z-1}\right)^{1/4} \left|\frac{4\sqrt{z}\sqrt{z-1}(3+\hat{p}_\infty) - (z+1)(z+2)\hat{\sigma}_\infty}{2z\frac{\hat{m}_s^2}{\hat{q}^2} + (4+z+z^2)}\right|^{1/2}\,, \tag{B.3c}$$

together with the constraint

$$(\hat{m}_s^2 - \hat{q}^2 h_\infty^2)\tilde{\psi}_\infty = 0\,. \tag{B.4}$$

Notice that after the rescaling (B.2) the system depends only on the ratio $\hat{m}_s/\hat{q}$, and not on $\hat{m}_s$ or $\hat{q}$ independently.

There are three different possibilities:

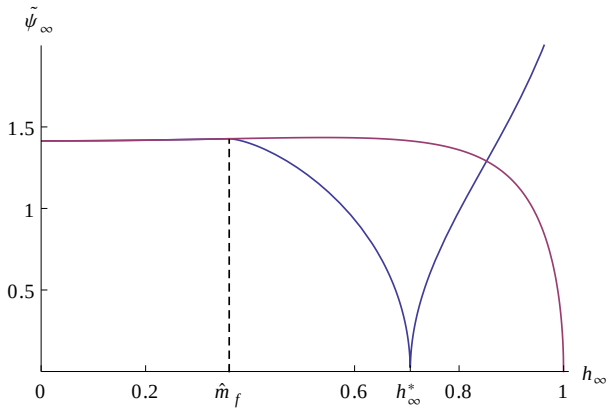


Figure B.1: The condensate $\tilde{\psi}_\infty$ as a function of $h_\infty = \hat{m}_s/|\hat{q}|$ for the Lifshitz solution at $\hat{m}_f = 0.36$ and $\hat{\beta} = 20$. The blue and purple lines represent the condensate with and without the star respectively. When there is no star forming, for $h_\infty = 1$, which corresponds to $z = \infty$, the condensate vanishes while it tends to a constant for $h_\infty = 0$ ($z \to 1$). When the star forms for $h_\infty > \hat{m}_f$, there is a particular point $h_\infty = h^*_\infty$ where the condensate vanishes. At this point, we recover the electron star solution.

1. **Fluid phase:** If the scalar field is trivial, Einstein-Maxwell equations impose the constraint

$$4\sqrt{z}\sqrt{z-1}(3+\hat{p}_\infty) - (z+1)(z+2)\hat{\sigma}_\infty = 0\,, \qquad \tilde{\psi}_\infty = 0\,, \tag{B.5}$$

   which gives a non-trivial relation between $z$ and the fluid parameters $\hat{m}_f$ and $\hat{\beta}$. This is the zero temperature electron star solution [39].

2. **Scalar field phase:** If the scalar field is non-trivial, the constraint (B.4) implies that $\hat{m}_s^2 > 0$ since $\hat{q}^2 h_\infty^2 > 0$, and the local chemical potential and dynamical exponents are

$$h_\infty = \frac{\hat{m}_s}{|\hat{q}|}\,, \qquad z = \frac{1}{1-\hat{m}_s^2/\hat{q}^2}\,. \tag{B.6}$$

   When the fluid is trivial, i.e. $\hat{\sigma}_\infty = \hat{p}_\infty = 0$, the condensate is given by

$$\tilde{\psi}_\infty = \frac{2\sqrt{3z}}{\sqrt{(z+1)(z+2)}}\,. \tag{B.7}$$

   This is the solution found in [51].

3. **Coexistence phase:** The fluid and the scalar field can coexist. In this case, Eq. (B.4) for $\tilde{\psi}_\infty \neq 0$ implies that the chemical potential is again $h_\infty = \hat{m}_s/|\hat{q}|$, related to the dynamical exponent by (B.3a). The value of the condensate is given in terms of $\hat{m}_f$, $\hat{\beta}$ and the ratio $\hat{m}_s/\hat{q}$ by Eq. (B.3c).

The space of solutions is depicted in Figure B.1, where we display $\tilde{\psi}_\infty$ as a function of $h_\infty$ for $\hat{m}_f = 0.36$ and $\hat{\beta} = 20$. Notice that for $h_\infty < \hat{m}_f$ the star cannot form, and only the solution with the scalar field alone exists. At $h_\infty = \hat{m}_f$ the star can start forming, so we have two branches. The special point $h_\infty = h^*_\infty$, which coincides with the vanishing of the right hand side of (B.3c), admits both a pure star and a pure condensate with the same Lifshitz exponent.

Although the phase structure of these solutions is interesting, one does not expect that these IR Lifshitz solutions will connect to the UV asymptotically $AdS_4$ space: the squared mass of the scalar field is positive, and the operator dual to the scalar field is an irrelevant operator in the UV. Thus, it is unlikely that one could find an RG flow from a UV $AdS$ region to these IR solutions.

# Appendix C

# The Dirac equation

Let us consider the action

$$S_\chi = \int \mathrm{d}^4x\sqrt{-g}\left[-i\left(\bar\chi\Gamma^a\mathcal{D}_a\chi - m_f\bar\chi\chi\right) + \eta J^{\mathrm{ferm}}_a J^a_{\mathrm{scal}}\right] \tag{C.1}$$

of a probe spinor field $\chi$ representing an electronic excitation of charge $|q_f|$, in a background solution of the form (3.27) of the theory of Section 3.3, where

$$J^a_{\mathrm{scal}} = -i\frac{q}{2}g^{ab}\left[\bar\psi(\partial_b - iqA_b)\psi - \psi(\partial_b + iqA_b)\bar\psi\right]\,, \tag{C.2a}$$

$$J^{\mathrm{ferm}}_a = -|q_f|\bar\chi\Gamma_a\chi\,, \tag{C.2b}$$

and

$$\mathcal{D}_a = \partial_a + \frac{1}{4}\omega_{ija}\Gamma^{ij} - i|q_f|A_a\,, \tag{C.3}$$

$$\bar\chi = \chi^\dagger\Gamma^0\,. \tag{C.4}$$

Notice that the field $\chi$ has positive electric coupling $|q_f|$ consistent with our background conventions. The Dirac equation is

$$i\,\Gamma^a\mathcal{D}_a\chi - im_f\chi + \eta|q_f|J^a_{\mathrm{scal}}\Gamma_a\chi = 0\,. \tag{C.5}$$

By setting $\chi = rf^{1/4}\xi(r)e^{ikx-i\omega t}$, it becomes

$$r^{-1}g^{-1/2}\left(\Gamma^1\partial_r - Lm_f g^{1/2}\right)\xi(r) + iK_i\Gamma^i\xi(r) = 0 \tag{C.6}$$

where

$$K_0 = -r^{-1}f^{-1/2}\left[\omega + \frac{eL}{\kappa}|q_f|h\left(1-\eta q^2\bar\psi\psi\right)\right]\,, \qquad K_2 = k\,, \qquad K_1 = K_3 = 0\,. \tag{C.7}$$

The Dirac equation does not depend on $\Gamma^3$. We choose the following basis for Gamma-matrices,

$$\Gamma^0 = \begin{pmatrix} i\sigma^1 & 0 \\ 0 & i\sigma^1\end{pmatrix}\,, \quad \Gamma^1 = \begin{pmatrix} -\sigma^3 & 0 \\ 0 & -\sigma^3\end{pmatrix}\,, \quad \Gamma^2 = \begin{pmatrix} -\sigma^2 & 0 \\ 0 & \sigma^2\end{pmatrix}\,, \quad \Gamma^3 = \begin{pmatrix} 0 & \sigma^2 \\ \sigma^2 & 0\end{pmatrix}\,, \tag{C.8}$$

where $\sigma^l$, $l = 1, 2, 3$, are Pauli matrices. By writing $\xi = (\Phi, \tilde{\Phi})$, we obtain two decoupled first order equations for the Dirac spinors $\Phi$ and $\tilde{\Phi}$ which differ only by the momentum $k \to -k$. The equation for $\Phi$ is [32]

$$\left(\partial_r + \gamma \hat{m}_f g^{1/2} \sigma^3\right) \Phi = g^{1/2} \left\{ i\gamma\sigma^2 \left[\hat{\omega} f^{-1/2} + \hat{\mu}_l\right] - \gamma \hat{k} r \sigma^1 \right\} \Phi \,, \tag{C.9}$$

or in components,

$$\frac{1}{\sqrt{g}} \partial_r \Phi_1 + \gamma \hat{m}_f \Phi_1 - \gamma \left( \frac{\hat{\omega}}{\sqrt{f}} + \hat{\mu}_l - \hat{k} r \right) \Phi_2 = 0 \,, \tag{C.10a}$$

$$\frac{1}{\sqrt{g}} \partial_r \Phi_2 - \gamma \hat{m}_f \Phi_2 + \gamma \left( \frac{\hat{\omega}}{\sqrt{f}} + \hat{\mu}_l + \hat{k} r \right) \Phi_1 = 0 \,. \tag{C.10b}$$

In the above equations, we have rescaled the momentum and the frequency by

$$\omega = \gamma \hat{\omega} \,, \qquad k = \gamma \hat{k} \,, \tag{C.11}$$

where $\gamma$ is given by (3.51). The equations (C.10) can be written in the form

$$\begin{aligned} \Phi_2'' =& \frac{\left[\sqrt{g}\left(\frac{\hat{\omega}}{\sqrt{f}} + \hat{\mu}_l + \hat{k} r\right)\right]'}{\sqrt{g}\left(\frac{\hat{\omega}}{\sqrt{f}} + \hat{\mu}_l + \hat{k} r\right)} \Phi_2' \\ &+ \left\{ \gamma^2 g \left[ \hat{m}_f^2 + \hat{k}^2 r^2 - \left( \frac{\hat{\omega}}{\sqrt{f}} + \hat{\mu}_l \right)^2 \right] - \gamma \hat{m}_f \sqrt{g} \frac{\left(\frac{\hat{\omega}}{\sqrt{f}} + \hat{\mu}_l + \hat{k} r\right)'}{\frac{\hat{\omega}}{\sqrt{f}} + \hat{\mu}_l + \hat{k} r} \right\} \Phi_2 \,, \end{aligned} \tag{C.12a}$$

$$\Phi_1 = \frac{1}{\frac{\hat{\omega}}{\sqrt{f}} + \hat{\mu}_l + \hat{k} r} \left( \hat{m}_f \Phi_2 - \frac{1}{\gamma} \frac{1}{\sqrt{g}} \Phi_2' \right) \,, \tag{C.12b}$$

where primes denote derivatives with respect to the radial coordinate $r$. In the large-$\gamma$ limit, it can be shown that the $\Phi_2'$ term in (C.12a) is negligible by putting it in a Schrödinger form. In this limit, the system (C.12) can be written as

$$\Phi_2'' = \left\{ \gamma^2 g \left[ \hat{m}_f^2 + \hat{k}^2 r^2 - \left( \frac{\hat{\omega}}{\sqrt{f}} + \hat{\mu}_l \right)^2 \right] - \gamma \hat{m}_f \sqrt{g} \frac{\left(\frac{\hat{\omega}}{\sqrt{f}} + \hat{\mu}_l + \hat{k} r\right)'}{\frac{\hat{\omega}}{\sqrt{f}} + \hat{\mu}_l + \hat{k} r} \right\} \Phi_2 \,, \tag{C.13}$$

$$\Phi_1 = \frac{1}{\frac{\hat{\omega}}{\sqrt{f}} + \hat{\mu}_l - \hat{k} r} \left( \hat{m}_f \Phi_2 - \frac{1}{\gamma} \frac{1}{\sqrt{g}} \Phi_2' \right) \,. \tag{C.14}$$

# Appendix D

# Solving the Schrödinger-like equation

We will solve the Schrödinger equation (3.52) in the WKB approximation. We focus here on the case where there is a region of the bulk where the Schrödinger potential is negative. This region is bounded by the turning points $r = r_1$ and $r = r_2$, with $r_1 < r_2$, where the potential vanishes. We recall that in the WKB approximation, the formal solution to the equation (3.52) is

$$\begin{aligned}\Phi_2 \simeq & C_+ \exp\left[\gamma \int_{r_0}^{r} \mathrm{d}s \sqrt{V(s)} - \int_{r_0}^{r} \mathrm{d}s \frac{V'(s)}{4V(s)}\right] \\ & + C_- \exp\left[-\gamma \int_{r_0}^{r} \mathrm{d}s \sqrt{V(s)} - \int_{r_0}^{r} \mathrm{d}s \frac{V'(s)}{4V(s)}\right]\end{aligned} \tag{D.1}$$

where $r_0$ is an arbitrary (fixed) point.

Close to a turning point $r = r_\star$, we have

$$\gamma \int_{r_\star}^{r} \mathrm{d}s \sqrt{|V(s)|} \sim \pm\varphi(r)\,, \qquad r \to r_\star^{\pm}\,, \tag{D.2}$$

where

$$\varphi(r) = \frac{2}{3}\gamma \sqrt{|V'(r_\star)|} \cdot |r - r_\star|^{3/2}\,. \tag{D.3}$$

The matching conditions around a turning point where $V(r)$ vanishes linearly are

$$\frac{1}{2} e^{-\varphi} \leftrightarrow \sin(\varphi + \pi/4)\,, \tag{D.4a}$$

$$e^{\varphi} \leftrightarrow \cos(\varphi + \pi/4)\,. \tag{D.4b}$$

## D.1 The WKB solution for one $V < 0$ region

We consider first the case where the potential $V$ is negative in one region bounded by $r_1$ and $r_2$ with $r_1 < r_2$. By imposing normalizability on the wave function, in the inner region $r > r_2$ we have

$$\Phi_2^{in} \sim C^{in}\, e^{-\gamma \int_{r_2}^{r} \mathrm{d}s \sqrt{V(s)}}\,. \tag{D.5}$$

In the intermediate region $r_1 < r < r_2$, the wave function is

$$\Phi_2^{inter} \sim C_+^{inter}\, e^{i\gamma \int_{r_1}^{r} \mathrm{d}s \sqrt{|V(s)|}} + C_-^{inter}\, e^{-i\gamma \int_{r_1}^{r} \mathrm{d}s \sqrt{|V(s)|}} \tag{D.6}$$

$$\sim C_+^{inter}\, e^{\theta_{12}}\, e^{i\gamma \int_{r_2}^{r} \mathrm{d}s \sqrt{|V(s)|}} + C_-^{inter}\, e^{-\theta_{12}}\, e^{-i\gamma \int_{r_2}^{r} \mathrm{d}s \sqrt{|V(s)|}} \tag{D.7}$$

where

$$\theta_{ij} = \gamma \int_{r_i}^{r_j} \mathrm{d}r \sqrt{|V(r)|}\,. \tag{D.8}$$

Finally, in the UV region, we have

$$\Phi_2^{out} \sim C_+^{out}\, e^{\gamma \int_{r_1}^{r} \mathrm{d}s \sqrt{V(s)}} + C_-^{out}\, e^{-\gamma \int_{r_1}^{r} \mathrm{d}s \sqrt{V(s)}} \tag{D.9}$$

$$\sim C_+^{out}\, e^{-\theta_\epsilon}\, e^{\gamma \int_{\epsilon}^{r} \mathrm{d}s \sqrt{V(s)}} + C_-^{out}\, e^{\theta_\epsilon}\, e^{-\gamma \int_{\epsilon}^{r} \mathrm{d}s \sqrt{V(s)}} \tag{D.10}$$

where

$$\theta_\epsilon = \gamma \int_{\epsilon}^{r_1} \mathrm{d}r \sqrt{V(r)} \tag{D.11}$$

and $\epsilon \ll 1$ is a UV cutoff. Close to the UV boundary, the WKB solution is

$$\Phi_2^{UV} \sim C_+^{UV} e^{-\theta_\epsilon} \left(\frac{r}{\epsilon}\right)^{\gamma \hat{m}_f} + C_-^{UV} e^{\theta_\epsilon} \left(\frac{r}{\epsilon}\right)^{-\gamma \hat{m}_f + 1}\,. \tag{D.12}$$

Notice that we have taken into account the $\mathcal{O}(\gamma^{-1})$-correction

$$-\gamma^{-1} \hat{m}_f \sqrt{g} \frac{\left(\frac{\hat{\omega}}{\sqrt{f}} + \hat{\mu}_l + \hat{k} r\right)'}{\frac{\hat{\omega}}{\sqrt{f}} + \hat{\mu}_l + \hat{k} r} \tag{D.13}$$

to the Schrödinger-like potential (3.55) to obtain the subleading power $r^1$ in the second term in (D.12). Applying the matching conditions (D.4) and using (3.75) and (3.76), we obtain the Green's function (3.77) with

$$\mathcal{G} = \frac{1}{2} \tan W \tag{D.14}$$

where

$$W = \gamma \int_{r_1}^{r_2} \mathrm{d}r \sqrt{|V(r)|}\,. \tag{D.15}$$

## D.2 The WKB solution for two $V < 0$ regions

Now we consider the case where $V$ is negative in two regions bounded by $r_1$, $r_2$ and $r_3$, $r_4$ respectively, with $r_1 < r_2 < r_3 < r_4$. We impose regularity on the wave function at infinity, so in the inner region $r > r_4$, $\Phi_2$ is given by (D.5) where $r_2$ is replaced by $r_4$. The UV expansion is again given by (D.12). By matching the solution in the different regions at the turning points, the constant $\mathcal{G}$ in the Green's function (3.77) is now given by

$$\mathcal{G} = \frac{4e^{2X} \sin Y \cos Z + \cos Y \sin Z}{8e^{2X} \cos Y \cos Z - 2 \sin Y \sin Z} \tag{D.16}$$

where

$$X = \gamma \int_{r_2}^{r_3} \mathrm{d}r \sqrt{V(r)}\,, \qquad Y = \gamma \int_{r_1}^{r_2} \mathrm{d}r \sqrt{|V(r)|}\,, \qquad Z = \gamma \int_{r_3}^{r_4} \mathrm{d}r \sqrt{|V(r)|}\,. \tag{D.17}$$

# Appendix E

# Duality symmetries and Very Special Kähler Geometry

We now summarize some key aspects of duality symmetries for very special Kähler geometry following [97, 98, 146]. Under the action of $Sp(2n_V+2,\mathbb{R})$, the prepotential transforms according to

$$\mathcal{S} = \begin{pmatrix} A & B \\ C & D \end{pmatrix} \in Sp(2n_V+2,\mathbb{R})\,, \tag{E.1}$$

$$\widetilde{F}(\widetilde{X}) = F(X) + X^\Lambda (C^t B)_\Lambda{}^\Sigma F_\Sigma + \frac{1}{2} X^\Lambda (C^t A)_{\Lambda\Sigma} X^\Sigma + \frac{1}{2} F_\Lambda (D^t B)^{\Lambda\Sigma} F_\Sigma\,. \tag{E.2}$$

The elements of $Sp(2n_V+2,\mathbb{R})$ which leave the prepotential invariant correspond to isometries of $\mathcal{M}_V$ and these have been classified by de Wit and Van-Proeyen. Working at the level of the Lie algebra we have an element

$$\underline{\mathcal{S}} = \begin{pmatrix} Q & R \\ S & T \end{pmatrix} \in \mathfrak{sp}(2n_V+2,\mathbb{R}) \tag{E.3}$$

with components

$$Q = -T^t = \begin{pmatrix} \beta & a_i \\ b^j & B^i{}_j + \frac{1}{3}\beta\delta^i_j \end{pmatrix}\,, \tag{E.4}$$

$$R = \begin{pmatrix} 0 & 0 \\ 0 & -\frac{3}{32}\widehat{d}^{ijk}a_k \end{pmatrix}\,, \tag{E.5}$$

$$S = \begin{pmatrix} 0 & 0 \\ 0 & -6d_{ijk}b^k \end{pmatrix}\,. \tag{E.6}$$

The scalar fields transform infinitesimally as

$$\delta z^i = b^i - \frac{2}{3}\beta z^i + B^i{}_j z^j - \frac{1}{2} R^i{}_{jk}{}^l z^j z^k a_l\,. \tag{E.7}$$

where $R^i{}_{jk}{}^l$ is the Riemann tensor on $\mathcal{M}_V$:

$$R^i{}_{jk}{}^l = 2\delta^i_{(j}\delta^l_{k)} - \frac{9}{16}\widehat{d}^{ilm}d_{mjk}\,. \tag{E.8}$$

In general these symmetries are constrained

$$B^i{}_{(j}d_{kl)i} = 0\,, \tag{E.9}$$

$$a_i E^i_{jklm} = 0 \tag{E.10}$$

where the $E$-tensor is given by

$$E^i_{jklm} = \widehat{d}^{inp}d_{n(jk}d_{lm)p} - \frac{64}{27}\delta^i_{(j}d_{klm)}\,. \tag{E.11}$$

When $\mathcal{M}_V$ is a homogeneous space, the case of most interest to us, $E^i_{jklm}$ vanishes and thus the constraint (E.10) is identically zero. As a consequence the $a_i$ and $b^j$ parameters are unconstrained.

To get a feeling for these symmetries, consider the fractional linear transformation of $z^i$ under $SL(2,\mathbb{R})$. To work out the infinitesimal transformation we take the standard generators of $\mathfrak{sl}(2,\mathbb{R})$

$$E = \begin{pmatrix} 0 & 1 \\ 0 & 0 \end{pmatrix}\,, \quad F = \begin{pmatrix} 0 & 0 \\ 1 & 0 \end{pmatrix}\,, \quad H = \begin{pmatrix} 1 & 0 \\ 0 & -1 \end{pmatrix} \tag{E.12}$$

then we have

$$\delta_E z^i \to \alpha\,, \qquad \delta_F z^i \to -\alpha(z^i)^2\,, \qquad \delta_H z^i \to 2\alpha z^i\,. \tag{E.13}$$

So one can interpret the matrix $\underline{\mathcal{S}}$ in (E.4)-(E.6) with $b^i \neq 0$ as raising operators and when $\mathcal{M}_V$ is a homogeneous space, the Riemann tensor is constant and one can interpret the matrix with $a_i \neq 0$ as lowering operators. The $(\beta, B^i{}_j)$ are then the Cartan elements. The full commutation relations can be easily worked out or found in [97, 98, 146].

# Appendix F

# Résumé long en français

Nous présentons dans cette thèse les applications de la correspondance AdS/CFT à l'étude des théories des champs fortement corrélées en adoptant deux approches, l'approche 'top-down' en termes de théorie des cordes et supergravité, et l'approche 'bottom-up', plus phénoménologique.

## F.1 La correspondance AdS/CFT

La correspondance AdS/CFT repose sur les deux descriptions des D-branes (M-branes) en théorie des cordes (théorie M, respectivement).

### F.1.1 Supergravité et $p$-branes

Les théories de supergravité contiennent des champs de jauge de rang supérieur qui généralisent les potentiels de l'électromagnétisme et des théories de Yang-Mills. Ces champs de jauge sont des $p$-formes $C_p$ invariantes sous des transformations de jauge généralisées. Les théories de supergravité admettent des objets massifs qui s'étendent dans $p$ directions spatiales et sont chargés sous le potentiel $C_p$. Ces objets sont connus sous le nom de $p$-branes.

Prenons l'exemple de la théorie de supergravité de type IIB, qui décrit le secteur des excitations non-massives de la théorie des cordes de type IIB. Cette théorie admet comme champs bosoniques la métrique dix-dimensionnelle, un tenseur antisymétrique de rang deux, le dilaton et les potentiels $C_0$, $C_2$ et $C_4$. Cette théorie admet en particulier des 3-branes où le potentiel de jauge $C_4$ est non-trivial. Les 3-branes préservent une partie de la supersymétrie de la théorie. Lorsque leur masse et leur charge sont égales, les 3-branes sont extrémales et peuvent être empilées. Une telle solution de la théorie est spécifiée par une unique fonction harmonique qui ne dépend que du nombre de branes.

La tension des $p$-branes est inversement proportionnelle à la constant de couplage de la corde $g_s$, ce qui traduit la nature non-perturbative des $p$-branes.

### F.1.2 Théorie des cordes et D$p$-branes

Il a été découvert dans les années 1990 qu'en théorie des cordes, les $p$-branes ont une description perturbative en termes de cordes ouvertes et fermées. Dans ce contexte ces objets sont appelés D$p$-branes et définis comme hypersurfaces $(p+1)$-dimensionnelles dans l'espace-temps dix-dimensionnel sur lesquelles les cordes ouvertes peuvent se rattacher.

Considérons l'exemple d'une D3-brane plane. Dans la limite de basse énergie, la quantification de la corde ouverte mène à un spectre non-massif constitué d'un multiplet vectoriel avec 16 supercharges vivant sur la D3-brane, menant à une théorie de jauge abélienne à 4 dimensions. Ce multiplet interagit avec les champs non-massifs issus de la corde fermée, qui vivent eux dans l'ensemble de l'espace-temps.

Lorsque l'on considère un empilement de plusieurs D3-branes, les cordes ouvertes peuvent être rattachées à des branes différentes, ce qui mène à une théorie de jauge non-abélienne sur les D3-branes. Les champs de cette théorie interagissent avec les champs du spectre de la corde fermée.

### F.1.3 Limite de découplage

Les branes ont donc deux interprétations, comme solutions non-perturbatives en supergravité, et comme hypersurfaces sur lesquelles les cordes ouvertes peuvent se rattacher en théorie des cordes. Nous allons maintenant voir comment la correspondance AdS/CFT émerge en considérant la même limite de découplage dans les deux cas.

Dans la description en termes de théorie des cordes, lorsque l'on zoome sur la région proche des D3-branes, le multiplet vectoriel issu de la quantification de la corde ouverte se découple des autres champs. La théorie se réduit dans ce cas à la théorie de Yang-Mills supersymétrique (SYM) $\mathcal{N} = 4$ à 4 dimensions avec groupe de jauge $U(N)$. Cela correspond à prendre la limite où l'inverse de la tension de la corde $\alpha' \to 0$.

Du côté de la supergravité, cette même limite mène à l'espace-temps $AdS_5 \times S^5$, où $AdS_5$ est l'espace Anti-de Sitter à 5 dimensions. Le potentiel $C_4$ reste lui aussi non-trivial.

La limite $\alpha' \to 0$ mène à penser qu'il y a équivalence entre la théorie SYM $\mathcal{N} = 4$ et la théorie des cordes de type IIB sur l'espace $AdS_5 \times S^5$. Nous donnons ci-dessous des raisons de croire en cette dualité.

### F.1.4 Tests et propriétés de la correspondance

Chacune des deux théories admet deux paramètres. Ces paramètres sont pour la théorie des champs le rang du groupe de jauge $U(N)$, égal à $N$, et le couplage de 't Hooft $\lambda = g_{YM}^2 N$, où $g_{YM}$ est la constante de couplage du champ de jauge non-abélien. Du côté de la théorie de gravité, ces paramètres sont le couplage de la corde $g_s$ et l'inverse de la tension de la corde $\alpha'$. Les relations entre les paramètres des deux théories sont très simples, et mènent à d'intéressantes conclusions. En particulier, la limite de basse énergie de la théorie des cordes, c'est-à-dire la supergravité de type IIB sur l'espace $AdS_5 \times S^5$ obtenue en prenant $\alpha' \ll 1$ et $g_s \to 0$, correspond du côté de la théorie des champs à prendre $N \to \infty$ et $\lambda \to \infty$. La théorie des champs est donc dans ce cas fortement couplée.

Les mêmes symétries sont réalisées des deux côtés de la correspondance. En effet, on pense que la théorie SYM $\mathcal{N} = 4$ est conforme à tous les ordres, ce qui signifie que c'est une théorie conforme des champs (CFT). Le groupe conforme en 4 dimensions est $SO(4,2)$. A cela s'ajoute la R-symétrie et les supercharges conformes nécessaires pour fermer l'algèbre. Toutes ces symétries forment le groupe superconforme $PSU(2,2|4)$ sous l'action duquel la théorie SYM $\mathcal{N} = 4$ est invariante. Notons que la théorie des champs contient 16 supercharges et 16 supercharges conformes.

La symétrie $PSU(2,2|4)$ est aussi réalisée dans la théorie des cordes duale. Les groupes $O(4,2)$ et $SO(6) \simeq SU(4)$ sont les groupes d'isométrie de $AdS_5$ et $S^5$, respectivement.

Aussi, la théorie des cordes de type IIB contient 16 supercharges. Sur l'espace-temps maximalement supersymétrique $AdS_5 \times S^5$, la supersymétrie est élargie menant à 32 supercharges.

Par exemple, le sous-groupe $SO(1,3)$ du groupe d'isométrie $O(4,2)$ de $AdS_5$ correspond au groupe de Lorentz de la théorie des champs. Aussi, le sous-groupe $SO(1,1)$ est dual aux dilatations dans la théorie des champs. Du côté de la gravité, ces transformations agissent sur les coordonnées de l'espace $AdS_5$, qui sont les coordonnées spatio-temporelles de la théorie des champs, ainsi que la coordonnée radiale, qui peut être assimilée à l'échelle d'énergie de la théorie des champs.

Le spectre de chacune des deux théories duales est aussi clairement relié. Les observables de la CFT sont les opérateurs primaires chiraux et non-chiraux. Les premiers sont des opérateurs composites 'single-trace' des opérateurs fondamentaux de la théorie et sont protégés sous renormalisation, ce qui signifie que leur dimension conforme est leur dimension canonique. Les seconds sont des opérateurs composites 'multi-trace' et ne sont pas protégés sous renormalisation. Ces opérateurs forment respectivement des multiplets courts (opérateurs chiraux) et longs (opérateurs non-chiraux). Dans la limite de 't Hooft $N \to \infty$, $\lambda$ fixé, les opérateurs chiraux et non-chiraux se découplent.

Du coté de la gravité, cette limite correspond à la limite de supergravité avec corrections dans l'action de dérives d'ordres supérieurs. Les champs 10-dimensionnels peuvent être réduits dimensionnellement sur la 5-sphère. Les champs résultant à 5 dimensions s'organisent en les mêmes multiplets chiraux du groupe superconforme que du côté de la théorie des champs. Chaque champ à 5 dimensions est dual à un opérateur de la CFT appartenant au même multiplet chiral. Ils ont les mêmes Casimirs que sont les nombres quantiques du groupe de Lorentz ainsi que la dimension conforme. Celle-ci est donné du côté de la gravité en termes de la masse du champ.

### F.1.5 Thermodynamique et fonctions de corrélation

La correspondance AdS/CFT établit l'égalité des fonctions de partitions des deux théories. Dans la limite où la théorie des champs est fortement couplée, la théorie des cordes se réduit à la supergravité et la fonction de partition est simplement donnée par l'action 'on-shell'. Les propriétés d'équilibre de la théorie des champs sont ainsi simplement obtenues en calculant l'action on-shell de la théorie de gravité.

La correspondance AdS/CFT permet aussi de calculer les fonctions de corrélations de la CFT fortement couplée. Celles-ci sont définies en théorie des champs comme dérivées de la fonction de partition par rapport à la source à laquelle se couple l'opérateur. Dans la correspondance AdS/CFT, elles peuvent être calculées en étudiant les perturbations du champ de la théorie de gravité dual à l'opérateur de la CFT. Ce champ obéit généralement à une équation différentielle du second ordre. Deux conditions aux bords doivent donc lui être imposées. La première a lieu dans l'IR, c'est-à-dire loin du bord conforme, où on doit imposer la régularité si on travaille en signature euclidienne. Si on travaille en signature lorentzienne, plusieurs conditions au bord peuvent être imposées: les conditions 'in-going' et 'out-coming', qui mènent, pour les fonctions de corrélation à deux points, aux fonctions de Green retardée et avancée, respectivement. Dans le cadre de l'étude des propriétés proche de l'équilibre de la théorie des champs, il est naturel de considérer la condition in-going pour laquelle l'onde se propage vers l'infini. Dans l'UV, c'est-à-dire proche du bord conforme d'AdS, la solution est donnée comme combinaison linéaire d'un mode normalisable et d'un autre non-normalisable. Le mode non-normalisable donne la

source de l'opérateur dual. En calculant l'action on-shell, il est alors possible d'obtenir les fonctions de corrélation de la théorie des champs en prenant des dérivées de celle-ci par rapport à cette source.

### F.1.6 Généralisations

Bien que la formulation originelle de la correspondance AdS/CFT proposée par Maldacena conjecture l'équivalence entre la théorie des cordes de type IIB sur $AdS_5 \times S^5$ et la théorie $\mathcal{N} = 4$ SYM, d'autres dualités ont été établies. Citons par exemple l'équivalence entre les théories de Chern-Simons couplées à de la matière en 3 dimensions et la théorie M sur $AdS_4$ fois une variété compacte à 7 dimensions. Plus généralement, la correspondance relie des CFT à $d$ dimensions à la physique sur l'espace $AdS_{d+1}$. Les détails de chaque dualité provient des deux descriptions des D-branes et M-branes en théorie des cordes et théorie M.

Il est aussi possible de considérer la théorie des champs à température non-nulle. Dans ce cas, les branes ne sont pas extrémales, et dans la description en termes de supergravité, cela se traduit par la présence d'un trou noir. La température de la théorie des champs n'est autre que la température de Hawking du trou noir, et les propriétés d'équilibre sont données par la thermodynamique du trou noir. La correspondance s'avère très utile pour l'étude de la dynamique proche de l'équilibre et des phénomènes de dissipation dans les théories des champs fortement couplées.

Dans la correspondance AdS/CFT, une symétrie globale de la théorie des champs est duale à une symétrie de jauge dans la théorie de gravité. Par exemple, si la CFT contient une symétrie globale $U(1)$ cela signifie que la théorie de gravité contient un champ de jauge $U(1)$. On peut alors considérer la théorie des champs à potentiel chimique non-nul pour cette symétrie. Puisque le potentiel chimique peut être vu comme une source pour la charge $U(1)$ conservée, du côté de la gravité cela correspond à changer le comportement asymptotique du champ de jauge proche du bord d'AdS. Plus spécifiquement, le mode non-normalisable devient dans ce cas non-nul.

Nous allons par la suite notamment nous intéresser à des théories des champs fortement couplées à la fois à température finie et à densité finie. La théorie de gravité va donc contenir un trou noir et un champ de jauge.

Dans la dualité AdS/CFT, on peut voir la théorie des champs comme vivant sur le bord conforme de l'espace AdS. La correspondance AdS/CFT est donc une réalisation du principe holographique, qui stipule que toute l'information contenue dans un volume est encodée dans son bord.

## F.2 AdS/CFT pour la matière condensée

La correspondance AdS/CFT est utile pour l'étude de certaines théories des champs supersymétriques qui ont une description duale en termes de supergravité. On peut élargir le domaine d'application de la correspondance et assumer qu'elle s'applique aussi à des modèles plus phénoménologiques.

Nous allons assumer l'équivalence entre une théorie des champs fortement couplée avec un grand nombre de degrés de liberté (similaire au rang $N$ du groupe de jauge $SU(N)$ dans la formulation de Maldacena de la dualité) vivant en $d$ dimensions, et une théorie classique de gravité sur un espace asymptotiquement $AdS_{d+1}$ (dans l'UV, proche du bord d'AdS).

Cela permet d'appliquer le dictionnaire de la correspondance qui relie les observables des deux théories et de calculer les fonctions de corrélation.

Du côté de la gravité, le fait de considérer un espace-temps non pas AdS mais seulement asymptotiquement AdS brise l'invariance conforme de la théorie des champs. Cela est réalisé en considérant des opérateurs relevants dans la théorie des champs ou en la considérant à température finie. Puisque l'invariance conforme est brisée, le groupe de renormalisation est non-trivial pour la théorie des champs.

### F.2.1 Systèmes de fermions à densité finie

Nous allons nous intéresser tout particulièrement aux applications possibles de la correspondance AdS/CFT aux systèmes de fermions fortement couplés. Ces systèmes sont à densité finie.

La plupart des métaux sont très bien décrits par la théorie de Landau des liquides de Fermi. Même si les électrons sont fortement couplés, dans de tels systèmes les excitations de basse énergie sont faiblement couplées et les méthodes perturbatives de la mécanique quantique et de la théorie des champs peuvent être appliquées. Ces excitations sont des 'électrons habillés' qui se comportent comme des particules quasi-libres grâce à la resommation des interactions fortes de courte distance. Le système à basse énergie est adiabatiquement connecté au gaz libre d'électrons. L'état de vide est symétrique sous la symétrie $U(1)$ et les excitations de basse énergie consistent en des paires électrons-trous.

Cette approche en termes de quasiparticules a aussi été utilisée pour décrire le mécanisme menant à l'état supraconducteur par formation de paires de Cooper rendue possible par l'interaction des électrons habillés avec les vibrations du réseau (les phonons). Dans ce cas la symétrie $U(1)$ est spontanément brisée.

Certains systèmes de fermions ne sont cependant pas décrits par la théorie de Landau. Cela se produit lorsque les excitations de basse énergie sont fortement couplées. Dans ce cas on ne parle plus de quasiparticules car les excitations ont un temps de vie court.

Certains systèmes de fermions qui ne sont pas décrits par la théorie de Landau admettent une transition de phase quantique, que l'on peut définir comme une transition de phase à température nulle qui n'est pas controlée par la température mais par un paramètre tel que le dopage. Au point critique, la longueur de cohérence diverge et le système est invariant sous une symétrie d'échelle émergente sous laquelle le temps et l'espace se transforment différemment: $t \to \lambda^z t$, $x \to \lambda x$. Le système est aussi invariant sous rotations et translations spatiales et temporelles. Cela forme le groupe de Lifshitz. La symétrie émergente est aussi présente à des températures non-nulles pour lesquelles les fluctuations quantiques sont négligeables par rapport aux fluctuations thermiques. Dans cette région critique quantique, le système est en principe décrit par une théorie critique à température finie.

Les cuprates sont des matériaux qui deviennent supraconducteurs en dessous d'une température critique anormalement haute d'un point de vue de la théorie BCS. A des températures supérieures à la température critique, ces matériaux sont conducteurs mais non décrits par la théorie de Landau à cause des fortes interactions et de l'absence de quasiparticules. On pense que cet état de 'métal étrange' appartient à la région critique quantique d'un point critique quantique qui se trouverait dans la phase supraconductrice du diagramme de phase. Pour comprendre le mécanisme menant à l'état supraconducteur dans de tels matériaux, il est intéressant de comprendre l'état de métal étrange. Cet état est cependant difficilement accessible en utilisant les méthodes perturbatives de la

mécanique quantique et de la théorie des champs puisqu'il est fortement corrélé à basse énergie. La dualité AdS/CFT fournit une nouvelle approche et de nouveaux outils pour l'étude de tels systèmes.

### F.2.2 La théorie d'Einstein-Maxwell

Nous souhaitons étudier les systèmes de fermions fortement corrélés en utilisant la correspondance AdS/CFT dans une approche phénoménologique. Puisque de nombreux matériaux se comportent à basse énergie comme s'ils vivaient dans un espace à 2+1 dimensions, nous allons considérer un espace-temps asymptotiquement $AdS_4$. Un tel espace peut être obtenu en considérant la théorie de gravité d'Einstein avec une constante cosmologique négative. De plus, les systèmes de fermions qui nous intéressent sont à densité finie, la théorie de gravité duale doit donc contenir un champ de jauge $U(1)$ responsable du potentiel chimique non-nul. Nous considérons donc la théorie d'Einstein-Maxwell en 4 dimensions.

Cette théorie admet une solution exacte, le trou noir de Reissner-Nordström, qui est un trou noir chargé. La charge totale de cette solution est aussi la charge $U(1)$ de la théorie des champs duale. Cette solution pose cependant quelques problèmes pour l'étude des systèmes de fermions. Il est facile de montrer que l'entropie de cette solution est non-nulle à température nulle, ce qui veut dire que l'état de la théorie des champs duale est dégénéré. Aussi, aucun champ de matière n'est présent dans cette solution, ce qui signifie que la matière est inaccessible dans la théorie des champs duale. Il est donc nécessaire d'introduire des champs de matière dans la théorie d'Einstein-Maxwell pour modéliser holographiquement plus précisément un système de fermions.

### F.2.3 Le modèle de l'étoile à électrons

Un premier modèle holographique important pour l'étude des systèmes de fermions fortement couplés est l'étoile à électrons. Ce modèle consiste en la théorie d'Einstein-Maxwell couplée à un fluide parfait de fermions chargés à température nulle. Dans ce modèle, les fermions sont traités semi-classiquement et les quantités du fluide fermionique, telles que la pression, la densité de charge et la densité d'énergie, sont fonctions d'un potentiel chimique local, lui-même fonction de la composante temporelle du champ de jauge (et de la métrique). Lorsque le potentiel chimique local est supérieur à la masse des fermions, les quantités du fluide sont non-nulles. Lorsqu'il est inférieur à la masse, ces quantités sont nulles et le fluide n'est pas présent.

Ce système admet une solution exacte qui reproduit l'invariance d'échelle émergente observée au point critique dans les systèmes critiques quantiques. Dans cette solution, le potentiel chimique local est constant, le fluide est non-trivial et ses quantités sont constantes. Cette solution est considérée comme la solution dans l'IR (loin du bord de l'espace AdS). En perturbant cette solution, il est possible de connecter cette géométrie de basse énergie à un espace-temps AdS proche du bord. La valeur du potentiel chimique local décroit lorsqu'on s'éloigne de la région IR jusqu'à un point où il est égal à la masse des fermions. A ce point les quantités du fluide deviennent nulles, ce qui définit le bord de l'étoile. En dehors de l'étoile, l'espace-temps est celui du trou noir de Reissner-Nordström.

En calculant l'action on-shell de cette solution, il peut être montré que l'énergie libre de la solution de l'étoile à électrons est inférieure à celle du trou noir de Reissner-Nordström extrémal, ce qui signifie que l'étoile à électrons est favorisée thermodynamiquement à température nulle.

En étudiant l'équation du mouvement d'un champ spinoriel test sur cette solution, il peut être montré que la théorie des champs duale admet un grand nombre de surfaces de Fermi. Aussi, il est possible d'étudier la réaction du système à l'application d'un champ magnétique. On trouve que celui-ci ne se comporte pas exactement comme un liquide de Fermi.

La solution de l'étoile à électrons est interprétée comme décrivant un système de fermions fortement couplé proche d'un point critique et qui n'est pas décrit par la théorie de Landau.

### F.2.4 Le supraconducteur holographique

On peut aussi coupler la théorie d'Einstein-Maxwell à un champ scalaire chargé. Cela a mené au concept de supraconducteur holographique.

Des solutions pour de telles théories ont été trouvées où un trou noir chargé coexiste avec un champ scalaire. Le champ scalaire est non-trivial dans tout l'espace-temps. En particulier, proche du bord d'AdS le mode non-normalisable, proportionnel à la vev de l'opérateur scalaire chargé dual, est non-nul. L'opérateur scalaire dual condense et la symétrie $U(1)$ est spontanément brisée. En interprétant cet opérateur comme l'équivalent à couplage fort des paires de Cooper, on en déduit que l'état est supraconducteur.

En dessous d'une certaine température critique, la solution où le champ scalaire est non-trivial est favorisée thermodynamiquement par rapport au trou noir chargé seul. Cependant, au dessus de cette température, seule la solution du trou noir chargé seul existe. On peut montrer qu'il y a une transition de phase du second ordre à la température critique interprétée comme le passage à l'état supraconducteur dans la théorie des champs duale.

Les supraconducteurs holographiques ont été découverts tout d'abord à température finie par Hartnoll, Herzog et Horowitz en 2008. L'année suivante une solution à température nulle a été trouvée par Horowitz et Roberts (voir aussi Gubser et Nellore). Dans ce cas le trou noir n'est plus présent et l'état supraconducteur dual est non-dégénéré. Cette solution est un des ingrédients majeurs de cette thèse.

L'appellation 'supraconducteurs holographiques' pour ces solutions n'est pas seulement justifiée par la condensation d'un opérateur scalaire chargé. En effet, il est possible de caractériser l'état supraconducteur en étudiant le comportement du système à l'application de champs électrique et magnétique. Dans le contexte de l'holographie, cela peut être fait en étudiant les perturbations du champ de jauge de la théorie de gravité. En appliquant le dictionnaire de la dualité AdS/CFT et la théorie de la réponse linéaire, on peut par exemple obtenir la conductivité électrique, dépendante de la fréquence, du système. Dans l'état supraconducteur, on observe un gap en énergie dans la partie réelle de la conductivité. Dans un métal, la conductivité n'a pas de gap: pour un champ électrique appliqué arbitrairement faible, le système est conducteur et le courant électrique induit est non-nul. Dans un supraconducteur BCS, un tel gap est présent et correspond à l'énergie de liaison des paires de Cooper. Dans les supraconducteurs holographiques, le gap observé est interprété comme l'énergie de liaison du condensat scalaire, qui est un opérateur composite de l'opérateur fermionique. Il est aussi possible d'étudier la réaction du système à l'application d'un champ magnétique. Il a été montré que les supraconducteurs holographiques réalisent l'effet Meissner: le supraconducteur expulse tout champ magnétique. Cependant, l'application d'un champ magnétique assez fort brise l'état supraconducteur. La transition de phase entre état supraconducteur et non-supraconducteur en fonction du

champ magnétique appliqué a été étudié dans le contexte holographique. Il est particulièrement intéressant de noter que les supraconducteurs holographiques sont de type II, tout comme les supraconducteurs à haute température critique tels que les cuprates (les supraconducteurs décrits par la théorie BCS sont de type I).

## F.3 Systèmes de Bose-Fermi holographiques

Comme nous l'avons vu ci-dessus, le trou noir de Reissner-Nordström admet deux instabilités, une fermionique et l'autre bosonique, qui sont *a priori* indépendantes. Ces instabilités ont mené à deux modèles importants pour l'étude des systèmes fortement couplés en matière condensée, l'étoile à électrons et le supraconducteur holographique.

Du point de vue de la matière condensée, l'étude de systèmes holographiques où à la fois des degrés de liberté fermioniques et bosoniques sont présents est intéressante. En effet, reprenons le diagramme de phase des cuprates. A basse température, ces systèmes sont supraconducteurs. A plus haute température, l'état est conducteur mais non décrit par la théorie de Landau des liquides de Fermi à cause des fortes interactions entre excitations fermioniques de basse énergie. Comme nous l'avons suggéré plus haut, cela pourrait signifier qu'il y a un point critique quantique dans la phase supraconductrice. L'étude de systèmes holographiques de Bose-Fermi pourrait permettre de décrire la transition de phase entre l'état conducteur et supraconducteur dans ce type de matériaux.

Certains modèles holographiques ont étudié le passage à l'état supraconducteur en considérant la formation de paires de Cooper dans le trou noir de Reissner-Nordström. Ces modèles sont toutefois limités car ils requièrent que la charge du condensat soit le double de celle des électrons. Cependant, il est possible que le condensat qui se forme dans l'état supraconducteur soit un opérateur scalaire composite de l'opérateur fermionique plus compliqué. Aussi, à cause de la possible existence d'un point critique quantique, le phénomène de fractionalisation peut avoir lieu. Dans ce cas, les excitations fermioniques de basse énergie ne portent pas la même charge que les électrons élémentaires.

Pour ces raisons, il est intéressant de considérer un modèle holographique où le rapport des charges des degrés de liberté bosoniques et fermioniques n'est pas fixé. Le modèle que nous proposons de considérer dans cette thèse est basé sur les modèles de l'étoile à électrons et du supraconducteur holographique. Nous allons nous focaliser sur le cas où la température du système est nulle.

### F.3.1 Modèle

Nous considérons la théorie d'Einstein-Maxwell couplée à la fois à un champ scalaire chargé libre et à un fluide parfait de fermions chargés. Du point de vue de la théorie des champs, on s'attend à ce que les degrés de liberté fermioniques et bosoniques interagissent directement. Nous choisissons de les faire interagir dans la théorie de gravité par un couplage courant-courant, entre les courants électromagnétiques du fluide et du champ scalaire. Cela permet de garder l'approximation semi-classique du fluide valide pour le traitement des fermions.

Ce modèle admet comme solutions connues le trou noir de Reissner-Nordström (solution pour laquelle le champ scalaire est trivial et le fluide n'est pas présent), le supraconducteur holographique (le fluide n'est pas présent) et l'étoile à électrons (le champ scalaire est trivial). Il est cependant possible d'imaginer qu'il existe d'autres solutions au système

où le champ scalaire et le fluide coexistent. Nous montrons dans cette thèse que de telles solutions existent.

### F.3.2 Solutions d'étoiles compactes

Nous commençons par étudier l'équation du mouvement d'un champ scalaire test dans l'étoile à électrons. Il peut être facilement montré que si la charge élémentaire du champ scalaire est suffisamment grande ou si sa masse est suffisamment petite, cette solution est instable et la contribution du champ scalaire aux équations d'Einstein et de Maxwell doit être prise en compte. Il faut alors résoudre le système d'équations du mouvement données par les équations d'Einstein, de Maxwell et de Klein-Gordon.

Il n'est pas possible de résoudre ces équations différentielles analytiquement. La méthode alors employée est de tout d'abord trouver une solution asymptotique dans l'IR et d'intégrer numériquement les équations jusqu'à la région asymptotiquement AdS dans l'UV. Deux types de solutions sont possibles dans l'IR. Premièrement, cette région peut être occupé à la fois par le champ scalaire et le fluide. Cependant dans ce cas les contraintes sont trop fortes sur le système et il n'existe pas de solutions. Deuxièmement, il est possible que la région IR ne soit occupée que par le champ scalaire et que les quantités de fluide soient non-nulles dans une région compacte de l'espace-temps (dans la direction radiale). Dans ce cas, la solution dans l'IR est la même que celle pour le supraconducteur holographique, le potentiel chimique local tend vers zéro.

En intégrant numériquement les équations du mouvement depuis l'IR jusqu'à l'UV et en considérant, comme pour le modèle de l'étoile à électrons, que le potentiel chimique local contrôle la présence du fluide, on peut montrer qu'il existe trois types de nouvelles solutions. Les solutions d'étoiles d'électrons compactes (eCS) correspondent à une densité de fluide confinée dans une région aux bords de laquelle le potentiel chimique local est égal à la masse des fermions. Dans ce cas, la densité de charge du fluide est positive et dans nos conventions, le fluide est constitué d'électrons. Les solutions d'étoiles de positrons compactes (pCS) correspondent de façon similaire à une densité de fluide confinée dans une région compacte de l'espace-temps (dans la direction radiale) pour laquelle la densité de charge est négative. Aux bords de cette région, le potentiel chimique local est égal à l'opposé de la masse des fermions et est négatif. Le troisième type de solutions sont les étoiles compactes de positrons et électrons (peCS) pour lesquelles le champ scalaire coexiste avec un fluide d'électrons et un fluide de positrons, qui sont confinés dans des régions distinctes de l'espace-temps.

Dans nos conventions, le champ de jauge est positif, ce qui détermine le signe de la charge électrique du champ scalaire, qui est aussi positive. La formation d'un fluide de positrons, de charge électrique négative, est rendue possible par l'écrantage de cette charge par le champ scalaire. Cela vient du fait que les deux entités interagissent directement à travers le couplage courant-courant. Dans le cas des solutions peCS, le système est polarisé où les fluides chargés positivement et négativement occupent des régions distinctes et sont immergées dans le champ scalaire non-nul. Du fait de l'écrantage de la charge électrique négative par le champ scalaire, les deux fluides se repoussent au lieu de s'attirer. Le système est maintenu stable par la force gravitationnelle qui annihile la répulsion électromagnétique.

### F.3.3 Energie libre

L'existence de ces nouvelles solutions d'étoiles compactes dépend des paramètres du système, que sont la masse et la charge élémentaire du champ scalaire ainsi que la masse et un paramètre lié au spin des fermions. Lorsque plusieurs solutions existent, il est nécessaire de calculer l'énergie libre de chacune des solutions pour déterminer celle qui est favorisée thermodynamiquement. Pour ce faire, il faut en théorie calculer l'action on-shell pour ces solutions. Cependant, il est possible de calculer l'énergie libre de chaque solution à partir de la solution asymptotique proche du bord de l'espace AdS.

Lorsqu'une solution d'étoile compacte existe à paramètres fixés, elle est favorisée thermodynamiquement par rapport au trou noir chargé, au supraconducteur holographique et à l'étoile à électrons. Lorsque la solutions peCS existe, les solutions eCS et pCS existent aussi, mais ne sont pas favorisées.

Lorsque les valeurs extrémales du potentiel chimique sont trop petites (en valeur absolue), les solutions d'étoiles compactes ne peuvent se former. Cela se produit par exemple lorsque la masse des fermions est suffisamment grande, à autres paramètres fixés. L'étude de l'énergie libre des différentes solutions comme fonction des paramètres du système tels que la masse des fermions ou la charge élémentaire du champ scalaire mène à d'intéressantes conclusions.

Nous avons trouvé des transitions de phase continues entre le supraconducteur holographique et les solutions d'étoiles compactes (eCS, pCS et peCS) comme fonction de la masse des fermions et de la charge élémentaire du champ scalaire. Les transitions de phase ont lieu aux points dans l'espace des paramètres où la valeur maximale ou minimale du potentiel chimique local dans la solution du supraconducteur holographique est égale à la masse des fermions (en valeur absolue).

Nous supposons qu'il existe aussi une transition de phase entre les solutions d'étoiles compactes et l'étoile à électrons. Cependant la précision de nos calculs numériques ne nous permet pas de calculer l'énergie libre proche du possible point critique dans l'espace des paramètres. Il est aussi possible qu'une autre phase inconnue existe entre ces deux solutions. Pour éclairer ce point, il serait intéressant d'obtenir une solution de supraconducteur holographique pour une charge élémentaire plus petite du champ scalaire. A ce jour, une telle solution n'est pas connue.

### F.3.4 Excitations fermioniques de basse énergie

Nous avons vu plus haut qu'il existait des solutions asymptotiquement $AdS_4$ contenant à la fois des degrés de liberté bosoniques et fermioniques, respectivement représentés par un champ scalaire chargé et un fluide parfait de fermions chargé. Nous nous posons maintenant la question de l'interprétation à donner à ces solutions du point de vue de la théorie des champs duale.

En utilisant le dictionnaire de la dualité AdS/CFT, l'interprétation du champ scalaire est claire. Tout comme pour le supraconducteur holographique, le champ scalaire dans les solutions d'étoiles compactes se traduit par la présence d'un condensat scalaire chargé dans la théorie des champs duale qui brise la symétrie $U(1)$ globale.

Même s'il est naturel de penser que la densité de fluide fermionique est un signe de la présence de degrés de liberté fermioniques dans la théorie des champs duale, cela n'est pas aussi simple que pour le champ scalaire. Dans l'approximation du fluide, l'interprétation des fermions de la théorie de gravité n'est pas obtenue directement à partir de la solution asymptotique dans l'UV comme pour le champ scalaire. Cela est dû au fait que l'opérateur

fermionique de la théorie des champs est 'caché' par l'approximation semi-classique appliquée aux fermions de la théorie de gravité.

Dans le but de caractériser l'état dual aux solutions d'étoiles compactes et en particulier ses propriétés fermioniques, nous avons étudié les modes (quasi)-normaux d'un champ spinoriel test dans ces solutions. Ces modes sont obtenus en résolvant l'équation de Dirac en imposant les conditions aux bords suivantes: dans l'IR, on impose la régularité ou la condition in-going, dans l'UV on impose la condition de Dirichlet faible où le terme dominant est nul. Du point de vue de la théorie des champs, cela correspond à considérer l'opérateur fermionique comme n'étant pas couplé à une source extérieure. Le champ spinoriel a l'interprétation duale d'une fluctuation de l'opérateur fermionique de la théorie des champs. La procédure holographique pour calculer les fonctions de corrélation peut être appliquée et on obtient le propagateur, c'est-à-dire la fonction de Green retardée à deux points, des excitations fermioniques de basse énergie. Les pôles de cette fonction de corrélation donnent la relation de dispersion des excitations fermioniques.

Nous avons trouvé que la présence du fluide d'électrons (positrons, respectivement) correspondait dans la théorie des champs duale à la formation d'un grand nombre de surfaces de Fermi de type électron (trou). Pour les solutions peCS, la théorie des champs duale contient ces deux types de surfaces de Fermi. Ces solutions peuvent être interprétées de la manière suivante. Le système contient un grand nombre de fermions avec différentes saveurs et un condensat scalaire chargé. Chaque saveur de fermions a une certaine structure de bandes mais avec un niveau d'énergie nulle des excitations qui est différent pour chaque saveur. Par conséquent, un potentiel chimique donné intersecte la bande de valence pour certains fermions et la bande de conduction pour d'autres, menant aux surfaces de Fermi de type trou et électron, respectivement.

L'étude des excitations de basse énergie dans les états de Bose-Fermi holographiques nous a aussi mené à des conclusions intéressantes dans l'étude de la transition entre l'état métallique (représenté holographiquement par la solution de l'étoile à électrons) et l'état de Bose-Fermi caractérisé par la présence de surfaces de Fermi et du condensat scalaire (représenté holographiquement par la solution eCS). En étudiant l'équation de Dirac du champ spinoriel test sous la forme d'une équation de Schrödinger, nous avons montré que le nombre de surfaces de Fermi de type électron dans l'état dual à la solution de l'étoile à électrons est infini alors que ce nombre est fini pour l'état dual à la solution eCS. Dans la transition de phase ES/eCS entre les solutions de l'étoile à électrons (ES) et de l'étoile compacte d'électrons (eCS), un gap s'ouvre pour une partie des surfaces de Fermi. Les fermions correspondants sont interprétés comme étant ceux qui condensent et forment le condensat scalaire. Les surfaces de Fermi pour lesquelles un gap s'ouvre en premier sont celles avec un moment de Fermi petit. Dans la théorie BCS, c'est l'inverse qui se produit puisque les surfaces de Fermi avec un moment de Fermi plus petit sont plus stables. Rappelons de plus que le condensat scalaire est un opérateur composite de l'opérateur fermionique plus compliqué que dans le cas de la théorie BCS. Cela suggère que le mécanisme qui gouverne le passage à l'état supraconducteur dans notre modèle holographique n'est pas décrit par la théorie BCS.

## F.4 Trous noirs asymptotiquement AdS en supergravité jaugée

La correspondance AdS/CFT est utile pour l'étude des théories des champs fortement couplées. Comme nous l'avons vu plus haut, on peut admettre que cette dualité s'applique à une classe de théories plus larges que celles données par la théorie des cordes et la

physique des D-branes. Cela nous a permis de construire des modèles holographiques simples basés sur la théorie d'Einstein-Maxwell. La correspondance AdS/CFT a cependant aussi été fortement étudiée dans une approche plus mathématique, dans le contexte de la théorie des cordes.

Dans l'exemple de la théorie des cordes de type IIB sur l'espace $AdS_5 \times S^5$, il n'y a pas de séparation d'échelle entre les différents multiplets chiraux résultants de la compactification des champs dix-dimensionnels sur la sphère $S^5$. Ceci est dû à la courbure non-nulle de l'espace AdS. Il est cependant possible d'écrire une action pour le multiplet gravitationnel, qui contient notamment la métrique 5-dimensionnelle et les champs duaux aux courants conservés de la théorie des champs duale. Cette action à 5 dimensions correspond à la théorie de supergravité $\mathcal{N} = 8$ à 5 dimensions. On pense que cette théorie est une troncation consistante de la théorie des cordes de type IIB sur $AdS_5 \times S^5$ dans le sens où chaque solution classique de cette théorie à 5 dimensions correspond (peut être 'upliftée') à une solution dans la théorie 10-dimensionnelle.

Les théories de supergravité jaugée sont intéressantes pour l'holographie car elles admettent des solutions asymptotiquement AdS. Ceci est dû au fait que le potentiel pour les champs scalaires est non-nul, celui-ci joue le rôle d'une constante cosmologique négative.

Dans cette thèse nous nous sommes particulièrement intéressés à la théorie de supergravité jaugée $\mathcal{N} = 2$ en 4 dimensions, qui est une troncation consistante de la théorie de supergravité jaugée $\mathcal{N} = 8$ obtenue par de Wit et Nicolai. Cette dernière est une troncation consistante de la théorie M sur la sphère $S^7$.

Nous nous sommes intéressés à un modèle STU simple de la supergravité jaugée $\mathcal{N} = 2$ en 4 dimensions. Cette théorie contient le multiplet gravitationnel et trois multiplets vectoriels. Lorsque les couplages au champ de jauge sont de type Fayet-Iliopoulos, le lagrangien est donné par le lagrangien de la théorie non-jaugée auquel s'ajoute un potentiel pour les champs scalaires. Nous avons considéré le cas où l'espace des modules est le coset (aussi appelé espace homogène) $[SL(2,\mathbb{R})/U(1)]^3$.

Nous avons montré que cette théorie admet un groupe de dualité $U(1)^3$ dont les transformations du sous-groupe $U(1)^2$ préservent les équations BPS. Nous avons appliqué les transformations de ce sous-groupe de dualité pour générer de nouvelles solutions de trous noirs supersymétriques analytiques à partir des solutions connues. Pour les trous noirs statiques, nous avons généralisé les solutions analytiques de Cacciatori et Klemm qui comportent trois charges magnétiques. En plus de ces trois charges magnétiques, nos solutions admettent aussi deux charges électriques et correspondent donc à des trous noirs dyoniques. Pour les trous noirs en rotation, nous avons généralisé les solutions connues à deux paramètres en y ajoutant un paramètre supplémentaire qui représente un mode normalisable scalaire.

# Bibliography


[1] F. Nitti, G. Policastro, and T. Vanel, "Dressing the Electron Star in a Holographic Superconductor," *JHEP* **1310** (2013) 019, arXiv:1307.4558 [hep-th].

[2] F. Nitti, G. Policastro, and T. Vanel, "Polarized solutions and Fermi surfaces in holographic Bose-Fermi systems," arXiv:1407.0410 [hep-th].

[3] N. Halmagyi and T. Vanel, "AdS Black Holes from Duality in Gauged Supergravity," *JHEP* **1404** (2014) 130, arXiv:1312.5430 [hep-th].

[4] J. M. Maldacena, "The Large N limit of superconformal field theories and supergravity," *Adv.Theor.Math.Phys.* **2** (1998) 231–252, arXiv:hep-th/9711200 [hep-th].

[5] G. 't Hooft, "A Planar Diagram Theory for Strong Interactions," *Nucl.Phys.* **B72** (1974) 461.

[6] J. Polchinski, "Dirichlet Branes and Ramond-Ramond charges," *Phys.Rev.Lett.* **75** (1995) 4724–4727, arXiv:hep-th/9510017 [hep-th].

[7] J. Dai, R. Leigh, and J. Polchinski, "New Connections Between String Theories," *Mod.Phys.Lett.* **A4** (1989) 2073–2083.

[8] O. Aharony, S. S. Gubser, J. M. Maldacena, H. Ooguri, and Y. Oz, "Large N field theories, string theory and gravity," *Phys.Rept.* **323** (2000) 183–386, arXiv:hep-th/9905111 [hep-th].

[9] E. Witten, "Anti-de Sitter space and holography," *Adv.Theor.Math.Phys.* **2** (1998) 253–291, arXiv:hep-th/9802150 [hep-th].

[10] M. Bianchi, D. Z. Freedman, and K. Skenderis, "Holographic renormalization," *Nucl.Phys.* **B631** (2002) 159–194, arXiv:hep-th/0112119 [hep-th].

[11] K. Skenderis, "Lecture notes on holographic renormalization," *Class.Quant.Grav.* **19** (2002) 5849–5876, arXiv:hep-th/0209067 [hep-th].

[12] P. Breitenlohner and D. Z. Freedman, "Positive Energy in anti-De Sitter Backgrounds and Gauged Extended Supergravity," *Phys.Lett.* **B115** (1982) 197.

[13] P. Breitenlohner and D. Z. Freedman, "Stability in Gauged Extended Supergravity," *Annals Phys.* **144** (1982) 249.

[14] I. R. Klebanov and E. Witten, "AdS / CFT correspondence and symmetry breaking," *Nucl.Phys.* **B556** (1999) 89–114, arXiv:hep-th/9905104 [hep-th].

[15] J. Casalderrey-Solana, H. Liu, D. Mateos, K. Rajagopal, and U. A. Wiedemann, "Gauge/String Duality, Hot QCD and Heavy Ion Collisions," arXiv:1101.0618 [hep-th].

[16] O. Aharony, O. Bergman, D. L. Jafferis, and J. Maldacena, "N=6 superconformal Chern-Simons-matter theories, M2-branes and their gravity duals," *JHEP* **0810** (2008) 091, arXiv:0806.1218 [hep-th].

[17] E. Witten, "Anti-de Sitter space, thermal phase transition, and confinement in gauge theories," *Adv.Theor.Math.Phys.* **2** (1998) 505–532, arXiv:hep-th/9803131 [hep-th].

[18] A. Karch and E. Katz, "Adding flavor to AdS / CFT," *JHEP* **0206** (2002) 043, arXiv:hep-th/0205236 [hep-th].

[19] G. 't Hooft, "Dimensional reduction in quantum gravity," arXiv:gr-qc/9310026 [gr-qc].

[20] L. Susskind, "The World as a hologram," *J.Math.Phys.* **36** (1995) 6377–6396, arXiv:hep-th/9409089 [hep-th].

[21] J. M. Luttinger and J. C. Ward, "Ground-state energy of a many-fermion system. ii," *Phys. Rev.* **118** (Jun, 1960) 1417–1427. http://link.aps.org/doi/10.1103/PhysRev.118.1417.

[22] J. M. Luttinger, "Fermi surface and some simple equilibrium properties of a system of interacting fermions," *Phys. Rev.* **119** (Aug, 1960) 1153–1163. http://link.aps.org/doi/10.1103/PhysRev.119.1153.

[23] J. Bardeen, L. Cooper, and J. Schrieffer, "Microscopic theory of superconductivity," *Phys.Rev.* **106** (1957) 162.

[24] J. Bardeen, L. Cooper, and J. Schrieffer, "Theory of superconductivity," *Phys.Rev.* **108** (1957) 1175–1204.

[25] S. A. Hartnoll, "Lectures on holographic methods for condensed matter physics," *Class.Quant.Grav.* **26** (2009) 224002, arXiv:0903.3246 [hep-th].

[26] S. Sachdev, "Quantum magnetism and criticality," *Nature Physics* **4** (Mar., 2008) 173–185, arXiv:0711.3015 [cond-mat.str-el].

[27] S. A. Hartnoll, "Horizons, holography and condensed matter," arXiv:1106.4324 [hep-th].

[28] J. Bednorz and K. Muller, "Possible high Tc superconductivity in the Ba-La-Cu-O system," *Z.Phys.* **B64** (1986) 189–193.

[29] S. Sachdev and B. Keimer, "Quantum criticality," *Physics Today* **64** no. 2, (2011) 29, arXiv:1102.4628 [cond-mat.str-el].

[30] S. Sachdev, "Condensed Matter and AdS/CFT," *Lect.Notes Phys.* **828** (2011) 273–311, arXiv:1002.2947 [hep-th].

[31] G. Gibbons and S. Hawking, "Action Integrals and Partition Functions in Quantum Gravity," *Phys.Rev.* **D15** (1977) 2752–2756.

[32] T. Faulkner, H. Liu, J. McGreevy, and D. Vegh, "Emergent quantum criticality, Fermi surfaces, and AdS(2)," *Phys.Rev.* **D83** (2011) 125002, arXiv:0907.2694 [hep-th].

[33] S. Sachdev, "Compressible quantum phases from conformal field theories in 2+1 dimensions," *Phys.Rev.* **D86** (2012) 126003, arXiv:1209.1637 [hep-th].

[34] H. Liu, J. McGreevy, and D. Vegh, "Non-Fermi liquids from holography," *Phys.Rev.* **D83** (2011) 065029, arXiv:0903.2477 [hep-th].

[35] M. Cubrovic, J. Zaanen, and K. Schalm, "String Theory, Quantum Phase Transitions and the Emergent Fermi-Liquid," *Science* **325** (2009) 439–444, arXiv:0904.1993 [hep-th].

[36] N. Iqbal, H. Liu, and M. Mezei, "Semi-local quantum liquids," *JHEP* **1204** (2012) 086, arXiv:1105.4621 [hep-th].

[37] N. Iqbal, H. Liu, and M. Mezei, "Quantum phase transitions in semi-local quantum liquids," arXiv:1108.0425 [hep-th].

[38] T. Faulkner, N. Iqbal, H. Liu, J. McGreevy, and D. Vegh, "Charge transport by holographic Fermi surfaces," *Phys.Rev.* **D88** (2013) 045016, arXiv:1306.6396 [hep-th].

[39] S. A. Hartnoll and A. Tavanfar, "Electron stars for holographic metallic criticality," *Phys.Rev.* **D83** (2011) 046003, arXiv:1008.2828 [hep-th].

[40] S. A. Hartnoll, J. Polchinski, E. Silverstein, and D. Tong, "Towards strange metallic holography," *JHEP* **1004** (2010) 120, arXiv:0912.1061 [hep-th].

[41] S. Kachru, X. Liu, and M. Mulligan, "Gravity duals of Lifshitz-like fixed points," *Phys.Rev.* **D78** (2008) 106005, arXiv:0808.1725 [hep-th].

[42] G. T. Horowitz and B. Way, "Lifshitz Singularities," *Phys.Rev.* **D85** (2012) 046008, arXiv:1111.1243 [hep-th].

[43] S. A. Hartnoll, D. M. Hofman, and A. Tavanfar, "Holographically smeared Fermi surface: Quantum oscillations and Luttinger count in electron stars," *Europhys.Lett.* **95** (2011) 31002, arXiv:1011.2502 [hep-th].

[44] S. A. Hartnoll, D. M. Hofman, and D. Vegh, "Stellar spectroscopy: Fermions and holographic Lifshitz criticality," *JHEP* **1108** (2011) 096, arXiv:1105.3197 [hep-th].

[45] S. El-Showk and K. Papadodimas, "Emergent Spacetime and Holographic CFTs," *JHEP* **1210** (2012) 106, arXiv:1101.4163 [hep-th].

[46] S. A. Hartnoll and P. Petrov, "Electron star birth: A continuous phase transition at nonzero density," *Phys.Rev.Lett.* **106** (2011) 121601, arXiv:1011.6469 [hep-th].

[47] A. Allais, J. McGreevy, and S. J. Suh, "A quantum electron star," *Phys.Rev.Lett.* **108** (2012) 231602, arXiv:1202.5308 [hep-th].

[48] A. Allais and J. McGreevy, "How to construct a gravitating quantum electron star," *Phys.Rev.* **D88** no. 6, (2013) 066006, arXiv:1306.6075 [hep-th].

[49] S. S. Gubser, "Breaking an Abelian gauge symmetry near a black hole horizon," *Phys.Rev.* **D78** (2008) 065034, arXiv:0801.2977 [hep-th].

[50] G. T. Horowitz, "Theory of Superconductivity," *Lect.Notes Phys.* **828** (2011) 313–347, arXiv:1002.1722 [hep-th].

[51] G. T. Horowitz and M. M. Roberts, "Zero Temperature Limit of Holographic Superconductors," *JHEP* **0911** (2009) 015, arXiv:0908.3677 [hep-th].

[52] S. S. Gubser and A. Nellore, "Ground states of holographics," *Phys.Rev.* **D80** (2009) 105007, arXiv:0908.1972 [hep-th].

[53] S. A. Hartnoll, C. P. Herzog, and G. T. Horowitz, "Building a Holographic Superconductor," *Phys.Rev.Lett.* **101** (2008) 031601, arXiv:0803.3295 [hep-th].

[54] S. A. Hartnoll, C. P. Herzog, and G. T. Horowitz, "Holographic Superconductors," *JHEP* **0812** (2008) 015, arXiv:0810.1563 [hep-th].

[55] T. Albash and C. V. Johnson, "A Holographic Superconductor in an External Magnetic Field," *JHEP* **0809** (2008) 121, arXiv:0804.3466 [hep-th].

[56] S. A. Hartnoll and L. Huijse, "Fractionalization of holographic Fermi surfaces," *Class.Quant.Grav.* **29** (2012) 194001, arXiv:1111.2606 [hep-th].

[57] A. Adam, B. Crampton, J. Sonner, and B. Withers, "Bosonic Fractionalisation Transitions," *JHEP* **1301** (2013) 127, arXiv:1208.3199 [hep-th].

[58] B. Gouteraux and E. Kiritsis, "Quantum critical lines in holographic phases with (un)broken symmetry," *JHEP* **1304** (2013) 053, arXiv:1212.2625 [hep-th].

[59] T. Hartman and S. A. Hartnoll, "Cooper pairing near charged black holes," *JHEP* **1006** (2010) 005, arXiv:1003.1918 [hep-th].

[60] Y. Liu, K. Schalm, Y.-W. Sun, and J. Zaanen, "BCS instabilities of electron stars to holographic superconductors," *JHEP* **1405** (2014) 122, arXiv:1404.0571 [hep-th].

[61] M. Edalati, K. W. Lo, and P. W. Phillips, "Neutral Order Parameters in Metallic Criticality in d=2+1 from a Hairy Electron Star," *Phys.Rev.* **D84** (2011) 066007, arXiv:1106.3139 [hep-th].

[62] Y. Liu, K. Schalm, Y.-W. Sun, and J. Zaanen, "Bose-Fermi competition in holographic metals," *JHEP* **1310** (2013) 064, arXiv:1307.4572 [hep-th].

[63] L. D. Landau and E. M. Lifshitz, *Quantum mechanics: non-relativistic theory.* Elsevier, 1977.

[64] M. Oshikawa, "Topological Approach to Luttinger's Theorem and the Fermi Surface of a Kondo Lattice," *Physical Review Letters* **84** (Apr., 2000) 3370–3373, cond-mat/0002392.

[65] T. Hartman and S. A. Hartnoll, "Cooper pairing near charged black holes," *JHEP* **1006** (2010) 005, arXiv:1003.1918 [hep-th].

[66] P. Basu, J. He, A. Mukherjee, M. Rozali, and H.-H. Shieh, "Competing Holographic Orders," *JHEP* **1010** (2010) 092, arXiv:1007.3480 [hep-th].

[67] A. Donos, J. P. Gauntlett, J. Sonner, and B. Withers, "Competing orders in M-theory: superfluids, stripes and metamagnetism," *JHEP* **1303** (2013) 108, arXiv:1212.0871 [hep-th].

[68] D. Musso, "Competition/Enhancement of Two Probe Order Parameters in the Unbalanced Holographic Superconductor," *JHEP* **1306** (2013) 083, arXiv:1302.7205 [hep-th].

[69] R.-G. Cai, L. Li, L.-F. Li, and Y.-Q. Wang, "Competition and Coexistence of Order Parameters in Holographic Multi-Band Superconductors," *JHEP* **1309** (2013) 074, arXiv:1307.2768 [hep-th].

[70] Z.-Y. Nie, R.-G. Cai, X. Gao, and H. Zeng, "Competition between the s-wave and p-wave superconductivity phases in a holographic model," *JHEP* **1311** (2013) 087, arXiv:1309.2204 [hep-th].

[71] I. Amado, D. Arean, A. Jimenez-Alba, L. Melgar, and I. Salazar Landea, "Holographic s+p Superconductors," *Phys.Rev.* **D89** (2014) 026009, arXiv:1309.5086 [hep-th].

[72] A. Donos, J. P. Gauntlett, and C. Pantelidou, "Competing p-wave orders," *Class.Quant.Grav.* **31** (2014) 055007, arXiv:1310.5741 [hep-th].

[73] L.-F. Li, R.-G. Cai, L. Li, and Y.-Q. Wang, "The competition between s-wave order and d-wave order in holographic superconductors," arXiv:1405.0382 [hep-th].

[74] M. Cubrovic, Y. Liu, K. Schalm, Y.-W. Sun, and J. Zaanen, "Spectral probes of the holographic Fermi groundstate: dialing between the electron star and AdS Dirac hair," *Phys.Rev.* **D84** (2011) 086002, arXiv:1106.1798 [hep-th].

[75] B. de Wit and H. Nicolai, "N=8 Supergravity," *Nucl.Phys.* **B208** (1982) 323.

[76] S. L. Cacciatori and D. Klemm, "Supersymmetric AdS(4) black holes and attractors," *JHEP* **1001** (2010) 085, arXiv:0911.4926 [hep-th].

[77] D. Klemm, "Rotating BPS black holes in matter-coupled $AdS_4$ supergravity," *JHEP* **1107** (2011) 019, arXiv:1103.4699 [hep-th].

[78] J. M. Maldacena and C. Nunez, "Supergravity description of field theories on curved manifolds and a no go theorem," *Int. J. Mod. Phys.* **A16** (2001) 822–855, hep-th/0007018.

[79] C. Nunez, I. Park, M. Schvellinger, and T. A. Tran, "Supergravity duals of gauge theories from F(4) gauged supergravity in six-dimensions," *JHEP* **0104** (2001) 025, arXiv:hep-th/0103080 [hep-th].

[80] J. P. Gauntlett, N. Kim, S. Pakis, and D. Waldram, "Membranes wrapped on holomorphic curves," *Phys.Rev.* **D65** (2002) 026003, arXiv:hep-th/0105250 [hep-th].

[81] S. Cucu, H. Lu, and J. F. Vazquez-Poritz, "A Supersymmetric and smooth compactification of M theory to AdS(5)," *Phys.Lett.* **B568** (2003) 261–269, arXiv:hep-th/0303211 [hep-th].

[82] S. Cucu, H. Lu, and J. F. Vazquez-Poritz, "Interpolating from AdS(D-2) x S**2 to AdS(D)," *Nucl.Phys.* **B677** (2004) 181–222, arXiv:hep-th/0304022 [hep-th].

[83] I. Bah, C. Beem, N. Bobev, and B. Wecht, "Four-Dimensional SCFTs from M5-Branes," *JHEP* **1206** (2012) 005, arXiv:1203.0303 [hep-th].

[84] A. Almuhairi and J. Polchinski, "Magnetic AdS x $R^2$: Supersymmetry and stability," arXiv:1108.1213 [hep-th].

[85] F. Benini and N. Bobev, "Two-dimensional SCFTs from wrapped branes and c-extremization," *JHEP* **1306** (2013) 005, arXiv:1302.4451 [hep-th].

[86] J. P. Gauntlett, "Branes, calibrations and supergravity," arXiv:hep-th/0305074 [hep-th].

[87] M. M. Caldarelli and D. Klemm, "Supersymmetry of Anti-de Sitter black holes," *Nucl.Phys.* **B545** (1999) 434–460, arXiv:hep-th/9808097 [hep-th].

[88] D. Klemm and W. Sabra, "Supersymmetry of black strings in D = 5 gauged supergravities," *Phys.Rev.* **D62** (2000) 024003, arXiv:hep-th/0001131 [hep-th].

[89] R. P. Geroch, "A Method for generating solutions of Einstein's equations," *J.Math.Phys.* **12** (1971) 918–924.

[90] L. Andrianopoli, M. Bertolini, A. Ceresole, R. D'Auria, S. Ferrara, *et al.*, "General matter coupled N=2 supergravity," *Nucl.Phys.* **B476** (1996) 397–417, arXiv:hep-th/9603004 [hep-th].

[91] B. de Wit and H. Nicolai, "N=8 supergravity with local so(8) x su(8) invariance," *Phys. Lett.* **B108** (1982) 285.

[92] M. J. Duff and J. T. Liu, "Anti-de sitter black holes in gauged n = 8 supergravity," *Nucl. Phys.* **B554** (1999) 237–253, hep-th/9901149.

[93] M. Cvetic, M. Duff, P. Hoxha, J. T. Liu, H. Lu, *et al.*, "Embedding AdS black holes in ten-dimensions and eleven-dimensions," *Nucl.Phys.* **B558** (1999) 96–126, arXiv:hep-th/9903214 [hep-th].

[94] H. Nicolai and K. Pilch, "Consistent Truncation of d = 11 Supergravity on $AdS_4 \times S^7$," *JHEP* **1203** (2012) 099, arXiv:1112.6131 [hep-th].

[95] B. de Wit and H. Nicolai, "The Consistency of the S**7 Truncation in D=11 Supergravity," *Nucl. Phys.* **B281** (1987) 211.

[96] G. Dall'Agata and A. Gnecchi, "Flow equations and attractors for black holes in N = 2 U(1) gauged supergravity," *JHEP* **1103** (2011) 037, arXiv:1012.3756 [hep-th].

[97] B. de Wit and A. Van Proeyen, "Special geometry, cubic polynomials and homogeneous quaternionic spaces," *Commun. Math. Phys.* **149** (1992) 307–334, arXiv:hep-th/9112027.

[98] B. de Wit, F. Vanderseypen, and A. Van Proeyen, "Symmetry structure of special geometries," *Nucl.Phys.* **B400** (1993) 463–524, arXiv:hep-th/9210068 [hep-th].

[99] R. Corrado, M. Gunaydin, N. P. Warner, and M. Zagermann, "Orbifolds and flows from gauged supergravity," *Phys. Rev.* **D65** (2002) 125024, arXiv:hep-th/0203057.

[100] A. Gnecchi and N. Halmagyi, "Supersymmetric black holes in $AdS_4$ from very special geometry," *JHEP* **1404** (2014) 173, arXiv:1312.2766 [hep-th].

[101] N. Halmagyi, "BPS Black Hole Horizons in N=2 Gauged Supergravity," *JHEP* **1402** (2014) 051, arXiv:1308.1439 [hep-th].

[102] A. Gnecchi, K. Hristov, D. Klemm, C. Toldo, and O. Vaughan, "Rotating black holes in 4d gauged supergravity," *JHEP* **1401** (2014) 127, arXiv:1311.1795 [hep-th].

[103] N. Halmagyi, M. Petrini, and A. Zaffaroni, "BPS black holes in $AdS_4$ from M-theory," *JHEP* **1308** (2013) 124, arXiv:1305.0730 [hep-th].

[104] D. D. K. Chow and G. Compère, "Dyonic AdS black holes in maximal gauged supergravity," *Phys.Rev.* **D89** (2014) 065003, arXiv:1311.1204 [hep-th].

[105] V. A. Kostelecky and M. J. Perry, "Solitonic black holes in gauged N=2 supergravity," *Phys.Lett.* **B371** (1996) 191–198, arXiv:hep-th/9512222 [hep-th].

[106] M. Cvetic, G. Gibbons, H. Lu, and C. Pope, "Rotating black holes in gauged supergravities: Thermodynamics, supersymmetric limits, topological solitons and time machines," arXiv:hep-th/0504080 [hep-th].

[107] D. Klemm and O. Vaughan, "Nonextremal black holes in gauged supergravity and the real formulation of special geometry," *JHEP* **1301** (2013) 053, arXiv:1207.2679 [hep-th].

[108] A. Gnecchi and C. Toldo, "On the non-BPS first order flow in N=2 U(1)-gauged Supergravity," *JHEP* **1303** (2013) 088, arXiv:1211.1966 [hep-th].

[109] K. Hristov, C. Toldo, and S. Vandoren, "Phase transitions of magnetic AdS4 black holes with scalar hair," *Phys.Rev.* **D88** (2013) 026019, arXiv:1304.5187 [hep-th].

[110] A. Anabalon and D. Astefanesei, "On attractor mechanism of $AdS_4$ black holes," *Phys.Lett.* **B727** (2013) 568–572, arXiv:1309.5863 [hep-th].

[111] A. Anabalon and D. Astefanesei, "Black holes in $\omega$-defomed gauged $N = 8$ supergravity," *Phys.Lett.* **B732** (2014) 137–141, arXiv:1311.7459 [hep-th].

[112] H. Lu, Y. Pang, and C. Pope, "AdS Dyonic Black Hole and its Thermodynamics," *JHEP* **1311** (2013) 033, arXiv:1307.6243 [hep-th].

[113] O. Lunin and J. M. Maldacena, "Deforming field theories with u(1) x u(1) global symmetry and their gravity duals," *JHEP* **05** (2005) 033, hep-th/0502086.

[114] S. Frolov, "Lax pair for strings in Lunin-Maldacena background," *JHEP* **0505** (2005) 069, arXiv:hep-th/0503201 [hep-th].

[115] O. Aharony, B. Kol, and S. Yankielowicz, "On exactly marginal deformations of N=4 SYM and type IIB supergravity on AdS(5) x S**5," *JHEP* **0206** (2002) 039, arXiv:hep-th/0205090 [hep-th].

[116] R. G. Leigh and M. J. Strassler, "Exactly marginal operators and duality in four-dimensional n=1 supersymmetric gauge theory," *Nucl. Phys.* **B447** (1995) 95–136, hep-th/9503121.

[117] M. Berkooz and B. Pioline, "5D Black Holes and Non-linear Sigma Models," *JHEP* **0805** (2008) 045, arXiv:0802.1659 [hep-th].

[118] O. Bergman, J. Erdmenger, and G. Lifschytz, "A Review of Magnetic Phenomena in Probe-Brane Holographic Matter," *Lect.Notes Phys.* **871** (2013) 591–624, arXiv:1207.5953 [hep-th].

[119] G. T. Horowitz, J. E. Santos, and D. Tong, "Optical Conductivity with Holographic Lattices," *JHEP* **1207** (2012) 168, arXiv:1204.0519 [hep-th].

[120] G. T. Horowitz and J. E. Santos, "General Relativity and the Cuprates," arXiv:1302.6586 [hep-th].

[121] D. Vegh, "Holography without translational symmetry," arXiv:1301.0537 [hep-th].

[122] M. Taylor, "Non-relativistic holography," arXiv:0812.0530 [hep-th].

[123] P. Horava, "Membranes at Quantum Criticality," *JHEP* **03** (2009) 020, arXiv:arXiv:0812.4287 [hep-th].

[124] P. Horava, "Quantum Gravity at a Lifshitz Point," *Phys. Rev.* **D79** (2009) 084008, arXiv:arXiv:0901.3775 [hep-th].

[125] T. Griffin, P. Horava, and C. M. Melby-Thompson, "Lifshitz Gravity for Lifshitz Holography," *Phys.Rev.Lett.* **110** no. 8, (2013) 081602, arXiv:1211.4872 [hep-th].

[126] D. Son, "Toward an AdS/cold atoms correspondence: A Geometric realization of the Schrodinger symmetry," *Phys.Rev.* **D78** (2008) 046003, arXiv:0804.3972 [hep-th].

[127] K. Balasubramanian and J. McGreevy, "Gravity duals for non-relativistic CFTs," *Phys.Rev.Lett.* **101** (2008) 061601, arXiv:0804.4053 [hep-th].

[128] C. P. Herzog, M. Rangamani, and S. F. Ross, "Heating up Galilean holography," *JHEP* **0811** (2008) 080, arXiv:0807.1099 [hep-th].

[129] J. Maldacena, D. Martelli, and Y. Tachikawa, "Comments on string theory backgrounds with non-relativistic conformal symmetry," *JHEP* **0810** (2008) 072, arXiv:0807.1100 [hep-th].

[130] A. Adams, K. Balasubramanian, and J. McGreevy, "Hot Spacetimes for Cold Atoms," *JHEP* **0811** (2008) 059, arXiv:0807.1111 [hep-th].

[131] K. Balasubramanian and K. Narayan, "Lifshitz spacetimes from AdS null and cosmological solutions," *JHEP* **08** (2010) 014, arXiv:1005.3291 [hep-th].

[132] A. Donos and J. P. Gauntlett, "Lifshitz Solutions of D=10 and D=11 supergravity," *JHEP* **1012** (2010) 002, arXiv:1008.2062 [hep-th].

[133] A. Donos, J. P. Gauntlett, N. Kim, and O. Varela, "Wrapped M5-branes, consistent truncations and AdS/CMT," *JHEP* **1012** (2010) 003, arXiv:1009.3805 [hep-th].

[134] R. Gregory, S. L. Parameswaran, G. Tasinato, and I. Zavala, "Lifshitz solutions in supergravity and string theory," *JHEP* **1012** (2010) 047, arXiv:1009.3445 [hep-th].

[135] N. Halmagyi, M. Petrini, and A. Zaffaroni, "Non-Relativistic Solutions of N=2 Gauged Supergravity," *JHEP* **1108** (2011) 041, arXiv:1102.5740 [hep-th].

[136] D. Cassani and A. F. Faedo, "Constructing Lifshitz solutions from AdS," *JHEP* **1105** (2011) 013, arXiv:1102.5344 [hep-th].

[137] F. Bigazzi, A. L. Cotrone, J. Mas, A. Paredes, A. V. Ramallo, *et al.*, "D3-D7 Quark-Gluon Plasmas," *JHEP* **0911** (2009) 117, arXiv:0909.2865 [hep-th].

[138] F. Bigazzi, A. L. Cotrone, J. Mas, D. Mayerson, and J. Tarrio, "D3-D7 Quark-Gluon Plasmas at Finite Baryon Density," *JHEP* **1104** (2011) 060, arXiv:1101.3560 [hep-th].

[139] U. Gursoy, E. Kiritsis, L. Mazzanti, G. Michalogiorgakis, and F. Nitti, "Improved Holographic QCD," *Lect.Notes Phys.* **828** (2011) 79–146, arXiv:1006.5461 [hep-th].

[140] S. Bhattacharyya, V. E. Hubeny, S. Minwalla, and M. Rangamani, "Nonlinear Fluid Dynamics from Gravity," *JHEP* **02** (2008) 045, arXiv:arXiv:0712.2456 [hep-th].

[141] Y. Neiman and Y. Oz, "Relativistic Hydrodynamics with General Anomalous Charges," *JHEP* **1103** (2011) 023, arXiv:1011.5107 [hep-th].

[142] I. Bredberg, C. Keeler, V. Lysov, and A. Strominger, "From Navier-Stokes To Einstein," *JHEP* **1207** (2012) 146, arXiv:1101.2451 [hep-th].

[143] D. T. Son and A. O. Starinets, "Minkowski space correlators in AdS / CFT correspondence: Recipe and applications," *JHEP* **0209** (2002) 042, arXiv:hep-th/0205051 [hep-th].

[144] C. Herzog and D. Son, "Schwinger-Keldysh propagators from AdS/CFT correspondence," *JHEP* **0303** (2003) 046, arXiv:hep-th/0212072 [hep-th].

[145] R. Kubo, "Statistical mechanical theory of irreversible processes. 1. General theory and simple applications in magnetic and conduction problems," *J.Phys.Soc.Jap.* **12** (1957) 570–586.

[146] B. de Wit and A. Van Proeyen, "Hidden symmetries, special geometry and quaternionic manifolds," *Int.J.Mod.Phys.* **D3** (1994) 31–48, arXiv:hep-th/9310067 [hep-th].